# Final Report-Watervliet Arsenal

## Diagnostic Tools for Performance Evaluation of Innovative In-Situ Remediation Technologies at Chlorinated Solvent-Contaminated Sites

## ESTCP Project ER-200318

July 2011

Michael Kavanaugh
Rula Deeb
Elisabeth Hawley
**Malcolm Pirnie, Inc.**



# REPORT DOCUMENTATION PAGE

*Form Approved*
*OMB No. 0704-0188*



**PLEASE DO NOT RETURN YOUR FORM TO THE ABOVE ORGANIZATION.**

| 1. REPORT DATE *(DD-MM-YYYY)* | 2. REPORT TYPE | 3. DATES COVERED *(From - To)* |
|---|---|---|
| 02-07-2011 | Final Report-Watervliet Arsenal | 2003-02-07-2011 |

**4. TITLE AND SUBTITLE**

Diagnostic Tools for Performance Evaluation of Innovative In-Situ Remediation Technologies at Chlorinated Solvent-Contaminated Sites

**5a. CONTRACT NUMBER**

**5b. GRANT NUMBER**

**5c. PROGRAM ELEMENT NUMBER**

**6. AUTHOR(S)**

Rula Deeb
Michael Kavanaugh
Elisabeth Hawley

**5d. PROJECT NUMBER**

ER-200318

**5e. TASK NUMBER**

**5f. WORK UNIT NUMBER**

**7. PERFORMING ORGANIZATION NAME(S) AND ADDRESS(ES)**

Malcolm Pirnie, Inc.
2000 Powell Street, Suite 1180
Emeryville, CA 94608

**8. PERFORMING ORGANIZATION REPORT NUMBER**

ER-200318

**9. SPONSORING/MONITORING AGENCY NAME(S) AND ADDRESS(ES)**

SERDP/ESTCP
901 North Stuart Street, Suite 303
Arlington, VA 22203

**10. SPONSOR/MONITOR'S ACRONYM(S)**

SERDP/ESTCP

**11. SPONSOR/MONITOR'S REPORT NUMBER(S)**

**12. DISTRIBUTION/AVAILABILITY STATEMENT**

Unlimited

**13. SUPPLEMENTARY NOTES**

**14. ABSTRACT**

This Demonstration Report provides an evaluation of innovative diagnostic tools used first for site characterization to support remediation design, and second to evaluate the performance of in situ chemical oxidation (ISCO) using permanganate at the Watervliet Arsenal (WVA). An area of groundwater contamination was discovered in 1998 in the eastern portion of the WVA, adjacent to the site boundary and in front of former manufacturing Building 40. Groundwater contaminants include chlorinated volatile organic compounds (CVOCs), predominantly tetrachloroethene (PCE), and cis-1,2-dichloroethene (DCE), with a lesser percentage of trichloroethene (TCE) and vinyl chloride.

**15. SUBJECT TERMS**

| 16. SECURITY CLASSIFICATION OF: | | | 17. LIMITATION OF ABSTRACT | 18. NUMBER OF PAGES | 19a. NAME OF RESPONSIBLE PERSON |
|---|---|---|---|---|---|
| a. REPORT | b. ABSTRACT | c. THIS PAGE | | 298 | Rula Deeb |
| | | | | | 19b. TELEPHONE NUMBER *(Include area code)* (510) 596-8855 |

Reset

**Standard Form 298** (Rev. 8/98)
Prescribed by ANSI Std. Z39.18

## INSTRUCTIONS FOR COMPLETING SF 298

**1. REPORT DATE.** Full publication date, including day, month, if available. Must cite at least the year and be Year 2000 compliant, e.g. 30-06-1998; xx-06-1998; xx-xx-1998.

**2. REPORT TYPE.** State the type of report, such as final, technical, interim, memorandum, master's thesis, progress, quarterly, research, special, group study, etc.

**3. DATES COVERED.** Indicate the time during which the work was performed and the report was written, e.g., Jun 1997 - Jun 1998; 1-10 Jun 1996; May - Nov 1998; Nov 1998.

**4. TITLE.** Enter title and subtitle with volume number and part number, if applicable. On classified documents, enter the title classification in parentheses.

**5a. CONTRACT NUMBER.** Enter all contract numbers as they appear in the report, e.g. F33615-86-C-5169.

**5b. GRANT NUMBER.** Enter all grant numbers as they appear in the report, e.g. AFOSR-82-1234.

**5c. PROGRAM ELEMENT NUMBER.** Enter all program element numbers as they appear in the report, e.g. 61101A.

**5d. PROJECT NUMBER.** Enter all project numbers as they appear in the report, e.g. 1F665702D1257; ILIR.

**5e. TASK NUMBER.** Enter all task numbers as they appear in the report, e.g. 05; RF0330201; T4112.

**5f. WORK UNIT NUMBER.** Enter all work unit numbers as they appear in the report, e.g. 001; AFAPL30480105.

**6. AUTHOR(S).** Enter name(s) of person(s) responsible for writing the report, performing the research, or credited with the content of the report. The form of entry is the last name, first name, middle initial, and additional qualifiers separated by commas, e.g. Smith, Richard, J, Jr.

**7. PERFORMING ORGANIZATION NAME(S) AND ADDRESS(ES).** Self-explanatory.

**8. PERFORMING ORGANIZATION REPORT NUMBER.** Enter all unique alphanumeric report numbers assigned by the performing organization, e.g. BRL-1234; AFWL-TR-85-4017-Vol-21-PT-2.

**9. SPONSORING/MONITORING AGENCY NAME(S) AND ADDRESS(ES).** Enter the name and address of the organization(s) financially responsible for and monitoring the work.

**10. SPONSOR/MONITOR'S ACRONYM(S).** Enter, if available, e.g. BRL, ARDEC, NADC.

**11. SPONSOR/MONITOR'S REPORT NUMBER(S).** Enter report number as assigned by the sponsoring/ monitoring agency, if available, e.g. BRL-TR-829; -215.

**12. DISTRIBUTION/AVAILABILITY STATEMENT.** Use agency-mandated availability statements to indicate the public availability or distribution limitations of the report. If additional limitations/ restrictions or special markings are indicated, follow agency authorization procedures, e.g. RD/FRD, PROPIN, ITAR, etc. Include copyright information.

**13. SUPPLEMENTARY NOTES.** Enter information not included elsewhere such as: prepared in cooperation with; translation of; report supersedes; old edition number, etc.

**14. ABSTRACT.** A brief (approximately 200 words) factual summary of the most significant information.

**15. SUBJECT TERMS.** Key words or phrases identifying major concepts in the report.

**16. SECURITY CLASSIFICATION.** Enter security classification in accordance with security classification regulations, e.g. U, C, S, etc. If this form contains classified information, stamp classification level on the top and bottom of this page.

**17. LIMITATION OF ABSTRACT.** This block must be completed to assign a distribution limitation to the abstract. Enter UU (Unclassified Unlimited) or SAR (Same as Report). An entry in this block is necessary if the abstract is to be limited.

## TABLE OF CONTENTS

## FIGURES

## TABLES

**APPENDICES**

# ACRONYMS

| | |
|---|---|
| CM | Corrective Measure |
| CMT | (Solinst) Continuous Multichannel Tubing |
| DCE | Dichloroethene |
| DNAPL | Dense Non-Aqueous Phase Liquid |
| DOD | U.S. Department of Defense |
| DQO | Data Quality Objective |
| EDS | Energy Dispersive Spectroscopy |
| EI | Environmental Indicator |
| EPA | Environmental Protection Agency |
| FLUTe | Flexible Liner Underground Technologies (multi-level system) |
| IRP | Installation Restoration Program |
| ISCO | In Situ Chemical Oxidation |
| LAM | Laser Ablation Microprobe |
| MCL | Maximum Contaminant Level |
| MLS | Multi-Level Monitoring System |
| MMA | Main Manufacturing Area |
| NMR | Nuclear Magnetic Resonance |
| NYSDEC | New York State Department of Environmental Conservation |
| PCE | Tetrachloroethene |
| PPE | Personal Protective Equipment |
| RCRA | Resource Conservation and Recovery Act |
| RFI | RCRA Facility Investigation |
| ROD | Rock Oxidant Demand |
| SEM | Scanning Electron Microscopy |
| TCE | Trichloroethene |
| UNB | University of New Brunswick |
| USACE | United States Army Corps of Engineers |
| USATAAC | U.S. Army Tank Automotive and Armaments Command |
| UW | University of Waterloo |
| VC | Vinyl Chloride |
| VOC | Volatile Organic Compound |
| WVA | Watervliet Arsenal |
| ZIST | (BESST) Zone Isolation Sampling Technology |

## Acknowledgements

Malcolm Pirnie, Inc. personnel prepared this report with the assistance of researchers from the University of Waterloo (Dr. Beth Parker, Dr. John Cherry, Steven Chapman, Maria Gorecka, Dr. Ramon Aravena) and the University of New Brunswick (Dr. Tom Al). The ESTCP demonstration was performed concurrently with an Interim Corrective Measure managed by the United States Army Corps of Engineers (Mr. Steven Wood and Mr. Grant Anderson). The United States Geological Survey (Mr. John Williams and Mr. Frederick Paillet) performed early geophysical testing that was integral to the project. The New York State Department of Environmental Conservation (Mr. Larry Rosenmann) facilitated integration of the demonstration into the WVA RCRA Corrective Action Program.

The authors are grateful to Ms. JoAnn Kellogg of the Watervliet Arsenal for her time and assistance in coordinating the multiple field efforts required for the demonstration.

# Executive Summary

This Demonstration Report provides an evaluation of innovative diagnostic tools used first for site characterization to support remediation design, and second to evaluate the performance of in situ chemical oxidation (ISCO) using permanganate at the Watervliet Arsenal (WVA). An area of groundwater contamination was discovered in 1998 in the eastern portion of the WVA, adjacent to the site boundary and in front of former manufacturing Building 40. Groundwater contaminants include chlorinated volatile organic compounds (CVOCs), predominantly tetrachloroethene (PCE) and cis-1,2-dichloroethene (DCE), with a lesser percentage of trichloroethene (TCE) and vinyl chloride. PCE has been detected at aqueous concentrations as high as 170 mg/L, suggesting the presence of dense non-aqueous phase liquid (DNAPL). VOCs are present in the bedrock groundwater from 20 feet to more than 150 feet below ground surface.

The overall objectives of the demonstration project were to:

- Characterize and delineate the VOC contamination in a fractured rock setting using innovative diagnostic tools.
- Use innovative diagnostic tools to evaluate the effectiveness of ISCO with permanganate in a fractured rock setting.
- Compare these innovative methods with conventional diagnostic tools that are currently used for fractured rock site characterization and for assessing ISCO performance.

The ESTCP demonstration was conducted simultaneously with a corrective measure (CM) for Building 40 at the WVA. The scopes of the CM and demonstration project included working with Drs. Beth Parker and John Cherry of the University of Waterloo and the United States Army Corps of Engineers to apply innovative diagnostic tools to characterize the site for remediation technology selection, design and performance assessment. The selected remediation technology, ISCO with permanganate, was applied as the CM at the WVA fractured rock site. A detailed description of the CM and the technical design are included in Section 3. **It is important to note that the objective of this demonstration was not to achieve site remediation; rather, it was to evaluate the diagnostic tools used to characterize the site and to monitor treatment performance.**

Table ES-1 provides an overview of each of the diagnostic tools. Several of the diagnostic tools used for this demonstration are specific to the selected remedial technology (i.e., ISCO using permanganate) and the site geology (fractured shale).

**Table ES-1-1: Overview of Innovative Diagnostic Tools**

| Diagnostic Tool | Data Obtained |
|---|---|
| 3-Dimensional Sampling using Multi-Level | ■ Fracture network characterization<br>■ Contaminant concentrations at various depth intervals |

| Diagnostic Tool | Data Obtained |
|---|---|
| Monitoring Systems | ■ Hydraulic information at various depth intervals<br>■ Permanganate solution delivery (not a feature of all systems)<br>■ Permanganate distribution and persistence monitoring (not a feature of all systems) |
| Rock Matrix Analysis | ■ Contaminant mass and phase distribution<br>■ Fracture network characterization including identification of contaminant migration pathways<br>■ Rock matrix physical property measurements (porosity, organic carbon content, diffusion coefficients, permeability, mineralogy, other lab tests)<br>■ Comparison of rock core analyses to aqueous phase samples from multi-level wells to understand relationship between matrix and fracture water contamination<br>■ Visual evidence of permanganate invasion into the rock matrix |
| Isotopic Analysis | ■ Carbon isotope ratios of PCE, TCE and DCE to confirm contaminant oxidation versus displacement<br>■ Charting of fracture pathways (permanganate-influenced groundwater may reach a sampling location prior to arrival of permanganate) |
| Mass Flux | ■ Mass discharge via two different methods not standard in fractured rock application:<br>1. Integrated mass flux test (12-hour constant rate pumping test)<br>2. Mass flux measurements along a transect at the site boundary at various times throughout the duration of the demonstration via groundwater flux estimates using Darcy's Law and VOC concentrations from nested monitoring wells |
| Laboratory Rock Oxidant Demand Tests and Permanganate Invasion Tests | ■ Laboratory testing of rock oxidant demand via batch tests to measure natural / mineral oxidant demand<br>■ Permanganate invasion rate tests to measure reactive diffusive transport of permanganate on intact core samples via specialized techniques |
| Numerical Modeling | ■ Projection of mass reduction and groundwater quality beyond the demonstration period using one and two-dimensional discrete fracture models<br>■ Not utilized beyond initial simulations, given the nature of the complex physical and chemical reactions, such as the precipitation of manganese and trace metals upon reaction with VOCs and aquifer minerals, the concentration dependence of permanganate density, influence of microfractures on back-diffusion of VOCs and the sensitivity of rock oxidant demand to permanganate solution concentration |

Various multi-level monitoring diagnostic systems were installed at WVA during various phases of site characterization, each having unique characteristics. Given that there are so many ways in which multi-level monitoring systems (MLSs) and nested well systems differ from one another, and that individual sites will have different monitoring objectives, geology/hydrogeology, and regulatory requirements, the task of selecting the MLS or nested system most appropriate for the particular sites needs is challenging. In Section 4, the features of each of the four types of MLSs, as well as the ZIST nested well system, are briefly described in the general context of contaminant hydrogeology and then the specific relevance and experiences gained through their use at WVA are indicated. The uses and performance of the MLSs and ZIST at WVA are most unique in the context of the permanganate injections in the pilot tests and the full scale permanganate remediation. To date, no previous reporting on uses of MLSs or ZIST for injections or monitoring involving permanganate exists.

At the WVA, conventional borehole geophysical characterization methods supported the initial conceptualization that the majority of the groundwater flow in the Building 40 treatment area was confined to three primary fracture zones, designated “Upper”, “Middle”, and “Lower” (see Figure 1-3). This conceptual model was consistent with results of conventional borehole fluid resistivity, temperature logging, and flow metering at other sites that typically indicated only two or three active fractures in each hole (Sterling et al., 2005; Pehme et al., 2007). These data also indicated that the greatest contributions to the baseline compliance boundary VOC mass discharge were from the compliance monitoring zones that intersect the upper flow zone fracture system. However, this conceptualization was not supported by the assessment of site conditions using closely spaced sampling of continuous rock core at WVA (i.e., rock crushing diagnostic tool). Rock crushing results support the conclusion that the there were numerous pathways for contaminant migration, which was consistent with visual observations of fracture occurrence in the cores. The WVA rock core VOC results support the conceptual model for fractured sedimentary rock in which the DNAPL initially occupied many, mostly small to intermediate aperture fractures, and then dissolved, allowing the mass to be transferred by diffusion into the nearby matrix. In this conceptual model, the plume forms in a network of many interconnected fractures of variable aperture and length without dominance over long distances by any large-aperture fractures (see Parker, 2007 provided in Appendix G). The rock crushing diagnostic tool was key to developing the site conceptual model.

Compound-specific carbon isotopes are becoming useful tools for assessing natural and induced degradation of chlorinated ethenes (Hunkeler et al., 1999). Laboratory studies have shown that strong carbon isotope fractionation occurs during chemical oxidation of chlorinated compounds by potassium permanganate (e.g., Hunkeler et al., 2003) which makes isotopic analyses a potentially powerful diagnostic tool for monitoring ISCO, since they can be used to verify that concentration declines in target compounds are due to degradation instead of physical (e.g., displacement) processes. The isotope data provided information about the competing processes of permanganate oxidation and VOC rebound (due to back-diffusion or advection), which control VOC concentration during and after a permanganate treatment. The isotope data showed that the rebound effect is dominant at the WVA site due to the large amount of VOC present in the shale rocks.

The mass that the source zone is contributing to the larger dissolved phase plume is an important attribute to determine, from both risk assessment and treatment performance perspectives. The source strength, or mass discharge, is defined as the rate at which contaminants pass through a defined cross-sectional area perpendicular to groundwater flow. Given the difficulty in locating and removing contaminant mass at the WVA, mass-based metrics were used to formulate an exit strategy, using mass discharge across the property boundary, where the multi-level wells are located, to monitor treatment progress. At the WVA, two techniques were used to estimate mass flux, and, subsequently, mass discharge: an integrated pump test and multi-level sampling and testing along the property boundary. The estimates of mass discharge determined from the integrated pump test were approximately one order of magnitude greater than those from the boundary transect method, and are believed to be overestimates of the contaminant mass discharge in the treatment area. The overestimation was likely due to the changes in hydraulic gradient inherent in this method versus the more passive boundary transect method, which is conducted under ambient gradient conditions. Since fractured bedrock systems have essentially no storage, the introduction of an artificial hydraulic gradient through pumping will cause a change in the natural flow regime in the area of the pumping, and, more importantly, may draw water from fractures that do not normally contribute to the boundary mass flux due to their location, size, and degree of connection. These “back-door” or “dead-end” fractures likely contain the highest VOC concentrations since they transmit little to no flow and are in equilibrium with the near-solubility pore water concentrations in the rock matrix. These data suggest that, in the case of fractured bedrock, use of the transect method of mass flux calculation may be preferable to the integrated test.

Two types of laboratory studies were conducted to support design of the ISCO remedy: (1) rock oxidant demand (ROD) studies using $KMnO_4$ and $NaMnO_4$ and (2) tests to examine permanganate diffusion and reaction into the shale matrix in a static system. The ROD values measured from the $NaMnO_4$ tests were a factor of two or three higher than those measured in the $KMnO_4$ tests. There appeared to be a concentration dependence on ROD – the higher the permanganate concentration, the higher the ROD exerted by the shale. Results of sulfate analyses indicated that pyrite oxidation accounted for about 30% to 75% of the 21-day ROD values observed. The higher the permanganate concentration, the lower the percentage of ROD accounted for by pyrite. The fraction organic carbon analyses indicated some contribution to the ROD from organic carbon oxidation, particularly for higher permanganate concentrations.

The permanganate invasion testing showed that after 24 months, $MnO_4^-$ had penetrated the shale matrix to a distance of approximately 120 to 150 µm. The short distance of penetration is attributable to the rapid reduction of $MnO_4^-$ by reaction with minerals and organic carbon in the shale, which results in precipitation of the Mn-oxide reaction product. The laboratory studies showed the shale at the WVA has a porosity of 0.7% to 3.1%, which is relatively low for shale but still appreciable enough to result in mass transfer of contaminants into the matrix.

# 1.0 Introduction

This Demonstration Report provides an evaluation of innovative diagnostic tools used first for site characterization to support remediation design, and second to evaluate the performance of in situ chemical oxidation (ISCO) using permanganate at the Watervliet Arsenal (WVA). The WVA is a 140-acre government-owned installation located in the City of Watervliet, New York, which is on the western bank of the Hudson River and five miles north of the City of Albany. During a Resource Conservation and Recovery Act (RCRA) Facility Investigation (RFI), an area of groundwater contamination was discovered in 1998 in the eastern portion of the WVA, adjacent to the site boundary and in front of former manufacturing Building 40 (see Figure 1-1). Groundwater contaminants include chlorinated volatile organic compounds (CVOCs), predominantly tetrachloroethene (PCE) and cis-1,2-dichloroethene (DCE), with a lesser percentage of trichloroethene (TCE) and vinyl chloride. PCE has been detected at aqueous concentrations as high as 170 mg/L, suggesting the presence of dense non-aqueous phase liquid (DNAPL). VOCs are present in the bedrock groundwater from 20 feet to more than 150 feet below ground surface. The original source of the chlorinated VOCs is unknown; however, based on the manufacturing history of the Arsenal, it is estimated that the release occurred more than 30 years ago. The affected portion of the bedrock aquifer is not used as a source of potable water.

**Figure 1-1: Building 40, Watervliet Arsenal**


Although the ESTCP project for which this report has been prepared took place during the period of 2004 to 2007, the project was based on experience using diagnostic tools and data

obtained over a much longer time period. During this period, six study phases occurred, which are outlined here to provide the context for this report.

1. **RCRA Facility Investigation [1998-1999]**: On behalf of the WVA, Malcolm Pirnie, Inc. (Malcolm Pirnie) conducted a RCRA Facility Investigation (RFI) at the Main Manufacturing Area (MMA) of the WVA. The RFI was conducted under contract with the U.S. Army Corps of Engineers (USACE), Baltimore District in accordance with an Administrative Order on Consent between the WVA, the New York State Department of Environmental Conservation (NYSDEC), and the United States Environmental Protection Agency (USEPA). Five wells were installed in the vicinity of Building 40 during the RFI, including a well screened in the overburden (MW-33) and four wells screened in the bedrock (MW-34, MW-51, MW-59, and MW-61; see Figure 1-2).
2. **USGS Borehole Geophysics (2000-2001)**: A group from the United States Geological Survey (USGS) specializing in borehole geophysics and borehole flow metering performed borehole geophysical logging and borehole flow metering including flow meter pulse tests. This work, which was performed at four monitoring wells (34, 51, 58, 59) and four coreholes (65, 68, 71, 72) resulted in a conceptual model for the fracture network (Williams and Paillet, 2002a, 2002b).
3. **Initial Rock Core Study (late 2001):** A team from the University of Waterloo (UW) [Waterloo, Ontario, Canada] led by Dr. Beth Parker in collaboration with Malcolm Pirnie applied the Parker method of rock core VOC analysis to two cored holes (74 and 75) for the purpose of determining the VOC distribution in the rock matrix. This study showed that nearly all of the VOC mass resides in the rock matrix and resulted in development of a new site conceptual model and the selection of chemical oxidation using permanganate for remediation.
4. **Pilot-scale permanganate trial (2002-2003):** Malcolm Pirnie teamed with the Parker group at UW to conduct a pilot scale trial using potassium permanganate. The pilot study involved conventional injections using wells and innovative depth-discrete injections and monitoring during March 5-11, 2002 in well MW-59 and April 1 in wells MW-71 and MW-65. The results of the pilot study are documented in a published report (Goldstein et al., 2004).
5. **Full-Scale Interim Corrective Measure (2004-2007):** Malcolm Pirnie in collaboration with the Parker team and Dr. Tom Al of the University of New Brunswick (UNB) initiated a Corrective Measure (CM) in September 2004 using sodium permanganate injections. Sodium permanganate injections continued until September 2006. The frequency and duration of permanganate injections are listed in Table 1-1. The injections were halted because permanganate delivery, distribution, and residence time metrics had not been met, and improvements to the injection system did not result in better performance. A Supplemental Corrective Measures Study is currently being performed.
6. **ESTCP Demonstration (2003 – 2007):** This demonstration was initiated in 2003 and was conducted simultaneously with the full-scale permanganate CM. Although the ESTCP project for which this report has been prepared took place during the period of 2003 to 2007, data collected prior to 2003 (e.g., rock matrix analyses) were compared to data collected during the project time period for evaluation of some diagnostic tools.

**Figure 1-2: Locations of Multi-Level Diagnostic Tools**

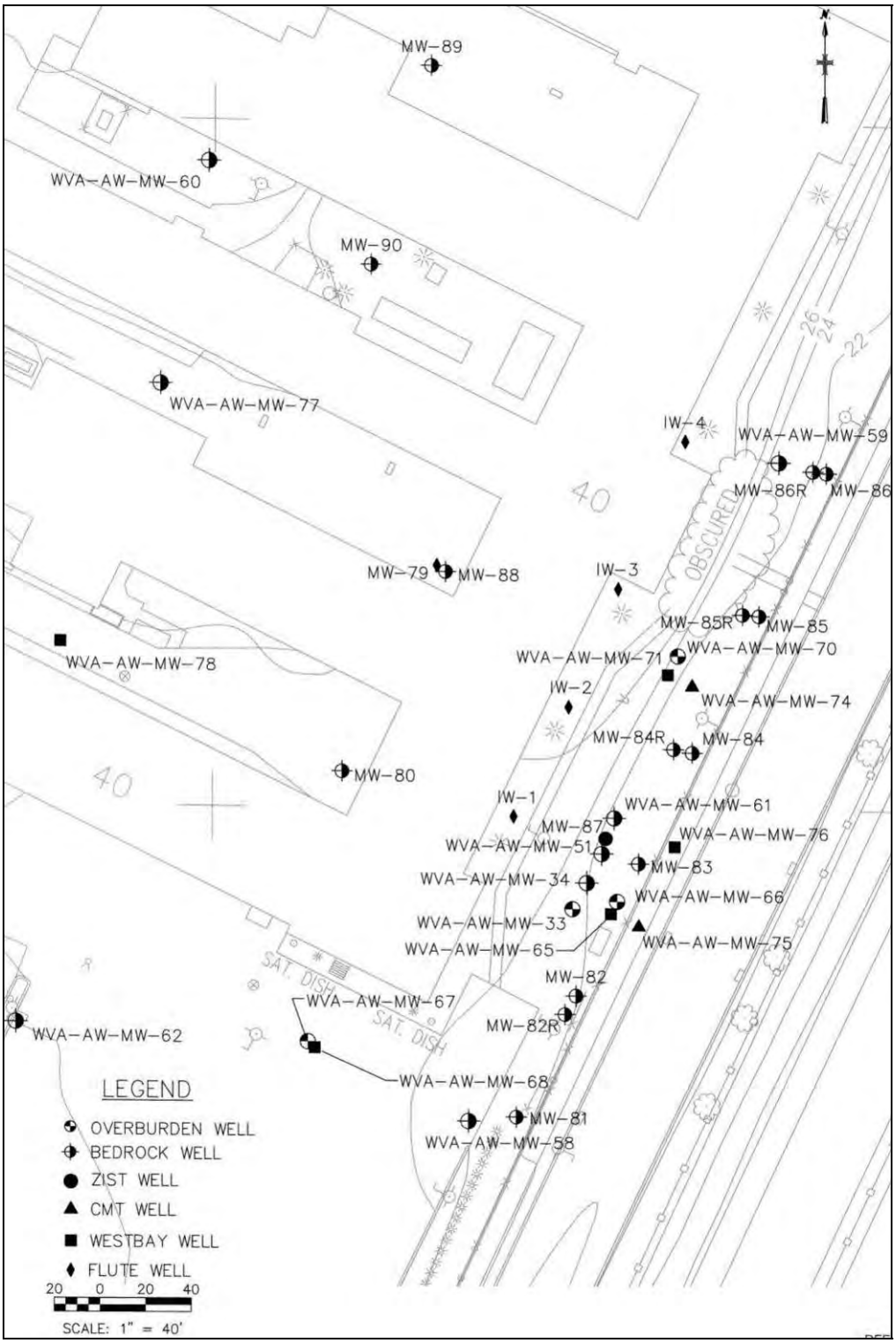

**Table 1-1: Permanganate Injections during the Full-Scale Interim Corrective Measure at the WVA**

| Injection Number | Date | Injection Location | Approximate $NaMnO_4$ Solution Concentration | Amount Solution Injected (gallons) | Amount 40% $NaMnO_4$ Injected (gallons) | Monitored Locations Where Permanganate Observed |
|---|---|---|---|---|---|---|
| 1 | 9/30/05-10/1/05 | MW-90 | 10% | 2,250 | 550 | Not observed |
| 2 | 1/31/05 - 2/11/05 | MW-90 | 10% | 4,500 | 1,100 | Not observed |
| 3 | 5/3/05 - 5/5/05 | MW-79 (lower) | 5% | 4,500 | 550 | IW-1, IW-2, IW-3 |
| 3a | 7/6/05 - 7/7/05 | MW-79 (upper) | 5% | 2,250 | 275 | MW-80 |
| 4 | 8/15/05 - 8/17/05 | MW-79 | 4% | 1,100 | | MW-80, 82R-3,83-1,83-3 |
| | | IW-1 | 4% | 1,100 | | 85R-2, 86R-2 |
| | | IW-2 | 4% | 1,100 | | |
| | | IW-3 | 4% | 1,100 | | |
| | | IW-4 | 4% | 1,100 | | |
| | | *Event Total* | | *5,500* | *550* | |
| 5 | 11/29/05 - 12/1/05 | MW-79 | 5% | 900 | | MW-80, 82R-3,83-1,83-3 |
| | | IW-1 | 5% | 895 | | 84R-1,85R-2, 85R-3, 86R-2 |
| | | IW-2 | 5% | 1,080 | | |
| | | IW-3 | 5% | 655 | | |
| | | IW-4 | 5% | 900 | | |
| | | *Event Total* | | *4,430* | *550* | |
| 6 | 4/3-06 - 4/7/06 | MW-79 | 5% | 900 | | MW-80, 81-2, 82R-2,83-3 |
| | | IW-1 | 5% | 1,730 | | 85R-2, 86R-2 |
| | | IW-2 | 5% | 930 | | |
| | | IW-3 | 5% | 70 | | |
| | | IW-4 | 5% | 970 | | |
| | | *Event Total* | | *4,600* | *550* | |
| 7 | 9/25/06 - 9/29/06 | MW-79 | 5% | 2,250 | | MW-80, 83-3 |
| | | IW-1 | 5% | 395 | | 85R-2, 86R-2 |
| | | IW-2 | 5% | 753 | | |
| | | IW-3 | 5% | 20 | | |
| | | IW-4 | 5% | 1,245 | | |
| | | *Event Total* | | *4,663* | *550* | |
| | | | **Totals to Date** | **32,693** | **4,125** | |

## 1.1 Background

Chlorinated solvents are the most common contaminants at U.S. Department of Defense (DOD) sites due to their widespread use for various industrial and commercial processes including metal degreasing and dry cleaning, and products, such as dyes, paints and adhesives. They are released into the subsurface as either aqueous-phase or non-aqueous phase liquids. When released in the non-aqueous phase, chlorinated solvents are referred to as "dense non-aqueous-phase liquids" (DNAPLs) since their density is greater than that of water. When released at the surface, DNAPLs move downward under the force of gravity and tend to follow preferential pathways such as fractures in soil or rock.

The previous understanding of a NAPL release in a fractured rock environment was that once the NAPL was released it would pool in rock fractures. As water flowed through NAPL-inhabited rock fractures, the more soluble constituents would partition into the water to generate a plume of dissolved contamination. This plume would expand to down-gradient areas from the NAPL-affected area, and the NAPL would continue to reside in the fractures until sufficient dissolution occurred for all of the NAPL to partition to the aqueous phase.

Recent advances in diagnostic tools have modified this conceptualization of fractured rock sites (especially sedimentary rock sites) contaminated with DNAPL. Although fractures

provide the only pathway for advective transport of groundwater and chlorinated solvents, often the ratio of the void space due to the presence of fractures to the bulk rock volume ("fracture porosity") is several orders of magnitude less than the matrix porosity of the rock itself. This means that the capacity of the rock matrix to store chlorinated solvent mass is orders of magnitude greater than the storage capacity in the fractures. This matrix storage capacity creates a diffusive gradient by which CVOCs present at high concentrations in the fractures can diffuse into the bedrock pore spaces. Thus, although DNAPL may still exist in some fractures, over time, the majority of the DNAPL that was initially present in the fractures will dissipate due to dissolution and diffusive mass transfer (Parker et al., 1994, 1997). This will cause most of the CVOC mass to reside in the rock matrix and not in the bedrock fractures. In this case, the "rock matrix" is defined as the intergranular porosity of the rock *and* micro-fractures that generally do not contribute to advective groundwater flow, but which behave in a similar manner as the intergranular porosity in terms of the potential for VOC mass storage. This site conceptualization has been verified at the WVA using a diagnostic tool allowing for the measurement of CVOC mass in rock matrix pore water. This technique involves the collection of small rock core samples over many depths of rock core, followed by crushing and methanol extraction.

The understanding that most of the CVOC mass resides in the rock matrix implies that effective remediation technologies for this class of sites will be those that will address the CVOC mass in the rock matrix in addition to treating the CVOC mass in the fractures that contribute to advective groundwater flow. Failure to treat the CVOC mass in the matrix (i.e., the source area) will result in a continuous diffusive transfer of mass out of the matrix to the groundwater.

In situ chemical oxidation (ISCO) via permanganate ($MnO_4$) was selected as the remedy for the fractured rock at the WVA. Unreacted $MnO_4$ in solution is chemically stable, allowing it to diffuse into low permeability media over time. Application of excess $MnO_4$ is expected to allow for diffusion of $MnO_4$ into the matrix at the same time as contamination is diffusing out of the matrix (i.e., the reactants will be moving towards each other) speeding the treatment of CVOC mass in the rock matrix.

To adequately characterize the site and to assess remedial success, various diagnostic tools were employed. Several types of depth-discrete multi-level monitoring systems were utilized to monitor the extent of treatment in the fracture network. Isotopic fractionation was used to verify VOC mass destruction by permanganate, as well as the extent of the injection displacement zone. Rock core analyses were used to characterize the VOC mass present in the rock matrix. Mass discharge measurements at the down-gradient treatment boundary were utilized to demonstrate the change in the rate of contaminant mass release from the treated zone. Laboratory studies were performed to enhance understanding of field observations, including rock oxidant demand tests and permanganate invasion rate tests.

## 1.2 Objectives of the ESTCP Demonstration Project

The overall objectives of the demonstration project were to:

- Characterize and delineate the VOC contamination in a fractured rock setting using innovative diagnostic tools.

- Use innovative diagnostic tools to evaluate the effectiveness of ISCO with permanganate in a fractured rock setting.

- Compare these innovative methods with conventional diagnostic tools that are currently used for fractured rock site characterization and for assessing ISCO performance.

As discussed above, the ESTCP demonstration was conducted simultaneously with a CM for Building 40 at the WVA. The scopes of the CM and demonstration project included working with Drs. Beth Parker and John Cherry of UW and the USACE to apply innovative diagnostic tools to characterize the site for remediation technology selection, design and performance assessment. The selected remediation technology, ISCO with permanganate, was applied as the CM at the WVA fractured rock site. A detailed description of the CM and the technical design are included in Section 3. **It is important to note that the objective of this demonstration was not to achieve site remediation; rather, it was to evaluate the diagnostic tools used to characterize the site and to monitor treatment performance.**

In a separate report, the results of this work will be evaluated in the context of two other sites, Fort Lewis, Washington and Vandenberg Air Force Base, California, where similar demonstrations in porous media (the WVA is the only fractured rock site) with different remediation systems were performed, using some of the same diagnostic tools being used at the WVA. The work at all three sites was conducted under ESTCP Project CU-0318.

## 1.3 Test Site Description

The WVA is a 140-acre government-owned installation under the command of the U.S. Army Tank Automotive and Armaments Command (USATAAC) located in the City of Watervliet, New York, which is west of the Hudson River, and five miles north of the City of Albany. The WVA currently manufactures large caliber cannons. Benet Labs, currently located within Building 40 of the WVA, conducts on-site research and development, prototyping and testing, and full-scale manufacturing of defense-related materials.

The WVA consists of two primary areas: the Main Manufacturing Area (MMA), encompassing approximately 125 acres, where manufacturing and administrative operations occur, and the Siberia Area, primarily used for the storage of raw and hazardous materials, finished goods, and supplies brought from the MMA. Building 40 is located in eastern portion of the MMA, adjacent to the eastern WVA property boundary. Broadway Street (New York State Route 32) and a six-lane interstate highway (Interstate 787) are located between Building 40 and the Hudson River.

### 1.3.1 *Test Site Geology*

The major overburden unit identified in the MMA is fill, consisting of brown or dark gray silty sand with angular gravel. The fill material is the only unit consistently found throughout the site. The fill is thickest in the eastern portion of the MMA. Native overburden materials, consisting of fine-grained alluvium, a coarser alluvium, and glacial till are present beneath the fill layer in various thicknesses throughout the MMA. However, these materials are not present in all areas of the MMA. The bedrock underlying the site is black, medium-hard laminated shale, showing some characteristics of minor metamorphism. This shale has been identified as part of the Snake Hill Formation. Both high-angle fractures (i.e., across bedding planes) and low-angle fractures (i.e., along bedding planes) are present throughout the bedrock. Veins of calcite and pyrite are commonly present along fracture and bedding planes. Competent bedrock is encountered in the Building 40 area at depths ranging from 15 to 20 feet below ground surface (bgs).

### 1.3.2 *Test Site Hydrogeology*

Groundwater flow in the MMA is primarily controlled by the degree of fracturing and degree of fracture hydraulic connectivity within the bedrock aquifer. Based on groundwater elevations measured during the RFI and subsequent studies, the direction of groundwater flow in the Building 40 area is to the east-southeast towards the Hudson River. Extensive hydrogeologic characterization studies were performed in the bedrock aquifer in the Building 40 area during the RFI and CMS Data Gap Study (1998 – 2001). These studies included discrete zone packer testing, down-hole geophysical profiling, video and acoustic televiewer profiling, and intra- and cross-borehole flow testing. The results of these studies are detailed in the United States Geological Survey (USGS) Open-File Report entitled Characterization of Fractures and Flow Zones in a Contaminated Shale at the Watervliet Arsenal, Albany County, New York: USGS Open File Report 01-385 (Williams and Paillet, 2002a, Appendix E). Based on the results of the hydrogeologic studies, groundwater in the bedrock aquifer in the Building 40 area flows along discrete, generally interconnected fracture pathways. The results of the USGS cross-borehole flow testing indicated that a highly transmissive fracture or series of fractures connects several of the wells in the Building 40 area. However, the USGS testing also demonstrated that other, less direct connections also exist between the monitoring wells installed in the Building 40 Area.

In conjunction with the field elements of the Pilot Study, representative rock core samples collected from monitoring wells drilled during the CMS Data Gap Study were sent to Golder Associates Ltd. of Mississauga, Ontario, Canada for analysis of physical and hydrogeologic parameters. Matrix diffusion tests were also performed on the rock cores to evaluate the rock matrix diffusion coefficient for the bedrock in the Building 40 area. The results of the rock core testing are summarized in Table 1-2. As shown in Table 1-2, the average hydraulic conductivity of the shale bedrock matrix is approximately $3x10^{-6}$ feet per day (ft/d) indicating that, as expected, advective groundwater transport in the bedrock is entirely controlled by fractures. The average porosity of the shale is approximately 2.3 percent, as compared to a typical range of five percent to 25 percent for sedimentary rocks (shale and sandstone). This low

porosity is likely a result of the low-grade metamorphism to which the rock has been exposed. The average chloride matrix diffusion coefficient (D) of the shale was $7.5x10^{-7}$ $cm^2$ per second.

**Table 1-2: Matrix Diffusion Testing Results**

| Core Sample No. | Sample Depth (feet) | Saturated Water Content (%) | Dry Density ($mg/m^3$) | Total Porosity (%) | Specific Gravity | Total Organic Carbon (%) | Hydraulic Conductivity (cm/s) | Hydraulic Conductivity (ft/d) | Chloride Matrix Diffusion Coeff., D@23 C ($cm^2/s$) | Matrix Tortuosity Factor, t |
|---|---|---|---|---|---|---|---|---|---|---|
| **MW-64** | 133.7 - 135 | 1.42 | 2.68 | 2.4 | 2.75 | 0.26 | 3.3E-09 | 9.4E-06 | 6.4E-07 | 0.042 |
| **MW-65** | 40 - 45 | 1.47 | 2.66 | 1.9 | 2.72 | 0.29 | 6.3E-10 | 1.8E-06 | 7.1E-07 | 0.047 |
| **MW-68** | 65 - 70 | 1.26 | 2.65 | 1.9 | 2.71 | 0.28 | 1.0E-10 | 2.8E-07 | 1.1E-06 | 0.071 |
| **MW-71** | 70.7 - 75.7 | 1.49 | 2.66 | 3.1 | 2.75 | 0.27 | 1.8E-09 | 5.1E-06 | 4.8E-07 | 0.032 |
| **MW-72** | 39.5 - 40.5 | 1.21 | 2.65 | 2.4 | 2.72 | 0.29 | 3.6E-11 | 1.0E-07 | 8.4E-07 | 0.056 |

**Table 1-3: Estimated Hydraulic Properties of Fracture-Flow Zones Detected in theMonitoring Wells and Coreholes at the WVA (Williams and Paillet, 2002a)**

| No. | Zone Depth (ft) | Zone Head (ft) | Transmissivity $ft^2$/day | | Storage | Hydraulic Connection | |
|---|---|---|---|---|---|---|---|
| | | | Single Borehole | Cross-hole | | Well No. | Zone Depth (ft) |
| 34 | 25 | 8.98 | 260 | 150 | 5.0E-05 | 71 | 65 |
| 34 | 25 | 8.98 | 260 | 100 | 5.0E-05 | 65 | 24 and 35 |
| 51 | - | 8.97 | - | - | - | - | - |
| 58 | 76 | 9.6 | 0.1 | - | - | - | - |
| 59 | 92 | 9.16 | 230 | 230 | 5.0E-05 | 71 | 65 |
| 59 | 92 | 9.16 | 230 | 230 | 1.0E-05 | 65 | 24 and 35 |
| 65 | 24<br>35 | 8.94 | 65<br>47 | 100 | 5.0E-05 | 34 | 25 |
| 65 | 24<br>35 | 8.94 | 65<br>47 | 100 | 1.0E-05 | 59 | 92 |
| 65 | 24<br>35 | 8.94 | 65<br>47 | 100 | 1.0E-05 | 71 | 65 |
| 65 | 78<br>88<br>110 | 9.1 | 37<br>3<br>3 | 80 | 1.0E-04 | 71 | 65 |
| 68 | 19 | 12.04 | 58 | - | - | - | - |
| 68 | 45 | 12.79 | 110 | - | - | - | - |
| 71 | 28 | 8.92 | 40 | - | - | - | - |
| 71 | 65 | 9.02 | 230 | 230 | 5.0E-06 | 59 | 92 |
| 71 | 65 | 9.02 | 230 | 150 | 5.0E-06 | 34 | 25 |
| 71 | 65 | 9.02 | 230 | 100 | 1.0E-05 | 65 | 24 and 35 |
| 71 | 65 | 9.02 | 230 | 80 | 1.0E-04 | 65 | 78,88, and 110 |
| 72 | 49 | 6.5 | 7 | - | - | - | - |
| 72 | 75 | 6.5 | 59 | - | - | - | - |

### 1.3.3 *Site Conceptual Model*

The conceptual model for the bedrock groundwater in the Building 40 area is summarized below. In addition, a draft manuscript describing the conceptual model for the fracture network is included in Appendix H to this report.

CVOCs are present in the bedrock aquifer in the Building 40 area. DNAPL, and dissolved-phase CVOC concentrations indicating the potential presence of DNAPL, have been detected in the bedrock groundwater. Advective transport of CVOCs in the bedrock aquifer takes place through a well-connected fracture network that extends to a depth of at least 150 to 200 feet bgs. This depth has been confirmed by both fracture groundwater and rock matrix CVOC analysis. Based on field observations, groundwater below approximately 150 feet is also affected by the presence of naturally-occurring hydrogen sulfide and methane gas. The original source of the CVOCs in the bedrock groundwater is presumed to be located in the northeastern portion of the building. Since significant CVOC concentrations were not detected in the overburden soil in this area, it is possible that the release occurred through a subsurface storm sewer that was once connected to floor drains in the source area of Building 40.

Parker et al. (1994; 1997) proposed a new conceptual model for chlorinated solvent DNAPL source zones, supported by analytical models for DNAPL behavior in water-saturated fractured porous media such as clay and sedimentary rock. In this model, the immobile DNAPL film in the fracture dissolves into the contiguous water film in the fracture, establishing an aqueous concentration gradient driving mass into the porous matrix by diffusion. In this case, the "rock matrix" is defined as the intergranular porosity of the rock *and* micro-fractures that generally do not contribute to advective groundwater flow, but which behave in a similar manner as the intergranular porosity in terms of the potential for VOC mass storage. This mass transfer can cause complete dissolution of the DNAPL phase after some period of time that depends on the thickness of the DNAPL film (i.e., fracture aperture and initial fracture DNAPL saturation) and the diffusion driven mass transfer rate into the matrix; however, this time is short relative to the time elapsed since contamination of some sites (on the order of decades ago). The lack of DNAPL persistence in all or major parts of the source zone represents a major difference between typical source zones in fractured porous sedimentary rock and those of granular aquifers where DNAPL as free product and / or residual can persist for extremely long times (Pankow and Cherry, 1996).

At the WVA, conventional borehole geophysical characterization methods supported the initial conceptualization that the majority of the groundwater flow in the Building 40 treatment area was confined to three primary fracture zones designated "Upper", "Middle", and "Lower" (see Figure 1-3). This conceptual model was consistent with results of conventional borehole fluid resistivity, temperature logging, and flow metering at other sites that typically indicated only two or three active fractures in each hole (Sterling et al., 2005; Pehme et al, 2007). These data also indicated that the greatest contributions to the baseline compliance boundary VOC mass discharge were from the compliance monitoring zones that intersect the upper flow zone fracture system.

This conceptualization was refined by the assessment of site conditions using closely spaced sampling of continuous rock core at WVA. Rock crushing results indicated that there were numerous pathways for contaminant migration, which was consistent with visual observations of fracture occurrence in the cores. This supports the conceptual model for fractured sedimentary rock in which the DNAPL initially occupied many, mostly small to intermediate aperture fractures, and then dissolved allowing the mass to be transferred by diffusion into the nearby matrix. In this conceptual model, the plume forms in a network of many interconnected fractures of variable aperture and length without dominance over long distances of any large-aperture fractures (see Parker, 2007 provided in Appendix G). This refined conceptual model differs from the traditional view of the distribution of contaminant mass; however, from a standpoint of mass transport, the majority of groundwater flow and long-distance contaminant transport appears to be consistent with the "macro" fracture system identified through the geophysical testing.

This site conceptualization implies that effective remediation technologies for the bedrock groundwater will be those that will address the CVOC mass in the rock matrix in addition to treating the CVOC mass in the fractures that contribute to advective groundwater flow. Failure to treat the CVOC mass in the matrix (i.e., the source area) will result in a continuous diffusive transfer of mass out of the matrix to the groundwater.

**Figure 1-3: Primary Fracture Zones**

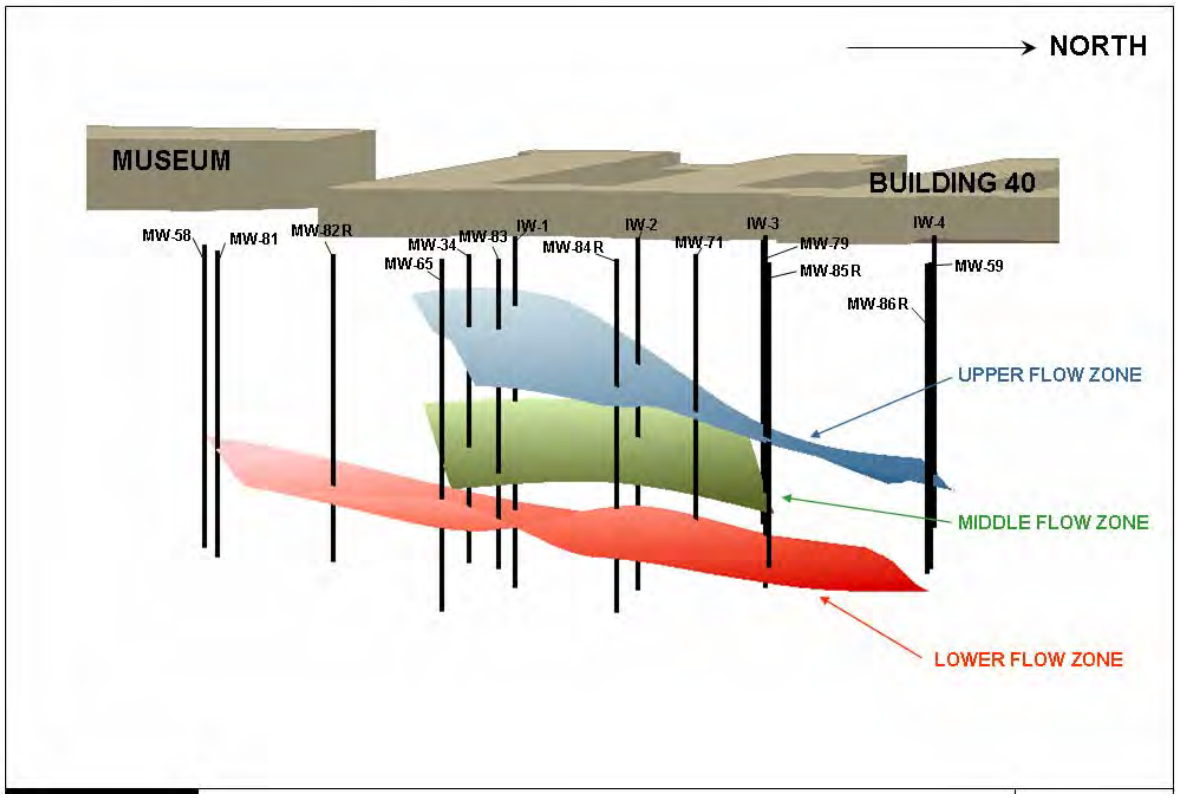

## 1.4 Regulatory Drivers

The environmental restoration program at the WVA is being regulated under the New York State RCRA program, and the lead regulatory agency is the NYSDEC. An Administrative Order on Consent between the WVA, the NYSDEC, and the USEPA was signed in 1993. The NYSDEC has stipulated that the long-term remedial goals for the groundwater at the WVA are NYSDEC Class GA groundwater standards (equivalent to USEPA Maximum Contaminant Limits [MCLs] for drinking water) as shown in Table 1-1 below.

**Table 1-4: NYSDEC Class GA Standards for WVA Contaminants of Concern**

| Compound | Regulatory Level (μg/L[a]) |
|---|---|
| TCE | 5 |
| PCE | 5 |
| cis-DCE | 5 |
| trans-DCE | 5 |
| vinyl chloride | 2 |
| a. 6 NYCRR Part 703 | |

## 1.5 Stakeholder/End-User Issues

There are several issues of concern to stakeholders/end-users related to the use of innovative tools for evaluating ISCO performance in fractured rock. These issues, which were addressed in this demonstration, include:

1. How do results from the new diagnostic tools compare to results from conventional monitoring techniques?
2. Will the new diagnostic tools provide increased understanding to yield more efficient (time and/or cost) operation of the treatment technology?
3. Are the costs of the diagnostic tools lower than the costs of traditional technologies, or do the benefits of using the diagnostic tools offset increased costs?

# 2.0 TECHNOLOGY DESCRIPTION

## 2.1 Technology Development and Application

Table 2-1 provides an overview of each of the diagnostic tools, and the sections below describe each of the diagnostic tools and how they were applied at the WVA. As shown in the table, several of the diagnostic tools used for this demonstration are specific to the selected remedial technology (i.e., ISCO using permanganate) and the site geology (fractured shale).

**Table 2-1: Overview of Innovative Diagnostic Tools**

| Diagnostic Tool | Data Obtained |
|---|---|
| 3-Dimensional Sampling using Multi-Level Monitoring Systems | ■ Fracture network characterization<br>■ Contaminant concentrations at various depth intervals<br>■ Hydraulic information at various depth intervals<br>■ Permanganate solution delivery (not a feature of all systems)<br>■ Permanganate distribution and persistence monitoring (not a feature of all systems) |
| Rock Matrix Analysis | ■ Contaminant mass and phase distribution<br>■ Fracture network characterization including identification of contaminant migration pathways<br>■ Rock matrix physical property measurements (porosity, organic carbon content, diffusion coefficients, permeability, mineralogy, other lab tests)<br>■ Comparison of rock core analyses to aqueous phase samples from multi-level wells to understand relationship between matrix and fracture water contamination<br>■ Visual evidence of permanganate invasion into the rock matrix |
| Isotopic Analysis | ■ Carbon isotope ratios of PCE, TCE and DCE to confirm contaminant oxidation versus displacement<br>■ Charting of fracture pathways (permanganate-influenced groundwater may reach a sampling location prior to arrival of permanganate) |
| Mass Flux | ■ Mass discharge via two different methods not standard in fractured rock application:<br>1. Integrated mass flux test (12-hour constant rate pumping test)<br>2. Mass flux measurements along a transect at the site boundary at various times throughout the duration of the demonstration via groundwater flux estimates using Darcy's Law and VOC concentrations from nested monitoring wells |
| Laboratory Rock | ■ Laboratory testing of rock oxidant demand via batch tests to measure natural / |

| Diagnostic Tool | Data Obtained |
|---|---|
| Oxidant Demand Tests and Permanganate Invasion Tests | mineral oxidant demand<br>■ Permanganate invasion rate tests to measure reactive diffusive transport of permanganate on intact core samples via specialized techniques |
| Numerical Modeling | ■ Projection of mass reduction and groundwater quality beyond the demonstration period using one and two-dimensional discrete fracture models<br>■ Not utilized beyond initial simulations, given the nature of the complex physical and chemical reactions, such as the precipitation of manganese and trace metals upon reaction with VOCs and aquifer minerals, the concentration dependence of permanganate density, influence of microfractures on back-diffusion of VOCs and the sensitivity of rock oxidant demand to permanganate solution |

### 2.1.1 *Multi-Level Monitoring Systems (MLS)*

Conventional groundwater monitoring is conducted using dedicated equipment to collect samples that represent an average measure from each well (blended values over open or screened interval). In contrast, multi-level monitoring systems (MLS) are designed to collect depth-discrete samples over a single vertical profile of the subsurface (ITRC, 2004; Einarson, 2006). The use of multi-level monitoring systems was incorporated into the characterization and remediation efforts at the WVA. Multi-level monitoring systems provide a better understanding of the location of contaminants as well as the changes in concentration with depth within the contaminant plume. MLSs were also used to evaluate fracture interconnectivity and hydraulic head distribution during subsequent testing and the efficacy of the chosen remedial treatment.

For clarity of discussion, a general nomenclature for these devices is presented here, followed by a description of their uses in general and at the WVA. Section 4.0 presents the advantages of using depth discrete MLS over conventional monitoring wells. The term "general purpose multilevel monitoring system" (MLS) refers to an engineered assembly of various components installed in a single borehole to:

1. obtain depth discrete measurements of water pressure (or hydraulic head);
2. acquire ground water samples for analysis; and
3. conduct tests to measure the hydraulic characteristics of the monitored interval.

For the purposes of this demonstration, an MLS is defined as a single-cased (or "single tube") entity capable of monitoring at least two discrete intervals within a borehole. Several MLSs fitting this definition are described in the literature; however, only four systems are available commercially. These four systems are manufactured by three companies:

- Flexible Liner Underground Technologies Limited (the Groundwater FLUTe™);
- Solinst Canada (the CMT® system and the Waterloo system), and;
- Schlumberger Water Services (Westbay system).

These four MLSs can be purchased to perform general purpose monitoring or to use for either sampling or head monitoring. Three of these systems were utilized at the WVA during the pilot study and CM:

- Westbay MP38 Multi-Level Sampling System (Schlumberger Water Services);
- Solinst Continuous Multichannel Tubing (CMT®) Model 403 System (Solinst Canada), and;
- Groundwater Flexible Liner Underground Technologies (FLUTe™) System (Flexible Liner Underground Technologies Ltd.).

In addition to these MLSs, two designs of nested wells were utilized. Nested wells are considered to be two or more wells installed in a single hole, stacked one above the other with seals placed in between. The systems used were a Zone Isolation Sampling Technology (ZIST™) System (Besst Inc.), which is inherently unique in its design and use, as well as conventional nested wells. The MLSs and nested wells were used at the WVA for a variety of purposes ranging from data acquisition for development of the site conceptual model to monitoring for permanganate distribution during in-situ remediation. Background on each system is provided below.

#### 2.1.1.1 *Westbay System*

***Description***

The Westbay system is a modular casing system comprised of a single, closed access tube made up of varying lengths of piping. The system is connected by regular couplings as well as two types of valved port couplings (measurement port and pumping port) to seal and provide access to a large number of monitoring zones in a single borehole. Hydraulically-filled packers or select backfill are used to seal the annulus between each of the monitoring zones. The access tube is hydraulically sealed during installation by using an end cap at the bottom of the access tube and incorporating O-rings whenever a coupling is used. As shown on Figure 2-1, a typical monitoring zone consists of a measurement port coupling, a magnetic collar that is used to locate each monitoring zone, and a pumping port coupling. The monitoring zone sequence is approximately five feet in length with the magnetic collar placed midway between the two ports.

**Figure 2-1: Westbay System with Monitoring Ports**

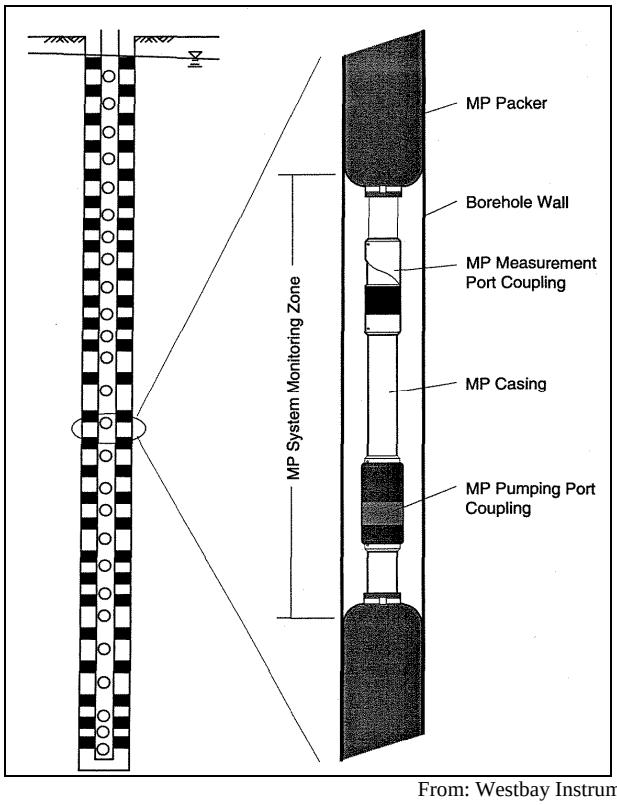


From: Westbay Instruments Inc. 1992-94, Multi-Level Groundwater Monitoring with the MP System

The Westbay system utilizes portable, wireline-operated tools to carry out various functions, including water level/pressure measurements, sample collection, and hydraulic tests.

***Installation Methods***

Casing used for the Westbay systems is available in two sizes to accommodate various borehole sizes. The MP38 System, which was used at the WVA, has an inside diameter of 38 millimeters (mm) or 1.5 inches and is generally used in boreholes or casing whose inside diameter ranges from three to five inches. The MP55 System has an inside diameter of 55 mm or 2.25 inches and is generally used in boreholes or casing whose inside diameter ranges from 3.9 to 6.25 inches. The casing used for the MP38 System consists of plastic, which is typically PVC, and some stainless steel components. The casing used for MP55 Systems are comprised of either plastic or stainless steel.

Westbay systems can be installed in an open borehole, through a temporary guide tube, or in a cased well. There is no limit to the number of monitoring zones that can be installed in a single borehole. An on-site technician from Westbay helps the consultant install the Westbay system and will train the consultant in how to set-up and use the system for the purposes in which it was installed.

***Operation***

Westbay tools and probes can be controlled by the user at the ground surface by using a MAGI interface, which displays the pressure, temperature, and status of the tool and/or probe. A manual or motorized winch with a cable connects to the tool and lowers and raises it in the borehole. The winch has a counter to guide the user on the depth of the tool and/or probe in the borehole.

Prior to groundwater sampling or collecting pressure measurements, each monitoring zone must be purged using the pumping port. Monitoring zones in a system can be pumped individually or several at a time. Prior to purging a monitoring zone, the water from inside the casing is removed and all other ports are closed, while the one port is left open. The water that remains in the casing is from the monitoring zone and once this water is removed from inside the casing, the monitoring zone is developed and can be sampled. Hydrogeologic tests, such as slug tests and hydraulic conductivity tests, and sampling can be conducted following development. Purging is not required prior to sampling a monitoring zone each time. It is only necessary to develop the monitoring zone once.

A pressure probe/sampling tool is used to measure fluid pressure and to collect groundwater samples from a monitoring zone. The fluid pressure is measured by the MOSDAX® pressure probe, which incorporates a location arm, a backing shoe, a face seal, and fluid pressure transducer. A groundwater sample is collected by attaching a sample container, which has a sampling valve that can be closed or open, to the pressure probe, which collectively is called a sampling tool. Groundwater samples are collected through the measurement port. A vacuum is created inside the sampling tool before lowering into the borehole. The pressure probe is lowered into the borehole and connects into the measurement port in the same way as that used for measuring fluid pressure of the formation. A sample from the formation is collected once the sampling valve is opened, allowing water from the formation to flow through the probe and enter the sample container. When the sampling valve is initially opened the fluid pressure decreases and then recovers as the water in the container builds to the formation pressure. Once the fluid pressure is equal to or slightly less than the formation pressure the sample container is considered full and the sampling valve is closed and the sample container can be brought to the ground surface.

#### 2.1.1.2 *CMT® System*

***Description***

The CMT® system uses a continuous length of polyethylene multichannel tubing. The number and location of ports may be determined prior to or following drilling the borehole. A port is created in up to seven channels per system to monitor specified depths determined from boring logs or geophysical tests conducted prior to assembly of the system. As shown on Figure

2-2, a plug is positioned and sealed in the channel just below the port opening and a stainless steel screen is placed over the port to prevent fines from entering. A vent hole is created just below the seal to allow air to escape as the system is lowered into the borehole. Each channel is sealed at the bottom of the tubing to prevent cross communication between zones. The CMT® system can be sealed in place using standard sand and bentonite layers placed via a tremie pipe.

**Figure 2-2: CMT® System Monitoring Port**

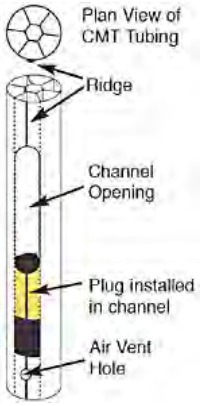


From: www.solinst.com/Prod/403/403d7.html

***Installation Methods***

There are two CMT® systems available to accommodate various borehole sizes. The 1.1-inch outer diameter polyethylene tubing is segmented into three channels, providing three depth-discrete sampling zones. The 3-Channel System was developed for smaller diameter installations, such as when direct push methods are used creating a narrow annulus for seal placement. The 1.7-inch outer diameter polyethylene tubing is segmented into seven channels and allows for up to seven depth-discrete zones of groundwater monitoring. This CMT® system was used at the WVA.

A CMT® system is built completely above ground and then inserted into the borehole. The tubing is laid out near the borehole and zones are marked on the tubing to show where the channel opening will be created. If packers and/or sand packs are used to seal the zones, they are installed or attached to the tubing in place outside of the borehole prior to installation. However, if the zones are sealed using traditional sand and bentonite layers, a mesh screen is placed over the port inlet holes. The CMT® system is installed as one continuous piece of tubing. The tubing comes in lengths of 100, 200, and 300 feet coils. Low-profile borehole centralizers are used to help center the system in the middle of the borehole so that a good seal can be created between the monitoring zones and prevent cross communication. Once the system is installed into the borehole, alternating layers of sand and bentonite are poured via a tremie-pipe into the annulus. The sand is poured around the monitoring zone, while the bentonite is used to seal the zones.

***Operation***

CMT® systems can be used for measuring water levels as well as for collecting groundwater samples from up to seven monitoring zones in one borehole. A peristaltic or double-valve pump is used for both purging and sampling groundwater in these systems. Purging of the monitoring interval is required prior to collecting a groundwater sample from the each channel. Equipment used for collecting groundwater samples from CMT® is dedicated to each channel or is disposable, reducing the risk of cross contamination between monitoring zones at one location.

2.1.1.3 *Water FLUTe™ system*

***Description***

A schematic of the FLUTe™ system is shown in Figure 2-3. The FLUTe™ system consists of a pressurized flexible polyurethane-coated Nylon liner that is emplaced in a borehole by interior water pressure – sealing the borehole completely. Sampling intervals are set using exterior spacers that are placed between the borehole wall and the liner. Each sampling interval is sealed from the remainder of the borehole by the water pressure inside the liner. A sample tube that is equipped with a check-valve system brings water from the formation up to the ground surface to be collected and monitored. The FLUTe™ system (1-20 ports) is typically used for deeper applications in stable holes (e.g., core holes in fractured bedrock).

**Figure 2-3: Water FLUTe™ Schematic**

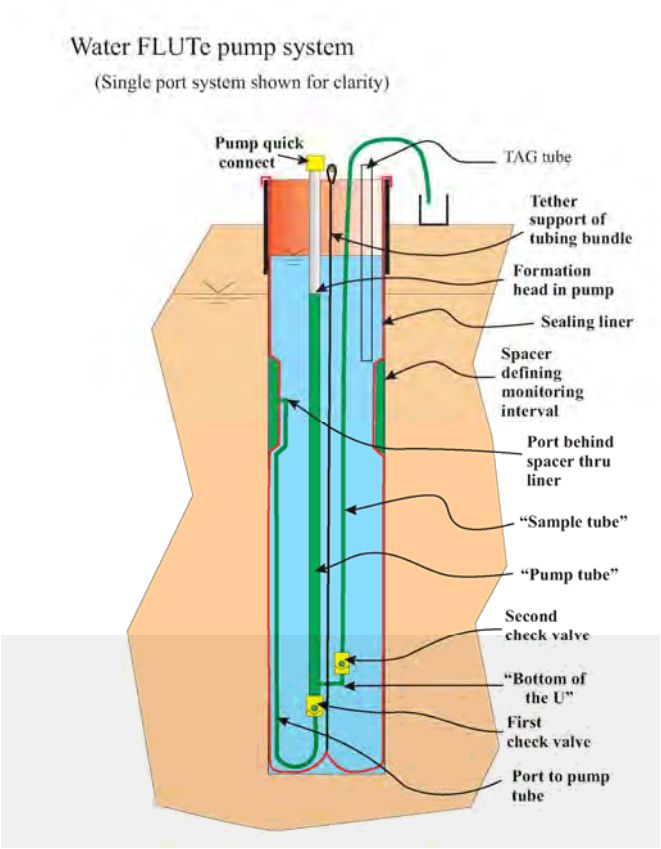

### *Installation Methods*

The installation of a FLUTe™ system is completed by a trained technician from Flexible Liner Underground Technologies, Inc. The liner is rolled off of a shipping reel and is emplaced into the borehole (Figure 2-4). Water is added to the interior of the liner, driving the liner deeper into the borehole, pulling the inside-out liner from the reel. It is this interior water pressure that is the driving force for the installation.

**Figure 2-4: FLUTe™ Installation at the WVA**

The installation of a FLUTe™ system is affected by many factors, including depth and diameter of the borehole, the relative transmissivity of the borehole, the depth to the water table, and the rate at which water can be supplied to fill the liner. A FLUTe™ system can be installed in most types of boreholes of varying diameters. Typically, a system can be installed in less than one day and can be removed by pumping out the water inside the liner and pulling the liner out of the well from the bottom up.

### *Operation*

The FLUTe™ system uses compressed nitrogen gas to purge and sample each of the ports installed within the system. The water flows directly from the formation through the spacer and into the sampling tube with the check-valve system, which prevents the water in the tube from contacting the nitrogen drive gas. The compressed nitrogen gas pushes the formation water to the surface. Since the water in the sample tube flows directly from the formation under natural hydrostatic pressure, it is only necessary to purge the small volume of water in the sampling tube before sampling. Because each sampling port/tube is self-contained, several sampling zones can be purged simultaneously.

2.1.1.4 *ZIST™ system*

***Description***

The ZIST™ system was specifically developed so that a well screen could be isolated, drawdown eliminated, and purge volume could be reduced. The system consists of a standard PVC well construction in which a pump (0.75 inch or 1.75 inch outer diameter) and sensor/data logger dock into the Well Screen Receptacle that is located between the well screen and riser pipe (Figure 2-5). When the pump and sensor/data logger are docked, the screened interval is sealed off for monitoring and sampling. A Simultaneous Control Unit is used by the operator to control the pressure of the nitrogen gas being used as the driver to push water up to the surface as well as the rate at which the water is pumped out. This Control Unit allows for the purging and sampling of multiple zones at the same time.

Various sensors can be placed in-line with the pump to measure pressure and the chemistry of the formation groundwater while operating. When the pump is not operating, the sensor can detect the same parameters under static conditions in the well screen and groundwater formation only. Electronic down-hole sensors with data loggers, or fiber optic sensors, can also provide information on the pore pressure, temperature, conductivity, and other useful chemical data within the well screen and formation groundwater. Due to the design of the Well Screen Receptacle, the riser pipe water does not come into contact with the water in the monitoring zone, allowing for continuous monitoring of groundwater conditions within the zone between sampling events, and greatly reduced purge volumes during sampling.

**Figure 2-5: ZIST™ System Schematic of Pump and/or Sensor Docked**

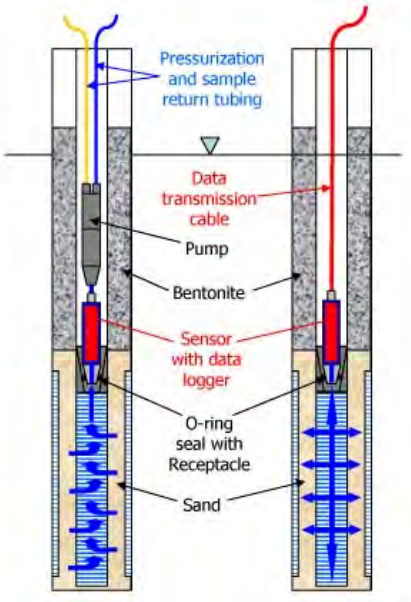

***Installation Methods***

The installation of a ZIST™ system is completed by the consultant along with assistance and training from a knowledgeable technician from BESST, Inc. A ZIST™ system can be easily integrated into a 0.75-inch to greater than four inch diameter borehole or monitoring well. The monitoring zones are constructed by pouring sand around the riser screen and pouring bentonite above the sand to create a seal between two monitoring zones and reducing the possibility of cross-contamination.

***Operation***

Water in the sample tube is pushed to the surface using compressed air or nitrogen. Because the water in the sample tube flows directly from the formation around the screened interval under natural hydrostatic pressure, it is only necessary to purge the small volume of water in the sample tube before sampling. Because each zone is self-contained with its own pump and tubing, all sampling zones can be purged simultaneously. The tubing, pump, and sensor/data logger can be removed from each well with relative ease in order to download data and maintain system components.

2.1.1.5 *Waterloo System*

***Description***

The Waterloo System is used to obtain groundwater samples, hydraulic head measurements and permeability measurements from many discretely isolated zones in a single borehole.

The Waterloo System uses modular components which form a sealed casing string of various casing lengths, packers, ports, a base plug and a surface manifold (Figure 2-6). Monitoring tubes attached to the stem of each port individually connect that monitoring zone to the surface. Thus formation water enters the port, passes into the stem, up into the monitoring tube attached to the stem, to its static level. A sampling pump or pressure transducer may be dedicated to each monitoring zone by attachment to the port stem. Dual stem ports are available to allow both sampling and hydraulic head measurements from the same port. Alternatively, the monitoring tubes may be left open to allow sampling and hydraulic head measurements with portable equipment. A manifold completes the system at surface. The manifold organizes, identifies, and coordinates the tubes and/or cables from each monitoring zone. The manifold allows connection to each transducer in turn, and a one-step connection for operation of pumps. When dedicated pumps are selected, it allows individual zones to be purged separately, or purging of many zones simultaneously to reduce field times.

**Figure 2-6: Waterloo System**

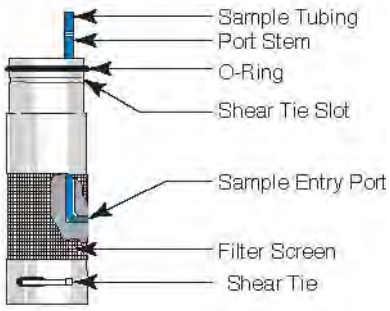


***Installation Methods***

The Waterloo System can be used to monitor multiple zones within unconsolidated formations, as well as in bedrock. There are three methods of System installation:

- Within hollow stem augers or temporary casing using natural formation collapse;
- Within hollow stem augers, temporary casing, or open bedrock boreholes using standard tremie methods to place sand around the ports and bentonite seals in the annular space between the monitoring zones;
- Within open bedrock boreholes or cased and screened well, using packers to seal zones.

***Operation***

The maximum number of monitoring zones for a System is determined by the number of tubes and/or cables that will fit inside the casing string. This number is dependent on the monitoring options chosen. Systems can be designed to monitor from 2 to as many as 24 zones. The most basic version uses open tubes attached to each port. This option allows monitoring with a portable sampler and a narrow diameter Water Level Meter. A mix of open tubes and dedicated equipment in different zones is also possible. This method combines the advantages of less expensive portable equipment for shallower zones (i.e., around 100 ft or 30 m) and the more time efficient dedicated equipment for deeper zones.

### 2.1.2 *Rock Matrix Analysis*

Shales are referred to as fractured porous media because their primary porosity typically ranges from 0 to 10 percent (Freeze and Cherry, 1979; Potter, 2005). It is the presence of fractures in the shale that provides the main pathways for flow through the rock because the rock pores are generally small and not interconnected. The ratio of the void space due to the presence of fractures to the bulk rock volume (fracture porosity) is expected to be at least a few orders of magnitude lower than the matrix porosity, and is estimated to be between 0.01 and 0.0001 percent. This large difference between fracture and matrix porosities greatly influences the distribution of chlorinated solvent mass in these deposits. The net result is that at field sites

where solvents have contaminated rock for a few decades, essentially all of the contaminant mass resides in the low permeability rock matrix, not in the fractures (Parker et al., 1994). Diffusion haloes form along the fractures where DNAPL flow or solute transport has occurred. The haloes, and therefore the pathways, can be determined from analysis of subsamples of rock core. This approach for pathway identification offers the potential for identifying smaller and/or lower transmissivity fractures than the conventional approaches of well sampling as it allows for the detailed analysis of actual contaminant migration pathways rather than just contaminant presence in relatively large groundwater monitoring zones.

The rate of expansion of plumes in fractured rock settings can be greatly retarded by the diffusion-driven chemical mass transfer from fractures where active flow occurs to the matrix blocks where the pore water is relatively immobile (Freeze and Cherry, 1979). Site-specific proof of this retardation of plume expansion lies in determination of the chemical mass distribution in the rock matrix and fracture network and matrix characteristics.

Dr. Beth Parker and colleagues at UW have developed a technique to assess VOC mass that has diffused into the rock matrix from hydraulically active fractures carrying VOC contaminant mass. The protocol entails the collection of three types of rock core subsamples:

1. VOC samples, which are crushed and preserved in the field by placing in vials with methanol for extraction and later laboratory analysis;
2. Physical property samples, consisting of intact sections of core that are analyzed for moisture content, matrix porosity, bulk density, specific gravity, hydraulic conductivity, and organic carbon content; and
3. Matrix diffusion samples, consisting of intact sections of core designated for laboratory diffusion tests and oxidant demand batch tests.

The protocol for collection of VOC samples includes collection of samples at fractures (i.e. one of the fracture faces) and bedding planes, at lithologic changes, and from matrix blocks between fractures. Sample lengths typically range from 0.1 to 0.4 feet of core. VOC samples are immediately wrapped in aluminum foil to minimize volatile losses and taken to an on-site field lab for crushing and processing. Prior to crushing, the outer rind of the core samples is chipped off to eliminate potential error from contact with the drilling fluids. Samples are then immediately crushed with a hydraulic rock crusher and placed into sample vials containing a known amount of high purity methanol (MeOH) to extract and preserve the VOC mass. Between samples, the cells are decontaminated using a four-part wash and rinse sequence. Field QA/QC procedures and decontamination procedures are designed to prevent cross-contamination.

Laboratory VOC analyses on the preserved crushed rock samples are conducted after allowing sufficient time for the VOCs to completely extract into the methanol. More recently a microwave assisted extraction technique has been developed to speed up the extraction. Following the extraction process, an aliquot of methanol is injected directly into a gas chromatograph (GC) for separation and quantification using a micro electron capture detector (μ−ECD). The list of target analytes quantified includes TCE, PCE and the DCE isomers, but

may be varied depending on the expected contaminants at the site. The direct, on-column injection of MeOH onto the gas chromatograph was tailored by UW for analysis of PCE, TCE and relevant breakdown products so that the resulting detection limits are very low (0.1 ug/L in MeOH for TCE and PCE, and <5 ug/L in MeOH for the DCE isomers).

The laboratory analysis provides the total mass of each VOC per unit mass of wet crushed rock sample ($c_t$) (e.g., μg PCE per g wet rock) and includes VOC mass present in the aqueous, sorbed and DNAPL (if present) phases. These concentrations are converted to equivalent pore water concentrations using partitioning calculations (see Feenstra et al., 1991) with measured or estimated rock matrix parameters (bulk density, porosity and sorption). In this case, equivalent pore water concentrations ($c_w$) were estimated using:

$$c_W = c_t \frac{\rho_{bwet}}{R\phi} \qquad [1]$$

where $\rho_{bwet}$ is the rock wet bulk density (g/cm$^3$), $\phi$ is the porosity and R is the retardation factor, accounting for VOC mass sorbed to organic carbon present in the rock. Retardation factors (R) were estimated using the relation:

$$R = 1 + \left[\frac{\rho_b}{\phi}\right] K_d \qquad [2]$$

where $K_d$ is the distribution coefficient (mL/g) and $\rho_b$ is the dry rock bulk density (g/cm$^3$). It is assumed that sorption is rapid, linear and reversible.

### 2.1.3 *Isotopic Analysis*

Compound-specific carbon isotope analysis is a diagnostic technique for use in the assessment of the effectiveness of permanganate treatment of chlorinated ethenes. A team from UW (Hunkeler et al., 2003) and others have shown that strong fractionation of the carbon isotopes in chlorinated solvents occurs when permanganate oxidation takes place. To apply this technique, representative groundwater samples from the treatment zone are analyzed prior to permanganate injection for their compound specific carbon-13 ($^{13}$C) / carbon-12 ($^{12}$C) ratio. Generally, the isotope values fall in a narrow range in the treatment zone before treatment. Then, after permanganate injections have occurred, groundwater samples from appropriate locations where permanganate treatment is expected are subjected to the isotopic analyses. If the carbon isotope ratio has shifted strongly towards a $^{13}$C enrichment value, and with consideration of other relevant factors, the cause of this shift can be attributed to permanganate oxidation. The strong $^{13}$C enrichment indicates that, although chlorinated ethene mass still remains at the sampling location, partial destruction of mass due to oxidation has occurred. The carbon isotope data may also provide information about rebound effects which may occur after the permanganate is consumed. Contaminant rebound may be identified if the carbon isotope composition of the VOC tends toward the original carbon isotopic composition of the VOC before oxidation.

This isotopic technique is particularly valuable at sites such as the WVA because background chloride values are generally too high (250 to 500 milligrams per liter) and too variable to allow chloride production as a result of permanganate oxidation to be a diagnostic tool. Several laboratories in North America perform compound-specific carbon isotope analyses on chlorinated ethenes; however, at the time of this demonstration, the UW had the best capability for analyzing a wide range of concentrations, including the extremely low concentrations (i.e., down to micrograms per liter).

### 2.1.4 *Mass Flux Analysis*

The mass that the source zone is contributing to the larger dissolved phase plume is an important attribute to determine, from both risk assessment and treatment performance perspectives. The source strength, or mass discharge, is defined as the rate at which contaminants pass through a defined cross-sectional area perpendicular to groundwater flow. In general, four techniques have been used to estimate contaminant mass discharge:

- Measure contaminant concentrations in samples recovered during continuous pumping groundwater extraction.
- Measure contaminant concentrations and groundwater discharge during short-term pumping tests ("integrated pump tests") (Bockelmann et al., 2001).
- Measure contaminant concentrations and groundwater flux at multiple locations across a transect of multi-level samplers (e.g., Einarson and Mackay, 2001).
- Measure contaminant concentrations and groundwater velocities at multiple locations and depths using passive borehole flux meters (e.g., Hatfield et al., 2004; Annable et al., 2005).

None of these techniques have been widely applied or tested in fractured rock. At the WVA, both the transect technique and an integrated pump test were used to estimate the VOC mass discharge over the treatment area. The transect technique involved the collection of a two-dimensional data set at six locations (18 total measurement points) located across the treatment zone discharge face (which is coincident with the property boundary).

The integrated pump test technique involved a 12-hour low flow rate pumping test performed in the contaminant source area. The Tubingen integrated pump test, developed by researchers at the University of Tubingen, Germany (Bockelmann et al., 2001) relies on capturing all of the contaminated groundwater flowing within the plume. An advantage of this method is that it does not require interpolation of contaminant concentrations between monitoring points, as is the case with transects of multi-level monitoring wells (described above). Contaminant mass discharge ($M_d$) is calculated as follows:

$$M_d = \sum_{i=1}^{n} Q_i C_i$$

Where
$M_d$ = contaminant mass discharge (mass/time)
$Q_i$ = extraction rate from well i (volume/time),
$C_i$ = contaminant concentration measured in effluent from well i (mass/volume)

Time-series VOC sampling was conducted during the test to evaluate integrated (average) contaminant concentrations in the treatment area. Initially, two pump tests were planned, one to be performed prior to permanganate injection and one to be performed at the completion of permanganate injections. The second pump test could not be performed due to clogging of the test borehole with what is presumed to be manganese dioxide or other permanganate by-products.

### 2.1.5 *Rock Oxidant Demand Tests and Permanganate Invasion Study*

Fine-grained sedimentary rocks, such as the Snake Hill Shale Formation at the WVA, offer unique challenges for investigating rates of VOC and permanganate ($MnO_4$) diffusion. These rocks commonly have very low matrix porosity, which limits the diffusion rates. In addition, organic carbon and reduced minerals, such as pyrite and chlorite, which commonly occur in these rocks may react with $MnO_4$, resulting in very small rates of diffusive penetration. As a result, investigations must be conducted using long time scales and/or very small distance scales to observe such processes. At sites such as the WVA, where contamination has existed for many decades, it is expected that the majority of the contaminant mass resides within the low permeability rock matrix as dissolved and sorbed phases. The rate of $MnO_4$ penetration into the rock matrix and rates of permanganate consumption are key design issues for considering the potential for $MnO_4$ as a remediation technology for destroying VOC mass present in the rock matrix. Both of these issues were targeted by laboratory studies and are discussed in detail in Sections 3.4.1.4 and 4.3.5.

### 2.1.6 *Numerical Modeling*

The goal of numerical modeling was to apply one and two-dimensional discrete fracture models to project mass reduction and groundwater quality beyond the demonstration period. One-dimensional simulations of PCE and TCE diffusion into the shale matrix were conducted using an analytical solution to Fick's Second Law of Diffusion. This early modeling assumed only organic carbon in the shale matrix contributes to ROD, permanganate can be maintained continuously in fractures, and the presence of microfractures can be neglected. Based on the laboratory testing (see Section 4.3.5), it was determined that these were not accurate assumptions. Therefore, modeling was not utilized beyond initial simulations, given the nature of the complex physical and chemical reactions, such as the precipitation of manganese and trace metals upon reaction with VOCs and aquifer minerals, the concentration dependence of permanganate density, influence of microfractures on back-diffusion of VOCs, and the sensitivity of rock oxidant demand to permanganate solution concentration. Modeling of contaminant and regent reactive transport in a complex fractured system is beyond current state of the science, and not understood well-enough to combine in models to be useful with any sense of reliability, especially in fractured porous media.

## 2.2 Previous Testing of the Technologies

The degree of previous testing of the diagnostic tools varies widely and is summarized below.

### 2.2.1 *Multi-Level Monitoring Systems (MLSs)*

MLSs are available commercially and have been used at many sites. There is substantial published literature concerning MLSs and other approaches to depth discrete groundwater monitoring. Einarson (2006) provides an overview encompassing all types of MLSs and well nests and clusters used in North America. The manufacturers provide detailed information about their MLSs on their web sites (also see discussion in Section 3). The Westbay system, which is described by Black et al. (1986) and Meyer et al. (2007), was the first MLS to enter the marketplace (late 1970s). This was followed by the Waterloo system in the late 1990s. Cherry and Johnson (1982) describe the first version of the Waterloo system and Parker et al. (2007) describe a recent version of the Waterloo system. The CMT® system described by Einarson, Cherry (2002) and the FLUTe system described by Cherry et al. (2007) entered the marketplace in the late 1990s. Each of these systems has been used in numerous investigations of contaminated rock sites distributed across North America, and some of the systems have been used on other continents. There is substantial reporting on the uses of MLSs in site characterization reports and conference proceedings.

### 2.2.2 *Rock Matrix Analysis*

Rock matrix analysis has been applied by UW researchers under the direction of Dr. Beth Parker and Dr. John Cherry at ten contaminated sites in fractured sedimentary rock to date, beginning in 1997. The sites are located throughout North America, with eight sites located in the U.S. (Arkansas, California, Kansas, Wisconsin and four in New York State, including WVA) and two sites in Canada (both in Ontario). The sites represent a range of lithologies including predominately sandstone (three sites), shale (four sites), limestone (one site), and dolomite (two sites), and varying types and ages of contamination.

The rock crushing technology and laboratory analytical techniques continue to be modified, refined, and tested on different sedimentary rock types and mineralogies. Such refinements have included design of improved hydraulic rock crushers and rock crushing cells, improvements in sample QA/QC procedures and development and testing of laboratory analytical techniques to speed the sample extraction process (e.g., microwave assisted extraction). Application of rock matrix analysis at different sites requires consideration of many factors including the type of rock, nature of the fracture network, and type and age of contamination. The sampling protocols are tailored to the unique characteristics of each site. The following is a list of selected publications by UW researchers (including conference proceedings and peer-reviewed manuscripts) related to application of rock crushing technology.

<u>Peer Reviewed Manuscripts</u>:

Sterling, S.N., B.L. Parker, J.A. Cherry, J.H. Williams, J.W. Lane, and F. P. Haeni. 2005. Vertical Cross Contamination of TCE in a Borehole in Fractured Sandstone. Ground Water, 43(4): 557-573.

Goldstein, K.J., Vitolins, A.R., Navon, D., Parker, B.L., Chapman, S., Anderson, G.A. 2004. Characterization and Pilot-Scale Studies for Chemical Oxidation Remediation of Fractured Shale. Remediation, 14(4): 19-37.

Conference Proceedings:

Parker, B.L., and S.N. Sterling. 1999. Rock core subsampling and analysis for volatile organic compounds (VOCs) in a fractured sandstone. In Symposium Proceedings "Dynamics of Fluids in Fractured Rocks: Concepts and Recent Advances", February 10-12, Berkeley, California. Abstracts pp. 175-177.

Parker, B.L., S.W. Chapman and S.N. Sterling. 2000. Evidence for strong diffusion effects on TCE behaviour in a fractured sandstone. 2000 GSA Annual Meeting, Nov. 13-16, Reno, Nevada, p. 64.

Sterling, S.N., B.L. Parker, and J.A. Cherry. 2000. Comparison of new and conventional field methods for characterizing trichloroethene distribution in a fractured sandstone. Groundwater 2000. International Conference on Groundwater Research, June 6-8, Copenhagen, Denmark. Bjerg et al. (eds). Balkema: Rotterdam, pp. 27-28. (Extended Abstract).

Hurley, J.C. and B.L. Parker, 2002. Rock core investigation of DNAPL penetration and TCE mobility in fractured sandstone. Ground and Water: Theory to Practice, D. Stolle, A.R. Piggott and J.J. Crowder (eds.), Proceedings of 55th CGS and 3rd Joint IAH-CNC Groundwater Specialty Conf. October 20-23, Niagara Falls, Ontario, pp. 473-480.

Parker, B.L., J.A. Cherry, M.A. Guilbeault, K.J. Goldstein, D. Navon, A.R. Vitolins, G.A. Anderson and S.P. Wood. 2002. Remedial investigation methods for shale contaminated by chlorinated hydrocarbons" Part 2 – Matrix influence on mass distribution. Presented at NGWA Northeastern FOCUS Ground Water Conf., Oct. 3-4, Burlington, Vermont.

Parker, B.L. 2003. Field evidence for abundant fracture connectivity in sedimentary rocks. Presented at the AGU Fall Meeting, December 8-12, San Francisco, CA. Eos Trans. AGU, Vol. 84 no. 46, Fall Meet. Suppl. Abstract H52B-04, 2003.

Parker, B.L. 2003. Strong matrix diffusion effects on contaminant behaviour in fractured sedimentary rocks. 2003 GSA Annual Meeting & Exposition, Seattle, WA, Nov. 2-5, Published in Abstracts with Programs Vol. 35 no. 6, pp. 54.

Parker, B.L, J.A. Cherry, K.J. Goldstein, A.R. Vitolins, D. Navon, G.A. Anderson, and S.P. Wood. 2004. Matrix Influence on Contaminant Mass Distribution in a Fractured Shale. Fourth International Conference on Remediation of Chlorinated and Recalcitrant Compounds, Monterey, CA, May 24-27, 2004.

Parker, B.L., 2004. Utility of rock core for characterizing contamination in fractured sedimentary rocks. Invited talk at: 2004 US EPA/ NGWA Fractured Rock Conf.: State of the Science and Measuring Success in Remediation, Portland, ME, Sept. 13-15, 2004.

Sterling, S.N., B.L. Parker, J.A. Cherry, J.W. Lane, J. H. Williams, F.P. Haeni. 2004. Vertical cross connection in a single borehole: A case study in fractured sandstone. Presented at: 2004 US EPA/ NGWA Fractured Rock Conf.: State of the Science and Measuring Success in Remediation, Portland, ME, Sept. 13-15, 2004.

Goldstein, K., Vitolins, A.R., Navon, D., Chapman, S.W., Parker, B.L., Al, T.A. 2007. Full-Scale Permanganate Remediation of Chlorinated Ethenes in Fractured Shale: Part 1 – Site Characterization and Design and Implementation of Full-Scale Remedy. 2007 U.S. EPA / NGWA Fractured Rock Conference: State of the Science and Measuring Success in Remediation, Portland, Maine, Sept 24-26, 2007.

Chapman, S.W., Parker, B.L., Goldstein, K.J., Vitolins, A.R., Navon, D., Al, T.A. 2007. Full-Scale Permanganate Remediation of Chlorinated Ethenes in Fractured Shale: Part 2 – Three-Year Interim Evaluation of Treatment Performance. 2007 U.S. EPA / NGWA Fractured Rock Conference: State of the Science and Measuring Success in Remediation, Portland, Maine, Sept 24-26, 2007.

Parker, B.L. 2007. Investigating contaminated sites on fractured rock using the DFN approach. Proceedings of the 2007 U.S. EPA/NGWA Fractured Rock Conference: State of the Science and Measuring Success in Remediation, Sept. 24-26, 2007, Portland, Maine, pp. 150-168.

### 2.2.3 *Isotopic Analysis*

Compound-specific carbon isotopes are becoming useful tools for assessing biodegradation of chlorinated ethenes and chlorinated ethanes in groundwater (Hunkeler et al., 1999). The rationale for the use of isotopes to monitor the fate of precursors and by-products during biodegradation is based on the process of isotope fractionation that leads to a progressive enrichment of the heavy isotope in the precursor, while the product becomes depleted in the heavy isotope. Significant carbon isotope fractionation has been reported for biodegradation of chlorinated ethenes and chlorinated ethanes in laboratory experiments (e.g., Bloom et al., 2000; Chartrand et al., 2005; Hunkeler et al., 1999) and isotopic analysis has been applied at field sites to demonstrate and evaluate biodegradation of these compounds in groundwater (e.g., Hunkeler et al., 1999; Sherwood Lollar and Slater, 2001; Vieth et al., 2003). Laboratory studies have also shown that strong carbon isotope fractionation occurs during chemical oxidation of chlorinated compounds by potassium permanganate (e.g., Hunkeler et al., 2003) which makes isotopic analyses a potentially powerful diagnostic tool for monitoring ISCO, since they can be used to verify that concentration declines in target compounds are due to degradation instead of physical (e.g., displacement) processes. The laboratory at the UW has the capability to analyze carbon isotopes of chlorinated ethenes over a wide concentration range, including very low (i.e. microgram per liter) concentration levels making it ideal for applications involving in-situ

oxidation. UW researchers have applied isotopic analyses at three sites to date as a tool to monitor ISCO: two of the sites are in sandy aquifers (Connecticut, Ontario), while the sampling conducted at the WVA during the pilot study potassium permanganate injection trial was the first application in a fractured rock setting (Hunkeler et al., 2003; Aravena et al., 2004). The following is a list of selected publications by UW researchers (including conference proceedings and peer-reviewed manuscripts) related to compound-specific isotopic analysis of chlorinated ethenes in potassium permanganate studies.

**Peer Reviewed Manuscripts:**

Hunkeler, D., Aravena, R., Butler, B.J., 1999. Monitoring microbial dechlorination of tetrachloroethene (PCE) using compound specific carbon isotope ratios: microcosms and field experiments. Environmental Science & Technology, 33 (16), 2733-2738.

Hunkeler, D., R. Aravena, B.L. Parker, J.A. Cherry, and X. Diao. 2003. Monitoring oxidation of chlorinated ethenes by permanganate in groundwater using stable isotopes: Laboratory and field studies. Environmental Science & Technology, Vol. 37, no. 4, p. 798-804.

**Conference Proceedings:**

Hunkeler, D., R. Aravena, B.L. Parker, and J.A. Cherry. 2002. Monitoring in situ oxidation of TCE by permanganate using carbon isotopes. In: A.R. Gavaskar and A.S.C. Chen (eds.), Remediation of Chlorinated and Recalcitrant Compounds – 2002. CD Proceedings of the Third International Conference on Remediation of Chlorinated and Recalcitrant Compounds. May 20-23, 2002, Monterey, California, Paper 2C-07, 7 pp.

Hunkeler, D., R. Aravena, B.L. Parker and J. A. Cherry. 2003. Assessment of the oxidation of chlorinated ethenes by permanganate in groundwater using isotope analysis. II International Seminar on In-Situ Remediation of Contaminated Sites, Sao Paulo, Brazil, November 3-5, 2003.

Hunkeler, D., R. Aravena, B.L. Parker and J.A. Cherry, 2004. Assessment of the oxidation of chlorinated ethenes by permanganate in aquifers using isotope analysis. First European Conference on Oxidation and Reduction Technologies for In-Situ and Ex-Situ Treatment of Water, Soil and Air (ECOR-1), Göttingen, Germany, April 25-28, 2004.

Aravena, R., Parker, B., Cherry, J., Navon, D., Vitolins, A.R., Goldstein, K.J. Anderson, G.A., and Wood, S.P. 2004. Use of carbon isotopes to monitor in situ oxidation of chlorinated ethenes in a fracture rock aquifer. The Third International Conference on Oxidation and Reduction Technologies for in Situ Treatment of Soil and Groundwater. San Diego, California, October 24-28.

Helsen, J.G., Aravena, R., Zhang, M., Shouakar-Stash, O, and Burns, L. 2007. Assessment of TCE oxidation by $KMnO_4$ using stable carbon and chlorine isotopes at a fractured bedrock site. NGWA-EPA Fractured Rock Conference. September 24-26, Portland, Maine.

### 2.2.4 *Mass Flux Analysis*

The concept of measuring mass discharge along a plane oriented perpendicular to flow direction is well understood and has been practiced widely using conventional monitoring devices. By collecting groundwater from closely spaced multi-level sampling points along a transect of wells intersecting a plume and aligned perpendicular to the groundwater flow direction, the total mass discharge across the transect can be estimated from the measured concentration distribution and groundwater discharge (e.g., Einarson and Mackay, 2001). It is presumed that this approach has been used at many sites, however there are few published discharge estimates in the literature (e.g., Guilbeault et al., 2005) and most of these are for porous media and not in fractured rock. This method involves intensive sampling using depth-discrete techniques to adequately characterize the plume, and also for estimation of groundwater flux.

More recently, an alternative to the application of detailed monitoring along transects, the Tübingen integrated pump test technique, has been in development. Field experience with this method is generally limited, especially in fractured rock. However, use of this technique in fractured rock may have limited utility, as it relies on the documentation of the complete capture of the contaminant plume through water level monitoring, which is extremely difficult to document in fractured bedrock. In addition, due to the lack of storage in bedrock groundwater systems, the induced gradient changes in individual fractures may result in over-estimation of the flux by inducing flow in contaminated fractures or matrix blocks (through microfractures) that do not normally contribute to the overall flux, or that normally contribute in a minimal nature.

## 2.3 Factors Affecting Cost and Performance

The following discussion outlines factors that may affect cost and performance of the various diagnostic tools.

**MLSs.** Many MLSs are commercially sold and costs vary based upon construction materials, manufacturing processes, and site requirements (e.g.,, length and diameter of borehole, and number of sampling intervals). A summary of the costs of each of the systems, as configured at the WVA, is provided in Section 5 of this report. Factors that may affect the performance of the multi-level systems including clogging (either by formation of manganese oxides or other mechanisms), borehole storage effects, and sampling in low hydraulic conductivity zones. These issues were evaluated throughout the demonstration period and are discussed in Section 4.0.

**Rock Matrix Analysis.** The costs for rock matrix analysis are fairly well defined and are comprised chiefly of drilling, labor costs for collecting and processing rock core samples, and laboratory analytical costs. Factors that may affect the performance of the rock matrix analysis include:

- A sufficient length of time allowed for the methanol extraction process.
- Accuracy in laboratory and field methods (e.g., minimizing volatile losses, following appropriate QA/QC protocols, decontamination, etc.).
- Variability in rock formation properties (e.g., $f_{oc}$, porosity and bulk density), which may affect the accuracy of equivalent pore water concentration calculations.

Rock core VOC measurements are highly location-specific in a fractured rock environment. Therefore, significant extrapolation is required to estimate the VOC mass over the entire treatment area [although it should be noted that this is not typically a primary goal of rock matrix analyses].

**Isotopic Analyses.** The costs for isotopic analyses are well defined and consist primarily of field labor to collect samples and laboratory analytical costs. Factors that may affect the performance of isotopic analyses are similar to those that exist for any field sampling effort involving collection of samples for laboratory chemical analyses. These include field protocols as well as laboratory protocols. Numbers of analyses required (in space and time) vary from site to site and from technology to technology. Collecting samples from the right places at the right times is key. Blended samples from longer monitoring intervals provides diluted effects and may mask important shifts. Also, adequate initial characterization is required to effectively monitor isotopic shifts.

**Mass Flux Analyses.** The costs for the integrated mass flux pumping tests consist of well installation costs, sampling labor, supplies, VOC analytical tests, and water handling and disposal charges. One of the primary factors that affects performance of this tool is the ability to achieve steady-state capture of the contaminated plume. The costs for mass discharge analyses via transect monitoring include well installation costs, multi-level system costs, geophysical tests to determine borehole transmissivities, sampling labor, supplies, and VOC analytical tests. Several factors affect performance of this technique, including application of transmissivity estimates over relatively large screened intervals and potential inaccuracies in transmissivity estimates. Likewise, potential inaccuracies in mass flux calculation will arise from the difficulty of measuring or estimating the hydraulic gradient in fractured rock, both in individual fractures and the groundwater flow system as a whole.

**Laboratory Testing.** The costs for laboratory testing consist primarily of labor for setup of laboratory experiments as well as costs for supplies and analytical costs. Costs for these tools are more difficult to quantify than those for the other tools because there are no well-defined endpoints, and this tool can be continually refined. There are many factors that could affect performance for these tools. The laboratory techniques being used to estimate diffusion of permanganate into the shale matrix are fairly standard techniques (but generally not widely available on a commercial basis), but the application is new.

**Numerical Modeling.** Simulation of reactive transport in fractured porous media and relevant processes (e.g., for in-situ remediation applications such as ISCO) is highly complex and not well-understood or incorporated into currently available models. It is therefore largely in the research domain. Also, many of the relevant parameters required for numerical modeling in fractured rock are not well-defined.

## 2.4 Advantages and Limitations of the Technology

Table 2-2 lists the capabilities and limitations of each of the diagnostic tools evaluated herein.

**Table 2-2: Capabilities and Limitations of Diagnostic Tools**

| Diagnostic Tool | Capabilities | Limitations |
|---|---|---|
| 3-Dimensional sampling using MLSs and nested wells | • Assess spatial variability of plume concentrations<br>• Determine vertical characteristics of treatment area including hydraulic, contaminant, and geochemical parameters<br>• Monitor vertical distribution of permanganate relative to contaminants<br>• Identify areas of predominant contaminant flux | • Requires the collection of numerous samples at any single well location and analysis of samples at additional cost |
| Rock Matrix Analysis | • Understand diffusion rates from preliminary testing including chloride diffusion coefficient<br>• Confirm diffusion of contaminants into rock matrix<br>• Identify active flow paths that are too small for detection using hydrogeophysical techniques<br>• Identify contaminant flow paths not discerned from aqueous phase sampling | • Very location-specific; results can differ when sample location moved by very small distance<br>• Requires collection of numerous samples (e.g., one sample per foot of core)<br>• Currently not available commercially |
| Isotopic Analysis | • Distinguish between VOC destruction via oxidation vs. displacement<br>• Chart active flow paths and fracture connections | • Relatively specialized analysis<br>• Additional costs for analyzing samples |
| Mass Flux Measurement | • Clearly demonstrate rate of contaminant mass releases from treatment zone<br>• Use as regulatory metric (e.g., RCRA EI) | • Difficult to quantify transmissivities and hydraulic gradients in fractured rock<br>• Not proven in fractured rock<br>• Degree of uncertainty in monitoring flow zones (e.g., backdoor fractures conveying mass past the discharge plane) |
| Rock oxidant demand tests and permanganate invasion studies | • Understand and quantify processes / controls on specific remediation technologies | • Uncertainty in scaling up lab-scale measurements to field setting |

| Diagnostic Tool | Capabilities | Limitations |
|---|---|---|
| Numerical Modeling | • Predict long-term remediation performance | • Simplifying assumptions limit accuracy of the model<br>• Process understanding and parameterization and incorporation in models for fractured rock applications largely in research domain<br>• Appropriate resolution of applicable processes / site-specific parameters unknown |

# 3.0 DEMONSTRATION DESIGN

This section describes the overall design of the technology demonstration and the implementation of the innovative diagnostic tools to characterize the site and to evaluate remedial performance. The detailed performance objectives are presented first, followed by a description of the selected site and its characteristics. A description of the CM is then presented, as this is required to provide a context for understanding the application of the diagnostic tools. Current operations at the site, as well as previous testing, are then briefly discussed. This is followed by a detailed description of the demonstration test.

## 3.1 Performance Objectives

The objectives of the demonstration were to evaluate innovative diagnostic tools used to:

1. Characterize the site to allow development / evaluation of the site conceptual model, and for selection of a remedial technology, and;
2. To monitor performance of ISCO treatment of a chlorinated solvent source area in fractured bedrock.

A comparison of the new diagnostic tools with conventional monitoring methods was performed (when possible/applicable), and the utility and cost effectiveness of the new methods was evaluated. It should be reiterated that the ESTCP demonstration was performed concurrently with a CM under a RCRA consent order agreement between the WVA, NYSDEC, and the USEPA. Accordingly, the diagnostic tools were utilized in conjunction with the consent order program and direct comparison of diagnostic tools was not always possible due to differing conditions and/or uses at the WVA. Performance criteria used to achieve the objectives are identified specifically in Table 3-1.

## Table 3-1: Performance Objectives

| Analytical Objective | Conventional Diagnostic Tool | Performance Metrics for Conventional Tool | Innovative Diagnostic Tool | Performance Metrics for Innovative Diagnostic Tool |
|---|---|---|---|---|
| **Qualitative** | | | | |
| Demonstrate that new diagnostic tools improve the implementation and optimization of ISCO using permanganate in fractured rock | Single point monitoring wells<br><br>Analyses of parameters such as VOCs, permanganate, ORP, sulfate, chloride and inorganics | Measure concentrations of parameters such as VOCs, permanganate, ORP, sulfate, chloride, and inorganics in two dimensions | Multi-level sampling systems and nested wells<br><br>Flux analyses using integrated mass flux testing and a transect of multi-level wells at the site boundary<br><br>Carbon isotope analyses as well as oxygen and deuterium isotope analyses<br><br>Rock matrix VOC analyses<br><br>Numerical modeling and laboratory analyses | Same performance metrics as for conventional tools, but evaluation of data in three dimensions<br><br>Compare the performance of several types of multi-level sampling systems in a fractured rock setting<br><br>Assess efficacy of ISCO using multi-level wells to determine zones of high contaminant flux. This differs from conventional metrics based on single point concentration data<br><br>Confirm VOC mass destruction using carbon isotopes<br><br>Determine distribution of VOCs in the rock matrix at discrete borehole locations<br><br>Optimize remedial strategy via numerical modeling combined with lab studies to interpret results and improve design, such as by optimizing time between $MnO_4$ injections to assessing impacts of diffusion of VOC mass back out of the shale matrix |
| **Quantitative** | | | | |
| Determine vertical and horizontal permanganate distribution, permanganate residence time, VOC concentrations over time, and mass flux across property boundary | Single point sampling wells<br><br>Analyses of parameters such as VOCs, permanganate, ORP, sulfate, chloride and inorganics | Determine VOC and permanganate concentrations vs. time in two dimensions<br><br>Determine baseline concentrations of all analytes in two dimensions | Multiple port sampling wells<br><br>Flux analyses using integrated mass flux testing and a transect of multi-level wells at the site boundary<br><br>Carbon isotope analyses | Assess same performance metrics as described for conventional tools except in three dimensions<br><br>Determine relative percent difference between calculated discharge using each of two methods and determine sensitivity and cost<br><br>Assess baseline conditions for stable carbon isotopes and monitor changes with time in three dimensions |

## 3.2 Selected Test Site

The area near Building 40 on the WVA was selected as the demonstration site. This site was selected for this demonstration to compliment funds already expended by the U.S. Army on detailed site characterization and on a pilot-scale study of ISCO. Extensive hydrogeologic studies were performed in conjunction with the U.S. Geological Survey in the bedrock aquifer in the vicinity of Building 40 (Williams and Paillet, 2002a). These studies have led to a unique understanding of the site hydrogeology on a fracture scale, allowing for more insightful data interpretation.

## 3.3 Pre-Demonstration Testing and Analysis

Initial characterization of fractures and flow zones at the WVA site was performed in 2001 (see Appendix E). A pilot study for ISCO using permanganate was completed in 2002 (see Appendix F). Boundary monitoring wells required for the CM were installed in October 2003 (see Section 3.6.1.4). Baseline rock crushing analyses were performed on several boreholes, including MW-87 (one of the designated ESTCP technology wells) in October 2003. Geophysical tests were performed at the nested boundary wells in May 2004 to determine borehole flow and transmissivity parameters.

## 3.4 Testing and Evaluation Plan

This section describes site activities required to implement the innovative diagnostic tools demonstration coincident with performance of full-scale remedial action at the WVA. Additional work items that were required to implement the evaluation of the diagnostic tools above and beyond what was required for implementation of the CM are as follows:

- Additional drilling and rock coring for new monitoring wells
- Additional hydraulic testing for new wells
- Additional sample collection and analysis for samples collected for rock core analysis
- Additional sample collection and analysis for samples collected from MLSs
- Additional sample collection and analysis for carbon isotopes, CVOCs, and geochemical parameters
- Laboratory supplies, equipment and labor for performing permanganate invasion tests and rock oxidant demand tests

### 3.4.1 *Demonstration Installation and Start-Up*

The selected diagnostic tools do not require the use of permanent above-ground structures or utilities. Specific elements of demonstration set-up and start-up are described below.

#### 3.4.1.1 *Multi-Level Monitoring Diagnostic Tools*

Table 3-2 provides a summary of the designs of all of the MLSs and well nests at the WVA. Figure 1-2 shows the locations of all of the MLSs and well nests. The boreholes in which these MLSs and wells are used range in diameter from 4 to 6 inches and the borehole depths range

from 65 to 160 feet. The spatial arrangement of the various boreholes and the sequence of uses of the different systems were driven by the evolution of site requirements during the site investigation and corrective measures. Therefore, the uses of the MLSs and wells were not selected to accommodate rigorous comparisons of advantages/disadvantages or performance. The following sections provide the construction and installation details of each of these systems. A discussion of the performance of each system is provided in Section 4.0.

**Table 3-2: Summary of MLSs and Well Nests at the WVA**

| | | | | | Monitoring Interval Lengths (ft) | |
|---|---|---|---|---|---|---|
| **System** | **Well ID** | **Total Depth (ft)** | **Borehole Diameter (inches)** | **# Monitoring Zones** | **Min** | **Max** |
| **Multilevel Monitoring Systems** | | | | | | |
| CMT | MW-74 | 131 | 4 | 6 | 15 | 16 |
| | MW-75 | 150 | 4 | 5 | 15 | 20 |
| Westbay | MW-65 | 160 | 4 | 7 | 15 | 20 |
| | MW-68 | 65 | 4 | 2 | 20 | 20 |
| | MW-71 | 100 | 4 | 3 | 15 | 25 |
| | MW-72 | 110 | 4 | 3 | 20 | 20 |
| | MW-67 | 145 | 4 | 5 | 20 | 25 |
| | MW-78 | 140 | 4 | 3 | 15 | 55 |
| FLUTe | MW-79 | 147 | 4 | 9 | 10 | 10 |
| | IW-1 | 150 | 6 | 9 | 5 | 10 |
| | IW-2 | 150 | 6 | 9 | 5 | 10 |
| | IW-3 | 148 | 6 | 9 | 10 | 10 |
| | IW-4 | 147 | 6 | 9 | 10 | 10 |
| **Conventional Well Nests** | | | | | | |
| Barcad (ZIST) | MW-87 | 150 | 4 | 3 | 10 | 10 |
| Traditional (Nested) | MW-81 | 150 | 6 | 3 | 30 | 40 |
| | MW-82R | 150 | 6 | 3 | 30 | 35 |
| | MW-83 | 150 | 6 | 3 | 30 | 40 |
| | MW-84R | 150 | 6 | 3 | 35 | 35 |
| | MW-85R | 150 | 6 | 3 | 30 | 35 |
| | MW-86R | 150 | 6 | 3 | 30 | 35 |

## Westbay System

Monitoring wells MW-65, MW-68, MW-71, MW-72, MW-76, and MW-78 were equipped with Westbay MP38 Multi-Level systems as part of the 2002 Pilot Study (Table 3-3). The number of monitoring zones per well ranged from two (MW-68) to seven (MW-65) and the maximum depth to which the system was installed was 160 feet bgs. The Westbay system was used for injecting potassium permanganate into the subsurface, monitoring permanganate distribution during the Pilot Test, further characterizing contaminant distribution at Building 40, and conducting hydraulic tests.

**Table 3-3: Westbay System Well Construction Details**

| Multi-level System | Monitoring Well | Zone ID | Monitoring Zone (feet bgs) |
|---|---|---|---|
| Westbay | MW-65 | 1 | 20-40 |
| | | 2 | 45-60 |
| | | 3 | 65-80 |
| | | 4 | 85-100 |
| | | 5 | 105-120 |
| | | 6 | 125-140 |
| | | 7 | 145-160 |
| Westbay | MW-68 | 1 | 20-40 |
| | | 2 | 45-65 |
| Westbay | MW-71 | 1 | 25-50 |
| | | 2 | 55-80 |
| | | 3 | 85-100 |
| Westbay | MW-72 | 1 | 40-60 |
| | | 2 | 65-85 |
| | | 3 | 90-110 |
| Westbay | MW-76 | 1 | 20-45 |
| | | 2 | 50-70 |
| | | 3 | 75-95 |
| | | 4 | 100-120 |
| | | 5 | 125-145 |
| Westbay | MW-78 | 1 | 20-35 |
| | | 2 | 40-80 |
| | | 3 | 85-140 |

## CMT® System

Monitoring wells MW-74 and MW-75 at WVA were equipped with a CMT® Model 403 multi-level system as part of the Pilot Study (Table 3-4). There were six monitoring zones at MW-74 and five monitoring zones at MW-75. The depths at which the systems were installed to were 131 feet bgs at MW-74 and 150 feet bgs at MW-75. The CMT® system was used to further characterize contaminant distribution at Building 40 and to monitor permanganate distribution during the Pilot Study and full-scale corrective measures.

**Table 3-4: CMT® System Well Construction**

| Multi-level System | Monitoring Well | Zone ID | Monitoring Zone (feet bgs) |
|---|---|---|---|
| CMT® | MW-74 | 1 | 20-36 |
| | | 2 | 40-55 |
| | | 3 | 59-74 |
| | | 4 | 78-93 |
| | | 5 | 97-112 |
| | | 6 | 116-131 |
| CMT® | MW-75 | 1 | 20-40 |
| | | 2 | Open* |
| | | 5 | 97-112 |
| | | 6 | 116-131 |
| | | 7 | 135-150 |

Open* - Bridged at 40 feet bgs

## Water FLUTe™ System

Injection wells IW-1, IW-2, IW-3, IW-4, and MW-79 at WVA were equipped with Water FLUTe™ systems as part of the CM program (Table 3-5). Nine ports were installed in each of the injection wells for purging and sampling and the depth of each well was approximately 150 feet bgs at the WVA. The FLUTe™ system was used to further characterize contaminant distribution at Building 40 and to monitor permanganate arrival during the initial CM injections (with the understanding that the systems were to be removed upon permanganate arrival – See Section 5.0).

**Table 3-5: FLUTe™ System Well Construction at WVA**

| Multi-level System | Monitoring Well | Zone ID | Monitoring Zone (feet bgs) | Multi-level System | Monitoring Well | Zone ID | Monitoring Zone (feet bgs) |
|---|---|---|---|---|---|---|---|
| FLUTe™ | MW-79 | 1 | 17-27 | FLUTe™ | IW-3 | 1 | 18-28 |
| | | 2 | 32-42 | | | 2 | 33-43 |
| | | 3 | 47-57 | | | 3 | 48-58 |
| | | 4 | 62-72 | | | 4 | 63-73 |
| | | 5 | 77-87 | | | 5 | 78-88 |
| | | 6 | 92-102 | | | 6 | 93-103 |
| | | 7 | 107-117 | | | 7 | 108-118 |
| | | 8 | 122-132 | | | 8 | 123-133 |
| | | 9 | 137-147 | | | 9 | 138-148 |
| FLUTe™ | IW-1 | 1 | 25-35 | FLUTe™ | IW-4 | 1 | 17-27 |
| | | 2 | 40-50 | | | 2 | 32-42 |
| | | 3 | 55-65 | | | 3 | 47-57 |
| | | 4 | 70-80 | | | 4 | 62-72 |
| | | 5 | 85-95 | | | 5 | 77-87 |
| | | 6 | 100-110 | | | 6 | 92-102 |
| | | 7 | 115-125 | | | 7 | 107-117 |

| Multi-level System | Monitoring Well | Zone ID | Monitoring Zone (feet bgs) | Multi-level System | Monitoring Well | Zone ID | Monitoring Zone (feet bgs) |
|---|---|---|---|---|---|---|---|
| | | 8 | 130-140 | | | 8 | 122-132 |
| | | 9 | 145-150 | | | 9 | 137-147 |
| FLUTe™ | IW-2 | 1 | 25-35 | | | | |
| | | 2 | 40-50 | | | | |
| | | 3 | 55-65 | | | | |
| | | 4 | 70-80 | | | | |
| | | 5 | 85-95 | | | | |
| | | 6 | 100-110 | | | | |
| | | 7 | 115-125 | | | | |
| | | 8 | 130-140 | | | | |
| | | 9 | 145-150 | | | | |

## ZIST™ System

Monitoring well MW-87 was equipped with a ZIST™ system as part of the CM program (Table 3-6). The ZIST™ system consisted of three screened intervals and the depth of the well was approximately 150 feet bgs. The ZIST™ system was used to further characterize contaminant distribution at Building 40 and to monitor permanganate distribution in the area between the injection wells and the compliance boundary during the CM. As part of the CM, the ZIST™ system, consisting of the pump and sensors, was also tested to evaluate its function in the presence of permanganate.

**Table 3-6: ZIST™ System Well Construction**

| Multi-level System | Monitoring Well | Zone ID | Monitoring Zone (feet bgs) |
|---|---|---|---|
| ZIST™ | MW-87 | 1 | 40-50 |
| | | 2 | 90-100 |
| | | 3 | 140-150 |

## Nested Wells

### *Description*

The compliance boundary monitoring wells, MW-81, MW-82R, MW-83, MW-84R, MW-85R, and MW-86R, at the WVA were all outfitted with three-zone nested well systems (Table 3-7). The three nested wells were 150 feet in depth and constructed using 30 to 40 feet screens and PVC riser pipe to the ground surface. The nested wells are constructed and installed within one borehole in the same manner as a single monitoring well. Since static water levels in all of the monitoring zones at the WVA are less than 20 feet bgs, purging and sampling is

conducted using dedicated tubing and a peristaltic pump. The nested wells were used to further characterize contaminant distribution at the Building 40 compliance boundary and to allow for the estimation/calculation of the compliance boundary VOC mass discharge. MLSs and ZIST were not utilized for these wells as it was necessary to maintain the option for permanganate injection if required during the later stages of the remedial program. As discussed further in Section 4.0, the Westbay system was the only MLS installed at the WVA that could be utilized for injections. However, clogging of the sampling and pumping ports by precipitates associated with oxidation of the permanganate and/or rock during the pilot study indicated that use of this MLS for full-scale permanganate injections was not viable.

**Table 3-7: Nested Well Construction**

| Multi-level System | Monitoring Well | Zone ID | Monitoring Zone (feet bgs) |
|---|---|---|---|
| Nested | MW-81 | I | 29-59 |
| | | II | 70-100 |
| | | III | 109-149 |
| Nested | MW-82R | I | 27-57 |
| | | II | 67-102 |
| | | III | 114-149 |
| Nested | MW-83 | I | 24-59 |
| | | II | 70-100 |
| | | III | 109-149 |
| Nested | MW-84R | I | 24-59 |
| | | II | 70-105 |
| | | III | 114-149 |
| Nested | MW-85R | I | 27-57 |
| | | II | 67-102 |
| | | III | 114-149 |
| Nested | MW-86R | I | 29-59 |
| | | II | 72-102 |
| | | III | 114-149 |

***Installation Methods***

Standard monitoring well installation methods were used to install the multi-level monitoring system in the compliance boundary wells. The nested wells were constructed at the borehole, starting with the deepest monitoring zone. Sand was poured around the screen and then bentonite was poured in to create a seal between adjacent zones. The next deepest well is then lowered to the top of the bentonite layer and is set using the same method as the deepest monitoring zone.

***Operation***

Water is purged and sampled using dedicated or disposable PVC tubing and a peristaltic, bladder, or double valve pump, depending on the water level. If a double valve or bladder pump is required to bring water to the surface, the pump has to be decontaminated before using in a different monitoring zone.

3.4.1.2 *Rock Matrix Analyses*

At the WVA, continuous HQ-size bedrock cores (2.5-inch diameter) were collected in five foot intervals from the competent bedrock surface to the final depth of the well from five monitoring well boreholes in 2001 and 2003 (see Table 3-8 and Figure 3-1).

**Table 3-8: Summary of Boreholes Sampled for Rock Matrix VOCs**

| Corehole ID | Start Date | End Date | Bedrock Depth (ft bgs) | Cored Interval (ft bgs) | | Total Interval Cored (ft) | Number Rock VOC Samples | Number Rock VOC Duplicates | Average VOC Sample Spacing (ft) | Number Intact Rock Samples |
|---|---|---|---|---|---|---|---|---|---|---|
| MW-74 | 5-Dec-01 | 7-Dec-01 | 18.5 | 20 | 150 | 130 | 112 | 7 | 1.16 | 12 |
| MW-75 | 10-Dec-01 | 13-Dec-01 | 16.5 | 17.5 | 150.5 | 133 | 109 | 6 | 1.22 | 10 |
| MW-80 | 14-Oct-03 | 16-Oct-03 | 10.0 | 15 | 150 | 135 | 184 | 9 | 0.73 | 13 |
| MW-83 | 17-Oct-03 | 21-Oct-03 | 14.5 | 19.5 | 200.5 | 181 | 216 | 11 | 0.84 | 15 |
| MW-87 | 22-Oct-03 | 23-Oct-03 | 12.5 | 17.5 | 151 | 133.5 | 150 | 8 | 0.89 | 12 |
| MW-88 | 23-Oct-03 | 24-Oct-03 | 13.3 | 18 | 40 | 22 | 32 | 2 | 0.69 | 3 |
| CH-91 | 4-Dec-06 | 11-Dec-06 | 14.5 | 15 | 150 | 135 | 161 | 10 | 0.84 | 14 |
| | | | | | **Totals** | **869.5** | **964** | **53** | **0.90** | **79** |

Samples from these cores were collected and analyzed using the techniques described in Section 2.1.2. Average parameter values for porosity and bulk (dry) density measured on representative site rock core samples by Golder Associates (Table 1-2; Mississauga, Ontario, Canada) were used for estimating equivalent porewater concentrations from the lab-measured total concentrations. Distribution coefficients were estimated using the correlation $K_d = K_{oc}\ f_{oc}$, and literature values of 380, 92 and 86 mL/g for PCE, TCE and cDCE, respectively were used for the organic carbon partitioning coefficients ($K_{oc}$) (Table 12.1, Pankow and Cherry, 1996). Fraction organic carbon ($f_{oc}$) was measured by the Organic Geochemistry Lab at UW, according to the procedure outlined by Churcher and Dickhout (1987). Based on fifteen samples collected from MW-74 and MW-75, $f_{oc}$ ranged from 0.31% to 0.68%, with an average of 0.40% which was used in the retardation factor estimates. (Note these $f_{oc}$ estimates are slightly higher than those for samples from five other cores, as presented in Table 1-2.) Using these parameters, average retardation factors of 177, 44 and 41 were estimated for PCE, TCE and cDCE,

respectively. For samples where the estimated pore water concentration approaches or exceeds the aqueous solubility (~200 mg/L for PCE and 1,100 mg/L for TCE; Table A1, Pankow and Cherry, 1996), it is possible that DNAPL was present in the fracture adjacent to where the sample was collected. However, such inferences must be made with caution, considering uncertainty in parameters used to estimate the pore water concentrations, particularly the estimated retardation factors (for example, the effect of metamorphism on the sorption capacity of the organic carbon is not known).

**Figure 3-1: Rock Coring Locations**

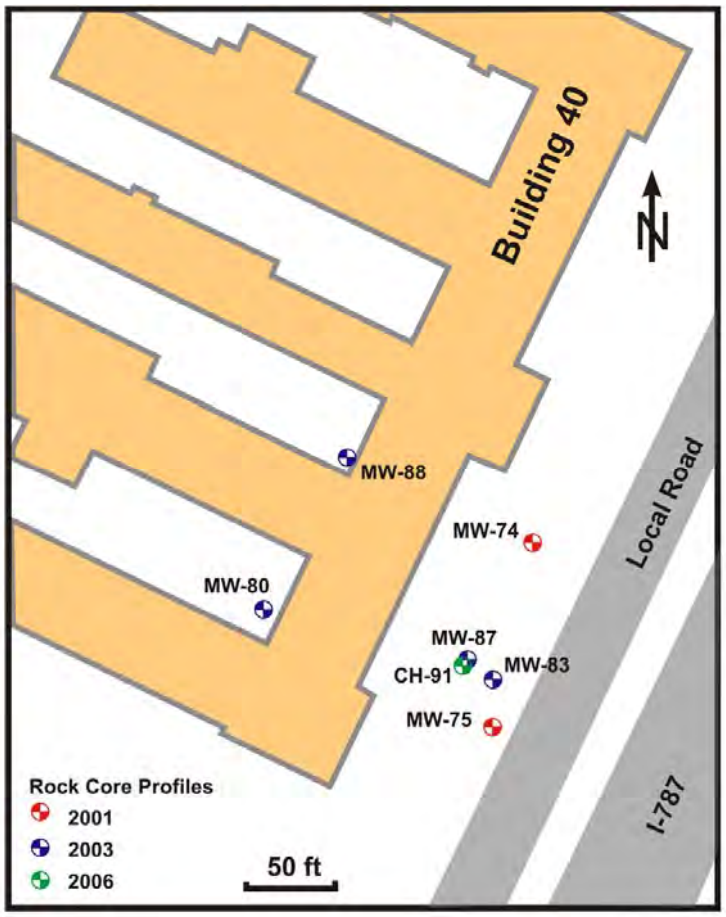


3.4.1.3 *Mass Flux Analyses*

The mass that the source zone is contributing to the larger dissolved phase plume is an important attribute to determine, from both risk assessment and treatment performance perspectives. The source strength, or mass discharge, is defined as the rate at which contaminants pass through a defined cross-sectional area perpendicular to groundwater flow. Given the difficulty in locating and removing contaminant mass at the WVA, mass-based metrics were

used to formulate an exit strategy, using mass discharge across the property boundary, where the multi-level wells are located, to monitor treatment progress. At the WVA, two techniques were used to estimate mass discharge: an integrated pump test and multi-level sampling and testing along the property boundary.

***Integrated VOC Mass Discharge Testing***

The integrated pump test relies on capturing all of the contaminated groundwater flowing within the plume, using one or more extraction wells. At the WVA, the testing consisted of a 12-hour constant rate pumping test during which groundwater samples were collected from the purged groundwater on an hourly basis and water levels were measured in the surrounding monitoring wells to evaluate the pumping radius of influence and overall hydraulic characteristics of the bedrock aquifer. The test was performed at injection well IW-2, which is located adjacent to the eastern side of Building 40 in the central portion of the VOC treatment area.

The pumping test was designed to extract water from the treatment area to evaluate contaminant discharge under known conditions (i.e., constant pumping rate). Water level measurements were recorded in 20 wells in the Building 40 vicinity prior to the pumping test to establish static water level conditions. Electronic pressure transducers (data loggers) were then installed in seven of these wells. Water levels in the remaining wells were measured manually using an electronic water level probe.

A submersible pump was positioned ten feet above the bottom of the borehole in injection well IW-2. The pump discharge hose was connected to an in-line flow meter capable of measuring flow to the nearest 0.1 gallons per minute (gpm). The pump test rate was maintained at 1 gpm. To ensure that discharge from the pump test did not provide recharge to the bedrock and to facilitate proper disposal of the purged groundwater, extracted water was temporarily staged in two 1,000 gallon polyethylene tanks during the pumping test. Water levels were measured continually during the pump test. The interval between measurements was approximately 10 minutes for the first hour of the test, 30 minutes for the second hour, and an hour for the remainder of the test.

Pumping test data were evaluated by comparing drawdown verses time relationships for each monitoring well using Theis and Neumann theoretical curves. Both of these methods assume that the aquifer is comprised of homogeneous porous media. For the purposes of this analysis, it was assumed that the bedrock aquifer would behave in a manner equivalent to that of a porous media. This assumption was based on the relatively high degree of fracture connectivity observed through the geophysical testing, as well vertical hydraulic head profiles that showed a generally constant upward trend in head between deep and shallow monitoring zones, indicating that the aquifer was relatively well connected. Water level data were plotted on log-log graph paper using the same scale as the Theis and Neumann “type curves”. Several of the observation wells and individual zones of multilevel wells monitored during the pumping test had erratic water level readings that rendered the data unusable for type curve matching. Values for

transmissivity were derived for each of the remaining observation wells once a "best fit" with the theoretical curves was obtained for the data. An average transmissivity for the pumping test area was then calculated.

Time-series VOC sampling was conducted during the pumping test to evaluate integrated (average) contaminant concentrations in the treatment area. Twelve groundwater samples were collected from the injection well IW-2 purge water during the pumping test from the pump discharge line. One sample was collected at the start of the test and one sample was collected every subsequent hour throughout the 12-hour test period. Samples were analyzed for VOCs by USEPA Method 8260B; magnesium, potassium, and sodium by USEPA Method 6010B; chloride and sulfate by USEPA Method 300; alkalinity by USEPA Method 310.1; and total dissolved solids (TDS) by USEPA Method 160.1. Prior to collecting each sample, conductivity, dissolved oxygen, oxidation-reduction potential, pH, temperature, and turbidity were measured.

***Boundary VOC Mass Discharge***

Borehole geophysical testing was conducted in boundary monitoring wells MW-81, MW-82R, MW-83, MW-84R, MW-85R, and MW-86R upon the completion of well installation and development in early July 2004. The objectives of the geophysical characterization were to:

- Evaluate groundwater flow parameters (i.e., transmissivity) in each boundary well borehole and in each of the anticipated monitoring zones; and
- Identify the depth and nature (i.e., width and relative flow) of major fractures intersecting each boundary well borehole.

The geophysical evaluation was designed to assess groundwater flow parameters (i.e., degree of hydraulic connection and transmissivity) in each of the compliance boundary monitoring wells. A secondary objective of the geophysical investigation was to identify the depth and nature (i.e., aperture and dip) of major fractures intersecting the borehole so that monitoring zones could be adjusted accordingly.

The following tests were performed in each boundary monitoring well:

- Gamma Ray;
- Spontaneous Potential (SP);
- Single Point Resistance (SPR);
- Short and long normal Resistivity (MW-81 and MW-83);
- 3-Arm Caliper;
- Fluid Temperature;
- Fluid Resistivity;
- Acoustic Televiewer
- Optical Televiewer (OBI);
- Full Waveform Sonic; and
- Heat pulse flow meter under ambient and pumping conditions.

During logging, fractures were identified in each borehole based on the combination of results from the various instruments. Single borehole heat pulse flow meter testing was then conducted to evaluate flow at each of the identified fractures and in the borehole as a whole. Limited cross borehole testing was then conducted at select wells to evaluate connectivity. The results of the geophysical testing are summarized in Table 1-3. Transmissivity calculations were performed using the same methods (United States Geological Survey (USGS) flow modeling code FWRAP) as those used previously at the WVA (see *Characterization of Fractures and Flow Zones in a Contaminated Shale at the Watervliet Arsenal, Albany County, New York: USGS Open File Report 01-385* (Williams and Paillet, 2002a)). As shown in Table 2-2, several fractures transmitting groundwater flow were found in each borehole; however, there are two highly transmissive fracture zones that are present along the compliance boundary. These fracture zones appear to be nearly planar sub-parallel features comprised of interconnected fractures dipping in many directions and with widths ranging from less than one foot to greater than several feet. Both features dip to the east and plunge to the north. The first feature, which was identified during previous testing at the WVA, intersects monitoring well MW-86R (94 feet bgs), MW-85R (77 feet bgs), MW-84R (49 feet bgs), and possibly, MW-83 (~36 feet bgs). This zone also appears to intersect MW-59 (91 feet bgs), MW-71 (65 feet bgs) and MW-34 (24 feet bgs). The second feature intersects MW-83 (121 feet bgs), MW-82R (94 feet bgs), and MW-81 (78 feet bgs), and probably in MW-65 (111 feet bgs). Cross-borehole testing shows that there is a connection between these two fractures features; however, the nature of this connection could not be identified during the testing.

Compliance boundary VOC mass discharge estimates were calculated for each compliance monitoring zone using the transmissivity values calculated for fractures that had detectable flow during the July 2004 geophysical testing. Mass discharge estimates were calculated as described in Section 4.3.2

#### 3.4.1.4 *Rock Oxidant Demand Tests and Permanganate Diffusion Studies*

Two types of laboratory studies were conducted: rock oxidant demand studies and tests to examine permanganate diffusion and reaction into the Snake Hill shale in a static system. Various studies were conducted from 2002 (i.e., during the Pilot Study trial) to 2005.

**Rock Oxidant Demand Tests**

The initial rock oxidant demand tests involved batch tests conducted on three representative rock core samples obtained from MW-74 and MW-75 to evaluate the permanganate rock oxidant demand (ROD) exerted by the shale, and to perform a preliminary assessment of the main contributors to the ROD. For the batch tests, subsamples of the sections of rock core were first manually broken into small fragments, and then crushed to a fine powder using a ring mill. The batch tests were initiated by placing approximately 10 grams (g) of crushed rock from each of the three samples into 125-millileter (mL) Erlenmeyer flasks and then adding ~100 mL of $KMnO_4$ solution. The tests were set up with three different initial concentrations of $KMnO_4$ solution: 1, 5, and 20 g/L (0.1, 0.5, and 2.0 percent by weight,

respectively). Aliquots of the solution were removed from the flasks at several times during the tests for $KMnO_4$ determination and estimation of the variation of ROD exerted over time. A second set of batch tests were conducted using sodium permanganate (NaMnO4) on two of the three samples for which the $KMnO_4$ batch tests were performed. The purpose of these tests was to investigate the dependence of the ROD on permanganate concentration using higher concentrations achievable with $NaMnO_4$. As with the $KMnO_4$ tests, three different initial concentrations of $NaMnO_4$ were used: 20, 50, and 100 g/L (2.0, 5.0, and 10.0 percent by weight, respectively). For comparison at the lower end, a parallel test was also performed using $KMnO_4$ at 20 g/L (2.0 percent by weight). Pre- and post-oxidation samples of the batch test solids from both tests were analyzed for fraction organic carbon. Post-oxidation samples from both batch tests were analyzed for sulfate concentrations using ion chromatography (IC) following reduction of any remaining permanganate with glucose. Sulfate concentrations determined from the IC analyses were used to evaluate the contribution of pyrite oxidation to the measured ROD. Results of this testing are described in Section 4.3.5.1.

**Permanganate Diffusion Testing**

Laboratory testing was initiated in September 2002 to measure the rate of permanganate invasion into the Snake Hill shale. The goal of the testing was to have rock core samples in contact with KMnO4 solution for a period of time during which diffusion into the core would take place. The initial plan called for the cores to be examined at various time intervals to determine the distance of KMnO4 invasion. This would be done by splitting the core to observe the invasion distance from the KMnO4 contact surface visually based on color change and also by chemical analyses of small samples obtained from the core by saw cutting or miniature core drilling. Several of these core diffusion experiments were to be set up to run concurrently and sacrificed over time so that the invasion distances after different invasion period could be determined.

The invasion tests were initiated on September 6, 2002. Five samples from intact rock (approximately 1 cm x 2 cm x 3 cm each) were immersed in a 2% potassium permanganate solution. The test samples were removed at 2, 4, 6, 12, and 24 months following immersion. Initially, it was thought that diffusion zones would be visible (i.e., would turn from black to dark brown) and could be chipped from the cores for analysis. However, given the very low permeability of the Snake Hill shale, diffusion rates were very slow and not visible over the span of the invasion tests. Therefore, following removal of each sample, thin-sections were prepared at the University of New Brunswick (UNB) by cutting along the longitudinal axis and mounting, so that the resulting section was about 3 cm by 1 cm with a thickness of about 200 microns. The thin sections were then analyzed for various elements using Laser Ablation Microprobe (LAM) ICP-MS analyses. This technique was used for the first three samples. However, the laser beam diameter (~50 microns) was of insufficient resolution to assess permanganate invasion in the thin-sections, as permanganate diffusion distances were less than 50 microns. Therefore, the remainder of the samples (as well as the three initial samples) were analyzed via scanning electron microscopy (SEM) and energy dispersive spectrometer (EDS).

### 3.4.2 *Period of Operation*

Although the ESTCP project for which this report has been prepared took place during the period of 2003 to 2007, the project was based on experience using diagnostic tools and data obtained over a much longer time period. Section 1.0 includes a summary of six study phases during which the WVA site was characterized and remedial actions using permanganate ISCO were performed.

### 3.4.3 *Residuals Handling*

Residuals that were generated during this technology demonstration included water generated during well development and equipment decontamination, purge water from sampling, drilling cores, field test kit wastes, sampling equipment decontamination wastes, and personal protective equipment (PPE). Water generated during well development, decontamination activities, and purge water generated during sampling, was temporarily stored in a tank(s), and was disposed in accordance with local, state, and federal regulations. Drill cuttings were containerized in drums for off-site disposal.

### 3.4.4 *Operating Parameters for the Technology*

Operating parameters for the technologies are discussed in detail in Section 3.4.5 below.

### 3.4.5 *Sampling Plan*

Table 3-9 summarizes the sample collection strategy. Injection and monitoring locations are illustrated on Figure 1-2. MLSs and well nests are detailed in Table 3-2. The monitoring network was designed to evaluate the following parameters:

- Horizontal and vertical distribution of CVOCs in groundwater;
- Horizontal and vertical distribution of permanganate during and after injections;
- CVOC mass flux within the treatment area (integrated flux) and across the property boundary discharge face (boundary flux);
- Horizontal and vertical distribution of the injection treatment/displacement zone; and
- Changes in rock matrix CVOC concentrations.

The sampling locations were grouped as follows:

- Property Boundary Wells: MW-81, MW-82R, MW-83, MW-84R, MW-85R, MW-86R
- Intermediate Wells: MW-79, MW-80
- ESTCP Technology Evaluation Wells (ESTCP Wells): MW-74, MW-87
- Rock Matrix Evaluation Well: MW-87

**CVOC Monitoring**

CVOC monitoring was conducted at the property boundary, which was designated as the compliance point for the corrective action program. The property boundary monitoring network consisted of six multi-level bedrock monitoring wells. CVOC monitoring was also conducted at the Intermediate and ESTCP Wells located up gradient of the property boundary. Baseline samples were collected from all wells prior to the initiation of permanganate injections. CVOC

samples were collected from all zones in the wells that did not contain permanganate during the injection period. Field parameters, including chloride and specific conductivity, were also monitored during CVOC sampling events.

**Permanganate Distribution and Injection Treatment Zone Monitoring**

Permanganate distribution and injection displacement zone monitoring was conducted at the Property Boundary, Intermediate, and ESTCP Wells and consisted of the following parameters:

- Permanganate presence and concentration: Presence of permanganate was used to evaluate distribution. Permanganate concentrations were used to evaluate residence time and efficacy of injections.
- Stable isotopes: Carbon isotope ratios were used to monitor the destruction of CVOCs.
- Geochemical parameters: Geochemical parameters were used to evaluate the effects of the permanganate on groundwater conditions and to evaluate the boundaries of the injection treatment zone.
- Inorganic precipitates: Visual observations of the presence/absence of inorganic precipitates resulting from reaction of the rock with the permanganate (i.e., managanese dioxide and iron/sulfur oxides) were utilized to empirically assess whether such precipitates could potentially contribute to clogging of the injection wells and/or fracture systems.

**Mass Flux Monitoring**

Mass discharge was monitored at the Property Boundary Wells before and after individual permanganate injections. Transmissivities derived from pre-injection borehole testing were used for the groundwater discharge. CVOC concentrations in groundwater samples collected during the injection monitoring events were used to calculate changes in CVOC mass discharge as the treatment program progressed. Integrated mass discharge testing was performed prior to initiation of permanganate injections. Property Boundary, Intermediate, and ESTCP wells were monitored for hydraulic response during the testing. The pumping well for the integrated mass discharge testing was the injection well with the greatest CVOC concentrations prior to the initiation of permanganate injections.

**Rock Matrix Evaluation**

Field rock matrix invasion and CVOC concentrations were evaluated prior to injection and 2.5 years after injections at monitoring well MW-87.

**Table 3-9: Sampling Strategy Summary**

| Monitoring Element | Purpose | Wells | Analyses | Frequency |
|---|---|---|---|---|
| CVOC Monitoring | Evaluate changes in CVOC groundwater concentrations | Property Boundary, Intermediate, and ESTCP Wells | • CVOCs<br>• Field parameters | Prior to each injection event |

| Monitoring Element | Purpose | Wells | Analyses | Frequency |
|---|---|---|---|---|
| Permanganate Distribution Monitoring | Evaluate permanganate distribution and residence time | Property Boundary and Intermediate Wells | • Permanganate | Monthly (initial)* |
| Treatment Zone Monitoring | Evaluate area affected by injections. | Property Boundary, Intermediate, and ESTCP Wells | • Permanganate<br>• Carbon isotopes<br>• Field parameters | 2 weeks after each injection |
| Property Boundary Mass Flux Monitoring | Evaluate CVOC mass flux across property boundary | Property Boundary Wells | • CVOCs | Prior to each injection event |
| Integrated Mass Flux Monitoring | Evaluate CVOC mass flux in entire treatment area | Property Boundary and Extraction Wells | • CVOCs (extraction well only) | Before first injection |
| Field Rock Matrix Evaluation | Evaluate permanganate invasion and changes in CVOC concentrations in field rock core samples | MW-87 | • CVOCs<br>• Permanganate | Prior to injections and 2.5 years after initiation of injections |

Table Notes:
* Permanganate monitoring frequency varied depending on trends in permanganate residence time in the monitored zones.

**Carbon Isotope Analyses**

Carbon isotope analyses were performed to verify that decreases in CVOC concentrations are the result of chemical oxidation, not displacement or other mechanisms. The carbon isotope data were also used to monitor the rebound in CVOC concentration during and after oxidation. The method is based on the observation that $MnO_4$ oxidation preferentially attacks the bond with the lighter carbon isotope (i.e., chlorinated compounds with the light isotope $^{12}C$ react faster than the molecules with the heavy isotope $^{13}C$). This preference causes the remaining CVOC carbon to become enriched in the heavier isotope (i.e., $^{13}C$). Once rebounding due to back-diffusion or advective transport becomes dominant, the carbon isotope composition of the CVOC will return to its original value.

The $^{13}C$ analyses are performed by mass spectrometry and reported in $\delta$ (‰) units defined as follows:

$$\delta^{13}C = (R_S - R_{ST})/R_{ST} * 1000$$

where $R_S$ and $R_{ST}$ are the $^{13}C/^{12}C$ ratio of the sample and an international standard, respectively. The analytical error is less than 0.5 ‰. Detailed information about the analytical protocol can be found in Hunkeler andAravena (2000).

During and after $MnO_4$ injection, there are three types of water in the system, classified based on chlorinated solvents status:

1. Type 1 – water with no chlorinated solvents (fully treated by $MnO_4$ - this water will be purple for a period of time).
2. Type 2 – water with remnant chlorinated solvent concentrations – some or much of the solvent mass at this location will be destroyed by $MnO_4$ oxidation.
3. Type 3 – water that will not have had any of its chlorinated solvent mass oxidized by $MnO_4$

Carbon isotope analyses were conducted on samples of Type 2 and Type 3 waters. The optimal sample type for $^{13}C$ analyses is Type 2 samples, where the solvent concentrations have declined but not disappeared completely. At the time of sampling in the field (after injections), chlorinated solvent concentrations were unknown; therefore, samples were collected for $^{13}C$ analyses along with separate samples for CVOC analyses. The UW laboratory analyzed the CVOC samples first, and based on those results selected the samples for $^{13}C$ analysis.

### 3.4.6 *Demobilization*

All equipment and materials used for implementing the technology demonstration were removed from the WVA at completion of implementation. No equipment, other than in-well sampling equipment, remains at the permanganate injection area. Wells installed as part of the ESTCP demonstration project have been left in place for future monitoring.

### 3.4.7 *Health and Safety Plan*

The site-specific Health and Safety Plan (HASP) was presented in Appendix D of the Demonstration Work Plan.

## 3.5 Selection of Analytical/Testing Methods

The selected analytical/testing methods have been identified in Section 3.5.

## 3.6 Selection of Analytical/Testing Laboratory

Samples collected during the performance of this demonstration were analyzed by the following laboratories:

| Laboratory | Types of Samples |
|---|---|
| Severn Trent Laboratories | Groundwater CVOCs |
| University of Waterloo, Dept. of Earth & Environmental Sciences | Rock core CVOCs<br>Specialized isotopic analysis |
| University of New Brunswick | Permanganate diffusion rate testing |
| PSC Analytical Services | Testing for inorganic parameters |

The laboratory addresses are as follows:

Severn Trent Laboratories
128 Long Hill Cross Road
Shelton, CT 06484
Tel: 203 929 8140
Fax: 203 929 8142

University of Waterloo
Department of Earth & Environmental Sciences
University of Waterloo
200 University Avenue West
Waterloo, Ontario N2L 3G1
Canada
Phone: (519) 888-4567

University of New Brunswick
Dr. Tom Al
Department of Geology
University of New Brunswick
Fredericton, New Brunswick E3B 5A3
P.O. Box 4400
Canada
Phone: 506-447-3189

PSC Analytical Services
5555 North Service Road
Burlington Ontario L7L 5H7
Canada
Phone: 905 332-8788

# 4.0 PERFORMANCE ASSESSMENT

## 4.1 Performance Criteria

The general performance criteria that were used to evaluate the diagnostic tools are listed in Table 4-1.

**Table 4-1: Performance Criteria**

| Performance Criteria | Description | Ranking |
|---|---|---|
| ***Multi-Level Monitoring Diagnostic Tools*** | | |
| Borehole Diameter | Borehole diameter required for the diagnostic tool | Secondary |
| Maximum depth | Maximum achievable depth of the multi-level monitoring diagnostic tool | Primary |
| Multiple Uses | Groundwater sampling and/or hydraulic head monitoring | Primary |
| Removability | Ease of system removal from hole | Secondary |
| Ease of installation | Avoidance of difficulties during installation | Primary |
| Nature of seal between monitoring intervals | Reliability of seals between monitoring intervals | Primary |
| System storage volume | Minimization of purging and sampling influence | Primary |
| Maximum purge/pumping rate | Ability to quickly purge and collect sample | Primary |
| Potential for sample bias | Factors that cause measured concentrations to be different from true formation concentrations | Primary |
| Ease of operation | Ease with which samples and /or hydraulic data may be collected | Primary |
| Durability/longevity under normal use | Materials, clogging, chemical corrosion, etc. | Primary |
| Durability/longevity when exposed to permanganate | Destruction of system due to exposure to permanganate | Secondary |
| Suitability for permanganate injection | Delivery of permanganate to fracture network | Secondary |
| Cost | Life-cycle costs | Secondary |
| ***Mass Discharge Evaluation*** | | |
| Accurate estimate of contaminant mass discharge | Contaminant mass discharge before, during, and after remedial actions | Primary |
| ***Rock Crushing*** | | |
| Quantify contaminant mass | Quantification of contaminant mass in | Primary |

| Performance Criteria | Description | Ranking |
|---|---|---|
| in rock matrix and map distribution of the mass | rock matrix | |
| Delineation of migration pathways | Identification of contaminant migration pathways | Secondary |
| ***Isotope Analyses*** | | |
| Method able to discern isotopic shifts in compound-specific stable carbon isotopes | Sufficient method sensitivity and detection limits to discern shifts that occur due to oxidation processes | Primary |
| Defensible QA/QC procedures | QA/QC procedures to quantify potential error limits and detection limits | Secondary |
| ***Laboratory Studies*** | | |
| Measure rock oxidant demand | Determination of whether ISCO using permanganate is a viable remedial action | Primary |
| Estimate permanganate diffusion distances into rock over time | Guidance of expectations regarding rock matrix treatment times and rebound monitoring time frames | Primary |

## 4.2 Performance Confirmation Methods

A Quality Assurance Project Plan (QAPP) was included as Appendix C of the project Demonstration Plan to ensure that data produced was of sufficient quality and quantity to measure the success of the project. The following six topics were presented and discussed in the QAPP:

1. Project organization and responsibilities
2. Data quality objectives
3. Laboratory analytical procedures
4. Sample collection procedures
5. Sample custody
6. Demobilization

The Data Quality Objectives (DQO) process (EPA, 1994) was used to ensure consistent and scientific evaluation of performance. The process uses qualitative and quantitative statements intended to clarify study objectives; define appropriate data types; determine appropriate conditions from which to collect the data; and specify acceptable levels of decision errors. EPA defines data quality levels as “screening” or “definitive” (EPA, 1994). Screening data are generated using rapid, less precise analytical methods with less rigorous sample preparation. Definitive data are generated using rigorous analytical methods such as approved EPA, American Society of Testing and Materials, or other well-established and documented test methods. Definitive data both identify and quantify analytes with relatively high precision and accuracy, and are typically used for compliance monitoring. Definitive data are typically used for

compliance monitoring and to confirm screening data. Decisions relevant to the performance objectives of the project as well as data required for their evaluation, data uses, and minimum data quality levels are summarized in Table 4-2. The data collection program of the DQO process is described in Section 3.4.5.

**Table 4-2: Decision Inputs**

| Decision | Data Required | Data Use | Minimum Data Quality Level Required |
|---|---|---|---|
| 1.Determine if innovative diagnostic tools provided significant benefits to operations and performance evaluations during the field demonstration | Permanganate<br>CVOCs<br>Carbon Isotope Ratio<br>Rock core VOC profiles<br>Numerical model results<br>Lab test results<br>Mass flux calculations | Performance monitoring – no quantitative action levels specified. Measurements will be made using the diagnostic tools as outlined in this work plan. The benefits of using the tools will be assessed. | Definitive |
| 2. Assess additional costs incurred using the additional diagnostic tools, as well as benefits realized by the project. | Same as above | Same as above | Same as above |
| 3. Determine if innovative diagnostic tools are more beneficial than conventional tools to assess groundwater and contaminant mass flux, contaminant degradation, and overall performance and implementation of ISCO using permanganate. | Same as above | Same as above | Same as above |

Performance confirmation metrics and methods are summarized in Table 4-2 as well as in Section 4.3.

**Table 4-3: Expected Performance and Performance Confirmation Methods**

| Performance Criteria | Expected Performance Metric | Performance Confirmation Method | Actual |
|---|---|---|---|
| ***Multi-Level Monitoring Diagnostic Tools*** | | | |
| Borehole Diameter | The expected performance metrics, performance confirmation methods, and actual performance of each multi-level monitoring diagnostic tool is discussed in Section 4.3.1 and summarized in Table 4-1. | | |
| Maximum depth | | | |
| Multiple Uses | | | |
| Removability | | | |

| Performance Criteria | Expected Performance Metric | Performance Confirmation Method | Actual |
|---|---|---|---|
| Ease of installation | | | |
| Seal characteristics | | | |
| System storage volume | | | |
| Maximum purge rage | | | |
| Potential for sample bias | | | |
| Ease of operation | | | |
| Durability/longevity under normal use | | | |
| Durability/longevity when exposed to permanganate | | | |
| Suitability for permanganate injection | | | |
| Cost | | | |
| ***Mass Discharge Evaluation*** | | | |
| Accurate estimate of contaminant mass discharge | Pioneering application in fractured rock for each method, so performance metrics unpredictable | Compare mass discharge using two techniques | One order of magnitude difference between the two techniques |
| ***Rock Crushing*** | | | |
| Quantify contaminant mass in rock matrix and map distribution of the mass | See discussion in Section 4.3.3 as well as data provided in Appendix A | | |
| Delineation of migration pathways | | | |
| ***Isotope Analyses*** | | | |
| Method able to discern isotopic shifts in compound-specific stable carbon isotopes | See discussion in Section 4.3.4 as well as data provided in Appendix B | | |
| Defensible QA/QC procedures | | | |
| ***Laboratory Studies*** | | | |
| Measure rock oxidant demand | See discussion in Section 4.3.5.1 as well as data provided in Appendix C | | |
| Estimate permanganate diffusion distances into rock over time | See discussion in Section 4.3.5.2 as well as data provided in Appendix D | | |

## 4.3 Data Analysis, Interpretation and Evaluation

### 4.3.1 *Multi-Level Monitoring Systems (MLSs) and Nested Wells*

The following list outlines the relevant factors, features, and capabilities utilized to evaluate the performance of MLSs and nested wells for this project:

a. Borehole diameter
b. Maximum depth
c. Multiple uses
d. Removability
e. Ease of installation
f. Nature of seal between monitoring intervals
g. System storage volume
h. Maximum purge/pumping rate
i. Potential for sample bias
j. Ease of operation
k. Durability when exposed to permanganate
l. Durability during normal use
m. Suitability for permanganate injections
n. Cost

There are many criteria that can be used for selection of a MLS and when a primary criterion is used, selection can be simplified. For example, if there is need for a relatively large number of monitoring intervals (>10) in a three to four inch borehole, the Westbay system is the only system capable of providing this number of intervals in one hole. Likewise, if there is need for an MLS to be removed from the borehole (without destroying the system) after installation, only the FLUTe system meets this criterion. However, at most sites, there are multiple usages desired and selection of the most appropriate MLS involves a balance between the various criteria.

Given that there are so many ways in which the MLS and nested well systems differ from one another, and that individual sites will have different monitoring objectives, geology/hydrogeology, and regulatory requirements, the task of selecting the MLS or nested system most appropriate for the particular sites needs is challenging. In this section, the features of each of the four types of MLSs, as well as the ZIST nested well system, are briefly described in the general context of contaminant hydrogeology and then the specific relevance and experiences gained through their use at the WVA are indicated. The uses and performance of the MLSs and ZIST at the WVA are most exceptional in the context of the permanganate injections in the pilot tests and the full scale permanganate remediation. To date, no previous reporting on uses of MLSs or ZIST for injections or monitoring involving permanganate exists.

Each of the system manufacturers makes improvements in the design of their systems in response to new field experiences. Therefore, the descriptions provided below should be viewed in this context. Some of the difficulties indicated have already been the subject of research and development by the manufacturers, resulting in subsequent improvements. Table 4-4 summarizes

the MLS and ZIST features with emphasis on elucidating the differences and discussion provided below. Although Einarson (2006) provides an extensive overview of all of the MLSs available in the marketplace, the publication does not discuss the various features and characteristics comparatively, and this is done in this report so that the particular MLS and ZIST uses at the WVA site have context.

# Table 4-4: Comparison of Multi-Level Diagnostic Tools

| Characteristic | Multi-level Sampling Systems | | | | Nested Monitoring Systems | |
|---|---|---|---|---|---|---|
| | Solinst CMT™ System | Westbay MP® System | Water FLUTe™ System | Solinst Waterloo™ System | BESST ZIST™ System | Conventional Wells |
| Utilized at Watervliet Arsenal? | yes | yes | yes | no | yes | yes |
| Minimum optimal borehole diameter (inches) | | | | | | |
| w/packers | N/A | 4 - 6 | 3 - 10[1] | 4 - 6 | N/A | N/A |
| w/bentonite seals | 6 | 6 | N/A | 6 | 3 - 10 | N/A |
| Maximum depth capability (feet below ground surface) | 300 | 4,000 | 1,000 | 750 | 3,000[2] | N/A |
| Nature of seal between monitoring intervals | bentonite backfill | inflatable packers, bentonite backfill | borehole liner with spacers | inflatable packers, bentonite backfill | bentonite backfill | bentonite backfill |
| Maximum number of sampling intervals | 7 | 20 per 100 feet | 20+ | 15 | borehole size dependent | borehole size dependent |
| Direct head measurement? | yes | no[3] | yes | yes | yes | yes |
| Hydraulic conductivity testing? | no | yes | no | no | yes | yes |
| Pumping/injection testing | no | yes | no | no | yes | yes |
| Removable?[4] | no | yes[5] | yes[6] | yes | no[7] | N/A |
| Sample collection methods | peristaltic or double-valve pump | Westbay sampling tool | compressed air | bladder or double-valve pumps | ZIST pump (compressed air driven) | bailer or pump |
| Continuous built-in data logging capability | no | yes | yes | yes | yes | yes |
| Relative purge volume | high[8] | low | low | high[8] | high[8] | high[8] |
| Observed durability/longevity with permanganate | good | poor | poor[9] | N/A[10] | good | good |

Notes:

1. The FLUTe system seals directly to the borehole wall and does not require packers.
2. Maximum capability of ZIST pump per manufacturer.
3. Head measurements calculated using monitoring zone hydraulic pressure.
4. Ability to remove any system will be highly dependent on borehole characteristics. Low borehole permeability may limit/prevent removal due to suction effect.
5. Westbay packers can only be deflated by destroying the packers with a specialized tool.
6. Water FLUTes typically require some degree of repair before re-use.
7. ZIST pump can be removed to leave open screen.
8. System requires purging of borehole around monitoring zone. Degree of purging dependent on borehole diameter and length of monitoring zone.
9. Performance based on nylon liner. Newer polyester liner may be more resistant to permanganate.
10. Not used at Watervliet Arsenal; however, rubber inflatable packers used in the Waterloo System are not compatible with permanganate.

#### 4.3.1.1 *Borehole Diameter*

Borehole diameter is normally influenced by several factors including the need for coring/core diameter, drilling cost, and ultimate use of the borehole. Prior to drilling, if there is the intention to install an MLS or ZIST in the borehole, then the borehole diameter selected must be compatible with the chosen system.

Each of the monitoring systems has restrictions on use imposed by the borehole diameter, but some are much more restricted than others. For the Westbay and Waterloo systems, the borehole diameter limitation is eased when the systems are used without packers. The FLUTe and ZIST systems are severely restricted in boreholes smaller than 3.5 inches diameter as installation is more difficult and the number of monitoring ports that can be fitted into the system is much less than for boreholes of 4 inches or larger. For the other systems, borehole diameter does not influence maximum number of ports available. The Westbay and Waterloo MLSs with attached packers require boreholes between three and five inches in diameter, with 4-inch diameter boreholes being optimum. However, these MLSs can also be used without packers in boreholes larger than 5-inches using sand/bentonite seals. The CMT system is only rarely used with attached packers and so its normal use is with backfilled sand packs and seals. However, because the outside diameter of the CMT tubing is smaller than that of the Westbay and Waterloo systems, the CMT system can be installed in smaller boreholes. Table 3-2 provides a summary of the borehole diameters for the MLSs and nested wells at the WVA.

#### 4.3.1.2 *Maximum Depth*

The maximum depth to which an MLS or nested well system can be installed is an important feature in some site studies, particularly sites with deep contamination such as chlorinated solvent sites where DNAPL is/was present. Of the systems evaluated, the CMT system is limited to the shallowest depths, generally less than 200 feet, and the Westbay system is capable of installation to the greatest depths, up to a few thousand feet. The maximum depth to which a particular system can be installed depends on several factors including the strength of the components, the capability of the sample collection equipment (i.e., pumps), packer inflatability, and borehole friction/deviation during installation. The Westbay and ZIST systems can be installed to deeper depths because the components of the system allow this, but, more importantly, because they can be installed through temporary casing placed inside the borehole. The temporary casing insures that the system reaches the bottom of the borehole regardless of borehole conditions. Conversely, the Waterloo system is not well suited for installation down dull casing and therefore goes down open uncased boreholes. Experience indicates that the Waterloo system generally should not be installed deeper than about 500 feet, but the maximum depth that should be attempted is very dependent on the borehole size and conditions. The maximum depth achievable with the FLUTe system depends strongly on the borehole diameter. Generally, larger boreholes better accommodate deeper installations. Also, the maximum depth for the FLUTe system is dependent on the number of monitoring systems included. The FLUTe

system has been installed commonly in the depth range of 100 to 300 feet bgs and occasionally to between 400 to 500 feet bgs.

At the WVA, the deepest boreholes were drilled to 200 feet bgs in competent bedrock and temporary casing was not required for installation of the MLSs and ZIST/nested wells.

4.3.1.3 *Multiple Uses*

An MLS or nested system can be utilized for groundwater sampling, hydraulic testing, hydraulic head monitoring, or a combination of these purposes. The CMT system, which is the simplest MLS, can be used for both hydraulic monitoring and groundwater sampling without need for particular design specifications. The CMT channels are too small to accommodate the equipment necessary for hydraulic testing. Conversely, the monitoring port/pumping port configuration of the Westbay system allows for water pressure measurements, groundwater sampling, and hydraulic testing. The FLUTe system and the Waterloo system can be configured only for head monitoring, or only for groundwater sampling, or for both. Nested well/ZIST systems, of course, can be used for head measurements, sampling, and hydraulic testing.

At the WVA, all of the systems were used for head measurements and groundwater sampling, but only the Westbay was utilized for hydraulic testing. In addition, as noted previously, the Westbay was also utilized for injection of permanganate.

4.3.1.4 *Removability*

Removability refers to the ease with which the MLS can be removed from the borehole at any time after installation. For example, there may be a desire to use the borehole for other purposes at some time after the MLS has yielded sufficient data or there may be a need to remove the MLS because the monitoring infrastructure at the site is being decommissioned. Of the four MLSs only the FLUTe system is designed to be removable. Nested well systems also cannot be removed; however, the design of the ZIST system allows for the pump assembly to be removed from the well without difficulty.

At the WVA, the FLUTe systems were removed after permanganate was detected in the boreholes. One of the FLUTes disintegrated in the borehole during removal due to damage caused by the permanganate. The project team was aware before the installation of the FLUTes that they were not compatible with permanganate and, therefore, they were installed with temporary monitoring as the objective.

4.3.1.5 *Ease of Installation*

Installation difficulties can arise because of borehole irregularities, MLS construction requirements, or bridging of well backfill materials. Non-ideal borehole conditions may prevent the MLS from reaching the bottom of the borehole. The Westbay system is least prone to installation difficulties because it can be installed inside temporary casing, if necessary, and does not require backfill of the borehole annulus. This is not the case for the other MLSs. Casing can also be used for installation of the CMT system, but, in this case, it needs to be used with rotosonic drilling to facilitate the positioning of the sand pack and seal. In certain circumstances

casing can be used to facilitate installation of the FLUTe system, but this is uncommon. The Waterloo system equipped with packers cannot be installed inside the casing and therefore good borehole conditions are required for it to have minimal installation risk. The Waterloo system was not used at the WVA because, for this particular site, it offered no particular advantages over the other systems. Nested well systems can be installed using temporary well casing.

At the WVA, difficulties were encountered during the installation of the CMT systems due to bridging of the well backfill materials in the boreholes. However, this problem was overcome in subsequent installation of nested wells by changing the backfill materials and the rate/method by which they were emplaced in the boreholes.

4.3.1.6 *Nature of Seal between Monitoring Intervals*

The seals used in the four MLSs and nested wells have different characteristics. The nature of the seal utilized in the FLUTe system is the most different in that the FLUTe seal is a long continuous seal with interruptions representing the monitoring intervals. Therefore in nearly all uses of this system, most of the borehole is sealed. In the other systems, the total seal length is a small percentage of the borehole length. The FLUTe seal is formed by the flexible urethane coated nylon fabric pressed against the wall by the head differential maintained by the higher water level inside the liner. The CMT system and nested wells utilize conventional sand, bentonite, and/or grout seals. The Westbay and Waterloo Systems have inflatable packers of similar size but very different materials and packer inflation method. The Waterloo packers are self inflating because they are formed in their interior of material, either bentonite or a chemical gel, that swells on contact with water. The Westbay packers are inflated with water and each packer is inflated individually to whatever pressure is desired. In the Waterloo system all of the packers inflate simultaneously after the system is fully in the borehole and water is added to the interior of the MLS casing.

4.3.1.7 *System Storage Volume*

System storage volume is an important factor influencing the contaminant concentrations obtained using MLSs or nested wells in fractured rock. The normal goal of sampling is to obtain a reliable and accurate value for the concentration in the formation immediately outside the borehole wall to represent undisturbed conditions. This measured concentration is typically used in assessment of contaminant distribution and contaminant transport and fate. Therefore , there is need to minimize the influences of the purging and sampling causing differences between what is measured and the actual formation concentration. Ideally, the system is purged to remove all of the stagnant water from the interior of the MLS ( i.e. from the plumbing ) and the annular water, and then pumped more to draw the sample from the formation domain very near the borehole wall.

The Westbay system has essentially no internal storage volume such that it is a "no purge" system. After the Westbay pumping port is used to purge the monitoring zones after installation, no further purging is required. The sample is collected down-hole into a canister connected to the monitoring port. The sample water comes from the annulus reservoir volume between the borehole wall and the system casing. This reservoir volume is large relative to the

sample volume. Therefore, the assumption is that the water in the annulus is well mixed naturally and that this mixture represents what is in the fractures near the borehole wall. If more than one fracture intersects the monitoring interval, with different concentrations, then the sample can be influenced mostly by one or more fractures in ways that are indeterminate.

The other MLSs and nested well systems require purging to remove the internal system stagnant water and the annular space (if present) to draw the sample from the formation into the system and pump it to surface. In fractured rock, drawing too much water from the formation causes the sample to be a mixture from increasing numbers of fractures in a larger volume of rock. Given that bulk fracture porosities are typically very small, excessive purging can cause the sample to become unrepresentative of the natural conditions in the fracture network. The FLUTe system has minimal annulus storage volume and this means that as soon as the internal system volume is purged, the sample can be collected with no substantial additional purging. The Waterloo, CMT, and nested well systems have relatively large annular storage volumes, and, therefore, more extensive purging is generally required.

4.3.1.8 *Maximum Purge/Pumping Rate*

The capability for MLS ports to yield water is different between the four MLSs and this can influence the MLS selection and how the MLS is used. This discussion assumes that the formation transmissivity is not the limiting factor on purging yield and the limitation is only due to the capabilities of the MLS to produce water yield from the system.

The purge rate of the Waterloo System is relatively low and depends strongly on depth to water, because each pump stroke pushes out the entire standing water column in the port tube. The FLUTe system has a much larger pumping rate than the Waterloo system due to the check-valve configuration of the tubing, which completely evacuates the standing water column in the tubing prior to the introduction of formation water. The CMT system has a relatively low purge rate, which depends on the mode of pumping (i.e., peristalitic or double-valve pump), but which is limited by the small size of the CMT channels.

The Westbay system is entirely different from the other systems in regard to pumping. This system is pumped using its pumping (purge) port, which is not designed to be used repetitively. It is intended for major purging after installation and then the system is intended to be a no purge system. When the Westbay purge port is opened, formation water flows into the Westbay casing and the water column in the casing can is pumped using a bladder pump, small diameter double-valve pump, or air lift pumping. In transmissive formations, the pumping rates can be as high as a few gallons per minute or more. The ZIST pump is capable of purging at rates similar to that of the Westbay in the open pumping port configuration.

4.3.1.9 *Potential for Sample Bias*

Sample bias refers to the influences on the contaminant concentrations during sampling and analysis that cause the measured concentrations to be different than the true concentrations in the formation immediately beyond the sampling internal. Many factors can cause sample bias, such as reaction with the MLS materials (e.g., sorption or leaching), volatilization losses, and formation mixing. The propensity for bias depends strongly on the type of containment under consideration. This discussion is directed at chlorinated solvents such as TCE, PCE and daughter

products. These components have only weak propensity for sorption, relative to many other categories of organic contaminants, but they are strongly volatile and therefore prone to volatilization losses. Biases are typically a concern at very low concentrations. Whether or not a particular level of bias is significant depends on the specific site.

Of the four MLS Systems, the Westbay system has the least propensity for biases because the sample is collected down-hole in a canister made of glass or steel without head space. In the CMT, Waterloo, FLUTe, and nested well systems, the sample water passes from the sampling interval to the surface via tubing, and the propensity for sample bias due to sorptional/ diffusion depends on the type of tubing selected. For example, the FLUTe system now uses PVDF tubing, which is less prone to sorption/diffusion effects. The CMT system is available in only one type of tubing, polyethylene, which is most prone to these effects. Sampling bias could not be evaluated at the WVA site due to the large variation and magnitude of VOC concentrations in the groundwater.

#### 4.3.1.10 *Ease of Operation*

The ease in which a sampling system can be operated is a function of several factors, including: the equipment necessary to conduct the sampling, the depth and size of the monitoring interval, purge volume, and the rate at which purging and sampling can be accomplished. Each of the MLSs and nested well systems included in this demonstration increase the efficiency of collecting groundwater samples by having multiple monitoring zones in one borehole, reducing the time it takes to set up and take down equipment needed to sample. Once a Westbay measurement port is purged, the port does not require purging again. This can reduce the time it takes to collect a sample from a port by not having to spend time purging the port prior to sampling. However, if a monitoring zone is set in a low transmissivity interval, sampling via the Westbay system can take hours since the rate of sample collection is dependent on the hydrostatic pressure in the sampling interval. In addition, collection of a sample using the Westbay system requires specialized equipment that must be broken down and decontaminated between sampling intervals. Conversely, sampling of the FLUTe system requires no specialized equipment and, since there is little borehole storage and several ports can be purged and sampled at once through dedicated tubing, requires relatively little time and effort. At the WVA, 45 groundwater samples were collected from five FLUTe systems in one day by a team of two people. Sampling of the CMT system also does not require specialized equipment; however, due to the potential for large purge volumes, sampling time can be extensive depending on the depth to water, the size of the borehole, and the length of the monitoring zone.

#### 4.3.1.11 *Durability When Exposed to Permanganate*

The WVA project is the first where several types of groundwater monitoring devices were exposed to permanganate. Permanganate is a common chemical used for in-situ remediation of chlorinated solvent sites and, therefore, the performance of monitoring devices exposed to permanganate has broad relevance. Permanganate is an oxidizing chemical that commonly maintains its oxidizing capacity for an extended time in the subsurface and has strong propensity for spreading far from its injection locations. For a monitoring device to be well

suited for use in permanganate projects it must withstand the permanganate effects. There are two types of effects:

1. Destruction of system components due to oxidation, and;
2. Clogging of components due to chemical precipitates.

Both of these adverse effects were encountered during the monitoring of permanganate distribution in the fractured shale at the WVA site. The strongest effects were seen in the failure of the FLUTe systems. This failure was expected because it was known prior to their use that high permanganate concentrations would cause the urethane coated fabric to disintegrate. Nevertheless, the FLUTe MLSs were used because there was need to monitor the early arrival of permanganate from distant injection points. The FLUTe system was selected for this because it has the smallest water storage volume in each monitoring interval. The very small storage volume in the annulus between the borehole wall and FLUTe fabric (casing) minimizes the dilution of the permanganate when it arrives into this reservoir from the fractures where it has been transported. The FLUTe systems used at the WVA site detected the early arrival of the permanganate and successfully monitored the permanganate concentration trends during and after the injections.

The Westbay systems were expected to withstand the permanganate effects as the materials used to construct the system are compatible with permanganate. However, over time, all of the ports in the Westbay wells used for permanganate injections (through the pumping ports) became inoperative – likely due to the formation of precipitates that clogged the ports and prevented either the attachment/sealing of the sampling tool and/or the movement of the pumping port cover. The Westbay systems not utilized for injection of permanganate remained operative throughout the project.

Neither the CMT nor nested well systems showed signs of deterioration in the presence of permanganate.

#### 4.3.1.12 *Durability/Longevity for Normal Use*

Many factors enter into the durability and longevity of MLSs. In general, MLS failure can occur due to three types of causes:

1. Failure of MLS materials due to strength loss;
2. Clogging of components due to formation of chemical precipitates, and;
3. Chemical corrosion of components.

The CMT system is the simplest of all the MLSs and is closest to a conventional monitoring well in terms of durability and longevity. Failure of a CMT or nested well system is generally caused by clogging of the sand pack or decomposition/degradation of the seal material. Next simplest in its down-hole components is the Westbay system. Its longevity depends on continuous functioning of its monitoring ports (i.e., its valves and its packers). There are a number of sites where Westbay systems have been used for monitoring since the early to mid-1980s without system failures. The Westbay system has the longest record for successful

deployment because Westbay systems have been available in the marketplace the longest and because its packers and ports are specifically designed to achieve longevity. The longevity of the Waterloo system depends on the particular configuration being used. If it is used with packers and down-hole pumps, its longevity will likely be less than if it is used with sand packs and seals and open tubes. There are sites where Waterloo systems have operated successfully for more than a decade. The FLUTe system is designed to be removable and, to achieve such removability and some of the other unique features of the FLUTe system, it has components that are less likely to allow extensive longevity. The FLUTe system entered common use only approximately five ago and therefore the record available to assess longevity is rather short.

The issue of MLS longevity at the WVA site is unusual in that permanganate has been injected into the groundwater system. As expected, the FLUTe systems could not withstand the strong chemical reactivity of the permanganate and therefore failed. This failure was expected as the FLUTe system used at the WVA was not designed specifically to withstand permanganate effects. The manufacturer of the system has since developed an alternative design intended specifically to function in groundwater systems that contain permanganate. The Westbay systems also had failures due to clogging of the sampling and pumping ports that made them inoperable. In addition, the wireline sampling system required for the Westbay required several repairs due to kinking of the line. The CMT and nested well systems showed no adverse effects of permanganate in their performance. Continued contact of the bentonite seals in these systems to permanganate may cause gradual deterioration of the seals; however, given the timeframe of the WVA project, this possibility was not a concern.

#### 4.3.1.13 *Suitability for Permanganate Injections*

A major challenge in the remediation of fractured rock sites is the injection of the treatment liquid in a manner that delivers it to those parts of the fracture network that have the contaminant mass needing ‘treatment’. At the WVA site the rock core VOC analysis show that much of the VOC mass is located in lower permeability zones. The prospects for successfully delivering permanganate into these low permeability, VOC mass-rich zones by injecting into the existing wells at the site were poor because these wells are connected primarily to zones of high hydraulic conductivity. This condition for sedimentary rock sites whereby much or most of the mass is in the low K parts of the system is likely not unusual (Parker 2007). The Westbay systems were installed at the WVA partially because they are the only MLS capable of injecting treatment solutions at useful rates into multiple low-conductivity intervals in the same borehole. Since each Westbay monitoring interval is equipped with a relatively large diameter pumping port that can be opened to allow direct access to the monitoring interval, it can potentially be used for the injection of treatment solutions. In addition, the Westbay packers can accommodate the relatively high hydraulic pressures during injection. At the WVA, permanganate was injected through two of the six Westbay systems installed at the site. At each location, the pumping ports in the low conductivity zone were opened and the wells were connected to the injection equipment through a removable seal set around the top of the Westbay casing. Injections were carried out every two weeks for a period of three months.

4.3.1.14 *Cost*

Comparison of costs between MLSs/nested well systems are complex and require specifications to narrow the monitoring purpose and scope in the context of the factors listed above, and also inclusion of the labor time required to conduct the monitoring and sampling. The cost of an MLS for any site will depend on the particular design options selected (i.e., with or without pumps or transducers), the hydrogeological characteristics of the site, the number and depth of required sampling intervals, and the required sampling frequency. Accordingly, direct comparison of the relative cost between these systems is not possible as these costs will vary greatly from site to site. The costs of the MLSs and nested well systems, as installed at the WVA, are listed in Table 4-5 below. The configurations of the MLSs and nested wells at WVA are presented in Section 3.

**Table 4-5: Monitoring System Installation Costs**

| Monitoring System | Installation Date | Number of Wells | Approximate Installation Cost* |
|---|---|---|---|
| Westbay MP 38 System | 2001-2002 | 6 | $104,000 |
| Solinst CMT System | 2002 | 2 | $10,500 |
| Flexible Underground Technologies FLUTe System | 2004 | 5 | $89,000 |
| Besst, Inc. ZIST System | 2006 | 1 | $24,000 |

Notes:

* Cost at time of installation. Includes purchase, shipping, and installation equipment/labor for all systems installed at the site. Does not include equipment, materials, and labor for drilling of borehole.

### 4.3.2 *Mass Discharge Evaluation*

***Integrated VOC Mass Discharge Testing***

Calculated transmissivity values for wells included in the pump test evaluation ranged from 2 to 77 $ft^2$/day using the Neumann method and from 6 to 64 $ft^2$/day using the Theis method. The average transmissivity calculated using the Neumann method was 29 $ft^2$/day. Although the average transmissivity was greater using the Theis method (37 $ft^2$/day), the results using the two methods generally correlated well.

Time-series VOC sampling was conducted during the pumping test to evaluate integrated (average) contaminant concentrations in the treatment area. Sample results for VOCs are summarized on Figure 4-1. The concentration of total VOCs in samples collected during the test ranged from 17,060 micrograms per liter (ug/L) to 26,870 ug/L. These data, coupled with the calculated transmissivity values for wells included in the pumping test, yielded a total VOC mass

discharge from IW-2 during the pumping test of approximately 0.32 pounds per day (approximately 115.8 pounds per year).

***Boundary VOC Mass Discharge***

Compliance boundary VOC mass discharge estimates were calculated for each compliance monitoring zone using the transmissivity values calculated for fractures that had detectable flow during the July 2004 geophysical testing. Mass discharge estimates were calculated using the following assumptions:

- **Discharge Zone Thickness**: Set as the thickness of the screened interval in each compliance monitoring zone.
- **Hydraulic Gradient**: Set at 0.003 ft/ft based on the hydraulic gradient in the Building 40 area calculated from WVA-wide water table groundwater elevations.
- **Horizontal Length of Discharge Zone**: Set as the distance between compliance monitoring wells.
- **VOC Concentration**: Set at the total VOC concentration in each compliance monitoring zone during each monitoring event (average of two baseline events used for the baseline estimate).

**Figure 4-1: Total VOCs vs. Time in IW-2 Pump Discharge**

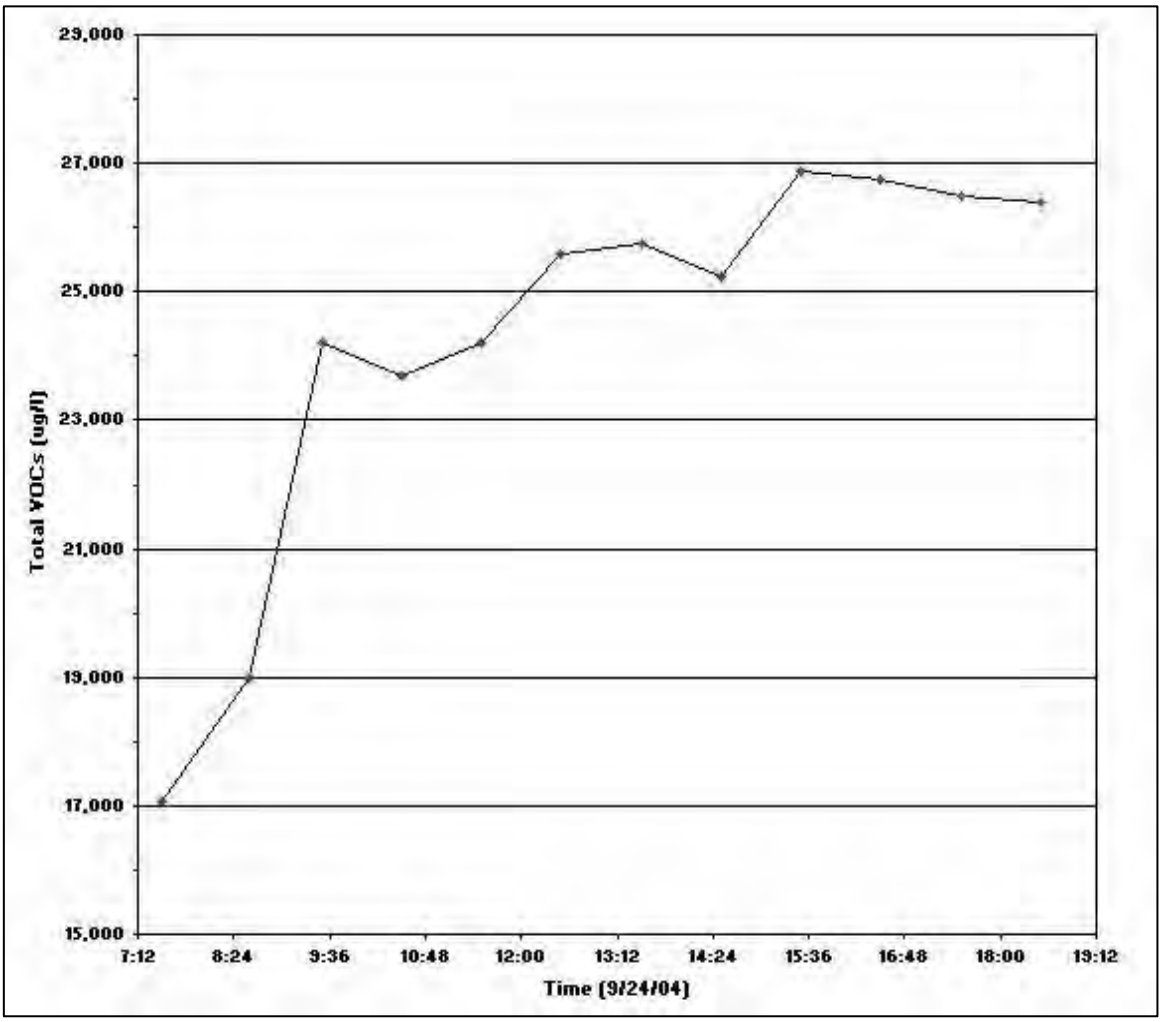

Compliance boundary VOC mass discharge estimates for the baseline and pre-injection monitoring events are presented in Table 4-6. Tthe estimated compliance boundary VOC mass discharge was similar to the baseline following the first three injection events. However, the estimated compliance boundary VOC mass discharge measured in November 2005 was approximately 34 percent less than the baseline, indicating that the permanganate injections on the east side of Building 40 in August 2005 resulted in significant VOC treatment in the area up-gradient of the compliance boundary. This was the first injection event to deliver the full volume and concentration of permanganate to all of the injection wells simultaneously. The subsequent rebound in March 2006 is likely attributed to the increased clogging of the injection wells and the inability to deliver the full volume of permanganate. By September 2006, only about two-thirds of the planned permanganate volume was able to be injected into the central portion of the plume, with the extra being injected into the periphery injection wells which had not experienced the same degree of clogging. Consequently, the estimated mass discharge across the compliance boundary increased, either as a result of decreased transmissivity of the fractures, or a mobilization of DNAPL/VOCs, or a combination of the two. The synchronous changes in mass discharge and permanganate distribution in the zones of the boundary compliance wells are illustrated in Figure 4-2.

**Table 4-6: Summary of Changes in Compliance Boundary VOC Mass Discharge**

| | Date | | | | | | |
|---|---|---|---|---|---|---|---|
| | **Baseline** | **Jan 2005** | **May 2005** | **Aug 2005** | **Nov 2005** | **Mar 2006** | **Sept 2006** |
| **Total VOC Mass Discharge (lb./yr.)** | 10.03 | 10.02 | 11.56 | 10.03 | 6.63 | 10.60 | 18.08 |

**Figure 4-2: Boundary Mass Discharge and $MnO_4^-$ Distribution**

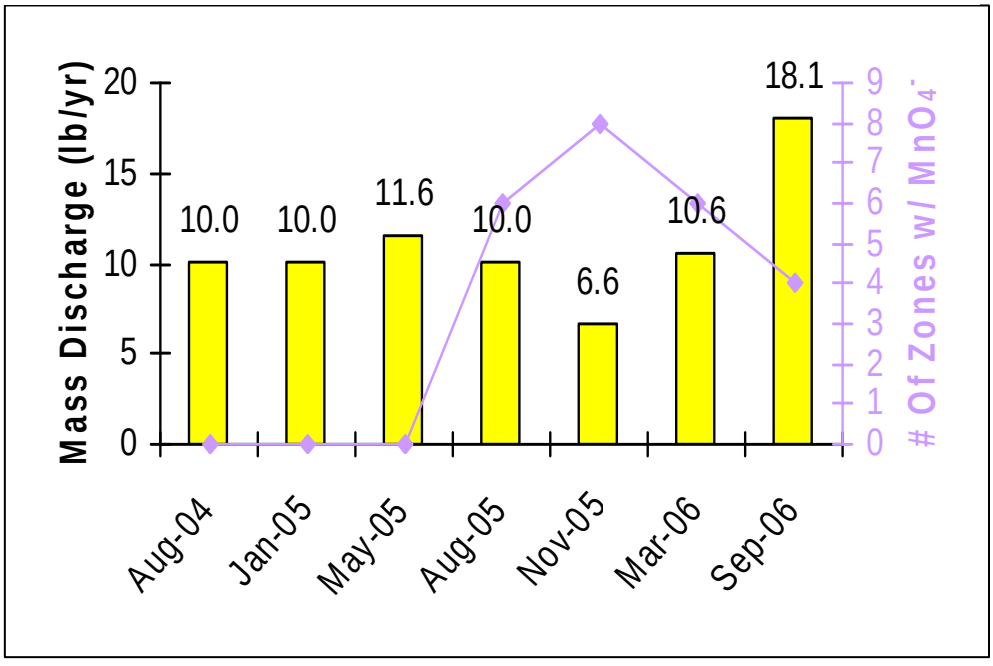

The greatest contributions to the baseline compliance boundary VOC mass discharge were from the compliance monitoring zones that intersect the "Upper" flow zone fracture system that was identified by the borehole geophysical testing. The percentage of the total estimated compliance boundary VOC mass discharge contributed by these zones is shown in Table 4-7 below. As shown in Table 4-7, these zones contribute approximately two thirds of the total compliance boundary VOC mass discharge.

**Table 4-7: Contribution to Total Compliance Boundary VOC Mass Discharge**

| Well (Zone) | Percentage of Total Estimated Compliance Boundary VOC Mass Discharge | | | | | | |
|---|---|---|---|---|---|---|---|
| | **Baseline** | **Jan 2005** | **May 2005** | **Aug 2005** | **Nov 2005** | **Mar 2006** | **Sept 2006** |
| **MW-83 (I)** | 5.5% | 22.5% | 25.1% | 29.9% | 35.0% | 27.4% | 44.7% |
| **MW-84R (I)** | 13.2% | 10.2% | 10.0% | 8.3% | 10.2% | 5.4% | 9.6% |
| **MW-85R (II)** | 25.1% | 21.8% | 18.4% | 25.8% | 1.3% | 22.7% | 17.5% |
| **MW-86R (II)** | 26.1% | 19.9% | 12.8% | 4.2% | 12.84% | 7.3% | 2.6% |
| **Total** | **69.9%** | **74.4%** | **66.3%** | **68.2%** | **59.3%** | **62.9%** | **74.4%** |

The estimates of mass discharge determined from the integrated pump test were approximately one order of magnitude greater than those from the boundary transect method (100 lbs/yr versus ~10 lbs/yr). As the scale of operations at WVA were not sufficient to cause a discharge of more than 100 lbs/yr for more than 30 years, we conclude the pumping test over-estimated the contaminant mass flux in the treatment area. The overestimation was likely due to the active nature of this method versus the more passive boundary transect method. Since fractured bedrock systems have essentially no storage, the introduction of an artificial hydraulic gradient through pumping will cause a change in the natural flow regime in the area of the pumping, and, more importantly, may draw water from fractures that do not normally contribute to the boundary mass flux due to their location, size, and degree of connection. These "back-door" or "dead-end" fractures likely contain the highest VOC concentrations since they transmit little to no flow and are in equilibrium with the near-solubility pore water concentrations in the rock matrix. Although the WVA site contains numerous monitoring points, complete documentation of the pumping test area of influence was not possible since it is not possible to monitor flow in all of the numerous fracture flow systems. Additionally, the proximity of the pumping well to the assumed source itself may be responsible for the higher estimates from the pump test, as estimates from the down-gradient transect may be affected by contaminant dilution and retardation. Based on these data, use of this method at fractured bedrock site is questionable.

The mass flux estimates from the compliance boundary transect are more realistic in light of the scale of operations conducted at the WVA. However, the transect mass flux estimates are entirely dependent on the transmissivity values derived for the major fracture pathways by the geophysical testing and may not be reflective of all of the fractures entering the borehole. In addition, since there is no way to periodically re-test the transmissivity (an open borehole is required), any changes in the transmissivity caused by the formation of permanganate treatment-

related precipitates (i.e., manganese, iron, and/or sulfur oxides) is not reflected in the mass flux calculations over time. Accordingly, it is not possible to determine whether the apparent increases in mass flux noted during the permanganate treatment program are due to actual changes in contaminant redistribution or to changes in fracture transmissvity, or a combination thereof.

These data suggest that, in the case of fractured bedrock, use of the transect method of mass flux calculation is preferable to the integrated test. However, this method is typically more expensive since it requires a greater number of monitoring points and sampling labor. In addition, since this method assumes that the transmissivity of the monitoring zone does not change, it may not yield accurate results at sites where chemical treatment is being conducted. Accordingly, in-well systems that allow for direct measurement of flux, or MLSs that can be removed so that transmissivity can be re-calculated, may be more useful in fractured bedrock settings where there is a potential for loss of transmissivity due to remedial efforts.

### 4.3.3 *Rock Matrix Analyses*

Current concepts for the nature of contaminant plumes in fractured rock are speculative. Although many techniques for borehole logging and hydraulic testing exist (e.g., review by Sara, 2003), general agreement in the literature indicates these techniques are severely limited in their prospects for providing quantitative information about the length and interconnectivity of the fractures in fracture networks (NRC, 1996; Berkowitz, 2002). Chlorinated solvents have been in the subsurface beneath many industrial properties for several decades allowing plumes to migrate down-gradient several hundreds to thousands of feet or more. These contaminants can now serve as tracers to study contaminant migration over the relevant large space and time scales most relevant in contaminant hydrogeology. Chlorinated solvent compounds are not naturally occurring in the environment; hence, even low-level detections serve as reliable evidence of contamination. The physical and chemical properties of the common chlorinated solvents make them good indicators of the physical hydrogeologic system characteristics, including the fracture network connectivity and distribution of groundwater flow.

Essentially all conventional fractured- rock borehole test methods relevant to the hydraulic conditions and properties, except for depth-discrete multilevel monitoring, (see comprehensive review by Sara, 2003), are done in open holes into which data acquisition equipment is inserted down-hole. Flow metering, fluid resistivity and conventional down-hole temperature logging and full-hole borehole dilution tests pertain to imposed (forced advection) hydraulic conditions, by applied fluid pressure as in the case of packer tests or vertical flow in the open hole caused by the hole itself (borehole cross connection between fractures). Price and Williams (1993), Sterling et al. (2005) and others have demonstrated that open holes in fractured rock commonly have borehole cross connection that disturbs the hydrochemical conditions.

The distribution of contaminants within chlorinated solvent plumes in fractured sedimentary rock has strong spatial variability due to heterogeneity in source zone contaminant mass distributions, fracture network, and matrix characteristics, accompanied by temporal variability in groundwater flow. One major reason why so little is known about contaminant

migration and fate in fractured sedimentary rock is that traditional research approaches involve only sampling water from the fractures. However, field studies using the rock core VOC analysis method show contaminant mass storage is dominated by the rock matrix rather than the fractures, and the contaminant concentrations in the fractures and the matrix are not in equilibrium (Hurley and Parker, 2002; Sterling et al., 2005; Parker et al., in review). This disequilibrium between fracture and matrix zones is evident in the WVA rock core concentration profiles shown on the figures contained in Appendix A. Therefore, sampling only the groundwater from the fractures cannot provide the overall mass distribution. Furthermore, when conventional boreholes are drilled, the water from a fracture in one section of the borehole migrates to another section of the borehole due to differences in head between the two sections. This creates an un-natural flow and contaminant transport condition within the system known as borehole cross-connection. This condition will also persist across the screened interval of a conventional monitoring well, and as a result, results from sampling the well do not reflect the natural system (Price and Williams, 1993; Sterling et al., 2005).

Rock core analyses provide contaminant mass and phase distributions more relevant to contaminant behavior than those obtained from monitoring wells or other types of borehole water sampling alone. The determination of the nature and extent of the contamination, with emphasis on elucidating the internal anatomy of contaminant plumes (including contaminant distribution in the rock matrix where groundwater is nearly immobile due to low permeability), is the foundation for understanding the processes governing the contaminant distribution. For example, Figure 4-3 shows VOC rock matrix concentrations in rock core collected at the WVA along with flow zones detected during geophysical testing. As shown in Figure 4-3, although the flow zones identified by the borehole geophysical testing correlate to elevated rock matrix VOC concentrations at two depths (approximately 35 and 50 feet bgs), they do not account for the large vertical span of elevated rock matrix VOC contamination from approximately 50 to 110 feet bgs, where, in many cases, PCE concentrations approach solubility. These data support the conclusion that numerous fracture pathways exist that are not detectable using conventional geophysical techniques. Likewise, Figure 4-4 shows the comparison between flow zones detected using geophysical methods, rock matrix VOC concentrations, and VOC concentrations/mass flux in groundwater samples collected from the same borehole. As shown in this figure, although the zone between approximately 50 to 110 feet bgs contains rock matrix VOC concentrations approaching solubility, groundwater VOC concentrations in this zone were only approximately 10 percent of the rock matrix pore water concentrations, indicating that the rock matrix and fracture groundwater are not in equilibrium. However, Figure 4-4 also shows that the mass flux from this zone is minimal due to low transmissivity. These data confirm that rock crushing is an invaluable tool in characterizing contaminated fractured bedrock sites.

**Figure 4-3: Estimated rock core porewater VOC concentrations at MW-83 (October 2003) and locations of flow zones identified during borehole flow testing**

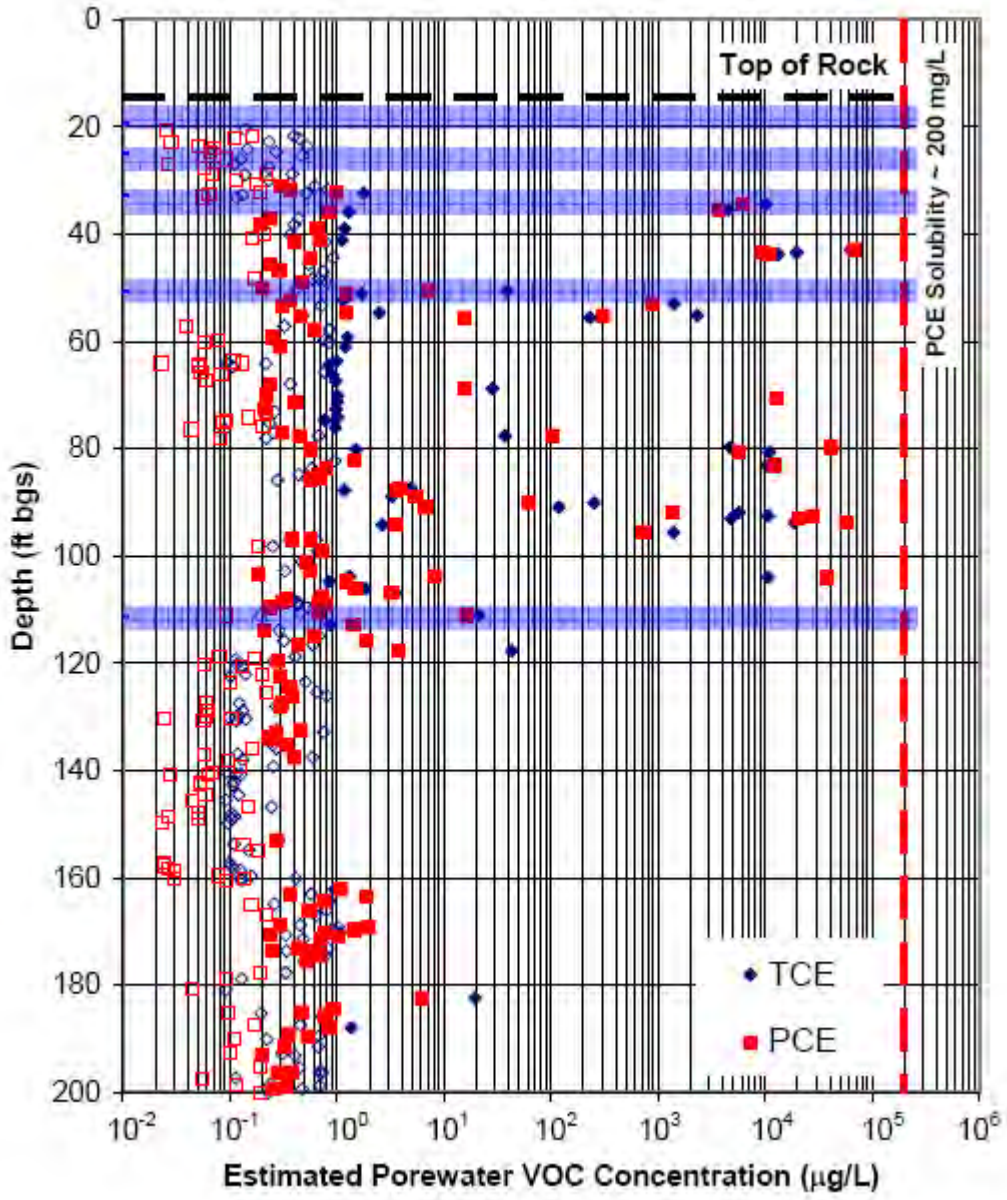

**Figure 4-4: Estimated rock core porewater VOC concentrations at MW-83 (October 2003) and comparison with multilevel-derived transmissivity, VOC concentrations and mass discharge.**

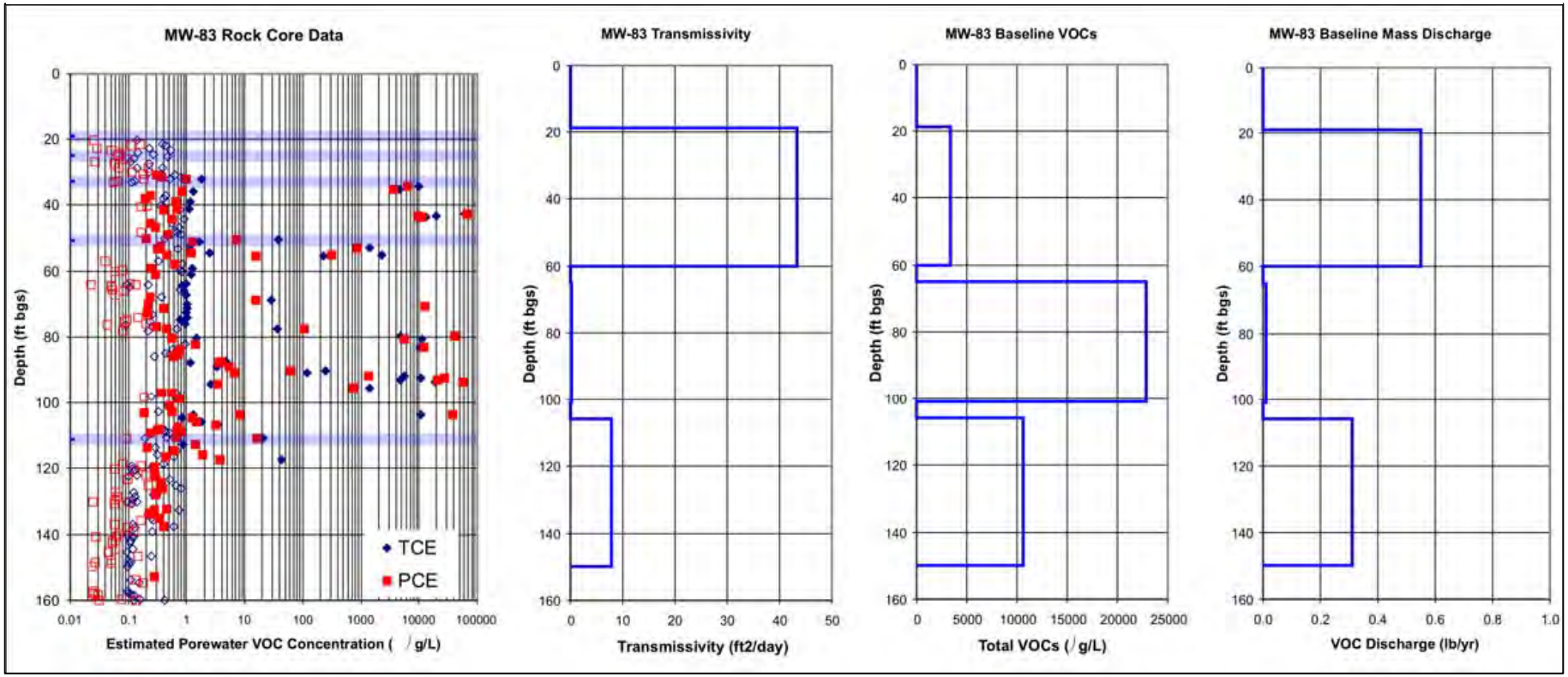

### 4.3.4 *Isotope Analyses*

Figures showing carbon isotope results in relation to well locations are presented in Appendix B and are discussed below.

**Pilot Test (2002-2003)**

In order to illustrate the use of carbon isotope analyses in the study area, a brief discussion of the carbon isotope data collected during the pilot test performed in 2002-2003 is presented. The data were collected during the injections performed during March 5-11, 2002 in well MW-59 and the injection carried out April 1, 2002 in wells MW-65 and MW-71. The monitoring multilevel wells were MW-74 and MW-76. No significant isotope differences were observed on March 6 in both monitoring wells comparing conditions pre-injection and during injection (Figures B-1 and B-2). This pattern was accompanied by a trend to lower PCE concentration in MW-74 and a change to higher concentration at some depths in MW-76.

During March 7, 2002, a significant trend toward more enriched $\delta^{13}C$ values was observed in monitoring depth 3 at MW-74 reaching a value of +5.1‰ (Figure B-3). The pre-injection $\delta^{13}C$ value was -31‰. However no significant difference was observed in PCE concentration at this depth. All the other monitoring depths in MW-74 and MW-76 showed no changes on the carbon isotopic composition of PCE (Figure B-3). During March 8, the enrichment pattern persisted at monitoring depth 3 in MW-74 and no changes were observed in the other depths at both monitoring wells (Figure B-4). During post injection monitoring (March 18-April 13) for the injections of March 5-11 (MW-59) and April 1-2 (MW-71 and MW-65), enriched values were observed at monitoring depths 3, 4 and 6 at well MW-74 and at monitoring depth 5 at well MW-76 (Figure B-5). The isotope data showed enriched isotope values even nine months after injections at well MW-74 accompanied by a relative high PCE concentration (Figure B-6). The isotope data at well MW-76 showed a shift toward the values representing pre-injection conditions and the PCE concentrations showed values much higher than pre-injection conditions (Figure B-6). The main observations inferred from the compound-specific carbon isotope and PCE concentration patterns during the pilot test were the following:

1) The changes in PCE concentration observed in wells MW-74 and MW-76 during the first two days of the March 2002 injection were the result of dilution and/or mass transport from areas of high PCE concentration due to the pressure front created by the injection process.

2) The $\delta^{13}C$ enrichment pattern observed only in one depth at MW-74 is a product of PCE oxidation by the permanganate solution. The permanganate solution traveled preferentially through a fracture network that is tapped by monitoring depth 3. The detection of permanganate only in this depth agreed with the isotope data.

3) The $\delta^{13}C$ enrichment pattern observed under post-injection condition for the March and April 1-2, 2002 injections showed the permanganate solution impacted a larger section of the fracture network in areas near the monitoring well MW-74 and only the deeper fractures in the case of

MW-76. This pattern agreed with the presence of permanganate at depths where the enriched $\delta^{13}C$ values were observed.

4) In the case of monitoring well MW-76, the shift to pre-injection $\delta^{13}C$ values after permanganate injection due to rebound implied that significant VOC mass is present in areas up-gradient of MW-76.

**Interim Corrective Measure - MW-79 and IW-1 to IW 4**

The first set of data that will be discussed are the results of the injections that were performed at well MW-90 corresponding to the first injection event of the CM (9/30/04-10/1/04) and the second injection event (1/31/05-2/11/05). The monitoring wells were FLUTe MLSs MW-79 and IW 4 and the results are presented in Appendix B. One of the patterns observed in some depths (MW-79-1, MW-79-3, MW-79-4, MW-79-5, MW-79-6) was an increase in VOC concentration under post-injection conditions. This pattern seemed to be accompanied at some depths by a significant increase in sulfate and sodium concentrations. The isotope data showed no changes in the carbon isotope composition of the PCE, TCE and cis-DCE, despite a large change in VOC concentrations. The isotope and the VOC concentration data showed that the concentration pattern observed at MW-79 is associated with mobilization of VOC mass along fractures due to a pressure front created by the injection solutions at MW-90. The isotope data showed no evidence of VOC oxidation and the sulfate pattern was associated with oxidation of the sulfide minerals present in the rock matrix by the potassium permanganate during transport toward the area monitored by MW-79. Batch experiments showed the shale bedrock has an extremely high oxidant demand in the range of 30 to 70 mg $MnO_4$/g rock (see discussion in following section).

A similar pattern of increasing VOC concentration after injections was observed at the IW-4 nest in the depths characterized by high VOC concentrations (IW-4-7, IW-4-8 and IW-4-9, Appendix B). The VOC concentration pattern was also accompanied by an increasing change in sulfate and sodium concentrations. No changes were observed in the carbon isotope data comparing pre and post injection conditions. The isotope data showed no evidence of VOC oxidation and the increase of VOC and sulfate concentrations is presumed to be related to mobilization of VOC mass due to a pressure front created by the injection solutions and reaction of the potassium permanganate with the rock matrix, respectively. The lack of the presence of $KMnO_4$ at MW-79 and IW-4 MLSs during injection events 1 and 2 is also a clear demonstration of the high oxidation demand of the shale bedrock.

A different pattern was observed in the IW-4 multilevel under post injections condition associated with the third permanganate injection event performed at MW-79 multilevel (lower part). The VOC concentrations in the depths characterized by the highest concentration showed no changes or a trend to lower VOC concentration with time (IW-4-6, IW-4-7, IW-4-8, IW-4-9, Appendix B). The sulfate concentration showed a significant increase under post injection conditions, again demonstrating the high oxidant demand of the shale rock. An increase in sodium concentration was also observed in these MLSs. The carbon isotope data showed a trend toward more enriched $\delta^{13}C$ values, especially for cis-DCE reaching values as high as -9.8 ‰ in

the relatively high VOC concentration areas. Some relatively low concentration areas such as IW-4-5 showed $\delta^{13}C$ values as high as +12.7‰. The $\delta^{13}C$ values for pre-injection conditions ranged between -26 and -24 ‰ (Appendix B). The trend toward enriched $\delta^{13}C$ values observed at IW-4 was also accompanied by a decrease in VOC concentration and it is clear evidence of the occurrence of VOC oxidation by potassium permanganate. $\delta^{13}C$ values as high as +200 ‰ have been observed in granular aquifers where the VOC source has been completely oxidized (Hunkeler et al., 2003). The relatively low $\delta^{13}C$ enrichment values observed in VOCs at the WVA are due to rebound (i.e., back-diffusion and advective transport; see discussion of conceptual site model).

A similar general pattern of decreasing VOC concentration and increasing sulfate and sodium concentration was observed in some of the other FLUTe MLSs (IW-1, IW-2 and IW-3). A trend toward enriched values was also observed in some depths in IW-2 and IW-3 reaching $\delta^{13}C$ values as high as -6.9 ‰. These patterns showed the effect of the rock oxidant demand and the oxidation of VOCs by potassium permanganate, which was observed in the IW-1, IW-2 and IW-3 but not in IW-4. It is important to highlight that in some wells characterized by high concentrations of VOC and sulfate and the presence of $KMnO_4$ (IW-2-1, IW-2-2, IW-3-4) no significant carbon isotope changes were observed. This type of pattern is likely due to the rebound effect during and after oxidation in areas that should be characterized by high concentration of VOC in the rock matrix.

**Boundary Nested Wells (MW-82, MW-84, MW-85, MW-86, MW-87)**

The isotope data collected in these wells correspond to pre-injection and post- injection conditions for injection event 1 and pre-injection conditions for injection events 6 and 7. One set of data corresponds to pre-injection and post-injection conditions for event 6**.** Most of the boundary wells are characterized by very high VOC concentrations. A significant increase in sulfate concentrations was observed in these wells comparing the pre-injection conditions in 2004 with post-injection conditions in 2006. No significant changes were observed in the $\delta^{13}C$ values except in some relatively low VOC wells (MW-82R-2, MW-85R-1, MW-86R-1) which showed values as high as -16.4 ‰. This trend was also accompanied by a decrease of VOC concentrations. The isotope pattern was expected under pre-injection conditions for events 6 and 7 due to rebound effects that occurred after the $MnO_4$ is consumed. However, no isotope changes were also observed between pre-injection and post-injection conditions at MW-85-2 during event 6. Due to the high rock oxidant demand at the site, the high VOC present in the rock matrix and the relatively large open intervals for the boundary wells, the carbon isotope composition of VOC should not change too much, in spite of VOC oxidation.

In summary, the isotope data provided information about the competing processes of permanganate oxidation and rebound, which control VOC concentration during and after a permanganate treatment. The isotope data showed that the rebound effect is dominant at the WVA due to the large amount of VOC present in the shale matrix. The expected isotope trend associated with oxidation was only observed at depths characterized by relatively low VOC concentrations where probably a relatively smaller mass of VOC is present in the shale matrix.

### 4.3.5 *Rock Oxidant Demand Tests and Permanganate Invasion Studies*

Laboratory studies were conducted at UW during at the same time as field activities were being performed to enhance understanding of field observations. The methods used for the laboratory studies were described in Section **Error! Reference source not found.**, and the following sections summarize the results of the laboratory studies.

#### 4.3.5.1 *Rock Oxidant Demand Tests*

Graphs and tables depicting the results of the ROD testing are provided in Appendix C. The results of the $KMnO_4$ batch tests indicated a maximum ROD after 21 days ranging from 19 to 32 mg $KMnO_4$ per g of rock, with about 83% to 91% of the 21-day ROD reached within the first seven days (Figures C-1 and C-2). The change in fraction of organic carbon (foc) was measured for batch test solids after 21 days. Based on the theoretical reaction of organic carbon and permanganate (Hønning et al., 2007), the oxidation of each milligram of organic carbon consumed 13.2 mg of $MnO_4$ (Figure C-3). Batch test solution sulfate concentrations were also measured after 21 days. Based on the theoretical reaction of pyrite and permanganate (Hønning et al., 2007), the oxidation of each milligram of pyrite consumed 5.0 mg of $MnO_4$ and produces 1.6 mg of $SO_4^{2-}$ (Figure C-4). Results suggest that pyrite oxidation accounted for 30-80% of the ROD.

The ROD values measured from the $NaMnO_4$ tests were a factor of two or three higher than those measured in the $KMnO_4$ tests (Figures C-5 and C-6). Therefore, there appears to be a concentration dependence on ROD – the higher the permanganate concentration, the higher the ROD exerted by the shale. Results of the sulfate analyses indicated that pyrite oxidation accounted for about 30% to 75% of the 21-day ROD values observed (Figures C-7 and C-8). The higher the permanganate concentration, the lower the percentage of ROD accounted for by pyrite. The fraction organic carbon analyses indicated some contribution to the ROD from organic carbon oxidation, particularly for higher permanganate concentrations. The batch test results on crushed samples must be evaluated with caution when applied to interpretation of anticipated ROD under field conditions with intact rock. Rates of reaction are much different between batch tests on crushed samples and intact rock, due to available surface area for reaction, and diffusion-limited permanganate transport to reactive minerals. Reaction rates in intact rock also may be hindered by deposition of $MnO_2$ coatings on reactive surfaces.

#### 4.3.5.2 *Permanganate Invasion Studies*

As discussed in Section 3.4.1.4, experiments were performed to measure the distance of $MnO_4^-$ diffusive penetration into the matrix of shale over a period of 24 months, and to assess the mineralogical controls on $MnO_4^-$ persistence. Graphs and tables depicting the results of these studies are included in Appendix D. Rock matrix properties including permeability, porosity, and density were measured (see Tables D-1 and D-2). The porosity of the rock ranged from 0.7 percent to 3.1 percent. A mineralogical analysis of the whole rock was performed via acid digestion and ICM-MS/ICP-AES. The results showed relatively high percentages of iron and sulfur, indicating the presence of pyrite in the rock (Table D-3). SEM images, visual inspections of rock cores, and Leica DM digital microscopy confirmed the presence of large pyrite-rich veins as well as calcite infilled microfractures (see Figures D-1, D-2, D-3, and D-4).

To conduct the permanganate invasion testing, five blocks of shale (1 x 2 x 3 cm) were immersed in a $KMnO_4$ solution (2 g/L). A single sample was removed at times of 2, 4, 6, 12 and 24 months following the immersion, and polished thin sections were prepared from each block. Profiles of relative Mn concentration versus distance from the block surface were measured in the directions parallel and normal to the bedding direction using LAM-ICP-MS and SEM-EDS (Table D-4). The Mn profiles reflect the presence of solid Mn-oxide which is the reaction product of $MnO_4^-$ reduction and they are used as an indicator of the depth of penetration into the shale. Initial core samples were examined using LAM-ICP-MS, which caused dispersion and broadening of the profiles, and over-estimation of Mn penetration distances (Figures D-5, D-6, D-7). Later, SEM-EDS and STEM-EDS were used to investigate reaction processes that influence the transport of $MnO_4^-$ in the shale matrix. Figures D-8, D-9, and D-10 show SEM/EDS profiles for samples removed from solution at 12.6 weeks, 52.6 weeks, and 104 weeks, respectively. Figure D-11 shows SEM/EDS profiles for all five samples to illustrate the progress of $MnO_4^-$ invasion over time. After 24 months, $MnO_4^-$ had penetrated the shale matrix to a distance of approximately 120 to 150 μm (Figure D-12). The short distance of penetration is attributable to the rapid reduction of $MnO_4^-$ by reaction with minerals and organic carbon in the shale which results in precipitation of the Mn-oxide reaction product (Figure D-13). This penetration distance corresponds to an apparent diffusion coefficient on the order of $10^{-17}$ $m^2/s$ which is four to five orders of magnitude lower than might be expected for a conservative solute in this shale and suggests a retardation factor between 104 and 105. There is abundant evidence of reaction between $MnO_4^-$ and pyrite (Figure D-14), and the data suggest that this reaction is initially limited by diffusion (Figure D-15). However, over time as a nano-scale network of Mn-oxide grows in the pore network, the reaction becomes limited by electronic conduction of electrons in Mn oxide between aqueous $MnO_4^-$ at the sample surface and pyrite embedded in the matrix (Figures D-16 and D-17).

The laboratory studies showed the shale at the WVA has a porosity of 0.7% to 3.1%, which is relatively low for shale but still appreciable enough to result in mass transfer of contaminants into the matrix. The tests also showed that an opinion of the suitability of permanganate as a technology at a site may be determined via mineralogical analyses, without the need to necessarily perform ROD studies. If reduced minerals are present in significant concentrations, then the ROD tests may not be required.

# 5.0 COST ASSESSMENT

## 5.1 Cost Reporting

Costs for the various diagnostic tools were tracked and are presented below. The cost elements, as defined in the Federal Remediation Technologies Roundtable format (FRTR 1998) are not directly applicable. Those cost elements apply to remedial technologies, whereas this demonstration is for diagnostic tools. Therefore, the presentation of costs was formatted to best convey the information for the diagnostic tools.

## 5.2 Cost Analysis

### 5.2.1 *Cost Comparison*

Because many of the diagnostic tools evaluated herein are unique, there is no conventional technology to which they may be directly compared. This is true for the mass discharge evaluation tools, rock crushing, isotope analyses, and laboratory studies. Although the costs for MLSs and nested wells may be compared to conventional single-point wells, even this comparison is not particularly useful because of the many configurations available for MLSs and nested wells.

### 5.2.2 *Cost Basis*

The cost basis for each innovative diagnostic tool is provided in Section 5.2.4.

### 5.2.3 *Cost Drivers*

Primary cost drivers for the diagnostic tools, as with most in situ diagnostic tools, include site conditions, nature and extent of contamination, scope of monitoring, and duration of operations. Many of these cost drivers are interrelated, which complicates a quantitative sensitivity analysis. Cost sensitivity of each of these cost drivers is therefore assessed qualitatively below.

#### 5.2.3.1 *Site Conditions*

Difficult lithologies or other surface and subsurface conditions that require expensive drilling technologies, e.g., rotosonic, and preclude less expensive drilling technologies, e.g., direct push, will increase capital costs for field preparation, depending on the numbers of wells (or MLSs), depths, number of completion intervals, and other site parameters. Hydrogeologic conditions including seasonally varying water table elevations and gradients can require more a more intensive well network and may also require control of the gradient by pumping from extraction wells.

Existing infrastructure, e.g., structures and access to utilities, can affect both capital and operation and maintenance (O&M) costs. For example, if power or water must be brought to the

site this increases capital costs for field preparation as well as O&M costs for generators, pumps, etc.

5.2.3.2 *Nature and Extent of Contamination*

Distribution of contaminants and contaminant types (e.g., presence of DNAPL) also affect costs for many of the diagnostic tools. Deep vertical distributions require deeper wells and/or rock cores (for rock crushing) to contact and monitor the contaminated intervals, increasing well construction/drilling costs. Presence of multiple contaminants may complicate analyses and thereby increase monitoring costs. Project costs are therefore sensitive to nature and extent of contamination.

5.2.3.3 *Scope of Monitoring*

Monitoring costs affect O&M costs for multi-level monitoring diagnostic tools. Monitoring costs are related to site conditions and to nature and extent of contamination, as well as to treatment requirements. The areal and vertical extents of monitoring are based on the nature and extent of contamination, and the size of the zone targeted for cleanup. Monitoring costs increase with numbers of monitoring locations, and with monitoring frequency. Also, monitoring costs increase as numbers of analyses are added. Monitoring frequency is based on system performance monitoring requirements and these vary with site conditions and nature and extent of contamination. If extraction and treatment of contaminated water are required (e.g., as for an integrated pump test for mass discharge calculation), additional compliance monitoring prior to discharge or re-injection may be required. Project costs are therefore very sensitive to monitoring requirements.

Monitoring costs may be increased during a field pilot test or during optimization of the treatment as compared with long-term operations. Understanding the system is important during the initial implementation of ISCO, especially in a fractured rock environment, and so increased numbers of wells per unit area, three-dimensional sampling, and more frequent sampling may occur during this period. Once the system has been optimized, however, monitoring locations, frequency and number of analytes will likely be greatly reduced.

5.2.3.4 *Duration of Operations*

The duration of ISCO operations would affect the cost of implementing certain diagnostic tools (e.g., multi-level monitoring diagnostic tools, boundary mass discharge measurements, carbon isotope measurements). Obviously, the longer the duration of active oxidant injection and groundwater monitoring, the greater the project costs. MNA may be implemented as a follow-on remedial alternative to reduce O&M costs, with the concurrence of regulators, to reduce the duration of active ISCO. Project costs are therefore sensitive to duration of operations.

### 5.2.4 *Life Cycle Costs*

The life-cycle costs for each of the diagnostic tools are summarized in the sections below.

5.2.4.1 *Multi-level Monitoring Diagnostic Tools*

The costs for multi-level monitoring systems include the following:

- MLS purchase and shipment to the site.
- MLS installation labor, including MLS manufacturer and site personnel.
- MLS installation equipment and materials, including backfill materials.
- Labor costs associated with MLS system sampling.
- Analytical costs for MLS sample analysis.
- MLS operations and maintenance costs (where applicable), including maintenance of down-hole equipment (Westbay).

After installation, the life cycle cost of an MLS system will be mostly dependent on the frequency of sampling, the number of samples to be collected, and the labor and equipment necessary to conduct the sampling. For example, the FLUTe system utilized at the WVA required relatively little labor and equipment for sampling and no operations and maintenance costs. Conversely, the Westbay system required a two person team to efficiently operate and decontaminate the down-hole equipment necessary for sampling, and maintenance of the down-hole equipment (wireline repairs) was required to keep it in proper working condition. Sampling costs for the CMT and nested well systems varied, but were generally greater than those of the FLUTe and less than those of the Westbay.

For a comparison of system costs, vendor quotes were obtained for the ZIST system and various MLS systems with the following configuration:

- Depth to groundwater: 10’ bgs
- Total depth for monitoring: 150’ bgs
- Number of monitoring zones: 3
- Geology: bedrock
- Borehole size: 6”
- Capabilities: groundwater sampling and water level measurement
- Channels for CMT: 7-channel
- Installation Method: sand and bentonite (i.e., no packers for Westbay or Waterloo systems)

The costs are summarized in Table 5-1 below. These costs do not include charges for drilling or sampling.

**Table 5-1: Cost Comparisons for ZIST and MLSs**

| System | Major Components | Cost |
|---|---|---|
| ZIST (BESST, Inc.) | Blatymini pumps; teflon tubing; riser pipe; well screens; bentonite pellets<br>ZIST transducer housings; Troll 500 transducers; Troll cables; programming cable | $7,487 (not including transducers)<br>$17,446 (including transducers) |

| System | Major Components | Cost |
|---|---|---|
| | ZIST training for installation and operation (2 days) | $3500 (includes travel and expenses) |
| CMT (Solinst, Inc.) | CMT-7-Channel tubing; centralizers; wellhead; installation tool kit | $1,844 |
| | Solinst training for installation and operation (2 days) | $3,600 (includes travel and expenses) |
| Westbay (Schlumberger) | Plastic MP38 casing | $6,400 (casing components)<br><br>$1,600 (2-day rental of sampling equipment)<br><br>$33,000 (purchase of sampling equipment) |
| | Westbay technical services – for training in equipment operation | $4,000 (includes travel and expenses) |
| FLUTe | 150 ft Water FLUTe with 3 ports<br><br>Ancillary equipment for installation – pump tube; wellhead roller rental; winch plate rental; pump plate rental; shipping reels | $10,412 (FLUTe only)<br><br>$13,302 (including ancillary installation equipment) |
| | FLUTe labor to install system | $6,000 (including travel and expenses) |

5.2.4.2 *Mass Discharge Evaluation*

The majority of the costs for the mass discharge evaluation were expended on the geophysical characterization of the boreholes from which the system transmissivity values were calculated. At the WVA, these costs were approximately $4,000 per 150-foot borehole, and included the flow modeling required to calculate transmissivities for individual fractures. Beyond the initial characterization costs, the primary mass discharge evaluation costs include sampling labor and sample analysis, which are also part of the MLS costs. In the case of the WVA, the cost for sampling and analysis of the compliance boundary monitoring wells, which included 18 separate monitoring zones, was approximately $6,500 to $7,500 per sampling event, depending on the time of year the samples were collected.

5.2.4.3 *Rock Crushing*

Costs for rock crushing include (a) additional drilling costs for collecting continuous (typically HQ-size) cores, ideally using a triple-tube core barrel system; (b) additional personnel costs (including daily rate, travel, lodging & per diem) including a field hydrogeologist who works with the geologist and collects the rock core samples during drilling and a two-person crew for sample crushing and processing; (c) rental of the hydraulic rock crusher, crushing cells and ancillary equipment (methanol dispenser, balance, hammers, chisels, etc); (d) expendable material costs including vials, methanol for sample processing and decontamination, coolers for shipping samples, etc.; (e) shipping costs; (f) sample extraction and analytical costs for VOC analyses; (g) costs for physical property analyses (e.g., moisture content, porosity, bulk density,

organic carbon content, matrix permeability, chloride diffusion coefficient) on a representative number of samples for the different lithologies encountered; and (g) costs associated with analyzing and reporting the results.

For the WVA site, the overall average sample frequency (seven rock core locations) was about just over one rock core VOC sample per foot (average spacing of 0.9 ft) and then an additional 20% or so for QA/QC (trip, equipment and methanol blanks and field duplicates). The samples were extracted and analyzed for a limited suite of analytes (including PCE, TCE, DCE isomers) at the University of Waterloo using a method that provides exceptionally low method detection limits (MDLs) for the analytes in methanol extract, and which is not available commercially. Analytical costs for a commercial lab would generally be much higher, and methods used typically involve diluting the methanol extract into water prior to analysis and this has much higher MDLs. For the physical parameter analyses, the full suite of analyses indicated above were performed by the Golder Associates Lab in Mississauga, Ontario at an approximate cost of $1,000 per sample. Golder Associates Lab is the only lab we are aware of that routinely performs all these types of measurements. At WVA, the average cost of rock crushing (assuming one sample collected per foot of core) ranged from $110 - $130 per linear foot of core. It is expected that these costs will rise if this technology is commercialized.

5.2.4.4 *Isotope Analyses*

Research laboratories at UW and at the University of Toronto specialize in compound-specific carbon isotope analyses. Microseeps is the first (and as far as we know, only) commercial laboratory in North America to offer compound specific isotope analysis. They currently offer analyses for various compounds including the chlorinated solvents. The cost ranges from approximately $300 to $500 per sample, depending on the number of compounds to be analyzed.

5.2.4.5 *Rock Oxidant Demand Tests and Permanganate Invasion Studies*

The costs of conducting laboratory studies varies widely depending on the scope and duration of the studies. Primary cost drivers include labor costs, equipment costs, and supply costs. Because the range of costs varies dramatically depending on the types of studies that are designed, it is not possible to accurately bracket these types of costs.

## 5.3 Cost-Benefit of Implementing Innovative Diagnostic Tools

A qualitative analysis of the cost-benefits of applying the innovative diagnostic tools is provided below. The cost-benefit of the tools was evaluated relative to the two primary objectives for the demonstration, which were to:

- Characterize and delineate the VOC contamination in a fractured rock setting using innovative diagnostic tools (see Table 5-2).

- Use innovative diagnostic tools to evaluate the effectiveness of ISCO with permanganate in a fractured rock setting (see Table 5-3).

**Table 5-2: Cost-Benefit Evaluation for Use of Innovative Tools in Characterizing and Delineating VOCs in Fractured Rock**

| Tool | Cost | Benefits | Limitations | Cost Savings for Use of Innovative Tool |
|---|---|---|---|---|
| Multi-Level Monitoring Systems | See Table 5-1 | Ability to evaluate vertical variability in aqueous VOC concentrations.<br><br>Contributes to more robust CSM, especially when comparing aqueous VOC results to rock matrix analysis data. | Additional costs for MLS components and installation. Also, additional analytical costs. | Cost savings due to reduced rock drilling compared to nested wells required to obtain similar information. |
| Mass Discharge Evaluation (boundary mass discharge) | $24,000 initial geophysics for 6 boreholes; $7000 per sampling event (18 monitoring zones) | Quantification of VOC mass being discharged from the site. | Difficult to quantify transmissivities and hydraulic gradients in fractured rock<br><br>Possibility of backdoor fractures conveying mass past the discharge plane. | If mass discharge at boundary is accepted as site metric, then could save on installation of more site-wide monitoring wells and focus on collection of data at boundary. |
| Rock Matrix Analyses | $130 per linear foot of core (1 sample per foot). Cost expected to increase when technology is available commercially. | Confirm diffusion of VOCs into rock matrix and estimate diffusion rates from preliminary testing.<br><br>Identify active flowpaths that are too small for detection using geophysical testing or aqueous phase sampling. | Results vary greatly with sample location.<br><br>Requires collection of numerous samples. | The realization that most of the VOC mass resided in the rock matrix influenced approach to remedy and expectations for cleanup time-frames. No other tools exist that provide this type of information. |
| Isotope Analyses | $300 - $500 / sample | Indication of degree of VOC degradation that has occurred prior to remedy application.<br><br>Baseline information for comparison to results obtained during remedy application. | Specialized analysis; regulators and other practioners may be unfamiliar with this tool.<br><br>Additional costs to the investigation program. | Tool provides unique information. No cost savings identified for its use during site characterization. |

**Table 5-3: Cost-Benefit Evaluation for Use of Innovative Tools in Evaluation of ISCO with Permanganate in Fractured Rock**

| Tool | Cost | Benefits | Limitations | Cost Savings for Use of Innovative Tool |
|---|---|---|---|---|
| Multi-Level Monitoring Systems | See Table 5-1 | Monitor vertical distribution of permanganate (not a feature of all systems).<br><br>Permanganate solution delivery (not a feature of all systems) | Additional costs for MLS components and installation. Also, additional analytical costs.<br><br>Incompatibilities with permanganate led to system failures in some instances (see Section 4.3.1.11) | Cost savings due to reduced rock drilling compared to nested wells required to obtain similar information. |
| Mass Discharge Evaluations | $24,000 initial geophysics for 6 boreholes; $7000 per sampling event (18 monitoring zones) | Quantification of VOC mass being discharged from the site.<br><br>Evaluation of ISCO success in reducing mass of VOCs being discharged from the site. | Difficult to quantify transmissivities and hydraulic gradients in fractured rock<br><br>Possibility of backdoor fractures conveying mass past the discharge plane. | If mass discharge at boundary is accepted as site metric, then could save on installation of more site-wide monitoring wells and focus on collection of data at boundary. |
| Rock Matrix Analyses | $130 per linear foot of core (1 sample per foot). Cost expected to increase when technology is available commercially. | Identify active flowpaths that are too small for detection using geophysical testing or aqueous phase sampling.<br><br>Determine whether permanganate is diffusing into the rock matrix. | Results vary greatly with sample location.<br><br>Requires collection of numerous samples.<br><br>Long time-frames for permanganate diffusion. | The realization that most of the VOC mass resided in the rock matrix influenced approach to remedy and expectations for cleanup time-frames. No other tools exist that provide this type of information. |
| Isotope Analyses | $300 - $500 / sample | Distinguish between VOC destruction via oxidation versus displacement.<br><br>Chart active flow paths and fracture connections by tracking permanganate-influenced water.<br><br>Gauge VOC rebound timeframe. | Specialized analysis; regulators and other practioners may be unfamiliar with this tool.<br><br>Additional costs to the monitoring program. | Cost savings due to acceptance of ISCO treatment.<br><br>Cost savings from understanding contaminant rebound timeframe, which guides permanganate application frequency. |
| Rock oxidant demand testing and permanganate invasion studies | Varies widely based on scope of studies | Aid in designing dosage for permanganate application.<br><br>Estimate cleanup timeframes for permanganate treatment. | Uncertainties in scale-up to field setting. | Cost savings due to more accurate calculation of permanganate dosage requirements. |

# 6.0 IMPLEMENTATION ISSUES

## 6.1 Environmental Checklist

No permitting requirements were required to implement the demonstration. All activities were performed in a previously disturbed, contaminated area. No emissions were produced by the in-situ treatment diagnostic tools.

## 6.2 Other Regulatory Issues

The permanganate injection program is being implemented under a Consent Order between the Watervliet Arsenal (WVA), the New York State Department of Environmental Conservation (NYSDEC), and the United States Environmental Protection Agency (USEPA). The consent order mandates that the WVA implement Facility Investigations and Corrective Measures under a site-wide Resource Conservation and Recovery Act (RCRA) Corrective Action program. The NYSDEC is the lead agency for the program. The permanganate injection program will become part of the Statement of Basis for the site upon approval of the regulator-required Work Plan documents. The Statement of Basis will be published for public comment prior to finalization by the regulatory agencies.

## 6.3 End-User Issues

End-users for the diagnostic tools are contractors, responsible parties, and agencies (including the DOD) who are responsible for mitigating risks to human health and the environment posed by CVOCs in groundwater – particularly in fractured bedrock systems. Listed below for each diagnostic tool are specific end-user concerns, reservations and decision-making factors, procurement issues, and planned technology transfer efforts.

**Table 6-1: End-User Issues**

| Diagnostic Tool | End-user concerns, reservations, decision-making factors | Procurement Issues | Planned technology transfer efforts |
|---|---|---|---|
| Multi-Level Monitoring Systems | The performance criteria described in Table 4-1 should be considered by an end-user. Each of the systems possesses positive attributes that would recommend it for an appropriate site-specific application. | All of the MLSs discussed in this report are commercially produced and readily available in whatever configuration is required for a site-specific application. | The MLSs tested for this study are already available. |

| Diagnostic Tool | End-user concerns, reservations, decision-making factors | Procurement Issues | Planned technology transfer efforts |
|---|---|---|---|
| Mass Discharge Evaluations | Depending on site-specific geology, size of the site, and other site parameters, there may be a significant cost to calculating mass discharge. It should be discussed with the appropriate regulatory agency prior to proceeding with this approach. The transect approach is fairly straight-forward to implement. The integrated mass flux test has not been used as commonly, and there are questions regarding its applicability to fractured rock systems. | The components required to perform these tests (i.e., monitoring wells, pumps, etc.) are readily available. | Not applicable. |
| Rock Crushing | Rock core analyses may provide valuable information regarding contaminant distribution at a fractured rock site. This insight can be used to identify valid treatment options and probable treatment time-frames. | Currently this procedure is not commercialized. It is only available through the University of Waterloo. | Dr. Beth Parker is working to produce a Standard Operating Procedure for rock core analyses. |
| Isotope Analyses | Isotope analyses may be used to confirm contaminant oxidation as opposed to displacement and for evaluation of VOC rebound. The timing for sample collection is important because no isotope measurement is obtained unless the water contains chlorinated solvent mass (i.e., if all of the solvent mass has been oxidized, then no isotope measurement is possible). Therefore, the | Isotope analyses are performed by several university research laboratories as well as by at least one commercial laboratory (Microseeps). | If the demand for this analysis rises, market forces dictate that more commercial laboratories will offer it as a service. |

| Diagnostic Tool | End-user concerns, reservations, decision-making factors | Procurement Issues | Planned technology transfer efforts |
|---|---|---|---|
| | sampling protocol will have to carefully planned prior to sample collection. | | |
| Rock oxidant demand testing and permanganate invasion studies | Vary widely depending on the scope of the laboratory studies. For rock oxidant demand testing, it is important to understand that the rock oxidant demand may be dependent on the concentration of the oxidant. For permanganate invasion testing, a detailed understanding of the matrix is required (e.g., presence of micro-fractures). | Generally require a cooperative agreement with an academic institution. | These tests are site-specific and technology-specific. |

# 7.0 POINTS OF CONTACT

**Table 7-1. Points of contact**.

| POINT OF CONTACT<br>Name: | ORGANIZATION<br>Name:<br>Address: | PHONE/FAX/E-MAIL | ROLE IN PROJECT |
|---|---|---|---|
| Mike Kavanaugh | Malcolm Pirnie, Inc.<br>2000 Powell Street, Suite 1180<br>Emeryville, CA 94608 | 510-735-3010 (phone)<br>510-596-3060 (fax)<br>mkavanaugh@pirnie.com | Principal Investigator |
| Ken Goldstein | Malcolm Pirnie, Inc.<br>104 Corporate Park Drive<br>White Plains, NY 10602 | 914-641-2863 (phone)<br>914-614-2455 (fax)<br>kgoldstein@pirnie.com | Project Coordinator |
| Rula Deeb | Malcolm Pirnie, Inc.<br>2000 Powell Street, Suite 1180<br>Emeryville, CA 94608 | 510-735-3005 (phone)<br>510-596-8855 (fax)<br>rdeeb@pirnie.com | Project Manager |
| Beth Parker | Department of Earth & Environmental Sciences<br>University of Waterloo<br>200 University Avenue West<br>Waterloo, Ontario N2L 3G1<br>Canada<br><br>School of Engineering<br>University of Guelph<br>50 Stone Road East<br>Guelph, Ontario N1G 2W1<br>Canada | (519) 888-4567 ext. 35371 (phone)<br>(519) 883-0220 (fax)<br>blparker@uwaterloo.ca<br><br>(519) 824-4120 ext. 53642 (phone)<br>519-836-0227 (fax)<br>bparker@uoguelph.ca | Technical Lead |

# 8.0 REFERENCES


Annable, M.D., Hatfield, K., Cho, J., Klammler, H., Parker, B.L., Cherry, J., and Rao, P.S. 2005. Field-scale evaluation of the passive flux meter for simultaneous measurement of groundwater and contaminant fluxes. Environ. Sci. Technol., 39, 7194-7201.

Aravena, R., Parker, B., Cherry, J., Navon, D., Vitolins, A.R., Goldstein, K.J. Anderson, G.A., and Wood, S.P. 2004. Use of carbon isotopes to monitor in situ oxidation of chlorinated ethenes in a fracture rock aquifer. The Third International Conference on Oxidation and Reduction Technologies for in Situ Treatment of Soil and Groundwater. San Diego, California, October 24-28.

Berkowitz, B. 2002. Characterizing flow and transport in fractured geologic media: a review. Advances in Water Resources, 25(8): 861-884.

Black, W.H., H.R. Smith, and F.D. Patton, 1986. Multiple-level ground water monitoring with the MP system. Proceedings of the Conference on Surface and Borehole Geophysical Methods and Ground Water Instrumentation, National Water Well Association, Dublin, OH, pp. 41-60.

Bloom, Y., Aravena, R., Hunkeler, D., Edwards, E. and Frape, S.K. 2000. Carbon isotope fractionation during microbial dechlorination of trichloroethene, cis-1,2-dichloroethene and vinyl chloride: Implications for assessment of natural attenuation Environ. Sci. Technol., 34: 2768-2772.

Bockelmann, A., T. Ptak, and G. Teutsch, 2001. An Analytical Quantification of Mass Fluxes and Natural Attenuation Rate Constants at a Former Gasworks Site. Journal of Contaminant Hydrology, 53(3-4): 429-53.

Cherry, J.A. and P.E. Johnson, 1982. A multi-level device for monitoring in fractured rock, Ground-Water Monitoring Review, 2(3), 41–44.

Cherry, J.A, Parker, B.L., Keller, C. 2007. A New Depth-Discrete Multilevel Monitoring Approach for Fractured Rock. Ground-Water Monitoring and Remediation, 27(2), 57-70.

Churcher, P.L., Dichhout, R.D. 1987. Analysis of ancient sediments for total organic carbon – some new ideas. J. Geochem. Explor. 29, 235-246.

Einarson, M. D., and D. M. Mackay. 2001. Predicting impacts of groundwater contamination, Environ. Sci. Technol., 35(3), 66A–73A.

Einarson, M.D. and J.A. Cherry, 2002. A new multi-level ground-water monitoring system utilizing multichannel tubing, Ground-Water Monitoring and Remediation, 22(4), 52–65.

Einarson, M. 2006. Multilevel Ground-Water Monitoring. Chapter 11 in Practical Handbook of Environmental Site Characterization and Ground-Water Monitoring, 2nd Ed. Edited by David M. Nielsen, CRC Press, Boca Raton, FL.

Feenstra, S., Mackay, D.M., Cherry, J.A. 1991. Presence of residual NAPL based on organic chemical concentrations in soil samples. Ground Water Monit. Rev. 11 (2), 128– 136.

Freeze, R.A. and J.A. Cherry . 1979. Groundwater. Prentice Hall, Englewood Cliffs, NJ.

Goldstein, K.J., Vitolins, A.R., Navon, D., Parker, B.L., Chapman, S., Anderson, G.A. 2004. Characterization and Pilot-Scale Studies for Chemical Oxidation Remediation of Fractured Shale. Remediation, 14(4): 19-37.

Guilbeault,M.A., B.L. Parker, and J.A. Cherry. 2005. Mass and flux distributions from DNAPL zones in sandy aquifers, Ground Water, 43(1), 70-86.

Hatfield, K.; Annable, M. D.; Cho, J.; Rao, P. S. C.; Klammler, H. 2004. A direct method for measuring water and contaminant fluxes in porous media. J. Contam. Hydrol. 75, 155-181.

Hønning, J., Broholm, M.M., Bjerg, P.L. 2007. Quantification of potassium permanganate consumption and PCE oxidation in subsurface materials. Journal of Contaminant Hydrology, 90,221–239. doi:10.1016/j.jconhyd.2006.10.002.

Hunkeler, D., Aravena, R., Butler, B.J. 1999. Monitoring microbial dechlorination of tetrachloroethene (PCE) using compound-specific carbon isotope ratios: microcosms and field experiments. Environ. Sci. Technol. 33 (16), 2733– 2738.

Hunkeler, D., and Aravena, R. 2000. Determination of stable carbon isotope ratios of dissolved chlorinated solvents by GC-C-IRMS: Comparison of headspace and solid-phase microextraction. Environ. Sci. Technol., 34: 2839-2844.

Hunkeler, D., R. Aravena, B.L. Parker, J.A. Cherry and X. Diao. 2003. Monitoring oxidation of chlorinated ethenes by permanganate in groundwater using stable isotopes: Laboratory and field studies. Environ. Sci. Technol., 37(4), pp. 798-804.

Hunkeler, D., R. Aravena, B.L. Parker and J.A. Cherry, 2004. Assessment of the oxidation of chlorinated ethenes by permanganate in aquifers using isotope analysis. First European Conference on Oxidation and Reduction Technologies for In-Situ and Ex-Situ Treatment of Water, Soil and Air (ECOR-1), Göttingen, Germany, April 25-28, 2004.

Hurley, J.C. and Parker, B.L. 2002. Rock core investigation of DNAPL penetration and TCE mobility in fractured sandstone. In: Ground and Water: Theory to Practice, Proceedings of the 55th Canadian Geotechnical and 3rd Joint IAH-CNC and CGS Groundwater Specialty Conferences. Eds. Stolle D., A.R. Piggott and J.J. Crowder, Southern Ontario Section of the

Canadian Geotechnical Society, October 20-23, Niagara Falls, Ontario, pp. 473-480.

Interstate Technology & Regulatory Control, Dense Non-Aqueous-Phase Liquids Team, 2004. Strategies for Monitoring the Performance of DNAPL Source Zone Remedies.

Meyer, J.R., Parker, B.L., Cherry, J.A. 2007. Detailed hydraulic head profiles as essential data for defining hydrogeologic units in layered fractured sedimentary rock. Environ. Geol. DOI 10.1007/s00254-007-1137-4.

Michelle M. G. Chartrand, M.,.G., Waller, A., Mattes, T.M., Elsner, M., Lacrampe-Couloume, G., Gossett, J.M., Edwards, E.A., and Sherwood Lollar, B. 2005. Carbon Isotopic Fractionation during Aerobic Vinyl Chloride Degradation, Environ. Sci. Technol., 39:1064-1070.

NRC (National Research Council). 1996. Rock fractures and fluid flow: contemporary understanding and applications. National Academy Press, Washington, DC, 551 pp.

Pankow, J.F., Cherry, J.A., 1996. Dense Chlorinated Solvents and other DNAPLs in Groundwater. Waterloo Press, Portland, OR.

Parker, B.L., Gillham, R.W. and Cherry, J.A. 1994. Diffusive disappearance of immiscible-phase organic liquid in fractured geologic media. Ground Water 32(5): 805-820.

Parker, B.L., McWhorter, D.B., and Cherry, J.A. 1997. Diffusive loss of non-aqueous phase organic solvents from idealized fracture networks in geologic media. Ground Water 35(6): 1077-1088.

Parker, B.L. and J.A. Cherry. 1999. Scale Considerations of Chlorinated Solvent Source Zones and Contaminant Fluxes: Insights from Detailed Field Studies. U.S. Geologic Survey Toxic Substances Hydrology Program – Proceedings of the Technical Meeting Charleson, SC March 8-12, 1999. Volume 3, Subsurface Contamination from Point Sources, Water-Resources Investigations Report 99-4018C.

Parker, B.L., Cherry, J.A., Swanson, B.J. 2006. A Multilevel System for High-Resolution Monitoring in Rotasonic Boreholes. Ground Water Monitoring and Remediation, 26(4), 57-73.

Parker, B.L. 2007. Investigating contaminated sites on fractured rock using the DFN approach. Proceedings of the 2007 U.S. EPA/NGWA Fractured Rock Conference: State of the Science and Measuring Success in Remediation, Sept. 24-26, 2007, Portland, Maine, pp. 150-168.

Pehme, P.E., Greenhouse J. P. and Parker B.L. 2007. The Active Line Source (ALS) technique, a method to improve detection of hydraulically active fractures and estimate rock thermal conductivity. Proceedings of 60th Canadian Geotechnical Conference & 8th Joint IAH-CNC Groundwater Conference, Ottawa, Ontario, October 21-24, 2007.

Potter, P.E., Maynard, J.B., Depetris, P.J. 2005. Mud & Mudstones. Springer, 205pp.

Poulson, S.R., Naraoka, H. 2002. Carbon Isotope Fractionation during Permanganate Oxidation of Chlorinated Ethylenes (cDCE, TCE, PCE). ES&T (36), pp. 3270-3274.
Price, M and Williams, A T, 1993. The influence of unlined boreholes on groundwater chemistry: a comparative study using pore-water extraction and packer sampling. *Journal of the Institution of Water and Environmental Management*, **7,** (6): 651-659.

Sara, M.N. 2003. Site Asssessment and Remediation Handbook, 2nd Edition. Lewis Publishers, CRC Press, 1160 pp.

Sherwood Lollar, B. and Slater, G.F. 2001. Stable Carbon Isotope Evidence for Intrinsic Bioremediation of Tetrachloroethene and Trichloroethene at Area 6, Dover Air Force Base Environ. Sci. Technol. 35 361-369.

Siegrist, R.L., M.A. Urynowicz, O.R. West, M.L. Crimi and K.S. Lowe. 2001. Principles and Practices of In Situ Chemical Oxidation Using Permanganate. Battelle Press. 2001.

Slater, G.F., Sherwood Lollar, B., Sleep, B. and Edwards, E., 2001. Variability in Carbon Isotopic Fractionation during Biodegradation of Chlorinated Ethenes: Implications for Field Applications. Environ. Sci. Technol., 35: 901-907.

Sterling, S.N., Parker, B.L., Cherry, J.A, Williams, J.H., Lane Jr., J.W., Haeni, F.P. 2005. Vertical Cross Contamination of Trichloroethylene in a Borehole in Fractured Sandstone. Ground Water 43(4): 557-573.

USEPA QA/G-4: Guidance for the Data Quality Objectives Process, EPA/600/R-96-055, September 1994.

Vieth, A., Müller, J., Strauch, G., Kästner, M., Gehre, M., Meckenstock, R.U. and Richnow, H.H. 2003. In-situ biodegradation of tetrachloroethene and trichloroethene in contaminated aquifers monitored by stable isotope fractionation. Isotopes Environmental and Health Studies, 39(2).

Williams, J.H. and F. Paillet. 2002a. Characterization of Fractures and Flow Zones in a Contaminated Shale at the Watervliet Arsenal, Albany County, New York. U.S. Geological Survey Open-File Report 01-385.

Williams, J.H., and Paillet, F.L. 2002b. Using flowmeter pulse tests to define hydraulic connections in the subsurface: a fractured shale example. Journal of Hydrology, 265: 100-117.

# Appendix A
Rock Core VOC Results

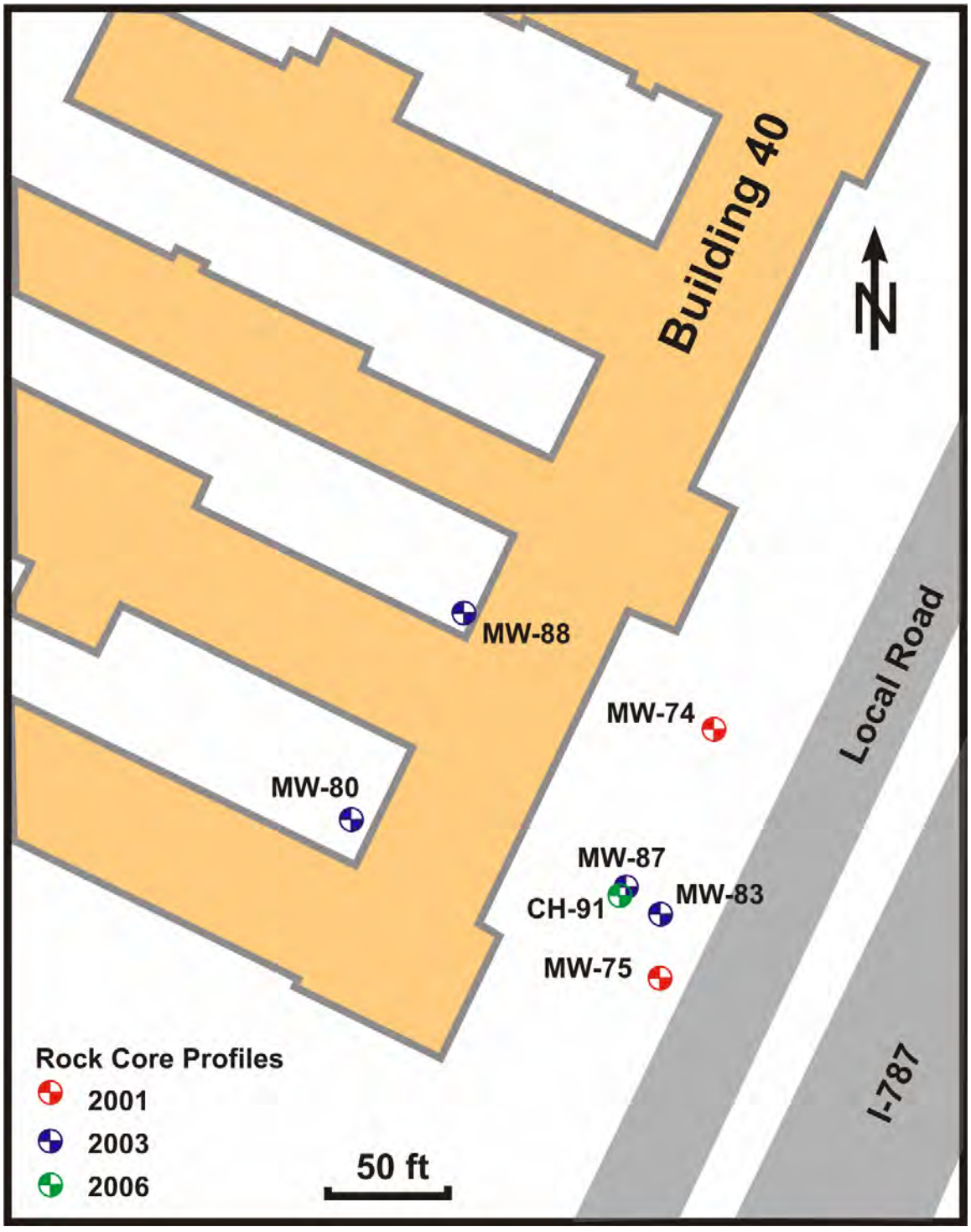


Figure A-1: Rock core VOC profile locations.

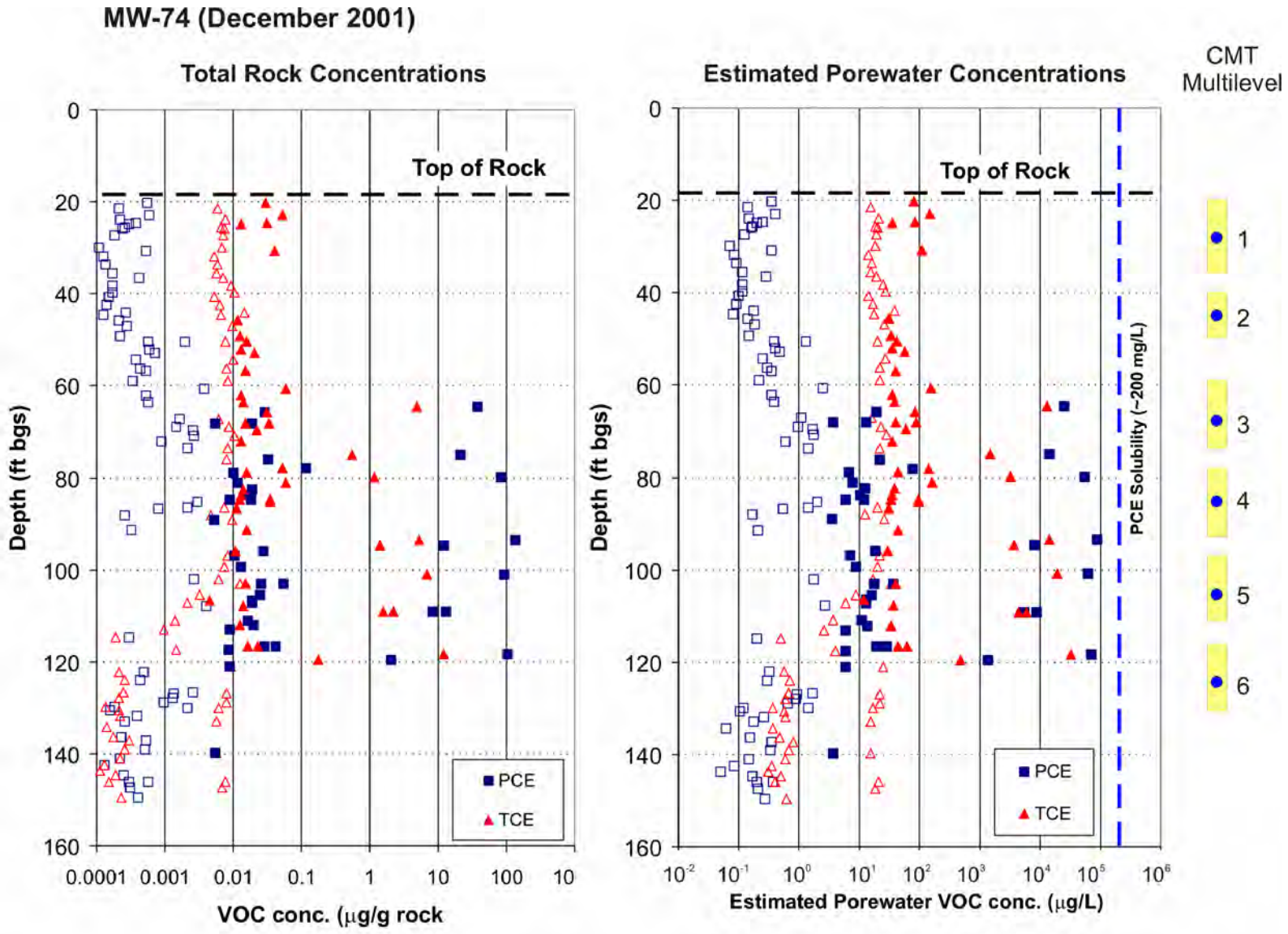


Figure A-2: Rock core VOC profiles at MW-74 (December 2001) and CMT multilevel system. Hollow symbols represent non-detects or samples flagged due to blanks contamination.

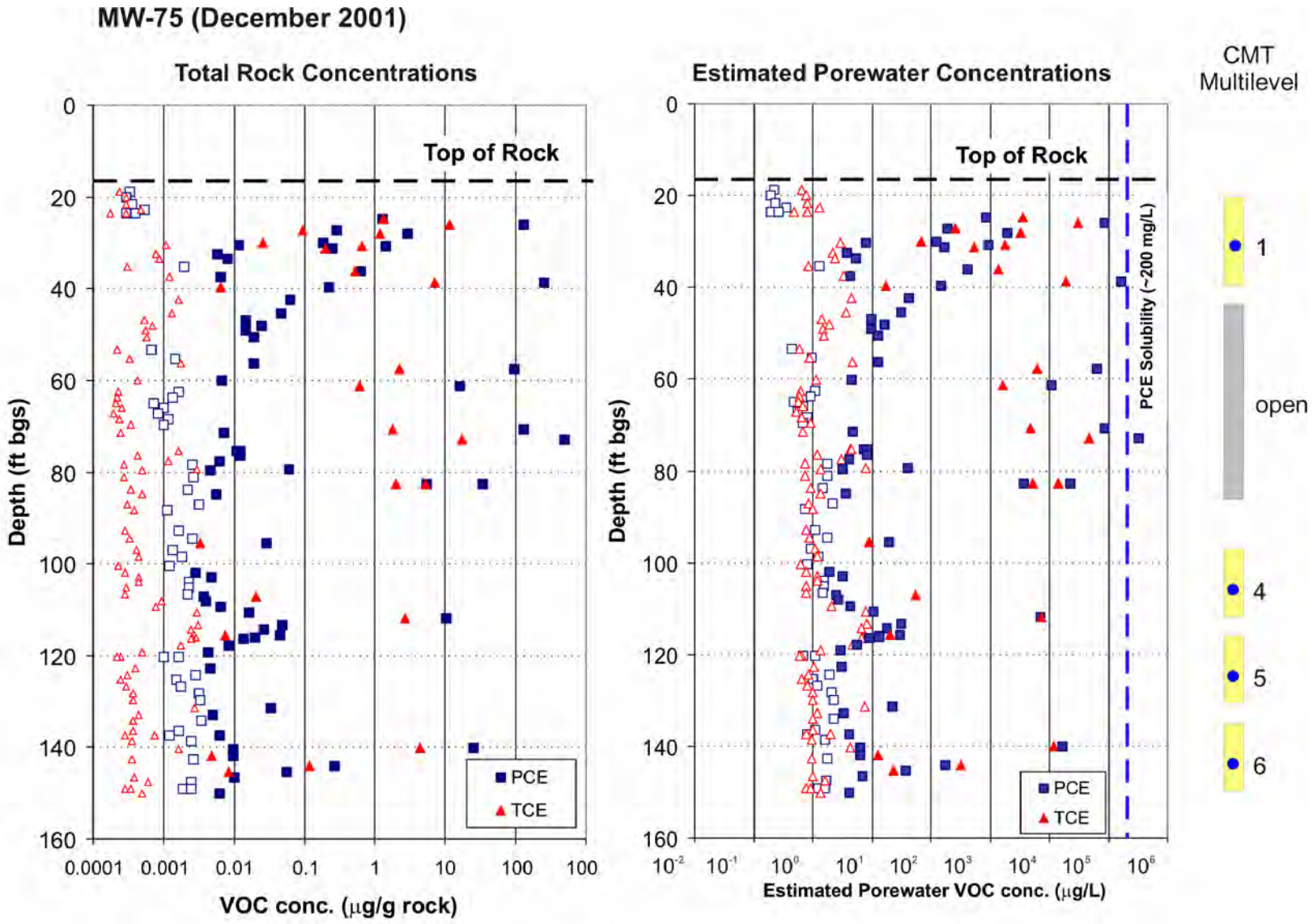


Figure A-3: Rock core VOC profiles at MW-75 (December 2001) and CMT multilevel system. Hollow symbols represent non-detects or samples flagged due to blanks contamination.

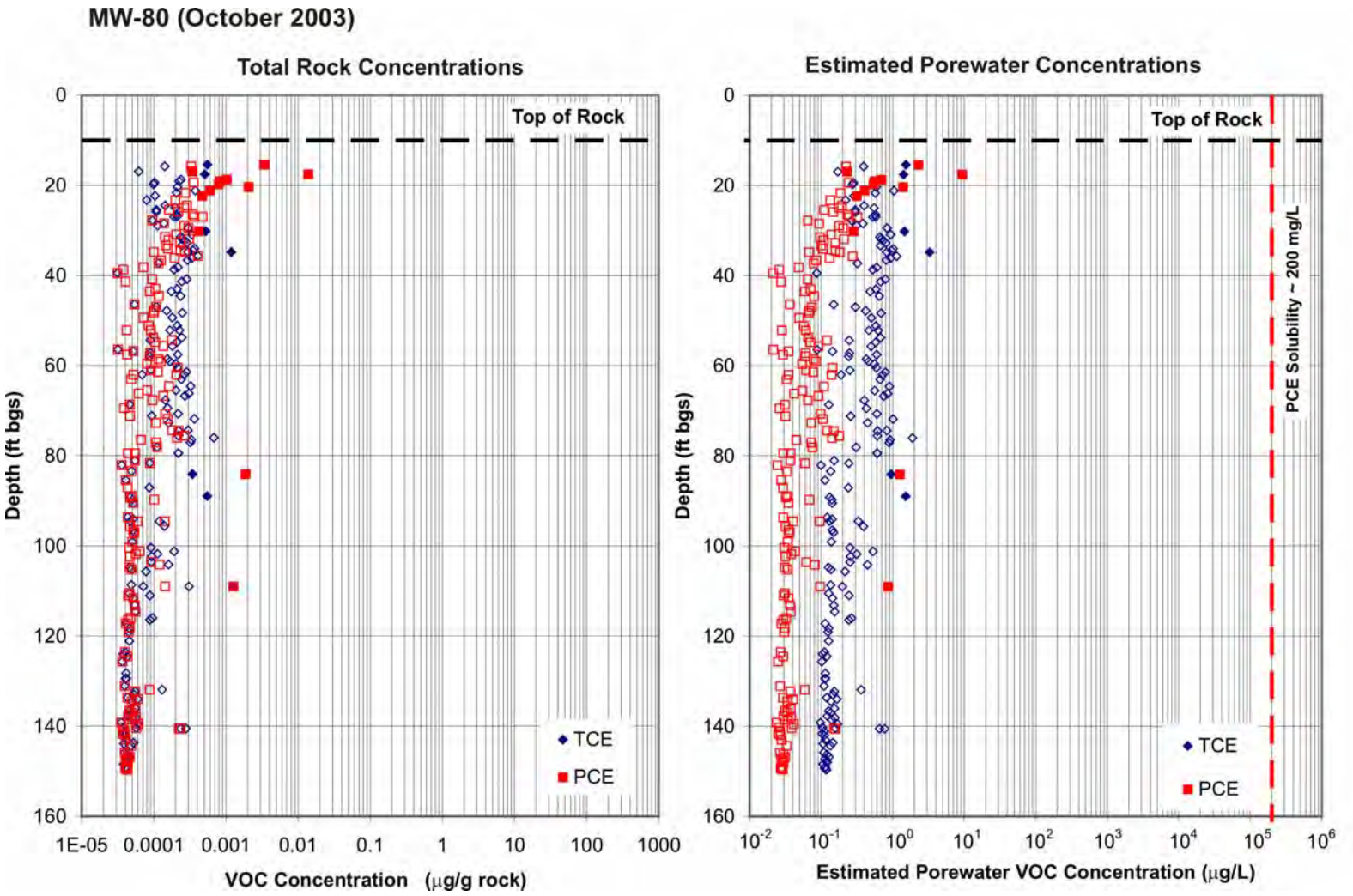


Figure A-4: Rock core VOC profiles at MW-80 (October 2003). Hollow symbols represent samples flagged with a J (between MDL and LOQ, or flagged due to blanks contamination).

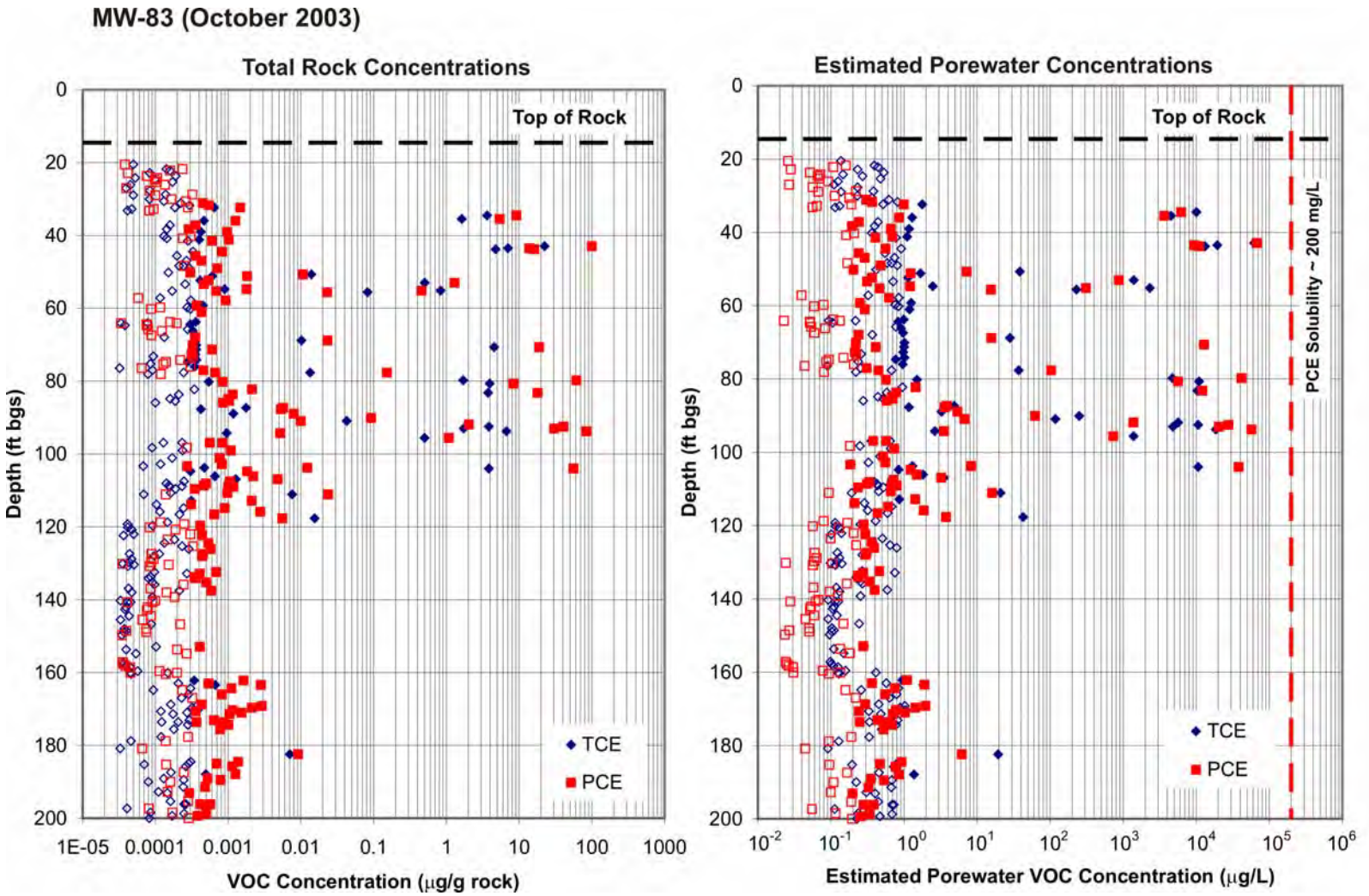


Figure A-5: Rock core VOC profiles at MW-83 (October 2003). Hollow symbols represent samples flagged with a J (between MDL and LOQ, or flagged due to blanks contamination).

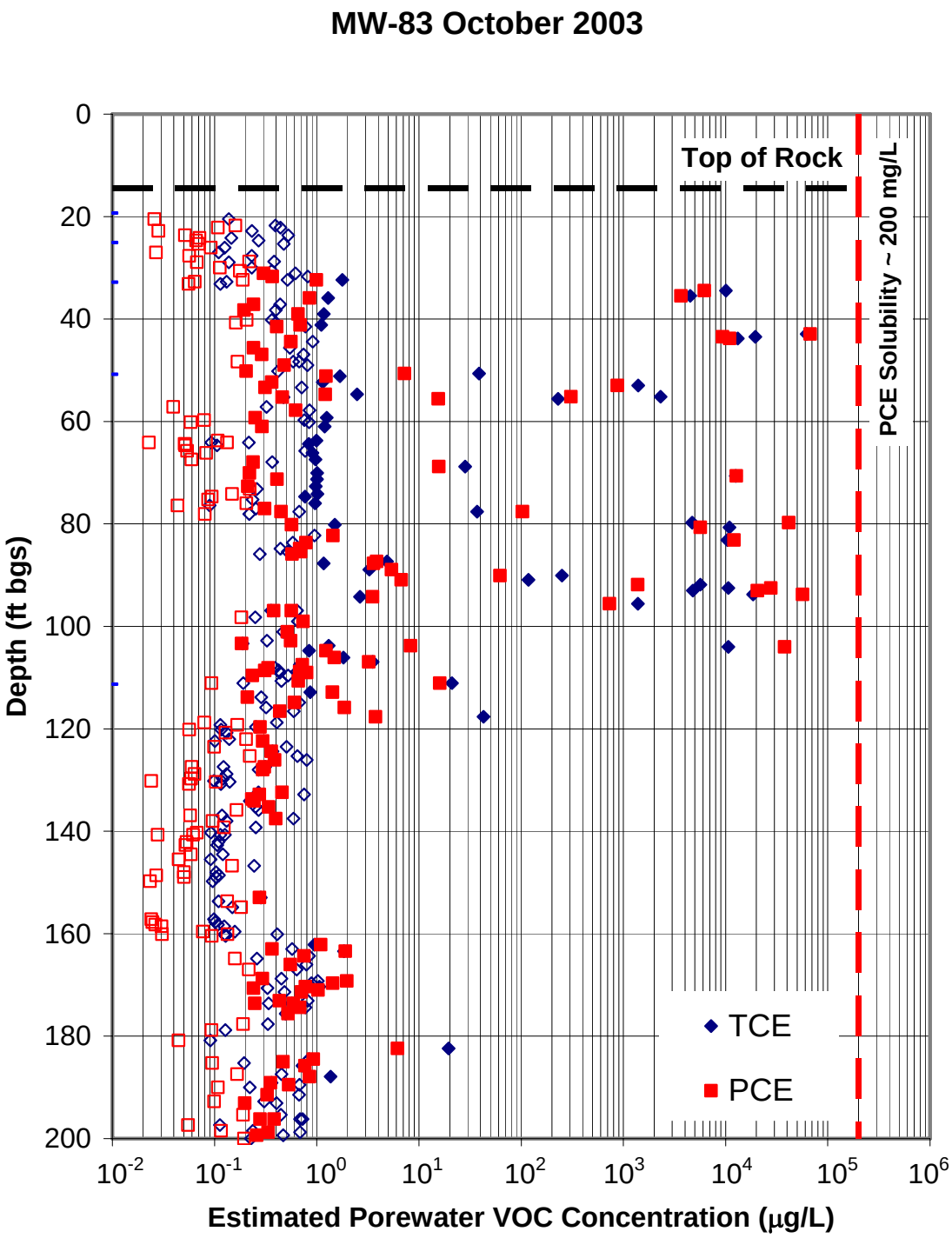


Figure A-6: Estimated rock core porewater VOC concentrations at MW-83 (October 2003) and locations of flow zones identified during borehole flow testing.

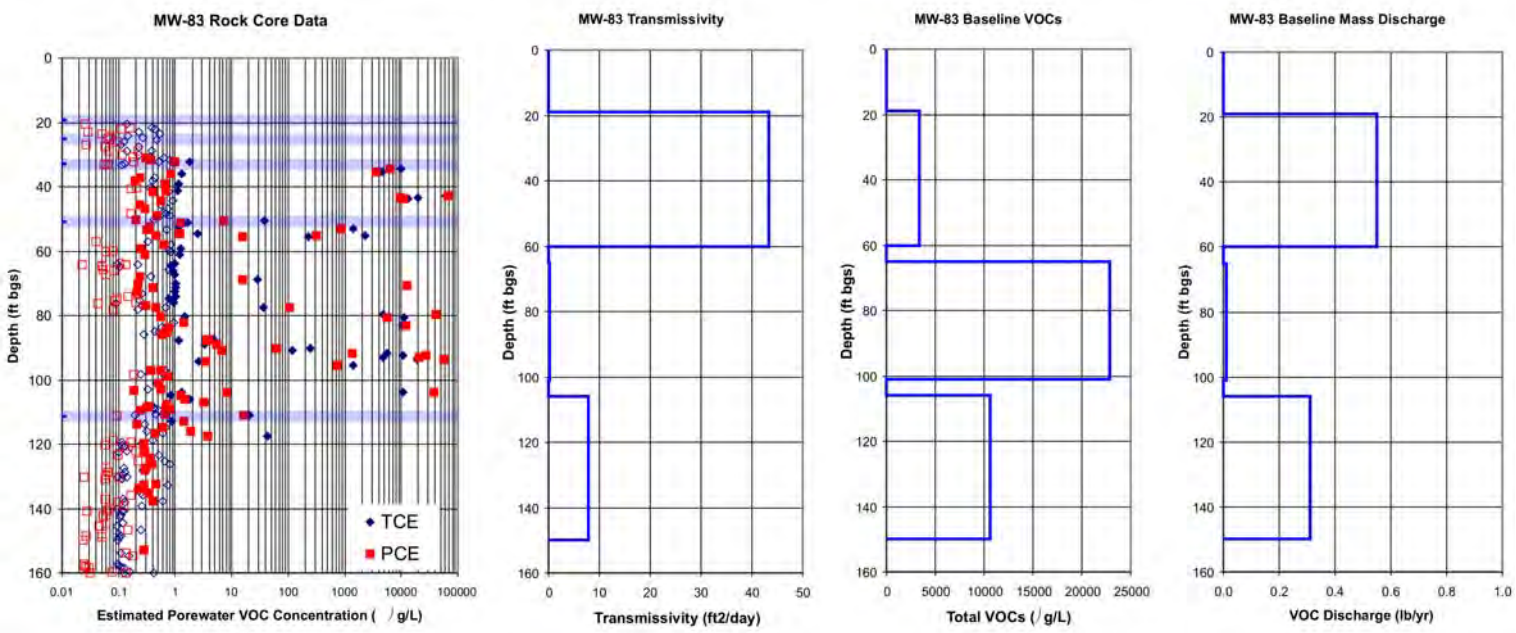


Figure A-7: Estimated rock core porewater VOC concentrations at MW-83 (October 2003) and comparison with multilevel-derived transmissivity, VOC concentrations and mass discharge.

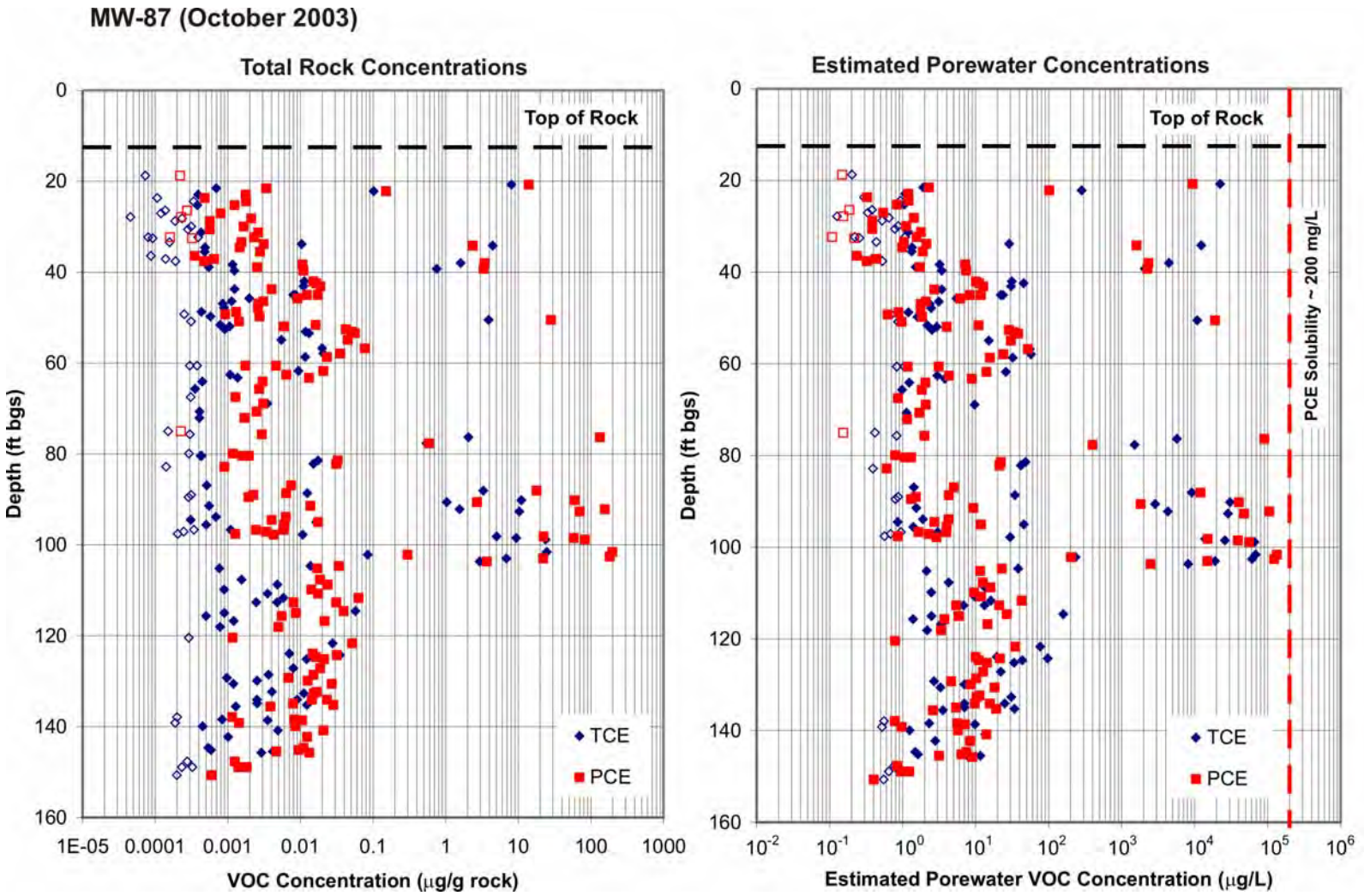


Figure A-8: Rock core VOC profiles at MW-87 (October 2003). Hollow symbols represent samples flagged with a J (between MDL and LOQ, or flagged due to blanks contamination).

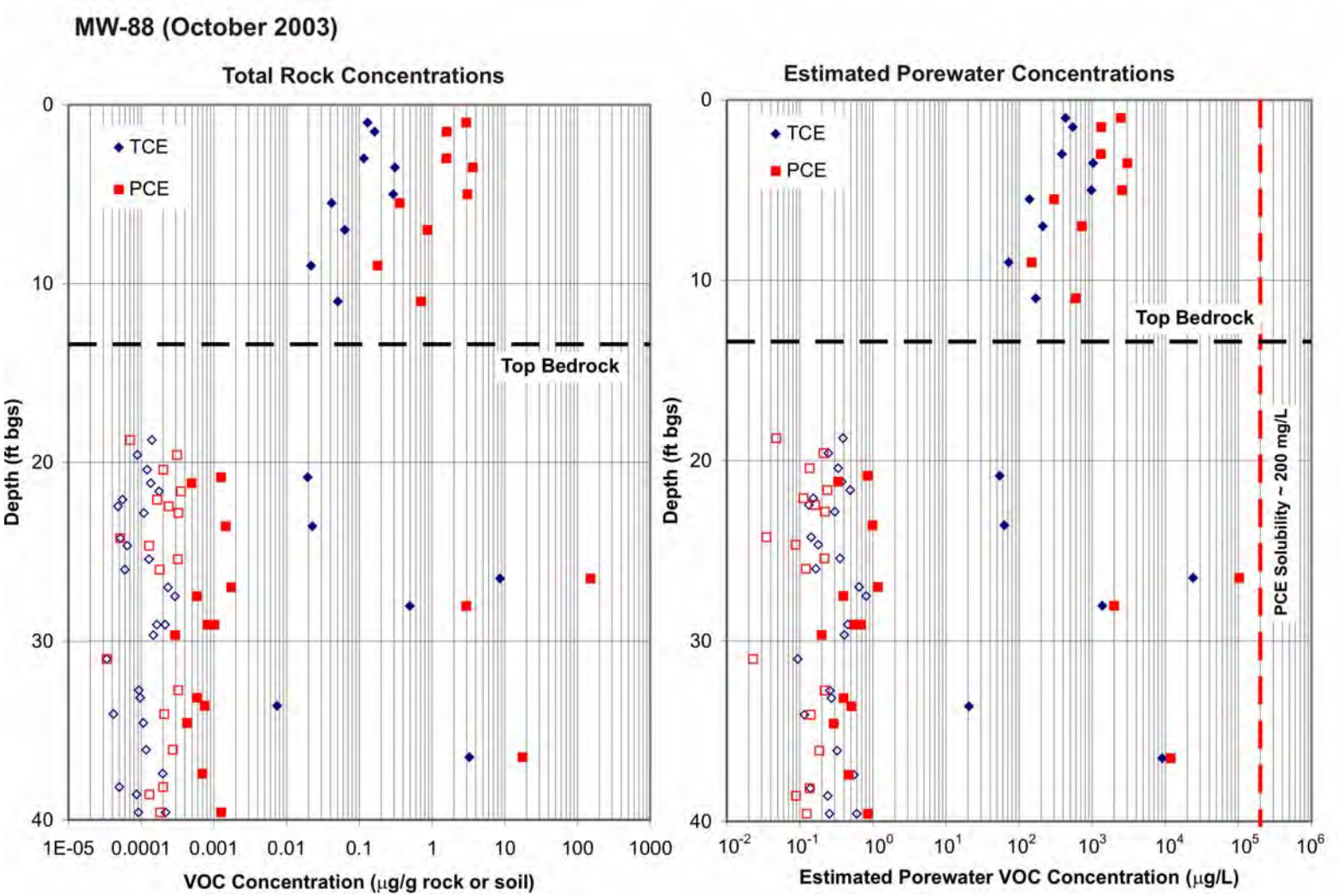


Figure A-9: Rock core / overburden VOC profiles at MW-88 (October 2003). Hollow symbols represent samples flagged with a J (between MDL and LOQ, or flagged due to blanks contamination).

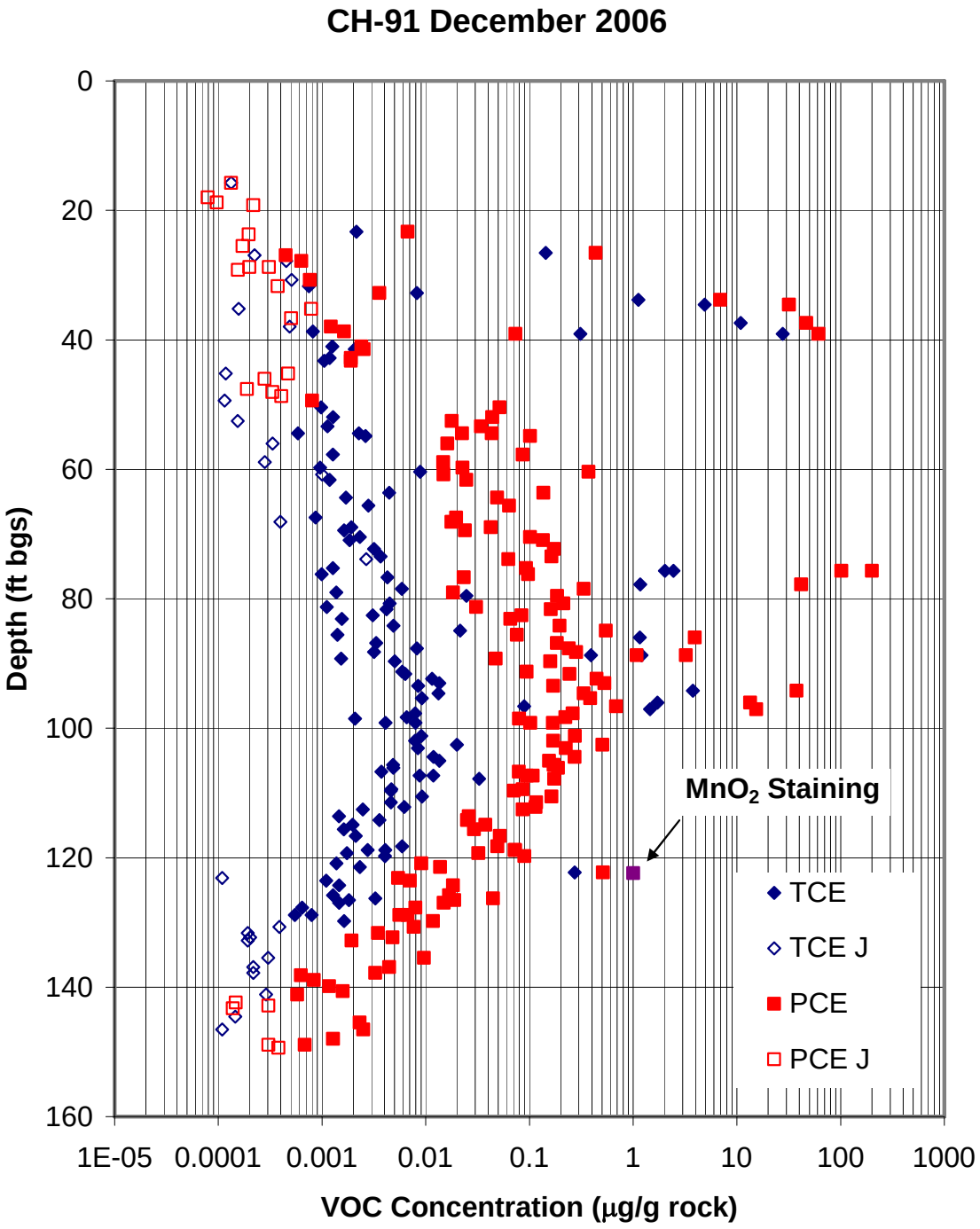


Figure A-10: Rock core VOC profiles at CH-91 (December 2006). Hollow symbols represent samples flagged with a J (between MDL and LOQ, or flagged due to blanks contamination).

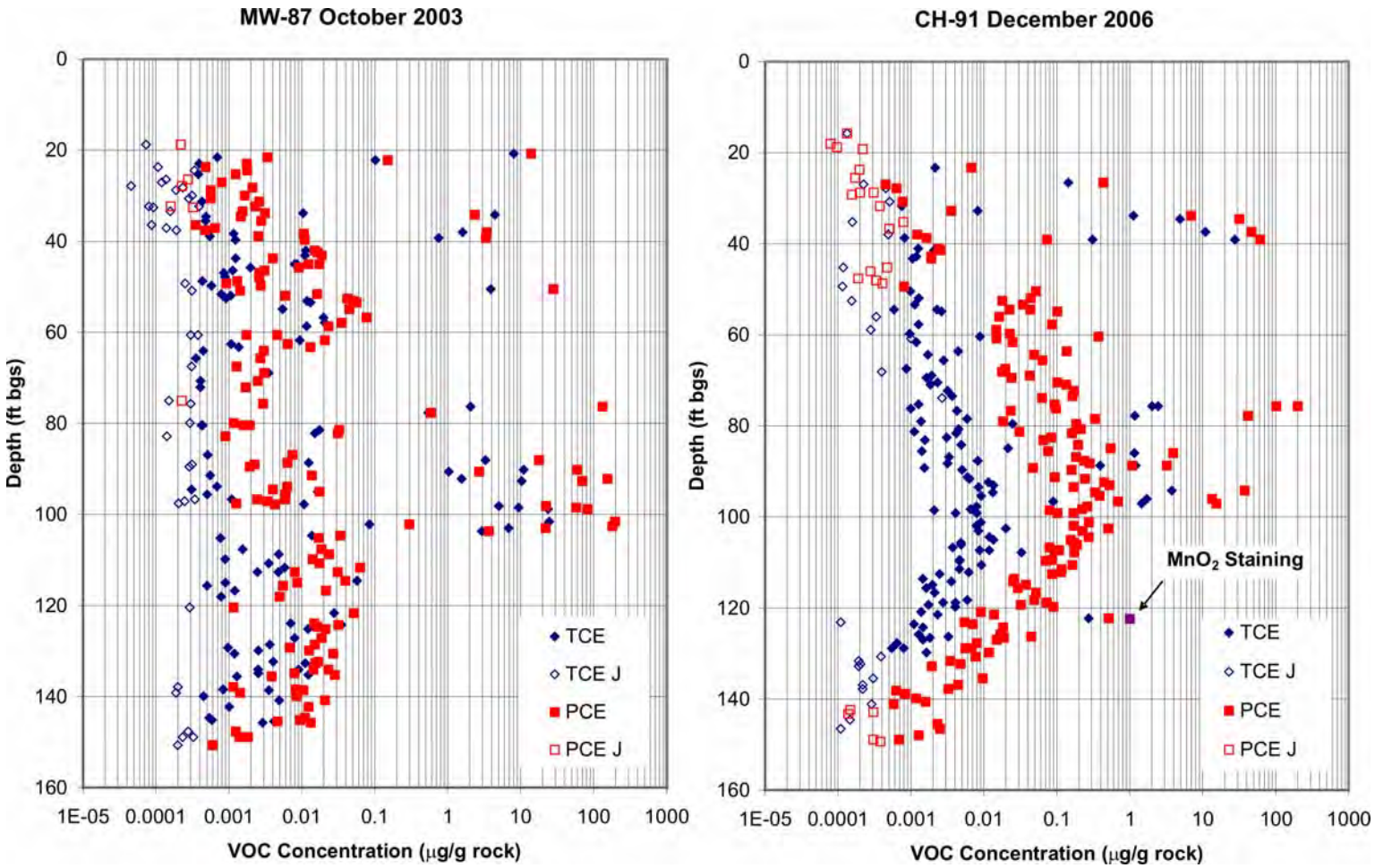


Figure A-11: Comparison of rock core VOC profiles at MW-87 (October 2003) conducted prior to full-scale permanganate injections and at CH-91 (December 2006) at about 2.3 years into the injection program (started September 2004). MnO2 staining was only observed in one fracture zone at 122.4 feet bgs at CH-91.

# Appendix B

Compound-Specific Carbon Isotope Results

Appendix B
Compound-Specific Stable Carbon Isotope Data
Watervliet Arsenal, Watervliet, New York

| | | Chlorinated VOCs (ug/L) | | | | | | Carbon Isotopes ($\delta^{13}C$) (‰ VPDB) | | |
|---|---|---|---|---|---|---|---|---|---|---|
| Well ID | Sampling date | PCE | TCE | c-DCE | t-DCE | 1,1-DCE | VC | PCE | TCE | c-DCE |
| MW-65-1 | 2/20/02 | 387 | 166.0 | 1356 | | | | -30.57 | -30.03 | -31.65 |
| | 3/6/02 | 1,961.5 | 387.6 | 1,948.8 | | | | -30.86 | -34.22 | -31.76 |
| | 3/7/02 | 1,466.5 | 332.3 | 1,871.3 | | | | -19.48 | | 45.03 |
| | 3/7/02 | 1,282.6 | 4.9 | 210.4 | | | | -31.61 | -35.40 | -32.09 |
| MW-65-2 | 2/20/02 | 391 | 170 | 1635 | | | | -30.48 | -29.08 | -33.41 |
| | 3/8/02 | 961.4 | 388.6 | 2,793.2 | | | | -30.34 | -30.78 | -33.39 |
| | 3/18/02 | 11 | 6 | 2154 | | | | -27.21 | -23.64 | -29.47 |
| MW-65-3 | 2/20/02 | 388 | 204 | 2404 | | | | -30.24 | -29.57 | -33.12 |
| | 3/8/02 | 85,627.5 | 13,739.9 | 8,115.8 | | | | -31.63 | -36.86 | -36.52 |
| MW-65-4 | 2/20/02 | 32040 | 5801 | 6211 | | | | -31.19 | -37.49 | -35.14 |
| | 3/8/02 | 11,487.0 | 4,239.2 | 7,236.7 | | | | -30.09 | -31.29 | -33.14 |
| MW-65-7 | 2/21/02 | 726 | 491 | 3776 | | | | -28.80 | | -30.95 |
| | 7/1/02 | 176.0 | nd | 44.0 | | | | -13.00 | | 63.75 |
| MW-74-1 | 2/20/02 | 7.9 | 5.2 | 350 | | | | | | -32.06 |
| | 3/5/02 | 8.7 | 23.9 | 288.3 | | | | | -24.89 | -30.65 |
| | 3/6/02 | 9.9 | 22.3 | 245.2 | | | | -31.79 | -25.56 | -31.26 |
| | 3/7/02 | 32.3 | 35.1 | 860.8 | | | | -27.88 | -27.75 | -29.66 |
| | 3/8/02 | 70.2 | 67.6 | < loq | | | | -27.54 | -27.54 | -32.26 |
| | 4/23/02 | 3.8 | 2.2 | < loq | < mdl | < mdl | | | | |
| | 1/3/03 | 101.0 | 4.0 | 16.0 | | | | - | - | -26.57 |
| | 9/29/04 | 5.5 | 7.2 | < mdl | < mdl | < mdl | < loq | ** | ** | ** |
| MW-74-2 | 2/20/02 | 4.1 | nd | 1088 | | | | -31.00 | | |
| | 3/6/02 | 5.5 | 13.8 | 688.3 | | | | | | -29.59 |
| | 3/7/02 | 23.3 | 22.3 | 811.6 | | | | -27.45 | -29.84 | -29.55 |
| | 3/8/02 | 59.7 | 52.0 | 1,118.4 | | | | -28.19 | -28.03 | -29.66 |
| | 3/18/02 | nd | nd | 206 | | | | -29.85 | | -28.54 |
| | 4/23/02 | 4 | < mdl | < mdl | < mdl | < mdl | | | | |
| | 1/3/03 | 7.4 | - | 18 | | | | | | |
| | 9/29/04 | 4.2 | 3.9 | < mdl | < mdl | < mdl | < loq | ** | ** | ** |
| MW-74-3 | 2/20/02 | 458 | 123 | 2802 | | | | -31.16 | | -32.45 |
| | 3/5/02 | 33.0 | 69.5 | 1,880.7 | | | | | | -31.42 |
| | 3/6/02 | 274.3 | 172.6 | 2,064.6 | | | | -28.44 | -26.15 | -31.92 |
| | 3/6/02 | 88.0 | 74.4 | 2,553.2 | | | | -26.99 | -23.36 | -28.08 |
| | 3/7/02 | 148.6 | 124.2 | 2,110.6 | | | | 5.14 | | |
| | 3/7/02 | 217.1 | < mdl | < mdl | | | | -14.74 | | |
| | 3/7/02 | 212.3 | 4.1 | < mdl | | | | -26.83 | -26.60 | -31.04 |
| | 3/8/02 | 109.5 | 7.9 | < mdl | | | | 6.09 | | |
| | 3/18/02 | 83 | 23 | 411 | | | | -11.07 | | 34.04 |
| | 4/23/02 | 239.2 | 20.6 | 475.4 | < mdl | < mdl | | | | |
| | 1/3/03 | 5959 | 107 | 1775 | | | | -19.99 | | 0.23 |
| | 9/29/04 | 2625.1 | 415.8 | 4529.9 | < mdl | < mdl | < loq | ** | ** | ** |
| MW-74-4 | 2/21/02 | 9183 | 382 | 524 | | | | -31.78 | -40.53 | -33.73 |
| | 3/6/02 | 3,065.4 | 858.8 | 3,580.9 | | | | -30.68 | -31.93 | -32.82 |
| | 3/7/02 | 5,751.6 | 1,563.9 | 3,618.0 | | | | -30.24 | -33.79 | -34.20 |
| | 3/8/02 | 11,000.8 | 2,274.3 | 2,274.6 | | | | -30.39 | -34.09 | -37.90 |
| | 4/23/02 | 283.8 | < mdl | < mdl | < mdl | < mdl | | | | |
| | 1/3/03 | 10,625.0 | 271.0 | 358.0 | | | | -15.80 | | 26.65 |
| | 9/29/04 | 8081.7 | 353.0 | 574.1 | < mdl | < mdl | < loq | -30.35 | -36.19 | -32.83 |
| MW-74-5 | 2/21/02 | 13988 | 3699 | 15155 | | | | -30.10 | -37.70 | -34.13 |
| | 3/6/02 | 6,754.8 | 14,399.9 | 34,851.3 | | | | -26.05 | -28.61 | -35.34 |
| | 3/7/02 | 8,716.1 | 18,832.9 | 30,984.8 | | | | -26.66 | -27.68 | -38.28 |
| | 3/8/02 | 22,630.0 | 24,781.7 | 21,254.2 | | | | -27.20 | -31.24 | -36.81 |
| | 4/23/02 | < mdl | 3.5 | < mdl | < mdl | < mdl | | | | |
| | 1/3/03 | 15,029.0 | 1,669.0 | 3,038.0 | | | | -29.59 | -33.56 | -31.54 |
| | 9/29/04 | 19224.7 | 5870.7 | 12207.8 | < mdl | < mdl | < loq | -27.88 | -32.14 | -31.91 |

Appendix B
Compound-Specific Stable Carbon Isotope Data
Watervliet Arsenal, Watervliet, New York

| | | Chlorinated VOCs (ug/L) | | | | | | Carbon Isotopes ($\delta^{13}C$) (‰ VPDB) | | |
|---|---|---|---|---|---|---|---|---|---|---|
| Well ID | Sampling date | PCE | TCE | c-DCE | t-DCE | 1,1-DCE | VC | PCE | TCE | c-DCE |
| MW-74-6 | 2/21/02 | 172 | 259 | 11745 | | | | -26.82 | -29.85 | -29.42 |
| | 3/6/02 | 57.3 | 103.3 | 13,358.4 | | | | -26.47 | -26.46 | -29.69 |
| | 3/8/02 | 4,878.2 | 4,185.3 | 16,599.0 | | | | -27.13 | -29.55 | -31.49 |
| | 3/8/02 | 8,146.3 | 1,672.5 | 12,746.8 | | | | -28.04 | -31.99 | -30.56 |
| | 4/23/02 | 17.6 | < mdl | < mdl | < mdl | < mdl | | | | |
| | 1/3/03 | 6,359.0 | 705.0 | 5,711.0 | | | | -24.96 | -14.84 | -8.06 |
| | 9/29/04 | 8121.3 | 3055.3 | 10863.6 | < mdl | < mdl | < loq | -28.81 | -31.33 | -29.11 |
| MW-75-1 | 9/29/04 | 166.5 | 162.5 | 3275.0 | < mdl | < mdl | < loq | BLOQ | BLOQ | -26.92 |
| MW-75-2 | 9/29/04 | 699.8 | 389.3 | 4979.3 | < mdl | < mdl | < loq | -28.83 | -28.70 | -26.25 |
| MW-75-5 | 9/29/04 | 1587.4 | 1209.6 | 4806.4 | < mdl | < mdl | < loq | -26.72 | -31.07 | -28.63 |
| MW-75-6 | 9/29/04 | 1195.2 | 487.5 | 4165.8 | < mdl | < mdl | < loq | -27.83 | -31.03 | -26.05 |
| MW-75-7 | 9/29/04 | 12477.3 | 2597.0 | 20424.8 | < mdl | < mdl | < loq | -- | -- | -- |
| MW-76-1 | 3/8/02 | 3,963.0 | 551.7 | 4,812.0 | | | | -31.49 | -31.53 | -31.13 |
| | 7/1/02 | 145.0 | 52.0 | nd | | | | -15.77 | | |
| | 4/24/02 | 1428.9 | 339.4 | 2052.6 | < mdl | < mdl | | | | |
| | 1/3/03 | 259.0 | 373.0 | 2700.0 | | | | -26.85 | -30.80 | -31.15 |
| | 9/28/04 | 912.4 | 299.0 | 1329.4 | < mdl | < mdl | < loq | -29.33 | -30.92 | -31.26 |
| MW-76-2 | 3/6/02 | 2,163.2 | 738.1 | 12,746.8 | | | | -29.68 | -32.05 | -31.30 |
| | 3/7/02 | 11,991.9 | 8,331.2 | 15,315.3 | | | | -29.14 | -31.53 | -32.50 |
| | 3/8/02 | 116,907.2 | 10,122.0 | 11,973.5 | | | | -31.12 | -34.21 | -34.12 |
| | 1/3/03 | 40,298.0 | 9,622.0 | 5,627.0 | | | | -30.49 | -35.48 | -34.95 |
| | 9/28/04 | 172.7 | 7.2 | 184.1 | < mdl | < mdl | < loq | -29.81 | | -8.86 |
| MW-76-3 | 2/22/02 | 2403 | 198 | 8742 | | | | -33.97 | -27.91 | -31.21 |
| | 3/6/02 | 100,242.2 | 19,202.5 | 23,265.0 | | | | -30.40 | -34.90 | -33.79 |
| | 3/7/02 | 110,534.1 | 20,706.2 | 24,537.7 | | | | -30.55 | -35.48 | -33.76 |
| | 3/8/02 | 136,501.2 | 19,048.5 | 21,775.6 | | | | -30.58 | -35.81 | -34.25 |
| | 7/1/02 | 57790.0 | 15437.0 | 7413.0 | | | | -29.89 | -35.42 | -33.13 |
| | 4/24/02 | 68871.2 | 17497.1 | 11763.4 | < mdl | < mdl | | | | |
| | 1/3/03 | 53186.0 | 11680.0 | 6552.0 | | | | -30.24 | -34.58 | -32.80 |
| | 9/28/04 | 76194.4 | 25098.5 | 7765.4 | < mdl | < mdl | < loq | -28.54 | -36.43 | -36.51 |
| MW-76-4 | 2/22/02 | 57672 | 8689 | 18105 | | | | -32.54 | -30.35 | -34.30 |
| | 3/6/02 | 6,400.6 | 1,833.8 | 10,925.2 | | | | -29.03 | -31.46 | -30.61 |
| | 3/7/02 | 6,383.0 | 1,870.5 | 10,697.5 | | | | -29.58 | -33.31 | -31.58 |
| | 3/8/02 | 8,146.3 | 1,672.5 | 12,746.8 | | | | -30.32 | -31.33 | -31.58 |
| | 7/1/02 | 93342.0 | 35571.0 | 20344.0 | | | | -29.10 | -33.55 | -34.88 |
| | 4/24/02 | 90040.8 | 61032.6 | 37339.7 | < mdl | < mdl | | | | |
| | 9/28/04 | 108211.4 | 34289.5 | 10786.8 | < mdl | < mdl | < loq | -28.67 | -36.70 | -36.08 |
| MW-76-5 | 4/23/02 | 13.2 | < mdl | < mdl | < mdl | < mdl | | | | |
| | 1/3/03 | 21225.0 | 412.0 | 3435.0 | | | | -30.04 | | -25.42 |
| | 9/28/04 | 3111.6 | 449.8 | 4261.2 | < mdl | < mdl | < loq | -27.32 | -29.48 | -25.82 |
| MW-79-1 | 9/30/04 | 988.3 | 122.8 | 438.8 | < mdl | < mdl | 2.5 | -26.95 | -28.48 | -26.57 |
| | 10/4/04 | 15644.2 | 1443.2 | 1544.0 | < mdl | < mdl | < loq | | | |
| | 10/13/04 | 11374.0 | 1405.5 | 1222.1 | < mdl | < mdl | < loq | -26.27 | -31.82 | -29.88 |
| | 11/16/04 | 5158.0 | 1542.9 | 1177.3 | <mdl | 4.5 | <mdl | | | |
| MW-79-2 | 9/30/04 | 64.9 | 14.2 | < mdl | < mdl | < mdl | 11.2 | ** | ** | ** |
| | 10/4/04 | 25.4 | 10.9 | < mdl | < mdl | < mdl | 7.9 | -- | -- | -- |
| | 10/13/04 | 45.3 | 18.0 | < loq | < mdl | < mdl | < loq | -25.28 | BLOQ | BLOQ |
| | 11/16/04 | 1281.2 | 268.4 | 637.7 | <mdl | 2.7 | <mdl | | | |
| | 2/24/05 | | | | | | | | | -24.28 |
| MW-79-3 | 9/30/04 | 357.4 | 83.1 | 645.3 | < mdl | < mdl | < loq | -24.51 | -25.67 | -25.30 |
| | 10/4/04 | 16867.0 | 98.2 | 507.5 | < mdl | < mdl | 7.9 | -26.62 | | |
| | 10/13/04 | 7635.1 | 179.9 | 845.3 | < mdl | < mdl | < loq | -25.14 | -27.82 | -24.35 |
| | 11/16/04 | 14520.1 | 2161.1 | 2648.8 | <mdl | 4.0 | <mdl | | | |
| | 2/24/05 | | | | | | | -25.50 | -26.20 | -29.20 |
| MW-79-4 | 9/30/04 | 509.4 | 166.2 | 1068.8 | < mdl | < mdl | < loq | -24.40 | -26.88 | -26.00 |
| | 10/4/04 | 765.8 | 180.8 | 905.8 | < mdl | < mdl | < loq | -26.16 | -26.65 | -27.08 |
| | 10/13/04 | 490.8 | 173.0 | 1297.4 | < mdl | < mdl | < loq | -24.27 | -27.00 | -25.65 |
| | 11/16/04 | 8382.6 | 4726.9 | 6717.8 | <mdl | 8.5 | <mdl | | | |
| | 2/24/05 | | | | | | | -23.97 | -25.49 | -29.50 |

Appendix B
Compound-Specific Stable Carbon Isotope Data
Watervliet Arsenal, Watervliet, New York

| | | Chlorinated VOCs (ug/L) | | | | | | Carbon Isotopes ($\delta^{13}C$) (‰ VPDB) | | |
|---|---|---|---|---|---|---|---|---|---|---|
| Well ID | Sampling date | PCE | TCE | c-DCE | t-DCE | 1,1-DCE | VC | PCE | TCE | c-DCE |
| MW-79-5 | 9/30/04 | 873.2 | 311.4 | 1593.9 | < mdl | < mdl | < loq | -23.28 | -25.89 | -25.03 |
| | 10/4/04 | 1656.9 | 616.1 | 2790.3 | < mdl | < mdl | < loq | | | |
| | 10/13/04 | 1560.8 | 583.3 | 4055.8 | < mdl | < mdl | < loq | -22.83 | -26.82 | -25.00 |
| | 11/16/04 | 785.7 | 404.3 | 4518.7 | <mdl | 8.1 | <mdl | | | |
| | 2/24/05 | | | | | | | -24.20 | | -25.33 |
| MW-79-6 | 9/30/04 | 137.5 | 74.9 | 734.0 | < mdl | < mdl | < loq | -23.19 | -25.50 | -23.97 |
| | 10/4/04 | 155.7 | 84.5 | 702.7 | < mdl | < mdl | < loq | -24.44 | -25.07 | -24.84 |
| | 10/13/04 | 511.0 | 268.6 | 1828.0 | < mdl | < mdl | < loq | -22.97 | -23.52 | -24.19 |
| | 11/16/04 | 827.5 | 515.3 | 3319.6 | <mdl | 5.9 | <mdl | | | |
| | 2/24/05 | | | | | | | -23.85 | -23.98 | -26.82 |
| MW-79-7 | 9/30/04 | 132.0 | 65.7 | 565.2 | < mdl | < mdl | < loq | -23.84 | -26.23 | -25.29 |
| | 10/4/04 | 34.6 | 15.0 | < loq | < mdl | < mdl | < loq | | | |
| | 10/13/04 | 31.5 | 18.9 | 196.7 | < mdl | < mdl | < loq | | | -24.00 |
| | 11/16/04 | 122.6 | 137.9 | 1110.8 | <mdl | 4.7 | <mdl | | | |
| | 2/24/05 | | | | | | | -23.45 | -22.41 | -27.29 |
| MW-79-8 | 9/30/04 | 69.1 | 31.3 | 328.7 | < mdl | < mdl | < loq | -24.73 | -26.38 | -25.63 |
| | 10/4/04 | 19.7 | 11.4 | < loq | < mdl | < mdl | < loq | | | |
| | 10/13/04 | 15.0 | 8.5 | < loq | < mdl | < mdl | < loq | | | -24.07 |
| | 11/16/04 | 212.8 | 88.2 | 279.1 | <mdl | 3.1 | <mdl | | | |
| | 2/24/05 | | | | | | | -23.71 | -22.43 | -27.45 |
| MW-79-9 | 9/30/04 | 101.8 | 67.5 | 585.6 | < mdl | < mdl | < loq | -23.97 | -24.86 | -24.76 |
| | 10/4/04 | 44.1 | 30.4 | 207.2 | < mdl | < mdl | < loq | | | |
| | 10/13/04 | 37.7 | 27.2 | 226.6 | < mdl | < mdl | < loq | -24.96 | | -25.27 |
| | 11/16/04 | -- | -- | -- | -- | -- | -- | | | |
| | 2/24/05 | | | | | | | -23.53 | -21.42 | -25.79 |
| IW-1-1 | 5/19/06 | 3.1 | 3.5 | 8002.0 | | | | -24.30 | -23.80 | -29.40 |
| IW-1-2 | 5/6/06 | 1030.0 | 504.0 | 3500.0 | | | | -27.10 | -28.10 | -27.40 |
| | 5/19/06 | 674.1 | 266.0 | 2351.0 | | | | -27.70 | -29.00 | -27.20 |
| IW-1-3 | 5/19/06 | 10.5 | 6.2 | 663.0 | | | | | | -23.50 |
| IW-1-4 | 5/19/06 | 355.0 | 99.8 | 562.0 | | | | -27.90 | -30.10 | -26.30 |
| IW-2-1 | 5/6/06 | 702.0 | 460.0 | 7103.0 | | | | -25.50 | -29.80 | -25.10 |
| | 5/19/06 | 885.5 | 582.0 | 7348.0 | | | | -27.90 | -32.30 | -24.70 |
| IW-2-2 | 5/6/06 | 2805.0 | 683.0 | 5583.0 | | | | -28.50 | -30.30 | -24.10 |
| | 5/19/06 | 4159.0 | 785.0 | 5307.0 | | | | -29.10 | -33.70 | -23.90 |
| IW-2-8 | 5/19/06 | 17239.0 | 1168.0 | 3996.0 | | | | -25.90 | -29.40 | -19.80 |
| IW-2-9 | 5/19/06 | 4289.0 | 417.0 | 4411.0 | | | | -25.10 | -28.60 | -15.70 |
| IW-3-1 | 5/6/06 | | | 615.0 | | | | | -30.30 | -3.20 |
| | 5/19/06 | | | 486.0 | | | | | | -2.00 |
| IW-3-2 | 5/19/06 | | | 629.0 | | | | | | -6.90 |
| IW-3-3 | 5/6/06 | 41.9 | 35.0 | 3224.0 | | | | | | -22.10 |
| | 5/19/06 | 15.2 | 13.6 | 2296.0 | | | | | | -23.10 |
| IW-3-4 | 5/6/06 | 454.0 | 186.0 | 45010.0 | | | | -27.10 | -31.50 | -26.90 |
| | 5/19/06 | 424.6 | 174.7 | 4190.0 | | | | -27.90 | -31.90 | -27.20 |
| IW-4-1 | 9/29/04 | 1.6 | < mdl | < mdl | < mdl | < mdl | < loq | ** | ** | ** |
| | 10/4/04 | < loq | < mdl | < mdl | < mdl | < mdl | < loq | ** | ** | ** |
| | 10/13/04 | < mdl | < loq | < mdl | < mdl | < mdl | < loq | ** | ** | ** |
| IW-4-2 | 9/29/04 | 3.3 | < mdl | < mdl | < mdl | < mdl | < loq | ** | ** | ** |
| | 10/4/04 | 3.3 | < mdl | < mdl | < mdl | < mdl | < loq | ** | ** | ** |
| | 10/13/04 | 2.5 | 1.8 | < mdl | < mdl | < mdl | < mdl | ** | ** | ** |
| IW-4-3 | 9/29/04 | 7.2 | 1.5 | < mdl | < mdl | < mdl | < loq | ** | ** | ** |
| | 10/4/04 | 7.1 | < loq | < mdl | < mdl | < mdl | < loq | ** | ** | ** |
| | 10/13/04 | 5.5 | 1.7 | < mdl | < mdl | < mdl | < loq | ** | ** | ** |
| | 2/24/05 | | | 221.0 | | | | | | -25.43 |
| | 5/19/06 | | | | | | | | | -9.90 |
| IW-4-4 | 9/29/04 | 4.6 | < loq | < mdl | < mdl | < mdl | < loq | ** | ** | ** |
| | 10/4/04 | 10.9 | < loq | < mdl | < mdl | < mdl | < loq | ** | ** | ** |
| | 10/13/04 | 12.8 | 2.6 | < mdl | < mdl | < mdl | < loq | ** | ** | ** |
| | 2/24/05 | | | 1046.0 | | | | | | -26.32 |
| | 5/6/06 | | | 581.0 | | | | | | -8.90 |
| | 5/19/06 | | | 341.6 | | | | | | 1.20 |

Appendix B
Compound-Specific Stable Carbon Isotope Data
Watervliet Arsenal, Watervliet, New York

| | | Chlorinated VOCs (ug/L) | | | | | | Carbon Isotopes ($\delta^{13}C$) (‰ VPDB) | | |
|---|---|---|---|---|---|---|---|---|---|---|
| Well ID | Sampling date | PCE | TCE | c-DCE | t-DCE | 1,1-DCE | VC | PCE | TCE | c-DCE |
| IW-4-5 | 9/29/04 | 37.1 | 8.0 | < mdl | < mdl | < mdl | < loq | ** | ** | ** |
| | 10/4/04 | 36.7 | 5.4 | < mdl | < mdl | < mdl | < loq | ** | ** | ** |
| | 10/13/04 | 38.5 | 5.1 | < mdl | < mdl | < mdl | < loq | ** | ** | ** |
| | 2/24/05 | 1.9 | | 861.0 | | | | | | -26.24 |
| | 5/6/06 | | | 605.0 | | | | | | 12.70 |
| | 5/19/06 | 2.1 | | 431.0 | | | | | | -1.00 |
| IW-4-6 | 9/29/04 | 79.9 | 12.5 | < mdl | < mdl | < mdl | < loq | ** | ** | ** |
| | 10/4/04 | 74.6 | 8.6 | < mdl | < mdl | < mdl | < loq | ** | ** | ** |
| | 10/13/04 | 70.4 | 7.2 | < mdl | < mdl | < mdl | < loq | ** | ** | ** |
| | 2/24/05 | 2.8 | | 876.0 | | | | | | -24.89 |
| | 5/6/06 | | 1.8 | 356.0 | | | | | | -19.50 |
| | 5/19/06 | 1.7 | 2.1 | 702.0 | | | | | | -10.70 |
| IW-4-7 | 9/29/04 | 168.3 | 31.0 | 225.1 | < mdl | < mdl | < loq | -24.98 | | -25.74 |
| | 10/4/04 | 499.1 | 110.0 | 842.6 | < mdl | < mdl | < loq | -25.16 | -26.14 | -25.99 |
| | 10/13/04 | 786.5 | 200.3 | 875.9 | < mdl | < mdl | < loq | -25.54 | -27.73 | -26.29 |
| | 2/24/05 | 103.8 | 55.3 | 2191.0 | | | | | | -24.79 |
| | 5/6/06 | 652.0 | 180.0 | 1809.0 | | | | -23.70 | -24.80 | -22.20 |
| | 5/19/06 | 176.9 | 43.2 | 1360.0 | | | | -23.40 | -25.80 | -21.00 |
| IW-4-8 | 9/29/04 | 212.0 | 17.1 | < loq | < mdl | < mdl | 3.7 | -23.81 | | -26.31 |
| | 10/4/04 | Dilute | 160.3 | 1148.3 | < mdl | < mdl | 3.7 | -25.09 | | -26.20 |
| | 10/13/04 | 3907.2 | 201.9 | 967.2 | < mdl | < mdl | < loq | -25.59 | -26.89 | -26.68 |
| | 2/24/05 | 1893.0 | 704.0 | 4476.0 | | | | -24.36 | -23.89 | -25.22 |
| | 5/6/06 | 1639.0 | 358.0 | 1843.0 | | | | -24.80 | -24.00 | -21.40 |
| | 5/19/06 | 201.2 | 49.8 | 2103.0 | | | | -23.90 | | -14.00 |
| IW-4-9 | 9/29/04 | 705.2 | 29.9 | < loq | < mdl | < mdl | < loq | -24.46 | | -25.83 |
| | 10/4/04 | 1461.3 | 44.9 | 319.8 | < mdl | < mdl | 1.5 | -25.03 | | -26.56 |
| | 10/13/04 | 822.4 | 57.9 | 519.8 | < mdl | < mdl | < loq | -25.30 | | -26.71 |
| | 2/24/05 | 36.0 | 26.2 | 4564.0 | | | | | | -24.65 |
| | 5/6/06 | 106.0 | 66.8 | 2164.0 | | | | -24.80 | -22.10 | -17.40 |
| | 5/19/06 | | | 1499.0 | | | | | | -9.80 |
| MW-81-1 | 9/16/04 | < mdl | 1.5 | < mdl | < mdl | < mdl | < loq | | | |
| | 10/25/04 | < loq | 2.1 | < mdl | < mdl | < mdl | < mdl | | | |
| | 11/16/04 | 1.2 | 0.9 | <mdl | <mdl | 3.3 | <mdl | | | |
| | 9/13/06 | | 3.3 | 10.4 | | | | | | |
| MW-81-2 | 9/16/04 | < mdl | 1.6 | < mdl | < mdl | < mdl | < mdl | | | |
| | 10/25/04 | < loq | < loq | < mdl | < mdl | < mdl | < mdl | | | |
| | 11/16/04 | 0.5 | 0.7 | <mdl | <mdl | 2.9 | <mdl | | | |
| | 9/13/06 | | | 6.4 | | | | | | |
| MW-81-3 | 9/16/04 | < mdl | < mdl | < mdl | < mdl | < mdl | < loq | | | |
| | 10/25/04 | < loq | < loq | < mdl | < mdl | < mdl | < mdl | | | |
| | 11/16/04 | 0.5 | 0.8 | <mdl | <mdl | 3.5 | <mdl | | | |
| | 9/13/06 | | | 9.5 | | | | | | |
| MW-82R-1 | 9/16/04 | 629.2 | 134.3 | 536.1 | < mdl | < mdl | < loq | -28.62 | -31.81 | -29.34 |
| | 10/25/04 | 904.7 | 167.1 | 547.8 | < mdl | < mdl | < mdl | | | |
| | 11/16/04 | 701.9 | 129.2 | 493.8 | <mdl | 5.0 | <mdl | | | |
| | 9/13/06 | 1760.0 | 403.0 | 572.0 | | | | -28.92 | -34.30 | -28.97 |
| MW-82R-2 | 9/16/04 | 3.1 | 2.0 | 219.6 | < mdl | < mdl | < loq | BLOQ | BLOQ | -25.28 |
| | 10/25/04 | 2.8 | 2.4 | < loq | < mdl | < mdl | < mdl | | | |
| | 11/17/04 | 1.6 | 1.4 | 246.2 | <mdl | 3.5 | <mdl | | | |
| | 9/13/06 | 12.6 | 2.9 | 83.3 | | | | | | |
| MW-82R-3 | 9/16/04 | < mdl | < mdl | < loq | < mdl | < mdl | < loq | ** | ** | ** |
| | 10/25/04 | < loq | < loq | < mdl | < mdl | < mdl | < mdl | | | |
| | 11/17/04 | 4.4 | 0.7 | 37.9 | <mdl | 3.8 | <mdl | | | |
| | 9/13/06 | | | 10.1 | | | | | | |
| MW-83-1 | 9/16/04 | 5654.0 | 2791.5 | 5610.5 | < mdl | < mdl | 16.2 | -28.93 | -33.66 | -31.64 |
| | 10/26/04 | 2520.4 | 1678.5 | 6745.1 | < mdl | < mdl | < mdl | | | |
| | 11/17/04 | 1549.5 | 1165.1 | 7458.4 | <mdl | 10.9 | <mdl | | | |
| | 9/13/06 | 14560.0 | 4170.0 | 3510.0 | | | | -30.02 | -36.34 | -32.29 |
| MW-83-2 | 9/16/04 | 2465.4 | 2664.6 | 6572.2 | < mdl | < mdl | < loq | -26.32 | -27.16 | -32.76 |
| | 10/26/04 | 7091.7 | 2614.4 | 5633.1 | < mdl | < mdl | < mdl | | | |
| | 11/17/04 | 6781.2 | 2803.8 | 6055.2 | <mdl | 9.5 | <mdl | | | |
| | 9/13/06 | 5660.0 | 3090.0 | 6130.0 | | | | -28.86 | -33.08 | -30.96 |

Appendix B
Compound-Specific Stable Carbon Isotope Data
Watervliet Arsenal, Watervliet, New York

| | | Chlorinated VOCs (ug/L) | | | | | | Carbon Isotopes ($\delta^{13}C$) (‰ VPDB) | | |
|---|---|---|---|---|---|---|---|---|---|---|
| Well ID | Sampling date | PCE | TCE | c-DCE | t-DCE | 1,1-DCE | VC | PCE | TCE | c-DCE |
| MW-83-3 | 9/16/04 | 747.1 | 348.4 | 3880.5 | < mdl | < mdl | < loq | -29.05 | -33.26 | -26.23 |
| | 10/26/04 | 758.6 | 403.8 | 3488.8 | < mdl | < mdl | < mdl | | | |
| | 11/17/04 | 605.7 | 281.3 | 2733.8 | <mdl | 5.9 | <mdl | | | |
| | 9/13/06 | 2.1 | | | | | | | | |
| MW-84R-1 | 9/20/04 | 9850.5 | 1792.3 | 5491.9 | < mdl | < mdl | < loq | -29.24 | -32.49 | -30.43 |
| | 10/26/04 | 3222.2 | 1794.2 | 5827.9 | < mdl | < mdl | < mdl | | | |
| | 11/17/04 | 3024.5 | 1673.5 | 6653.3 | <mdl | 9.3 | <mdl | | | |
| | 9/13/06 | 7670.0 | 5610.0 | 6590.0 | | | | -27.25 | -33.44 | -29.89 |
| MW-84R-2 | 9/20/04 | 1734.5 | 740.3 | 2767.1 | < mdl | < mdl | < loq | -28.51 | -36.55 | -30.89 |
| | 10/26/04 | 55220.0 | 8000.0 | 4866.9 | < mdl | < mdl | < mdl | | | |
| | 11/17/04 | 12890.2 | 7381.9 | 5310.4 | <mdl | 8.7 | <mdl | | | |
| | 9/13/06 | 74150.0 | 12980.0 | 6330.0 | | | | -30.02 | -36.66 | -32.46 |
| MW-84R-3 | 9/20/04 | 601.6 | 582.7 | 4270.0 | < mdl | < mdl | < loq | -27.62 | -34.99 | -28.65 |
| | 10/26/04 | 14666.3 | 3793.9 | 5923.6 | < mdl | < mdl | < loq | | | |
| | 11/17/04 | 9282.3 | 3348.1 | 5650.5 | <mdl | 9.3 | <mdl | | | |
| | 9/13/06 | 12100.0 | 8910.0 | 7370.0 | | | | -28.14 | -34.43 | -31.12 |
| MW-85R-1 | 9/20/04 | 438.1 | 135.0 | 964.2 | < mdl | < mdl | < loq | -28.11 | -30.15 | -29.39 |
| | 10/26/04 | 72.5 | 66.2 | 824.5 | < mdl | < mdl | < mdl | | | |
| | 11/17/04 | 38.2 | 28.8 | 636.7 | <mdl | 4.4 | <mdl | | | |
| | 9/13/06 | 7.1 | 3.1 | 66.7 | | | | | | |
| MW-85R-2 | 9/20/04 | 132.1 | 88.8 | 1330.6 | < mdl | < mdl | < loq | -28.82 | -30.91 | -30.78 |
| | 10/26/04 | 1401.1 | 307.8 | 1897.4 | < mdl | < mdl | < mdl | | | |
| | 11/17/04 | 932.8 | 280.9 | 2171.1 | <mdl | 6.2 | <mdl | | | |
| | 9/13/06 | 2066.0 | 487.0 | 1420.0 | | | | -28.98 | -34.31 | -29.27 |
| MW-85R-3 | 9/20/04 | 312.0 | 44.5 | 1260.3 | < mdl | < mdl | < loq | missing | missing | missing |
| | 10/26/04 | 12353.0 | 340.2 | 2489.1 | < mdl | < mdl | < mdl | | | |
| | 11/17/04 | 10198.5 | 371.2 | 2707.3 | <mdl | 6.6 | <mdl | | | |
| | 9/13/06 | 20340.0 | 1074.0 | 1580.0 | | | | -29.04 | -36.48 | -24.52 |
| MW-86R-1 | 9/20/04 | 731.3 | 120.2 | 601.8 | < mdl | < mdl | 5.5 | -28.53 | -32.98 | -29.60 |
| | 10/26/04 | 142.5 | 103.1 | 411.6 | < mdl | < mdl | < loq | | | |
| | 11/17/04 | 96.0 | 60.4 | 422.9 | <mdl | 2.5 | <mdl | | | |
| | 9/13/06 | | | 35.2 | | | | | | |
| MW-86R-2 | 9/20/04 | 2611.1 | 122.8 | 597.7 | < mdl | < mdl | < loq | -29.93 | -36.09 | -29.78 |
| | 10/26/04 | 4194.3 | 339.3 | 1093.2 | < mdl | < mdl | < mdl | | | |
| | 11/17/04 | 2638.8 | 235.8 | 858.3 | <mdl | 5.2 | <mdl | | | |
| | 9/13/06 | 1516.0 | 294.0 | 959.0 | | | | -29.05 | -33.30 | -29.51 |
| MW-86R-3 | 9/20/04 | 2659.9 | 334.1 | 1568.7 | < mdl | < mdl | 3.8 | -28.96 | -33.36 | -30.00 |
| | 10/26/04 | 2691.5 | 743.5 | 3992.4 | < mdl | < mdl | < loq | | | |
| | 11/17/04 | 1163.0 | 491.0 | 5038.1 | <mdl | 8.3 | <mdl | | | |
| | 9/13/06 | 4791.0 | 1990.0 | 7780.0 | | | | -28.4 | -35.1 | -29.1 |
| MW-87-1 | 9/13/06 | 13185.0 | 10634.0 | 3494.0 | | | | -30.11 | -36.80 | -33.08 |
| MW-87-2 | 9/13/06 | 262.0 | 120.0 | 3230.0 | | | | -28.85 | -30.43 | -24.20 |
| MW-87-3 | 9/13/06 | | | 22.4 | | | | | | |
| MW-34 | 2/19/02 | 401 | 188.0 | 2375.0 | | | | -29.25 | -36.24 | -31.96 |
| | 3/6/02 | 530.8 | 291.5 | 3287.3 | | | | -29.19 | -31.97 | -32.43 |
| | 3/7/02 | 1201.2 | 471.8 | 3127.9 | | | | -30.00 | -34.84 | -31.78 |
| | 3/18/02 | 169.0 | 92.0 | 1674.0 | | | | -25.38 | -27.10 | -30.07 |
| | 1/3/03 | 2632.0 | 356.0 | 948.0 | | | | -28.00 | -30.55 | -30.28 |
| | 9/15/04 | 1818.8 | 769.8 | 3459.9 | | | | -28.91 | -32.12 | -30.14 |
| MW-51 | 2/19/02 | 8551.0 | 5826.0 | 10666 | | | | -30.85 | -31.74 | -35.71 |
| | 3/8/02 | 12723.4 | 8732.7 | 12,985.5 | | | | -29.94 | -32.47 | -33.25 |
| | 7/1/02 | 40997.0 | 14364.0 | 6,738.0 | | | | -29.00 | -31.99 | -34.93 |
| | 1/3/03 | 19391.0 | 8108.0 | 6,189.0 | | | | -28.79 | -31.69 | -31.95 |
| | 9/15/04 | 17553.8 | 1761.5 | 1135.5 | | | | -28.76 | -32.67 | -31.20 |
| MW-60 | 9/15/04 | < mdl | < mdl | < mdl | | | | ** | ** | ** |
| MW-80 | 9/15/04 | < mdl | < mdl | < mdl | | | | ** | ** | ** |
| MW-87 | 9/15/04 | 5657.3 | 1627.0 | 5070.2 | | | | -28.60 | -32.42 | -28.81 |
| MW-89 | 9/15/04 | < mdl | < mdl | < mdl | | | | ** | ** | ** |

# Figure B-1: March 2002 Pre-Injection PCE and Isotope Analysis Results

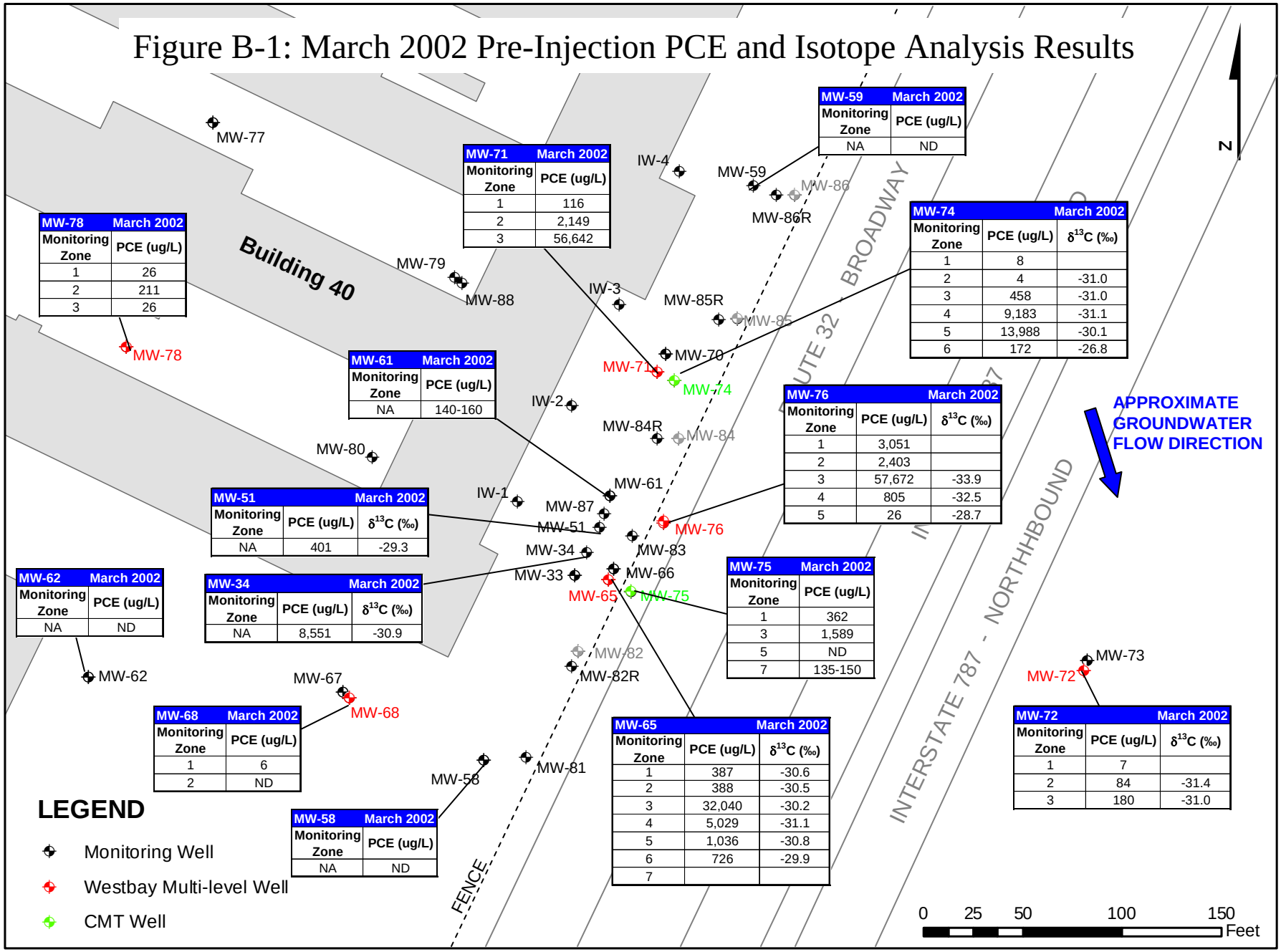


| MW-78 | March 2002 |
|---|---|
| Monitoring Zone | PCE (ug/L) |
| 1 | 26 |
| 2 | 211 |
| 3 | 26 |

| MW-71 | March 2002 |
|---|---|
| Monitoring Zone | PCE (ug/L) |
| 1 | 116 |
| 2 | 2,149 |
| 3 | 56,642 |

| MW-59 | March 2002 |
|---|---|
| Monitoring Zone | PCE (ug/L) |
| NA | ND |

| MW-74 | March 2002 | |
|---|---|---|
| Monitoring Zone | PCE (ug/L) | $\delta^{13}C$ (‰) |
| 1 | 8 | |
| 2 | 4 | -31.0 |
| 3 | 458 | -31.0 |
| 4 | 9,183 | -31.1 |
| 5 | 13,988 | -30.1 |
| 6 | 172 | -26.8 |

| MW-61 | March 2002 |
|---|---|
| Monitoring Zone | PCE (ug/L) |
| NA | 140-160 |

| MW-76 | March 2002 | |
|---|---|---|
| Monitoring Zone | PCE (ug/L) | $\delta^{13}C$ (‰) |
| 1 | 3,051 | |
| 2 | 2,403 | |
| 3 | 57,672 | -33.9 |
| 4 | 805 | -32.5 |
| 5 | 26 | -28.7 |

| MW-51 | March 2002 | |
|---|---|---|
| Monitoring Zone | PCE (ug/L) | $\delta^{13}C$ (‰) |
| NA | 401 | -29.3 |

| MW-34 | March 2002 | |
|---|---|---|
| Monitoring Zone | PCE (ug/L) | $\delta^{13}C$ (‰) |
| NA | 8,551 | -30.9 |

| MW-75 | March 2002 |
|---|---|
| Monitoring Zone | PCE (ug/L) |
| 1 | 362 |
| 3 | 1,589 |
| 5 | ND |
| 7 | 135-150 |

| MW-62 | March 2002 |
|---|---|
| Monitoring Zone | PCE (ug/L) |
| NA | ND |

| MW-68 | March 2002 |
|---|---|
| Monitoring Zone | PCE (ug/L) |
| 1 | 6 |
| 2 | ND |

| MW-65 | March 2002 | |
|---|---|---|
| Monitoring Zone | PCE (ug/L) | $\delta^{13}C$ (‰) |
| 1 | 387 | -30.6 |
| 2 | 388 | -30.5 |
| 3 | 32,040 | -30.2 |
| 4 | 5,029 | -31.1 |
| 5 | 1,036 | -30.8 |
| 6 | 726 | -29.9 |
| 7 | | |

| MW-72 | March 2002 | |
|---|---|---|
| Monitoring Zone | PCE (ug/L) | $\delta^{13}C$ (‰) |
| 1 | 7 | |
| 2 | 84 | -31.4 |
| 3 | 180 | -31.0 |

| MW-58 | March 2002 |
|---|---|
| Monitoring Zone | PCE (ug/L) |
| NA | ND |

**LEGEND**

- Monitoring Well
- Westbay Multi-level Well
- CMT Well

# Figure B-2: March 6, 2002 During Injection PCE and Isotope Analysis Results

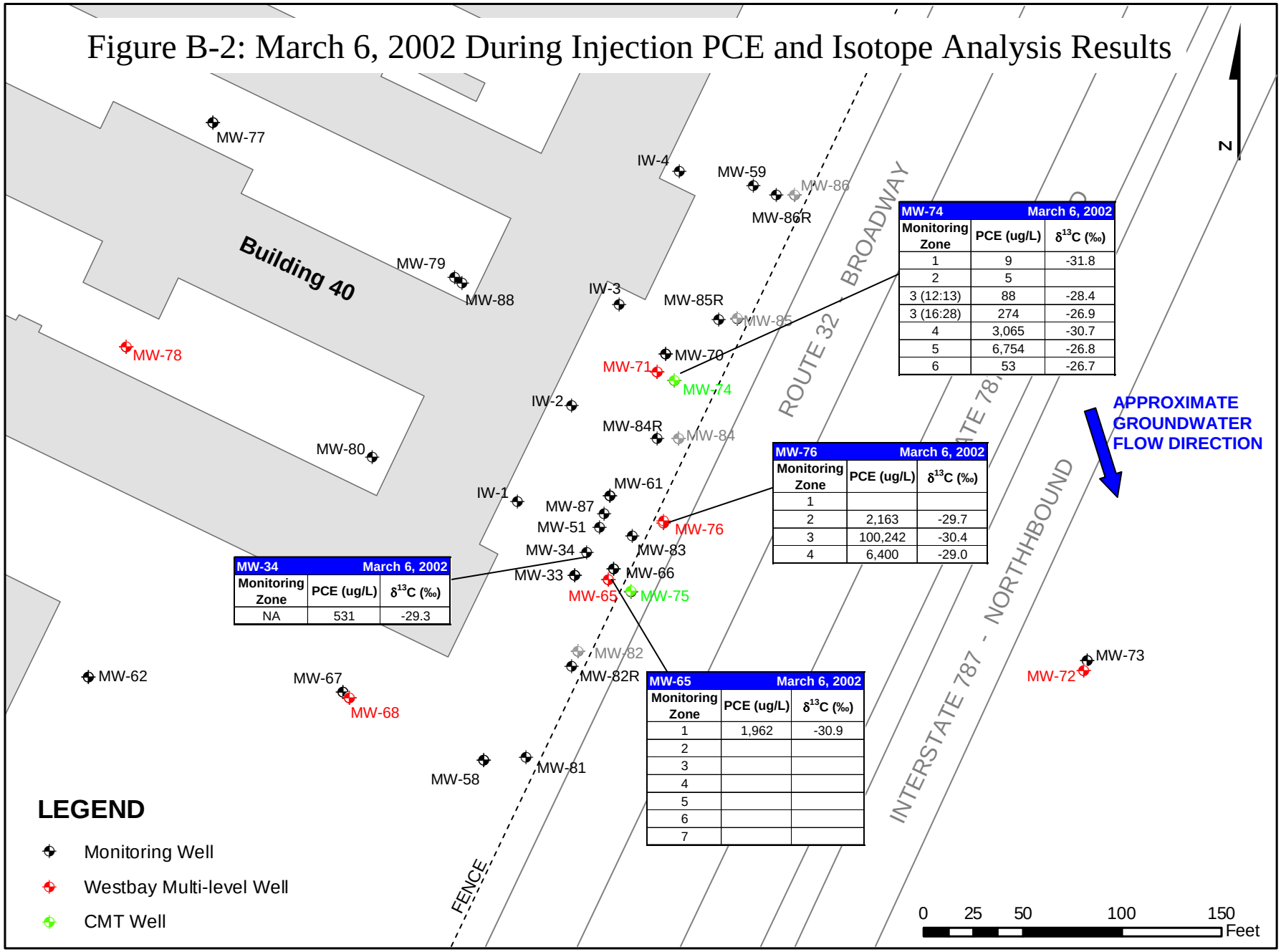


| MW-74 | March 6, 2002 | |
|---|---|---|
| Monitoring Zone | PCE (ug/L) | $\delta^{13}C$ (‰) |
| 1 | 9 | -31.8 |
| 2 | 5 | |
| 3 (12:13) | 88 | -28.4 |
| 3 (16:28) | 274 | -26.9 |
| 4 | 3,065 | -30.7 |
| 5 | 6,754 | -26.8 |
| 6 | 53 | -26.7 |

| MW-76 | March 6, 2002 | |
|---|---|---|
| Monitoring Zone | PCE (ug/L) | $\delta^{13}C$ (‰) |
| 1 | | |
| 2 | 2,163 | -29.7 |
| 3 | 100,242 | -30.4 |
| 4 | 6,400 | -29.0 |

| MW-34 | March 6, 2002 | |
|---|---|---|
| Monitoring Zone | PCE (ug/L) | $\delta^{13}C$ (‰) |
| NA | 531 | -29.3 |

| MW-65 | March 6, 2002 | |
|---|---|---|
| Monitoring Zone | PCE (ug/L) | $\delta^{13}C$ (‰) |
| 1 | 1,962 | -30.9 |
| 2 | | |
| 3 | | |
| 4 | | |
| 5 | | |
| 6 | | |
| 7 | | |

# Figure B-4: March 8, 2002 During Injection PCE and Isotope Analysis Results

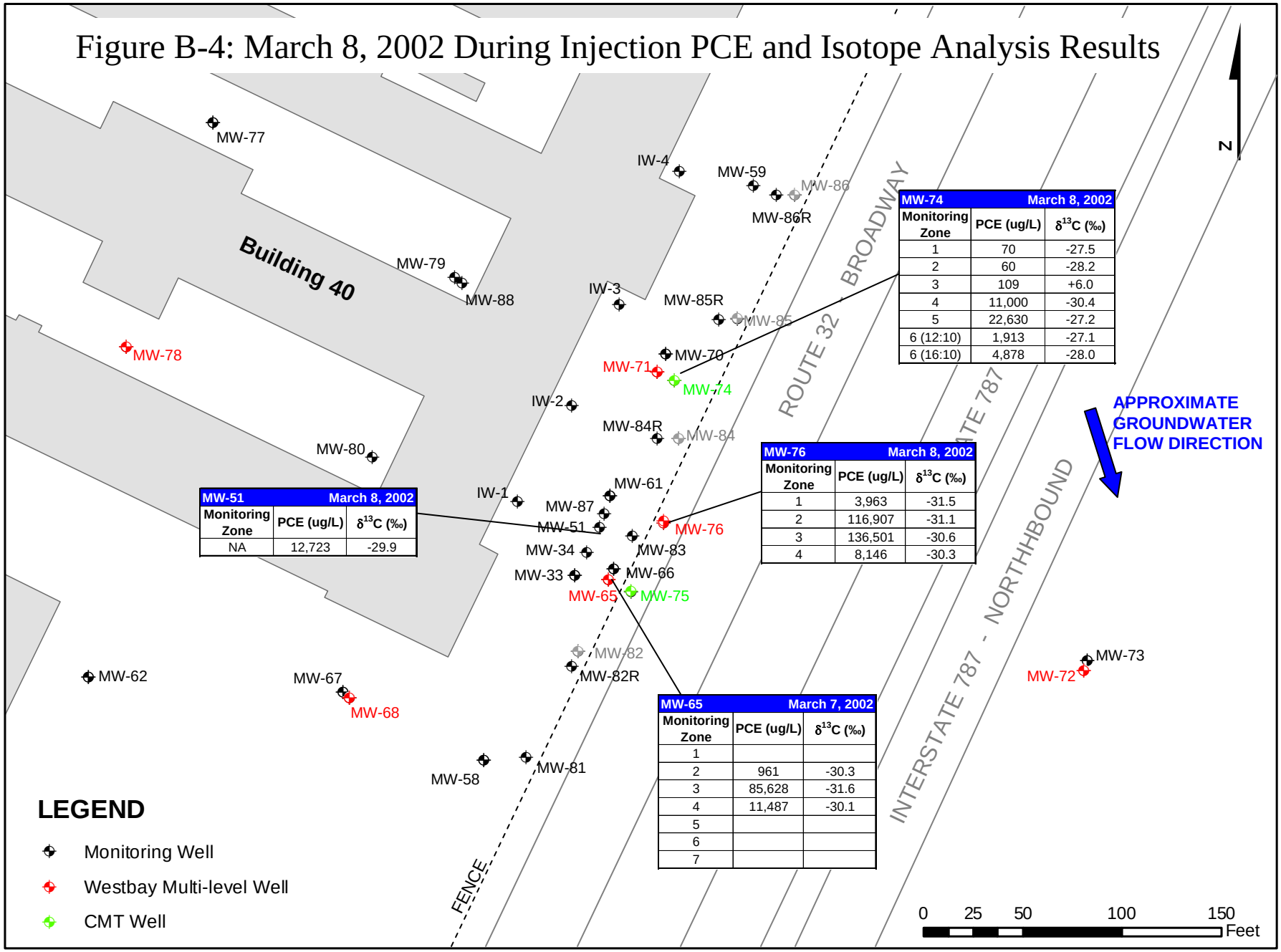


| MW-74 | March 8, 2002 | |
|---|---|---|
| Monitoring Zone | PCE (ug/L) | $\delta^{13}C$ (‰) |
| 1 | 70 | -27.5 |
| 2 | 60 | -28.2 |
| 3 | 109 | +6.0 |
| 4 | 11,000 | -30.4 |
| 5 | 22,630 | -27.2 |
| 6 (12:10) | 1,913 | -27.1 |
| 6 (16:10) | 4,878 | -28.0 |

| MW-76 | March 8, 2002 | |
|---|---|---|
| Monitoring Zone | PCE (ug/L) | $\delta^{13}C$ (‰) |
| 1 | 3,963 | -31.5 |
| 2 | 116,907 | -31.1 |
| 3 | 136,501 | -30.6 |
| 4 | 8,146 | -30.3 |

| MW-51 | March 8, 2002 | |
|---|---|---|
| Monitoring Zone | PCE (ug/L) | $\delta^{13}C$ (‰) |
| NA | 12,723 | -29.9 |

| MW-65 | March 7, 2002 | |
|---|---|---|
| Monitoring Zone | PCE (ug/L) | $\delta^{13}C$ (‰) |
| 1 | | |
| 2 | 961 | -30.3 |
| 3 | 85,628 | -31.6 |
| 4 | 11,487 | -30.1 |
| 5 | | |
| 6 | | |
| 7 | | |

# Figure B-5: March 18 – April 13, 2002 Post-Injection PCE and Isotope Analysis Results

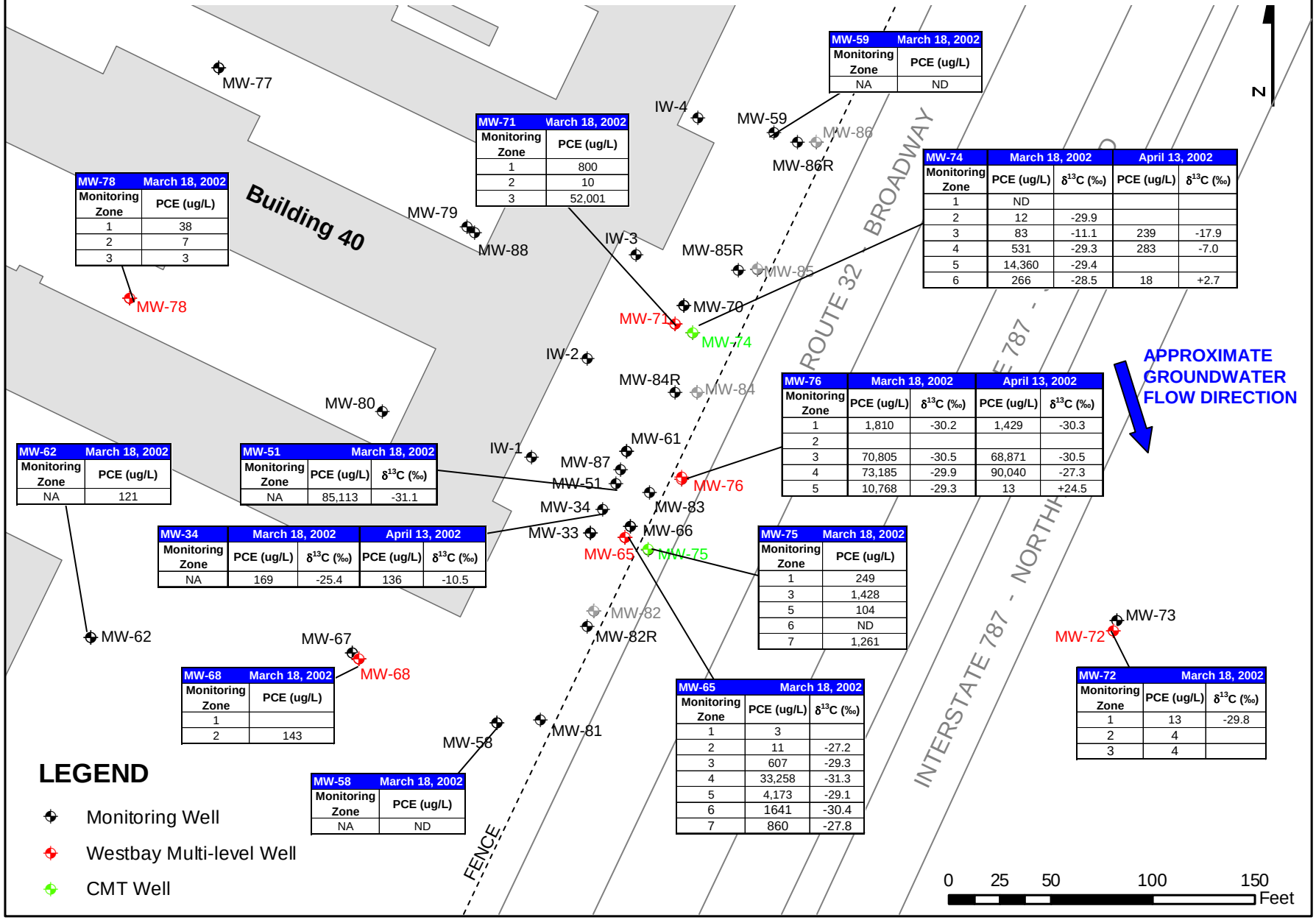


| MW-78 | March 18, 2002 |
|---|---|
| Monitoring Zone | PCE (ug/L) |
| 1 | 38 |
| 2 | 7 |
| 3 | 3 |

| MW-71 | March 18, 2002 |
|---|---|
| Monitoring Zone | PCE (ug/L) |
| 1 | 800 |
| 2 | 10 |
| 3 | 52,001 |

| MW-59 | March 18, 2002 |
|---|---|
| Monitoring Zone | PCE (ug/L) |
| NA | ND |

| MW-74 | March 18, 2002 | | April 13, 2002 | |
|---|---|---|---|---|
| Monitoring Zone | PCE (ug/L) | $\delta^{13}C$ (‰) | PCE (ug/L) | $\delta^{13}C$ (‰) |
| 1 | ND | | | |
| 2 | 12 | -29.9 | | |
| 3 | 83 | -11.1 | 239 | -17.9 |
| 4 | 531 | -29.3 | 283 | -7.0 |
| 5 | 14,360 | -29.4 | | |
| 6 | 266 | -28.5 | 18 | +2.7 |

| MW-76 | March 18, 2002 | | April 13, 2002 | |
|---|---|---|---|---|
| Monitoring Zone | PCE (ug/L) | $\delta^{13}C$ (‰) | PCE (ug/L) | $\delta^{13}C$ (‰) |
| 1 | 1,810 | -30.2 | 1,429 | -30.3 |
| 2 | | | | |
| 3 | 70,805 | -30.5 | 68,871 | -30.5 |
| 4 | 73,185 | -29.9 | 90,040 | -27.3 |
| 5 | 10,768 | -29.3 | 13 | +24.5 |

| MW-62 | March 18, 2002 |
|---|---|
| Monitoring Zone | PCE (ug/L) |
| NA | 121 |

| MW-51 | March 18, 2002 | |
|---|---|---|
| Monitoring Zone | PCE (ug/L) | $\delta^{13}C$ (‰) |
| NA | 85,113 | -31.1 |

| MW-34 | March 18, 2002 | | April 13, 2002 | |
|---|---|---|---|---|
| Monitoring Zone | PCE (ug/L) | $\delta^{13}C$ (‰) | PCE (ug/L) | $\delta^{13}C$ (‰) |
| NA | 169 | -25.4 | 136 | -10.5 |

| MW-75 | March 18, 2002 |
|---|---|
| Monitoring Zone | PCE (ug/L) |
| 1 | 249 |
| 3 | 1,428 |
| 5 | 104 |
| 6 | ND |
| 7 | 1,261 |

| MW-68 | March 18, 2002 |
|---|---|
| Monitoring Zone | PCE (ug/L) |
| 1 | |
| 2 | 143 |

| MW-65 | March 18, 2002 | |
|---|---|---|
| Monitoring Zone | PCE (ug/L) | $\delta^{13}C$ (‰) |
| 1 | 3 | |
| 2 | 11 | -27.2 |
| 3 | 607 | -29.3 |
| 4 | 33,258 | -31.3 |
| 5 | 4,173 | -29.1 |
| 6 | 1641 | -30.4 |
| 7 | 860 | -27.8 |

| MW-72 | March 18, 2002 | |
|---|---|---|
| Monitoring Zone | PCE (ug/L) | $\delta^{13}C$ (‰) |
| 1 | 13 | -29.8 |
| 2 | 4 | |
| 3 | 4 | |

| MW-58 | March 18, 2002 |
|---|---|
| Monitoring Zone | PCE (ug/L) |
| NA | ND |

# Figure B-6: January 2003 Post-Injection PCE and Isotope Analysis Results

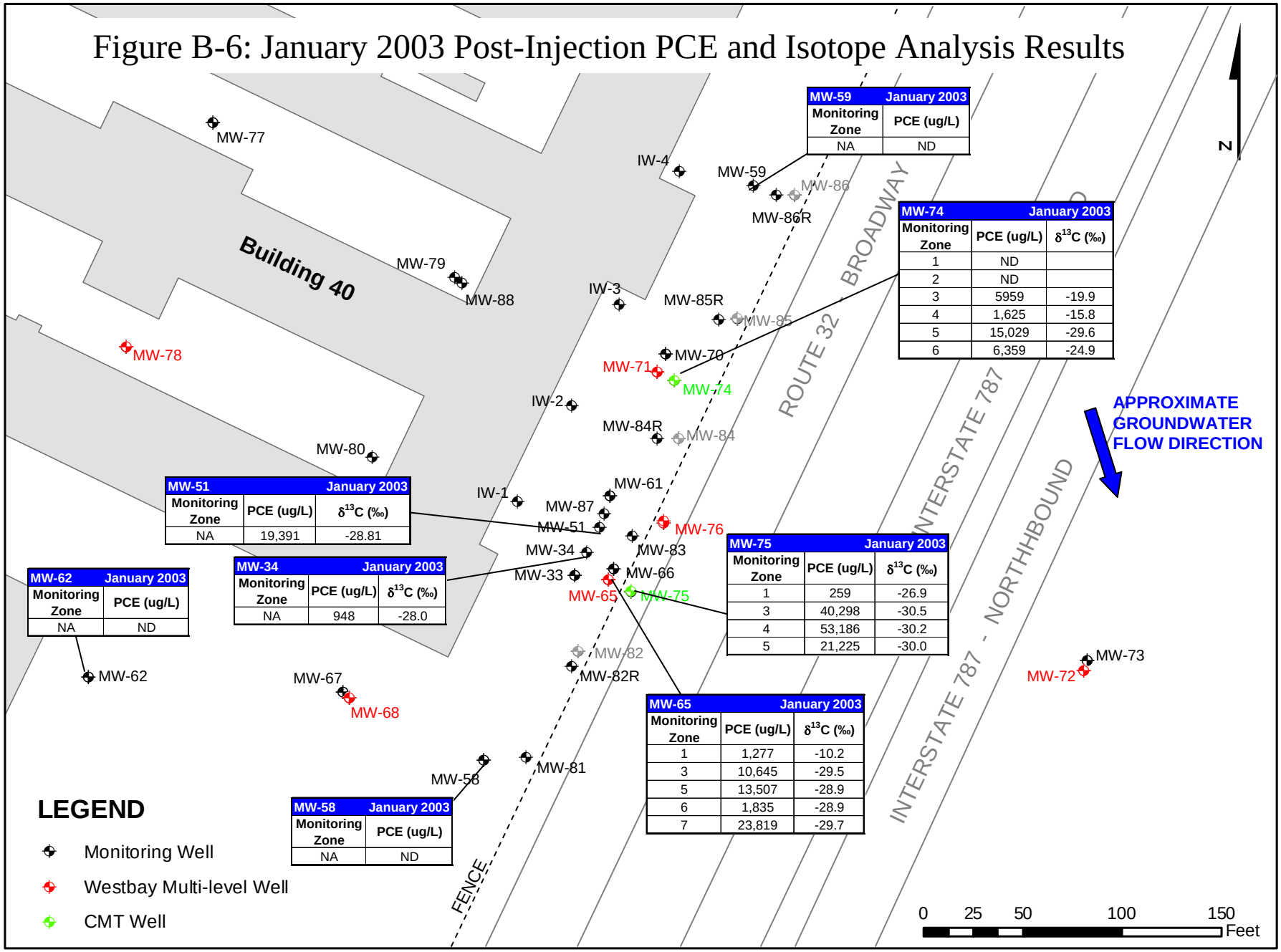


| MW-59 | January 2003 |
|---|---|
| Monitoring Zone | PCE (ug/L) |
| NA | ND |

| MW-74 | January 2003 | |
|---|---|---|
| Monitoring Zone | PCE (ug/L) | $\delta^{13}C$ (‰) |
| 1 | ND | |
| 2 | ND | |
| 3 | 5959 | -19.9 |
| 4 | 1,625 | -15.8 |
| 5 | 15,029 | -29.6 |
| 6 | 6,359 | -24.9 |

| MW-51 | January 2003 | |
|---|---|---|
| Monitoring Zone | PCE (ug/L) | $\delta^{13}C$ (‰) |
| NA | 19,391 | -28.81 |

| MW-34 | January 2003 | |
|---|---|---|
| Monitoring Zone | PCE (ug/L) | $\delta^{13}C$ (‰) |
| NA | 948 | -28.0 |

| MW-62 | January 2003 |
|---|---|
| Monitoring Zone | PCE (ug/L) |
| NA | ND |

| MW-75 | January 2003 | |
|---|---|---|
| Monitoring Zone | PCE (ug/L) | $\delta^{13}C$ (‰) |
| 1 | 259 | -26.9 |
| 3 | 40,298 | -30.5 |
| 4 | 53,186 | -30.2 |
| 5 | 21,225 | -30.0 |

| MW-65 | January 2003 | |
|---|---|---|
| Monitoring Zone | PCE (ug/L) | $\delta^{13}C$ (‰) |
| 1 | 1,277 | -10.2 |
| 3 | 10,645 | -29.5 |
| 5 | 13,507 | -28.9 |
| 6 | 1,835 | -28.9 |
| 7 | 23,819 | -29.7 |

| MW-58 | January 2003 |
|---|---|
| Monitoring Zone | PCE (ug/L) |
| NA | ND |

**LEGEND**

- Monitoring Well
- Westbay Multi-level Well
- CMT Well

# Figure B-3: March 7, 2002 During Injection PCE and Isotope Analysis Results

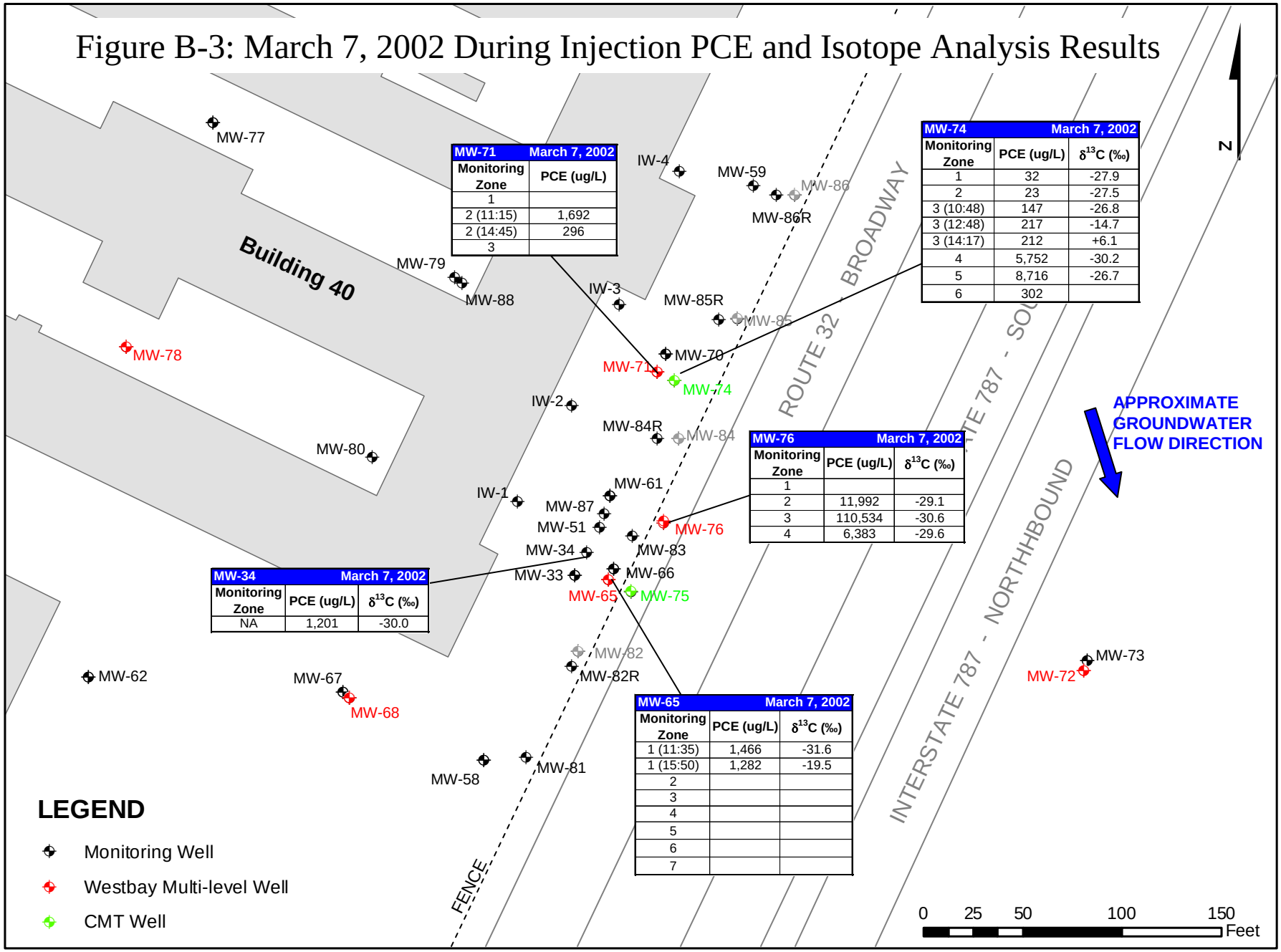

# Appendix C
Laboratory Rock Oxidant Demand Results

**Batch Rock Oxidant Demand (ROD) Tests – Watervliet Arsenal**

**Purpose:**

- determine upper end values for rock oxidant demand (ROD) on rock core samples using batch tests on samples of crushed/pulverized rock
- assess reaction mechanisms contributing to ROD by measurements on pre- and post-oxidation solids ($f_{oc}$) and solution ($SO_4^{2-}$)

**Methods:**

Two sets of batch tests:

(1) September 2002

- 3 samples
- Initial $KMnO_4$ at 1, 5, 20 g/L
- 10 g crushed rock and 100 mL of solution (rock mass: solution volume = 0.1 g/mL)
- sampled at 2, 4, 7, 9, 11, 14, 16, 18, 21 days

(2) March 2003

- 2 samples
- Initial $NaMnO_4$ at 2%, 5%, 10%, $KMnO_4$ at 20 g/L
- range of rock mass : solution volume ratios from 0.4 to 2.0 g/mL
- sampled at 4, 7, 14, 21 days

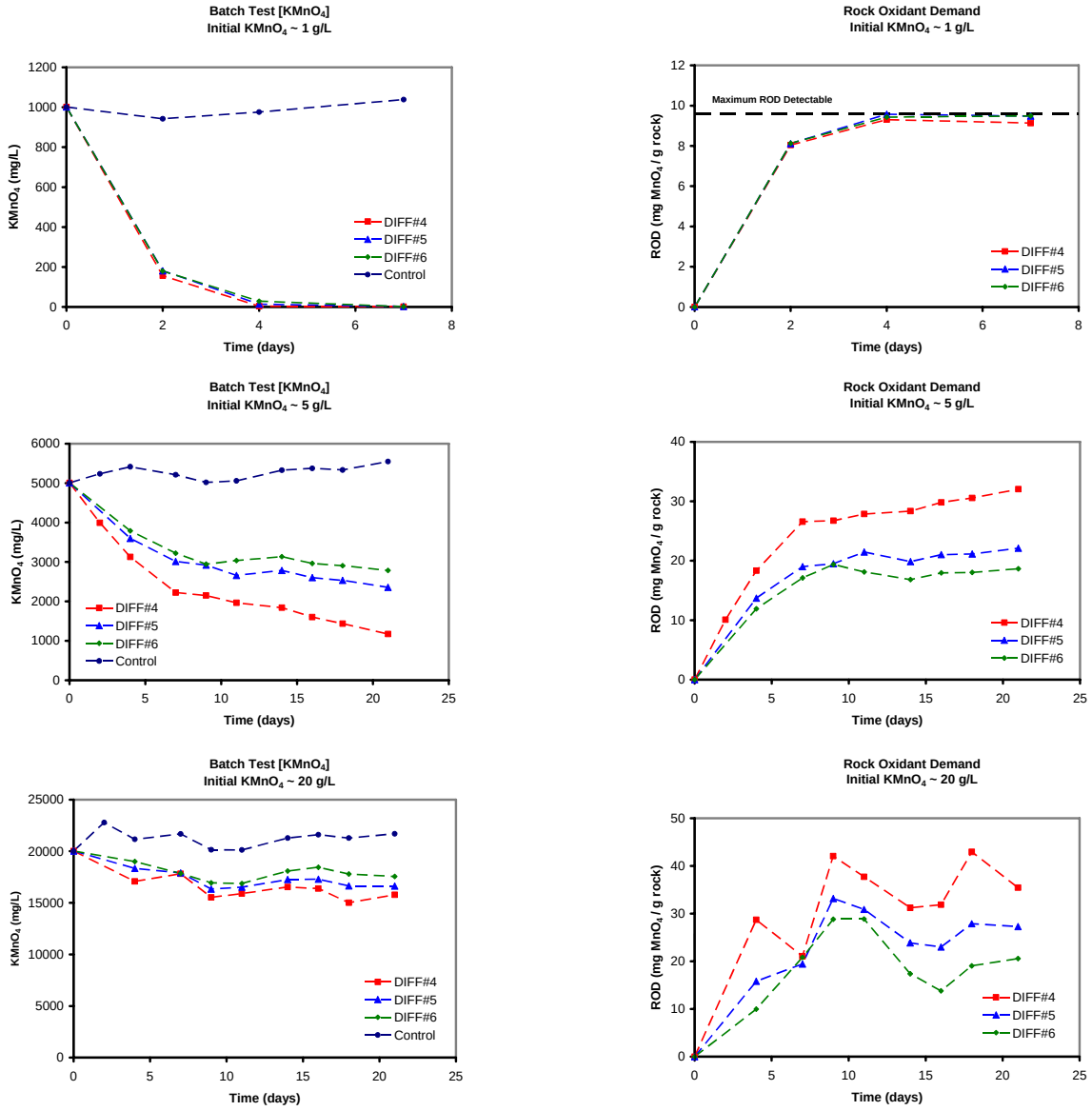


Figure C-1: Results of rock oxidant demand tests: $KMnO_4$ concentrations versus time and estimated ROD versus time for first set of batch tests.

(a)

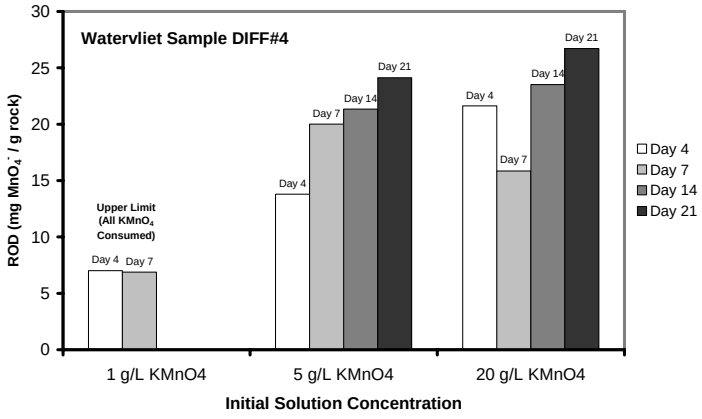


(b)

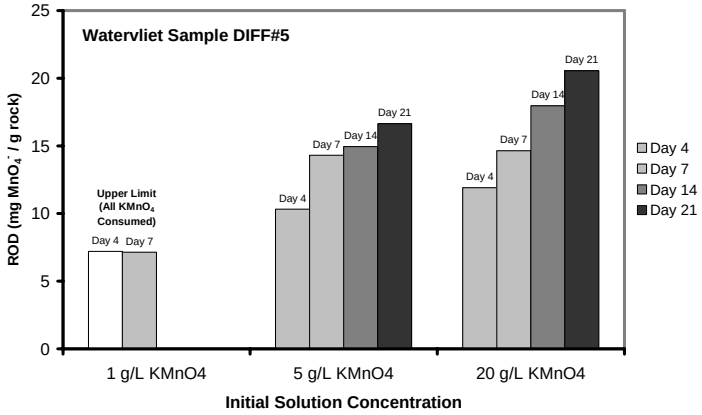


(c)

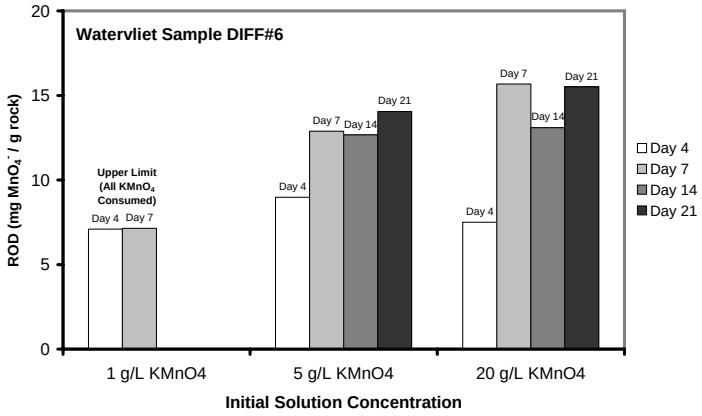


Figure C-2: Rock oxidant demand batch test results on first set of batch test samples using initial $KMnO_4$ concentrations of 1, 5 and 20 g/L.

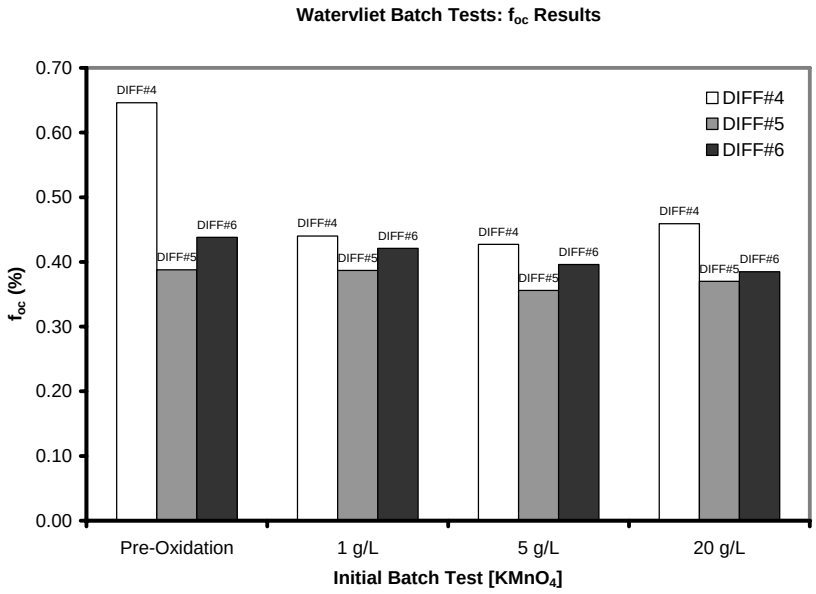


$$28MnO_4^- + 3C_7H_8O_4 + 28H^+ \rightarrow 28MnO_2(s) + 21CO_2 + 26H_2O$$

Figure C-3: Change in $f_{oc}$ for batch test solids after 21 days for first set of batch tests. Based on the above theoretical reaction of organic carbon (OC) and permanganate (Hønning et al., 2007) oxidation of each mg of OC consumes 13.2 mg of $MnO4^-$.

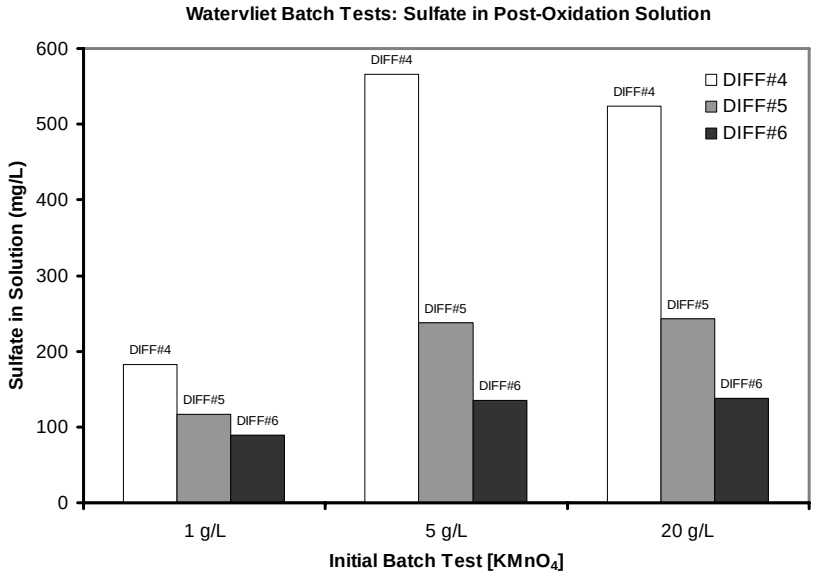


$$FeS_{2(s)} + 5MnO_4^- + H_2O + H^+ \rightarrow Fe(OH)_{3(s)} + 5MnO_{2(s)} + 2SO_4^{2-}$$

Figure C-4: Batch test solution sulfate concentrations after 21 days for first set of batch tests. Based on the above theoretical reaction of pyrite and permanganate, oxidation of each mg of pyrite consumes 5.0 mg of $MnO4^-$ and produces 1.6 mg of $SO_4^{2-}$. Results suggest pyrite oxidation accounts for 30-80% of ROD.

(a)

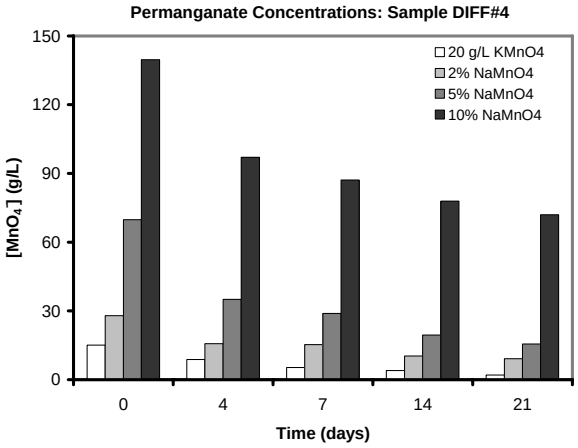


(b)

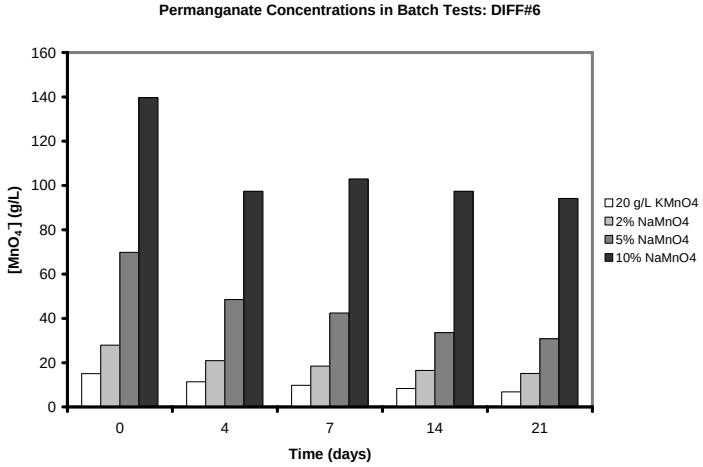


(c)

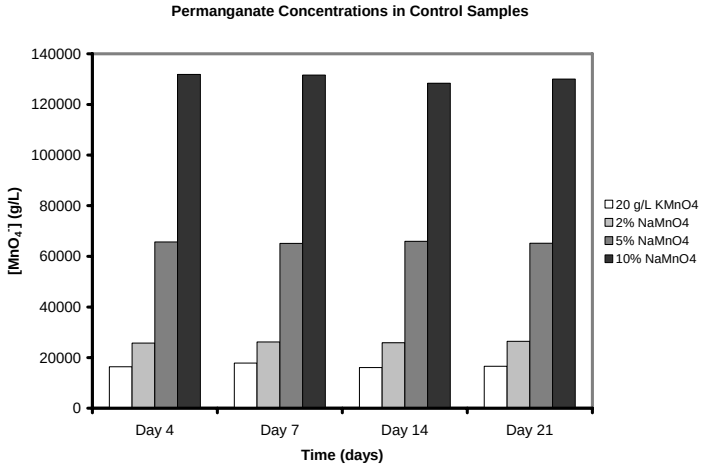


Figure C-5: Results of rock oxidant demand tests: $MnO_4^-$ concentrations versus time for second set of batch tests: (a) sample DIFF#4, (b) sample DIFF#6, and (c) control samples.

(a)

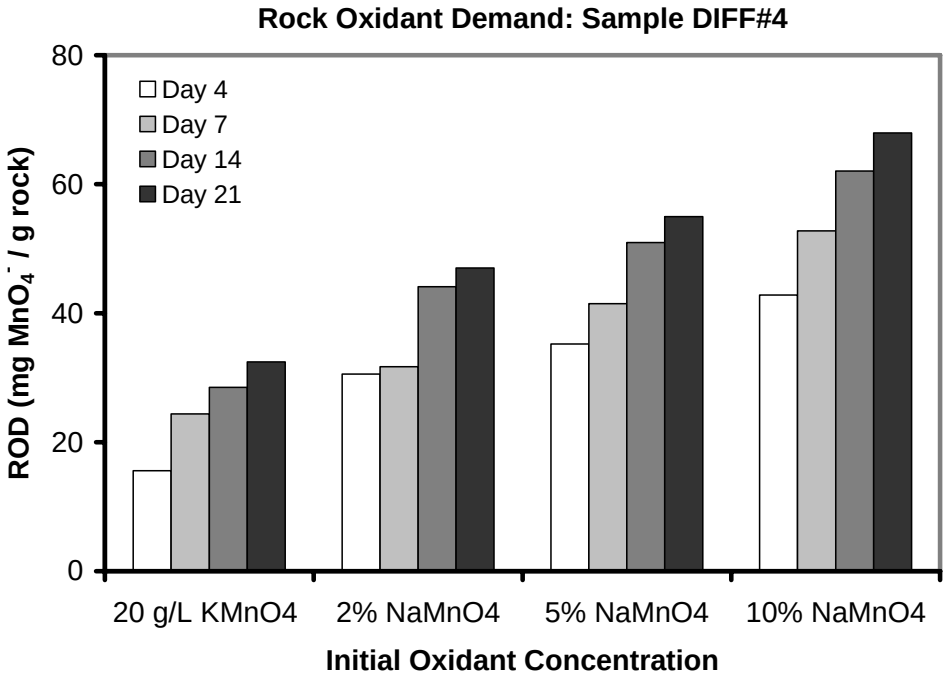


(b)

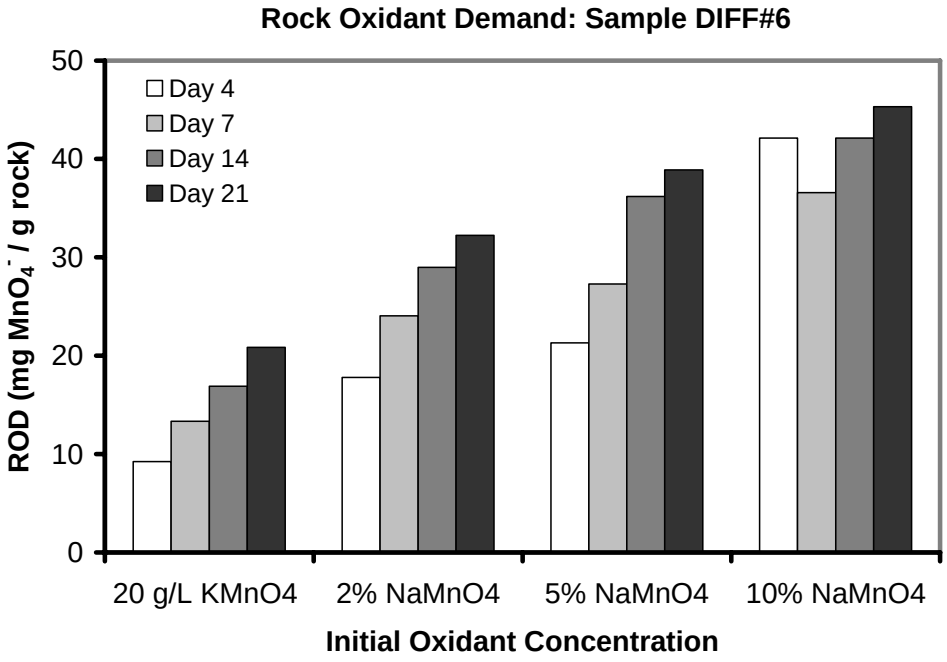


Figure C-6: Rock oxidant demand batch test results on second set of batch test samples using initial $KMnO_4$ concentration of 20 g/L and initial $NaMnO_4$ concentrations of 2, 5 and 10%.

(a)

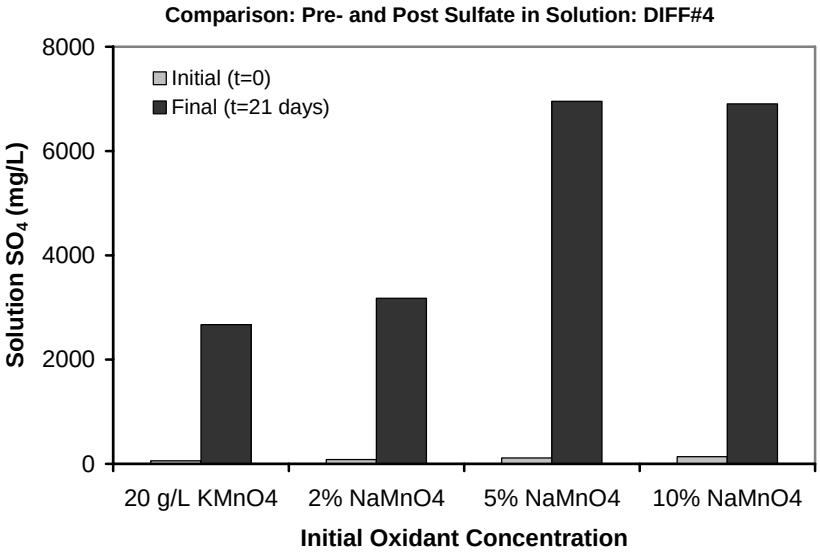


(b)

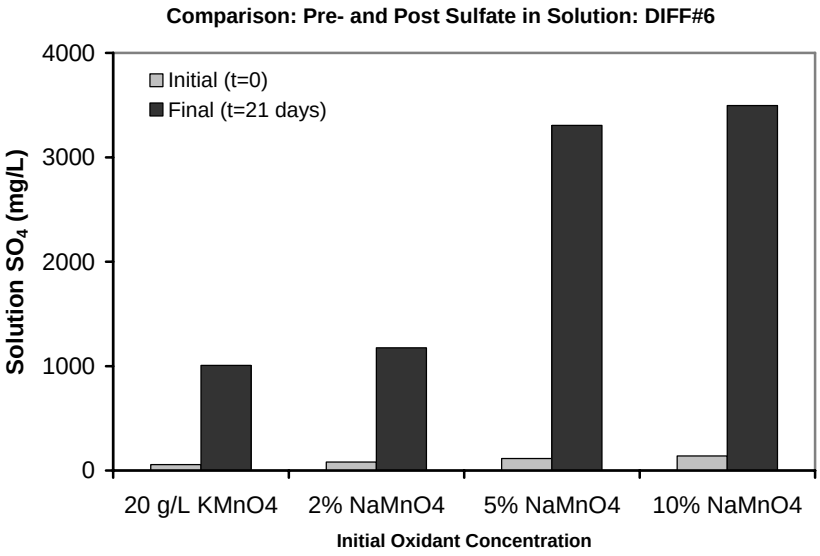


$$FeS_{2(s)} + 5MnO_4^- + H_2O + H^+ \rightarrow Fe(OH)_{3(s)} + 5MnO_{2(s)} + 2SO_4^{2-}$$

Figure C-7: Batch test solution sulfate concentrations after 21 days for second set of batch tests: (a) sample DIFF#4, and (b) sample DIFF#6. Based on the above theoretical reaction of pyrite and permanganate, oxidation of each mg of pyrite consumes 5.0 mg of $MnO4^-$ and produces 1.6 mg of $SO_4^{2-}$. Results suggest pyrite oxidation accounts for 30-75% of ROD.

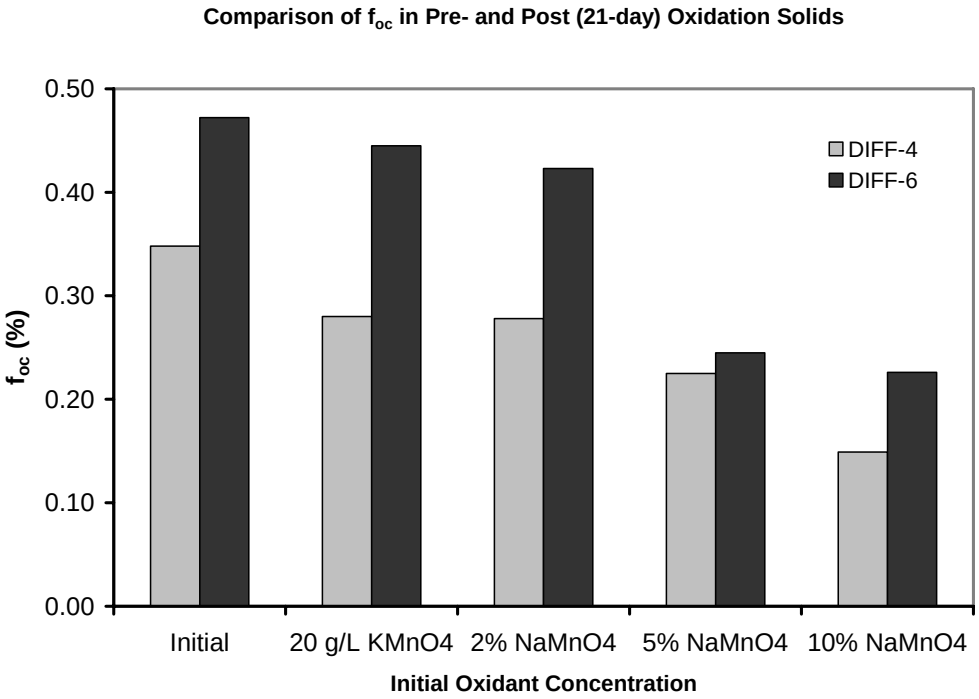


$$28MnO_4^- + 3C_7H_8O_4 + 28H^+ \rightarrow 28MnO_2(s) + 21CO_2 + 26H_2O$$

Figure C-8: Change in $f_{oc}$ for batch test solids after 21 days for second set of batch tests. Based on the above theoretical reaction of organic carbon (OC) and permanganate (Hønning et al., 2007) oxidation of each mg of OC consumes 13.2 mg of $MnO4^-$.

# Appendix D
Laboratory Diffusion Study Results

Table D-1: Results of rock matrix properties based on analysis of samples by Golder Associates (Mississauga, ON)

| **Borehole ID** | **Depth Range** (ft bgs) | **Saturated Water Content** (%) | **Dry Bulk Density** ($g/cm^3$) | **Total Porosity** ( % ) | **Specific Gravity** (-) | **Total Organic Carbon** (%) | **Hydraulic Conductivity** (cm/s) | **Chloride Matrix Diffusion Coeff., D** ($cm^2/sec$) | **Matrix Tortuosity Factor,** $\tau$ (-) |
|---|---|---|---|---|---|---|---|---|---|
| MW-64 | 133.7 - 135 | 1.42 | 2.68 | 2.4 | 2.75 | 0.26 | 3.3E-09 | 6.4E-07 | 0.042 |
| MW-65 | 40 - 45 | 1.47 | 2.66 | 1.9 | 2.72 | 0.29 | 6.3E-10 | 7.1E-07 | 0.047 |
| MW-68 | 65 - 70 | 1.26 | 2.65 | 1.9 | 2.71 | 0.28 | 1.0E-10 | 1.1E-06 | 0.071 |
| MW-71 | 70.7 - 75.7 | 1.49 | 2.66 | 3.1 | 2.75 | 0.27 | 1.8E-09 | 4.8E-07 | 0.032 |
| MW-72 | 39.5 - 40.5 | 1.21 | 2.65 | 2.4 | 2.72 | 0.29 | 3.6E-11 | 8.4E-07 | 0.056 |

Report: Attachment#1, Appendix B in Draft ICM Work Plan (October 2003)

Table D-2: Results of rock matrix properties based on analysis of samples by University of Waterloo (Ioanidis Lab).

| **Sample ID** | **Borehole ID** | **Depth Range** (ft bgs) | **Length** (cm) | **Permeability** (mDarcy) | **Dry wt** (g) | **Bulk Volume** ($cm^3$) | **Wet Wt** (g) | **Pore volume ($V_p$)** ($cm^3$) | **Porosity** ( % ) | **Dry bulk Density** ($g/cm^3$) | **Wet bulk Density** ($g/cm^3$) | **Formation Factor** (F) | **Cementation Exponent** (m) |
|---|---|---|---|---|---|---|---|---|---|---|---|---|---|
| WTV-UW-1 | MW-83 | 41.6 - 42.8 | 3.7 | <.0001 | 109.267 | 40.329 | 109.763 | 0.495 | 1.2 | 2.71 | 2.72 | 208.8 | 1.214 |
| WTV-UW-2 | MW-83 | 71.1 - 72.7 | 3.9 | <.0001 | 117.057 | 43.202 | 117.624 | 0.567 | 1.3 | 2.71 | 2.72 | 262.9 | 1.286 |
| WTV-UW-3 | MW-83 | 86.6 - 87.3 | 4.6 | <.0001 | 139.099 | 51.157 | 139.585 | 0.486 | 0.9 | 2.72 | 2.73 | 339.8 | 1.252 |
| WTV-UW-4 | MW-83 | 111.5 - 112.3 | 4.6 | <.0001 | 138.908 | 50.826 | 139.281 | 0.373 | 0.7 | 2.73 | 2.74 | 1675.7 | 1.511 |
| WTV-UW-5 | MW-83 | 134.4 - 135.2 | 5.0 | <.0001 | 150.398 | 55.246 | 150.835 | 0.437 | 0.8 | 2.72 | 2.73 | 452.9 | 1.263 |
| WTV-UW-6 | MW-83 | 151.6 - 152.3 | 3.0 | <.0001 | 90.291 | 33.147 | 90.851 | 0.561 | 1.7 | 2.72 | 2.74 | 198.9 | 1.297 |
| WTV-UW-7 | MW-83 | 174.5 - 175.6 | 3.4 | <.0001 | 103.405 | 37.898 | 103.916 | 0.511 | 1.3 | 2.73 | 2.74 | 414.7 | 1.400 |
| | | | | | | | | **Averages** | **1.1** | **2.72** | **2.73** | **507.7** | **1.318** |

Table D-3: Fraction organic carbon ($f_{oc}$) and carbonate content (December 2001 cores)

| Sample ID | Borehole ID | Depth (ft bgs) | | | Average Depth (ft bgs) | foc (%) | CaCO3 (equivalent %) |
|---|---|---|---|---|---|---|---|
| WVT FOC 1 | AV-1 | 31.90 | - | 32.05 | 31.98 | 0.397 | 2.7 |
| WVT FOC 2 | AV-1 | 43.70 | - | 43.85 | 43.78 | 0.342 | 4.6 |
| WVT FOC 3 | AV-1 | 44.30 | - | 44.00 | 44.15 | 0.338 | 3.0 |
| WVT FOC 4 | MW-74 | 22.00 | - | 22.30 | 22.15 | 0.449 | 3.3 |
| WVT FOC 5 | MW-74 | 48.00 | - | 48.20 | 48.10 | 0.363 | 2.1 |
| WVT FOC 6 | MW-74 | 58.60 | - | 58.80 | 58.70 | 0.409 | 3.9 |
| WVT FOC 7 | MW-74 | 82.70 | - | 83.00 | 82.85 | 0.401 | 2.7 |
| WVT FOC 8 | MW-74 | 87.60 | - | 88.00 | 87.80 | 0.355 | 3.2 |
| WVT FOC 9 | MW-74 | 114.40 | - | 114.70 | 114.55 | 0.680 | 3.6 |
| WVT FOC 10 | MW-74 | 127.10 | - | 127.40 | 127.25 | 0.363 | 4.7 |
| WVT FOC 11 | MW-74 | 147.30 | - | 147.40 | 147.35 | 0.343 | 3.6 |
| WVT FOC 12 | MW-75 | 23.90 | - | 24.30 | 24.10 | 0.367 | 4.6 |
| WVT FOC 13 | MW-75 | 53.45 | - | 53.65 | 53.55 | 0.384 | 7.0 |
| WVT FOC 14 | MW-75 | 67.45 | - | 67.60 | 67.53 | 0.331 | 2.9 |
| WVT FOC 15 | MW-75 | 87.35 | - | 87.55 | 87.45 | 0.400 | 3.0 |
| WVT FOC 16 | MW-75 | 91.00 | - | 91.20 | 91.10 | 0.412 | 2.8 |
| WVT FOC 17 | MW-75 | 122.00 | - | 122.10 | 122.05 | 0.474 | 3.9 |
| WVT FOC 18 | MW-75 | 144.20 | - | 144.40 | 144.30 | 0.313 | 4.0 |
| | | | | | **Average** | 0.396 | 3.6 |

**Notes:**

(1) $f_{oc}$ measured by Organic Geochemistry Laboratory (University of Waterloo)

(2) Carbonate content measured by Soil and Nutrient Laboratory (University of Guelph)

Table D-4: ALS Chemex results of whole rock analysis via acid digestion and ICM-MS / ICP-AES

| | Core ID | AV-1 | MW-74 | MW-74 | MW-74 | MW-74 | MW-75 | MW-75 | MW-75 |
|---|---|---|---|---|---|---|---|---|---|
| | Depth (ft bgs) | 43.5 - 45.8 | 24.2 - 24.6 | 30.9 - 31.7 | 60.8 - 61.9 | 137.6 - 138.9 | 53.7 - 55.2 | 53.7 - 55.2 | 87.5 - 89.2 |
| **Parameter** | **Units** | **WVT-DIFF-1** | **WVT-DIFF-2** | **WVT-DIFF-3** | **WVT-DIFF-4** | **WVT-DIFF-5** | **WVT-DIFF-6A** | **WVT-DIFF-6B** | **WVT-DIFF-7** |
| Ag | ppm | 0.36 | 0.3 | 0.34 | 0.38 | 0.48 | 0.38 | 0.32 | 0.42 |
| Al | % | 7.53 | 7.75 | 7.61 | 7.7 | 8.17 | 8.26 | 7.57 | 8.85 |
| As | ppm | 12.4 | 7.6 | 12.2 | 16 | 34.6 | 9.2 | 9.4 | 38.6 |
| Ba | ppm | 505.3 | 523.9 | 533.8 | 519.8 | 538.1 | 648.7 | 785.2 | 687.2 |
| Be | ppm | 1.95 | 2.05 | 2.2 | 2.3 | 2.4 | 2.4 | 1.95 | 2.75 |
| Bi | ppm | 0.39 | 0.3 | 0.34 | 0.25 | 0.3 | 0.29 | 0.28 | 0.33 |
| Ca | % | 0.84 | 1.25 | 1.2 | 1.05 | 1.4 | 0.93 | 1.4 | 1.1 |
| Cd | ppm | 0.38 | 0.06 | 0.22 | 0.1 | 0.18 | 0.18 | 0.32 | 0.08 |
| Ce | ppm | 73.2 | 73.8 | 74.8 | 74.5 | 94.5 | 88.3 | 86.6 | 89.3 |
| Co | ppm | 18.4 | 12.8 | 17.5 | 22.8 | 51.7 | 17.7 | 14.4 | 28.2 |
| Cr | ppm | 72 | 71 | 71 | 64 | 59 | 52 | 64 | 64 |
| Cs | ppm | 6.95 | 7.65 | 7.95 | 7.85 | 8.25 | 9.05 | 7.35 | 9.3 |
| Cu | ppm | 51.3 | 45.6 | 67 | 49.2 | 53.8 | 70.5 | 67.1 | 62.9 |
| Fe | % | 4.19 | 4.31 | 4.2 | 4.26 | 5.4 | 4.34 | 4.59 | 4.42 |
| Ga | ppm | 19.65 | 20.75 | 20.95 | 20.75 | 23.2 | 23.05 | 20.25 | 25.6 |
| Ge | ppm | 0.25 | 0.25 | 0.25 | 0.25 | 0.3 | 0.3 | 0.3 | 0.3 |
| Hf | ppm | 2.6 | 2.6 | 2.7 | 2.8 | 3 | 3 | 2.6 | 3.2 |
| In | ppm | 0.085 | 0.07 | 0.08 | 0.07 | 0.085 | 0.07 | 0.07 | 0.075 |
| K | % | 2.55 | 2.72 | 2.7 | 2.75 | 2.88 | 2.94 | 2.52 | 3.22 |
| La | ppm | 32.5 | 34 | 35 | 35 | 42 | 41 | 36 | 44 |
| Li | ppm | 43.8 | 48.8 | 48.8 | 46.8 | 56.6 | 58 | 56.4 | 57.6 |
| Mg | % | 1.52 | 1.64 | 1.57 | 1.53 | 1.71 | 1.66 | 1.68 | 1.66 |
| Mn | ppm | 730 | 1020 | 905 | 895 | 1140 | 845 | 980 | 905 |
| Mo | ppm | 2.35 | 0.95 | 1.35 | 2.45 | 4.9 | 1.05 | 1.05 | 4.3 |
| Na | % | 0.78 | 0.75 | 0.74 | 0.77 | 0.87 | 0.82 | 0.82 | 0.87 |
| Nb | ppm | 10 | 10.6 | 11.2 | 11.4 | 12.3 | 12.6 | 10.7 | 13.8 |
| Ni | ppm | 41.6 | 38.8 | 44.8 | 48.2 | 68 | 48.6 | 48.2 | 51.1 |
| P | ppm | 500 | 470 | 410 | 430 | 500 | 490 | 520 | 550 |
| Pb | ppm | 25.5 | 14.5 | 19 | 24 | 37 | 21 | 30.5 | 23 |
| Rb | ppm | 139 | 143 | 142 | 148 | 158.5 | 166.5 | 133.5 | 176.5 |
| Re | ppm | 0.002 | 0.002 | <0.002 | 0.002 | 0.002 | 0.002 | 0.002 | 0.002 |
| S | % | 0.67 | 0.24 | 0.39 | 0.72 | 1.17 | 0.22 | 0.21 | 0.61 |
| Sb | ppm | 1.4 | 0.85 | 1.15 | 1.8 | 3.7 | 0.75 | 0.5 | 2.45 |
| Se | ppm | 1 | 1 | 1 | 1 | 2 | 1 | 1 | 2 |
| Sn | ppm | 2 | 2.2 | 2.2 | 2.2 | 2.2 | 2.4 | 2 | 2.4 |
| Sr | ppm | 105 | 145.5 | 156.5 | 134.5 | 151 | 157 | 160 | 159.5 |
| Ta | ppm | 0.65 | 0.65 | 0.65 | 0.65 | 0.65 | 0.7 | 0.6 | 0.75 |
| Te | ppm | 0.15 | 0.1 | 0.1 | 0.05 | 0.15 | 0.05 | 0.05 | 0.1 |
| Th | ppm | 13.2 | 13.2 | 13.6 | 13.8 | 15 | 14.4 | 12.8 | 17 |
| Ti | % | 0.38 | 0.39 | 0.39 | 0.4 | 0.41 | 0.43 | 0.37 | 0.46 |
| Tl | ppm | 0.66 | 0.66 | 0.6 | 0.62 | 0.68 | 0.64 | 0.56 | 0.78 |
| U | ppm | 3.6 | 3.7 | 3.7 | 4 | 4.2 | 3.9 | 3.6 | 4.7 |
| V | ppm | 130 | 130 | 130 | 134 | 141 | 144 | 126 | 157 |
| W | ppm | 1.2 | 1.1 | 1.2 | 1.2 | 1.3 | 1.3 | 1.1 | 1.4 |
| Y | ppm | 18.9 | 19 | 18.7 | 17.9 | 19.7 | 20 | 19.3 | 20.9 |
| Zn | ppm | 96 | 60 | 180 | 68 | 132 | 140 | 254 | 78 |
| Zr | ppm | 87 | 91 | 99 | 95 | 113 | 113.5 | 89 | 114 |

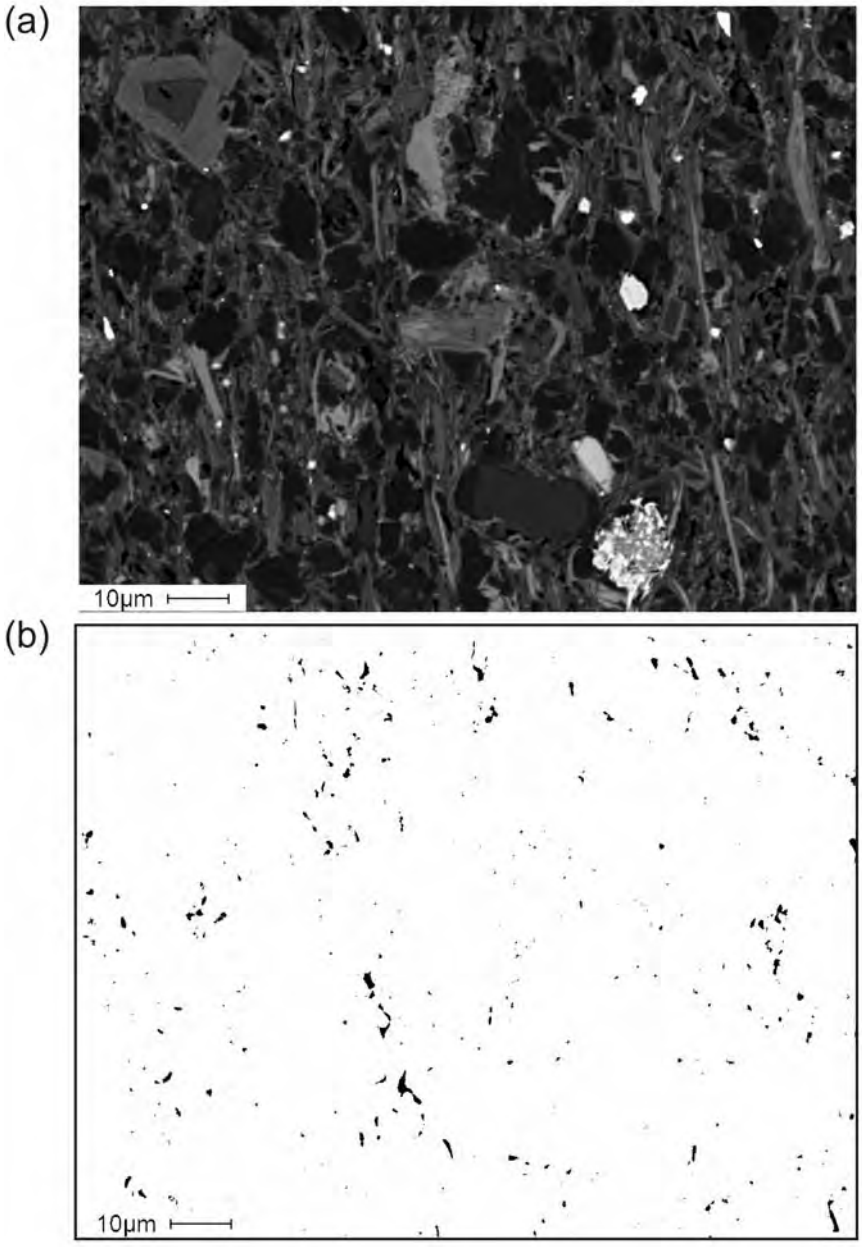


Figure D-1: SEM image of shale porosity: (a) backscattered SEM image of Watervliet shale sample, and (b) paired binary image showing matrix porosity (~1%) (from Tom Al, UNB).

**Microfractures: Examples**

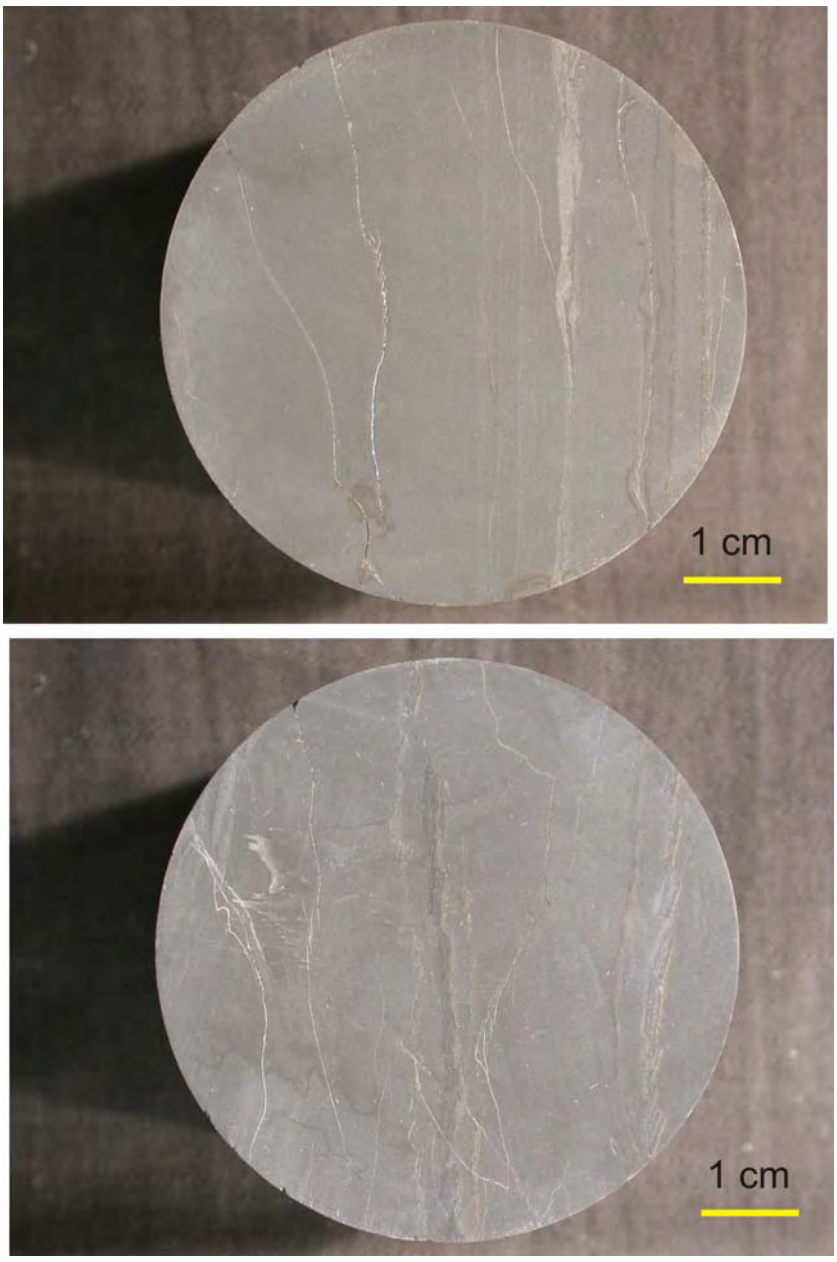


Figure D-2: Example photos of core samples cut along core-axis for invasion / disappearance tests; note presence of microfractures (some infilled with calcite), pyrite-rich zones, etc.

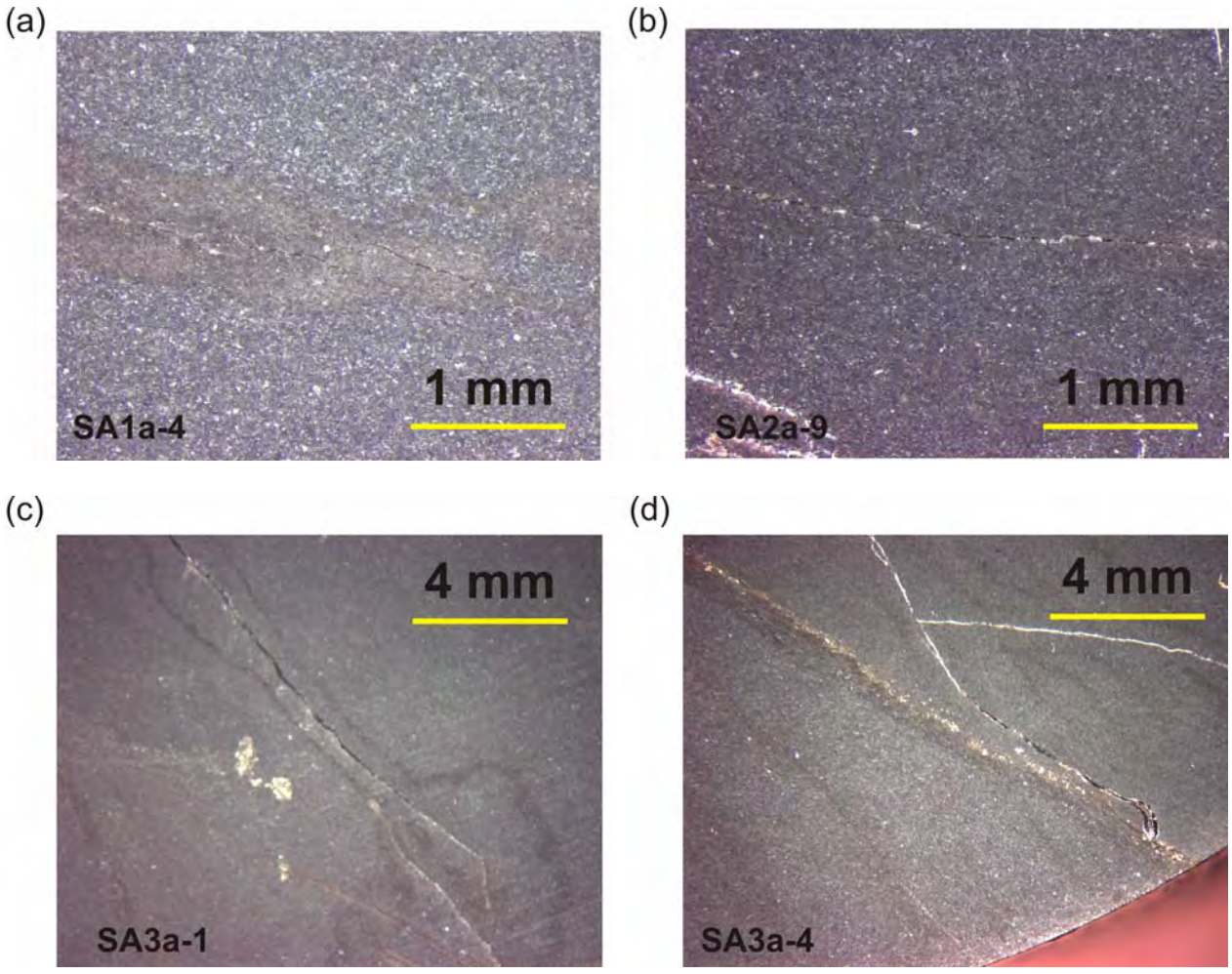


Figure D-3. Example photos using Leica DM Digital Microscope equipped with digital camera: (a) oxidation halo around microfracture, (b) microfracture partially infilled with pyrite, (c) large pyrite grain and open microfracture, (d) pyrite-rich vein and calcite infilled microfractures.

Figure D-4: Example photos of field core samples with pyrite accumulation on fracture surfaces.

Table D-5: Summary of invasion test samples initiated September 2002

| Sample ID | Date Removed | Time Sample in Solution | | Invasion Distance Determination | |
|---|---|---|---|---|---|
| | | weeks | months | LAM-ICP-MS | SEM/EDS |
| WINV#1 | 30-Oct-02 | 7.7 | 1.8 | X | X |
| WINV#2 | 03-Dec-02 | 12.6 | 2.9 | X | X |
| WINV#3 | 06-Mar-03 | 25.9 | 6.0 | X | X |
| WINV#4 | 09-Sep-03 | 52.6 | 12.1 | | X |
| WINV#5 | 02-Sep-04 | 103.9 | 24.0 | | X |

**Notes:**
Samples immersed in 2 g/L $KMnO_4$ solution
Tests initiated on September 6, 2002

## Methods of profile collection

(1) Laser Ablation Microprobe (LAM)-ICP-MS - Memorial University of Newfoundland (MUN)
http://www.mun.ca/earthsciences/facilities/analytical/LAMICP_Analysis.php

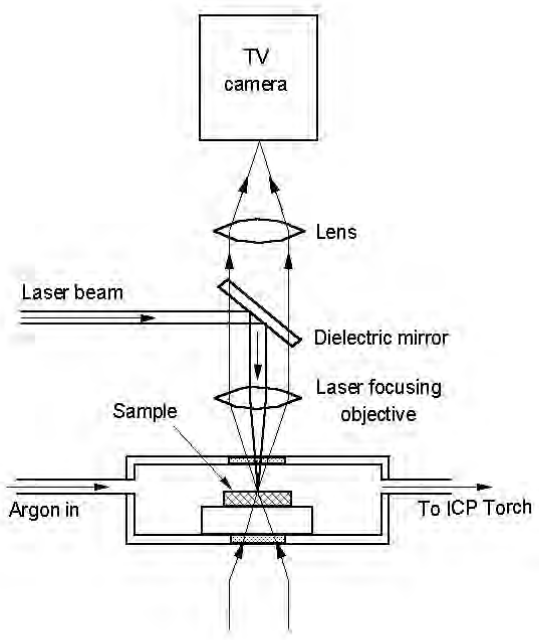


(2) Scanning Electron Microscopy / Energy Dispersive Spectroscopy (SEM/EDS) - University of New Brunswick (UNB)
http://www.unb.ca/fredericton/science/emunit/jeol6400.html

## Permanganate Invasion Tests – Initial Trial

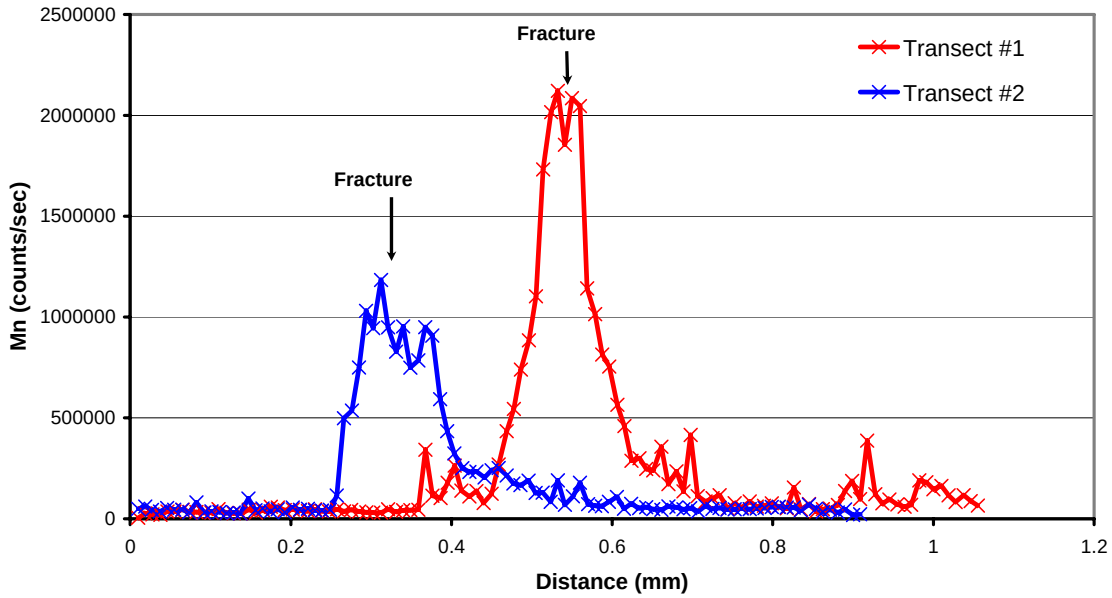


Figure D-5: Manganese profiles collected by laser ablation ICP-MS along transects perpendicular to microfractures (first trial on Watervliet samples). This sample was immersed in a 10 g/L $KMnO_4$ solution for about 6 weeks prior to thin-section preparation. Note that results are affected by the diameter of the laser beam (~50 microns) causing dispersion / broadening of the profiles and overestimation of Mn penetration distances.

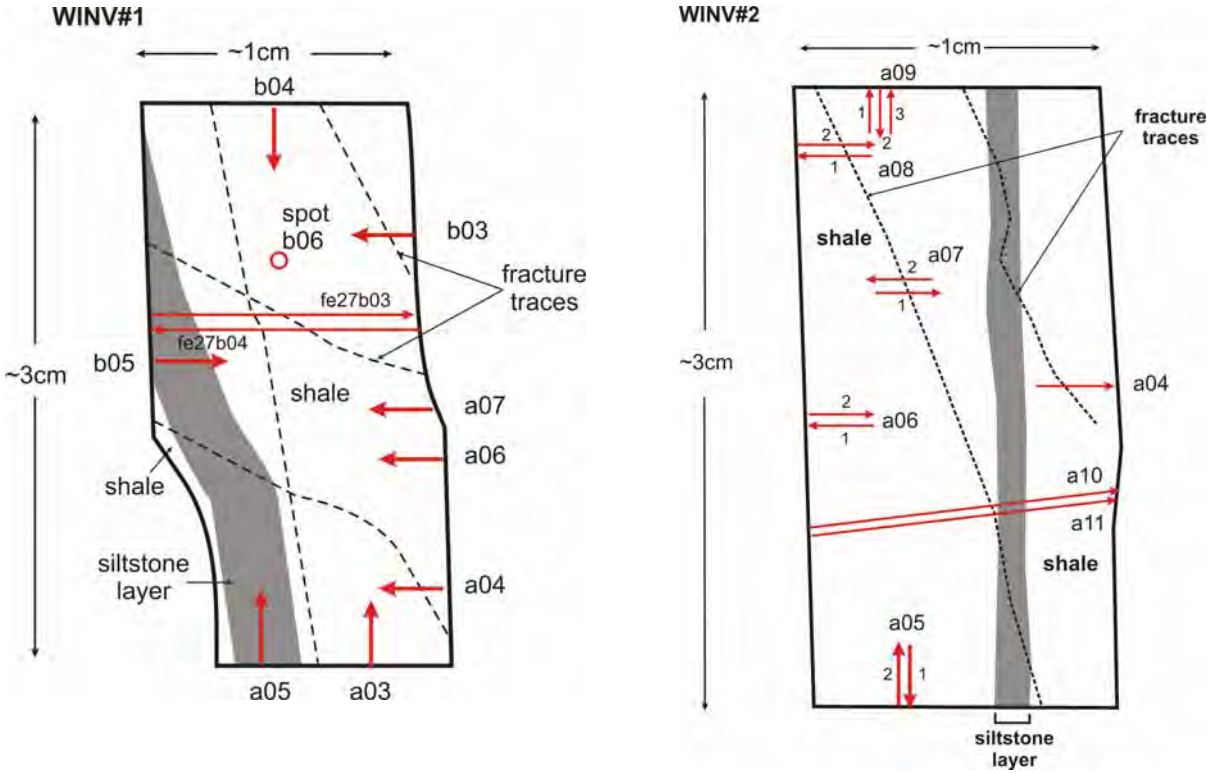


Figure D-6: Sketch of invasion test sample sections: (a) WINV#1, and (b) WINV#2 and locations of LAM-ICP-MS profiles collected.

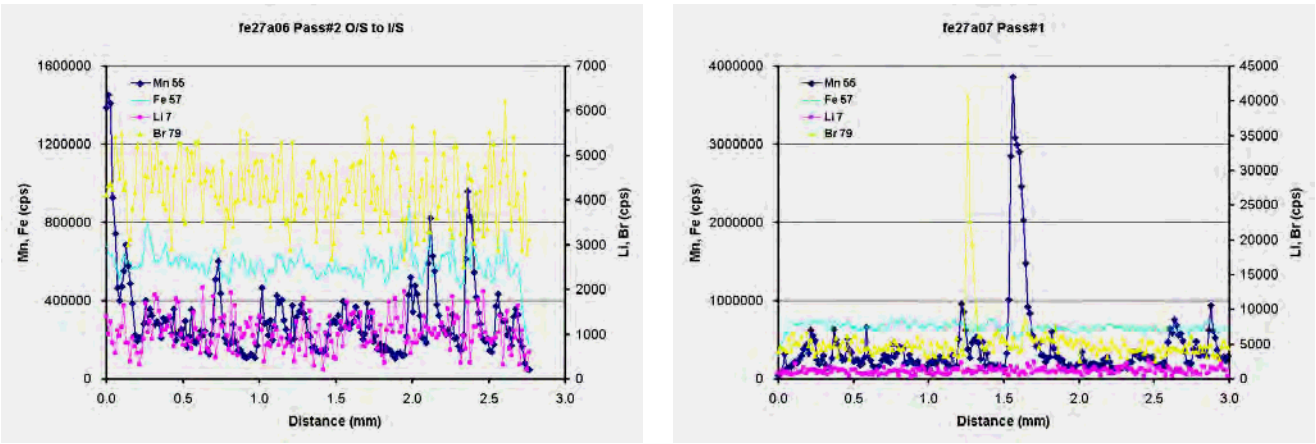


Figure D-7: Example LAM-ICP-MS profiles for WINV#2 (removed from solution at 12.6 weeks): (a) profile in from edge of sample, (b) profile across microfracture. Note that results are affected by the diameter of the laser beam (~50 microns) causing dispersion / broadening of the profiles and overestimation of Mn penetration distances.

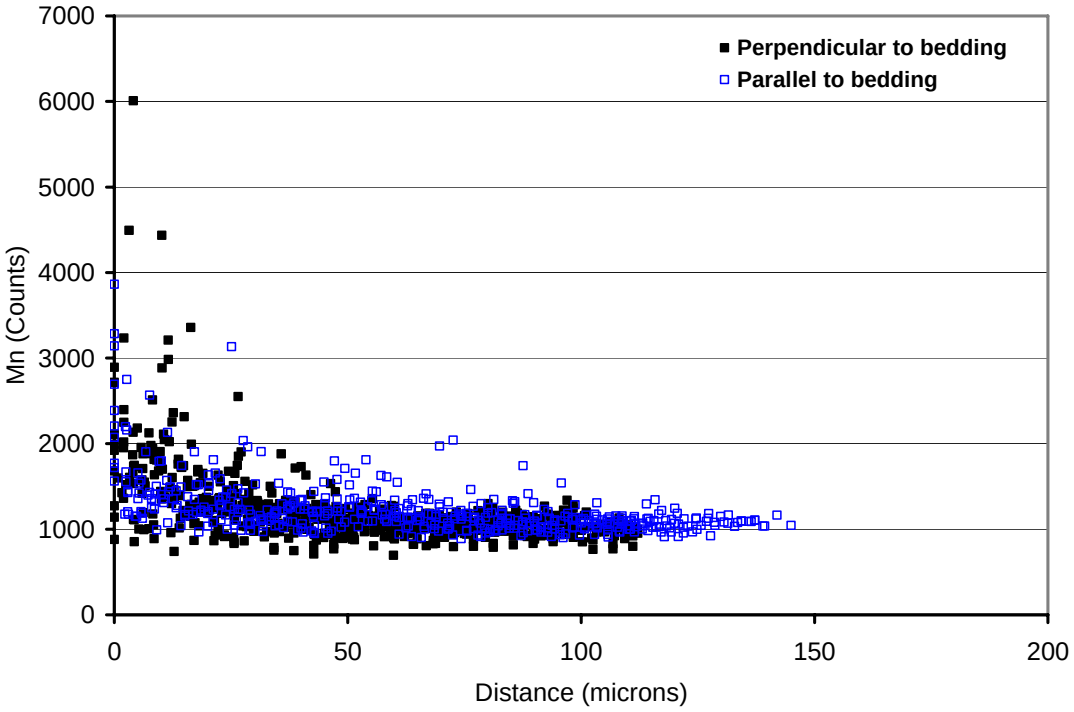


Figure D-8: SEM/EDS profiles for WINV#2 (removed from solution at 12.6 weeks): multiple profiles in from edges of sample parallel and perpendicular to bedding.

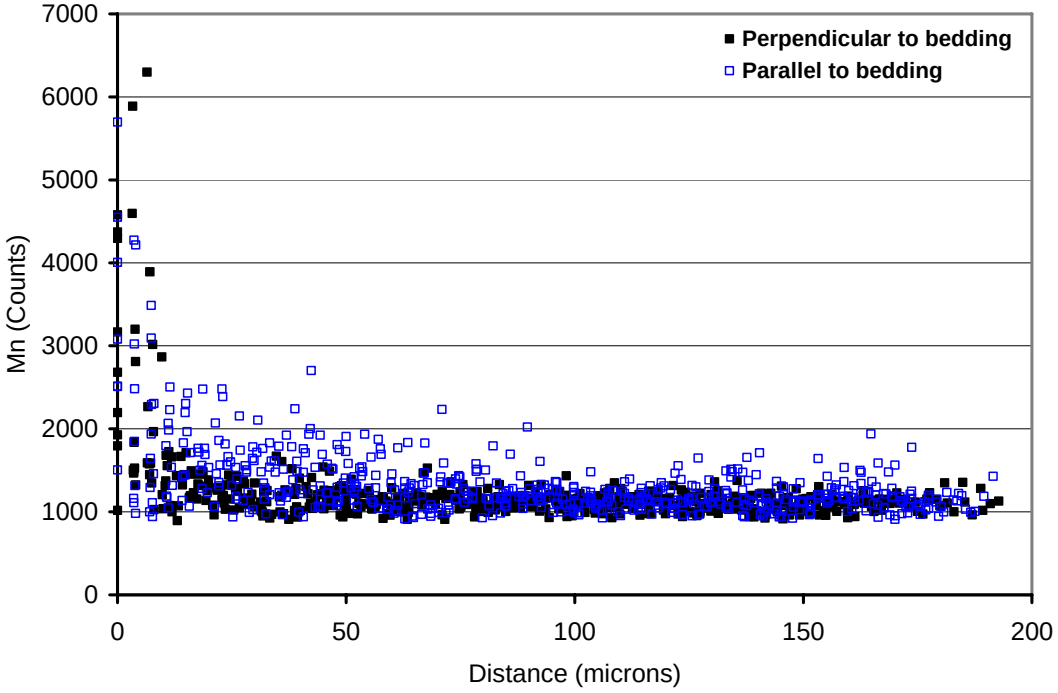


Figure D-9: SEM/EDS profiles for WINV#4 (removed from solution at 52.6 weeks): multiple profiles in from edges of sample parallel and perpendicular to bedding.

(a)

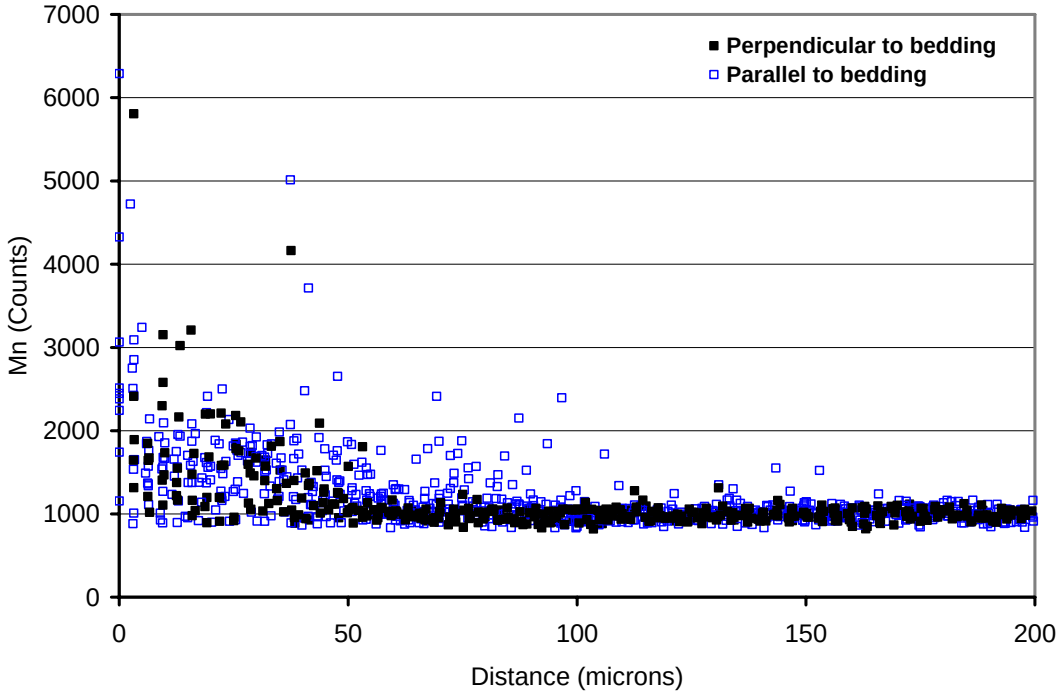


(b)

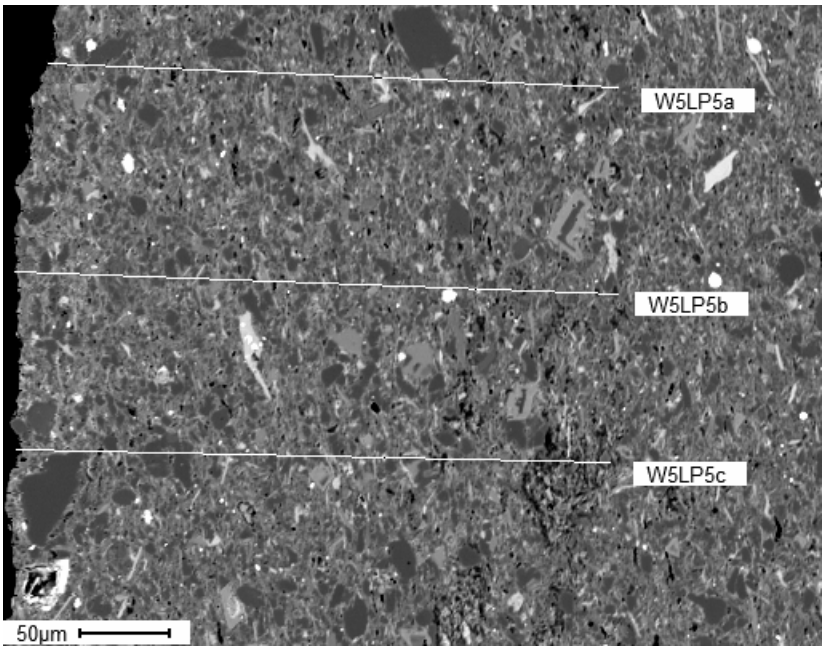


Figure D-10: Plots showing (a) SEM/EDS profiles for WINV#5 (removed from solution at 104 weeks): multiple profiles in from edge of sample perpendicular to bedding, and (b) SEM image showing locations of three of the profiles.

(a)

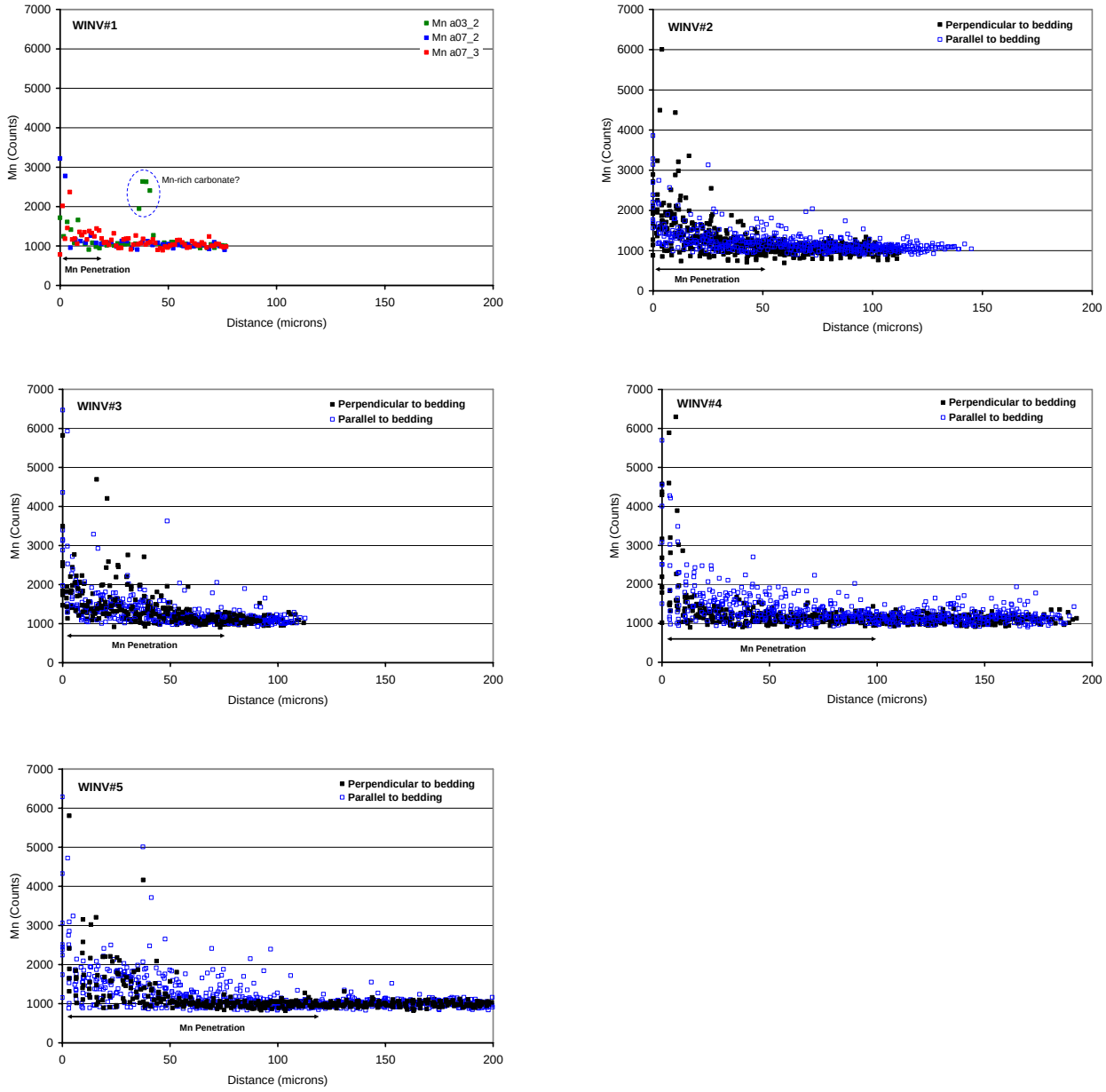


Figure D-11: Plots showing (a) SEM/EDS profiles for all five samples to illustrate the progression of $MnO_4$ invasion over time.

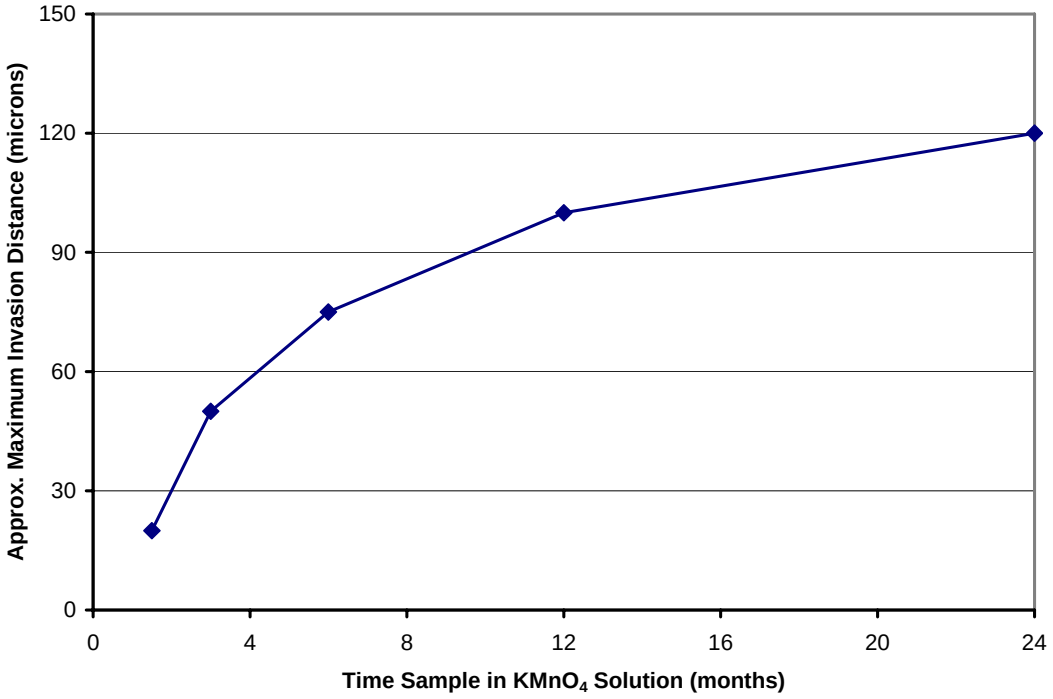


Figure D-12: Approximate maximum invasion distance versus time interpreted for the five samples suspended in 2 g/L $KMnO_4$ solution determined via SEM/EDS analysis of line profiles in from edges of the samples.

## Investigation of Reaction Mechanisms

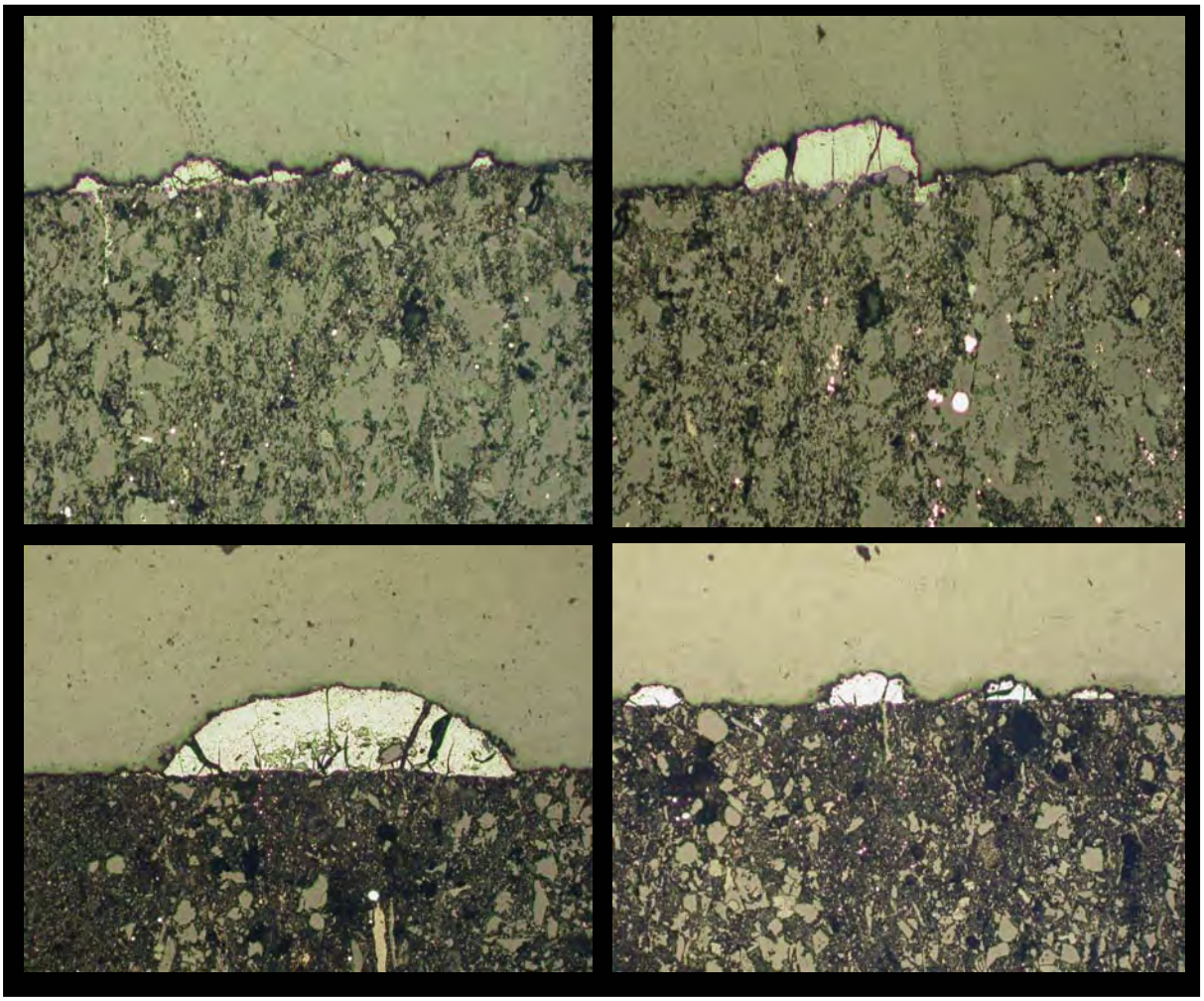

Figure D-13: SEM images of $MnO_2$ nodule formation on sample periphery (from Tom Al, UNB).

(a)

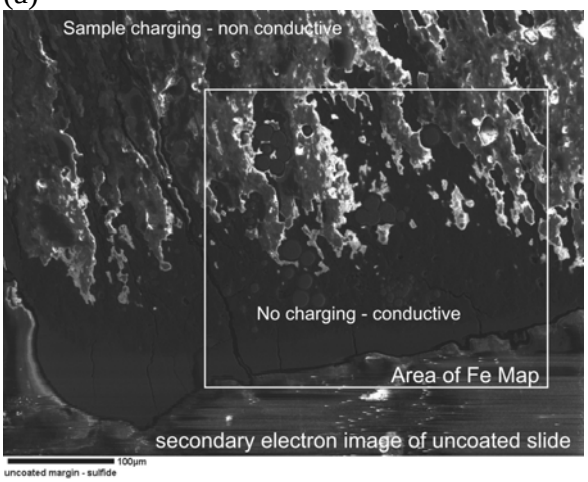


(b)

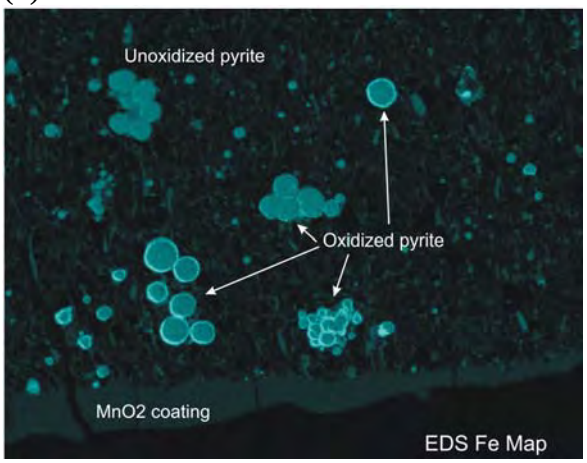


Figure D-14: SEM images obtained at periphery of sample WINV#5 (2 years in KMnO4 solution) to assess hypothesis that accumulation of MnO2 in the matrix leads to an increase in the electrical conductivity of the rock, allowing for solid-state electron transfer from sulfides in the matrix to MnVII in the bulk solution, which would explain accumulation of MnO2 "lumps" at the sample surface: (a) SEM secondary electron image on sample without conductive coating, and (b) SEM/EDS map of the Fe distribution. Generally, when a sample is prepared for SEM imaging, it must be coated up to a few nanometres thick with a conductive material such as carbon or gold to dissipate charge that develops from the large flux of electrons on the sample in the electron beam (if the sample is not coated the non-conductive charging spots will appear as extremely bright areas in the image). Rocks are mostly non conductive so thin sections are almost always coated before SEM analysis. However, assuming that MnO2 precipitation in the shale matrix would lead to an increase in conductivity this slide was imaged without the conductive coating. In (a) note the dark region around the margins of the slide (near the bottom of the image) and relatively bright region toward the top of the image away from the margins; the dark region is the area where charge from the beam is easily dissipated because the sample in those areas is conductive, the bright areas are regions that are charging. Thus dark areas represent the MnO4/MnO2 diffusion / precipitation front, which has been confirmed by Mn analyses. This 2D image provides a more satisfactory analysis of penetration compared to the analytical line profiles. Results suggest MnO4 consumption can occur much more rapidly with sulfide oxidation occurring via electron transfer through the solid (i.e. sulfides are oxidized within the matrix and electrons are transferred through the conductive MnO2 reaction products to reduce MnVII at the solution-sample interface) than if MnO4 were required to diffuse into the matrix and react with the sulfides through direct contact. In (b) the sulfides (bright spots in the Fe map) in the conductive region display weathered Fe-oxyhydroxide rims, while the sulfides in the unconductive regions of the slide are not visibly weathered, which further supports the hypothesis that the sulfide oxidation and permanganate reduction half reactions can be separated in space when there is an intervening zone of conductive MnO2 (from Tom Al, UNB).

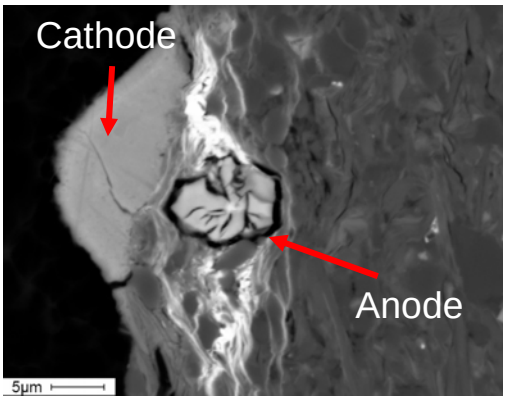


Anode Reaction:

$FeS_2 \rightarrow FeO(OH) + 2SO4^{2-} + 19\ H^+ + 15e^-$

Cathode Reaction:

$15e^- + 5MnO_4^- \rightarrow 5MnO_2$

Figure D-15: SEM Image of $MnO_2$ nodule formation on periphery of sample coupled with pyrite mineral oxidation (from Tom Al, UNB).

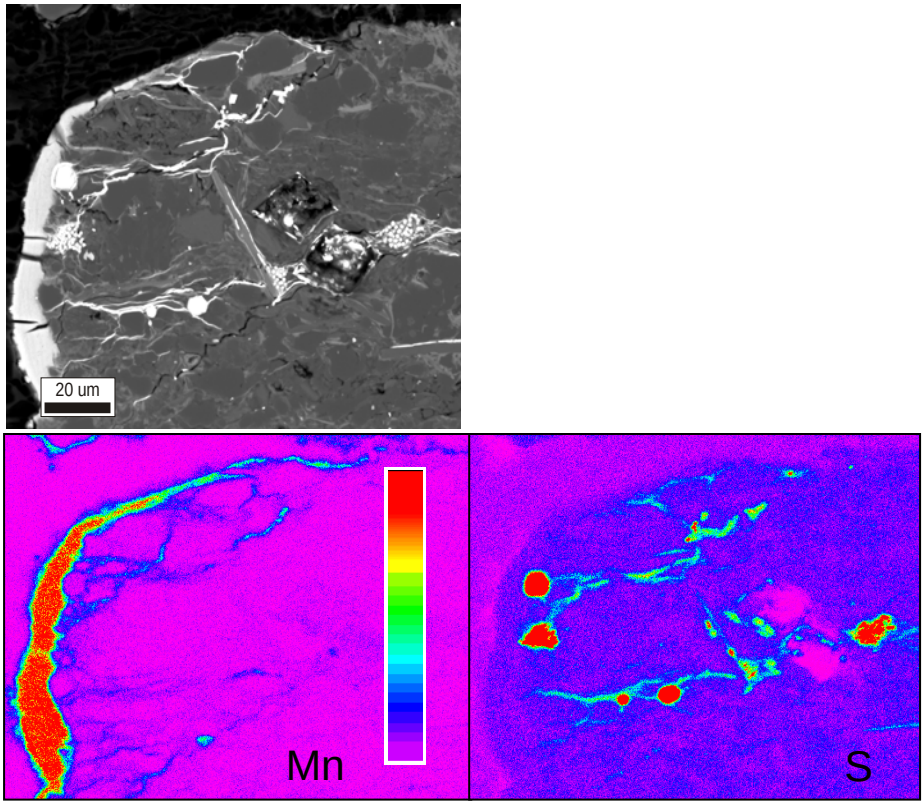


Early Time:

- $MnO_4$ diffusion along grain boundaries
- reaction occurs where $MnO_4$ contacts $f_{oc}$, Fe- silicates/carbonates/sulfides
- reactions lead to formation of a conductive $MnO_2$ network

Later Time:

- $MnO_2$ network provides electrical connection between "hidden" sulfide grains and $MnO_4$ in bulk solution

Figure D-16: SEM images: (a) backscattered SEM image at sample periphery, and elemental (b) Mn and (c) S maps obtained via SEM/EDS (from Tom Al, UNB).

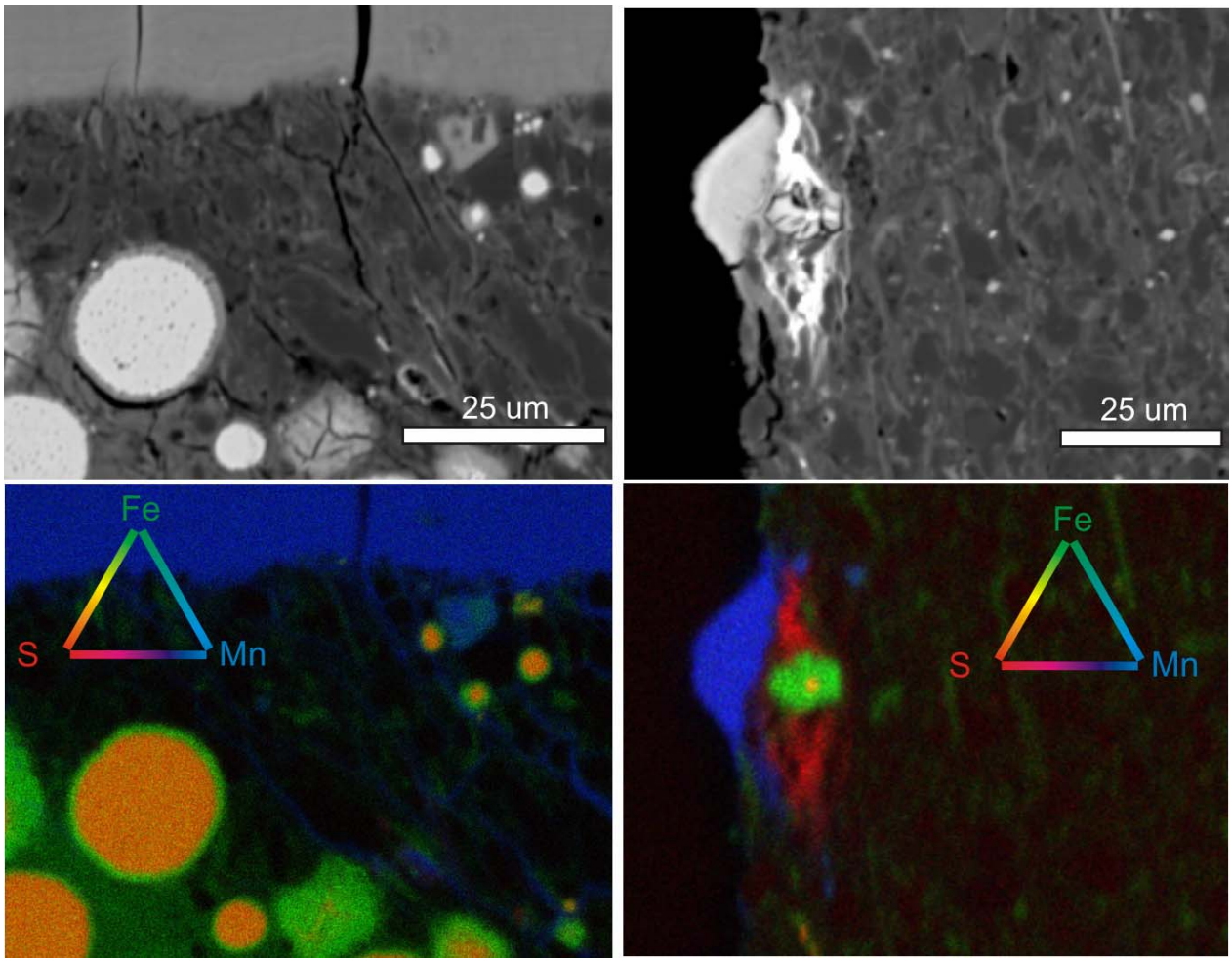


Figure D-17: SEM images showing Mn-precipitation and sulfide mineral oxidation near the sample periphery of WINV#5 (from Tom Al, UNB).

**Appendix E**

Williams and Paillet, USGS Open-File Report 01-385, 2002

USGS
science for a changing world

# Characterization of Fractures and Flow Zones in a Contaminated Shale at the Watervliet Arsenal, Albany County, New York

Open-File Report 01-385

U.S. Department of the Interior
U.S. Geological Survey

**This page has been left blank intentionally.**

# Characterization of Fractures and Flow Zones in a Contaminated Shale at the Watervliet Arsenal, Albany County, New York

By John H. Williams and Frederick L. Paillet

U. S. GEOLOGICAL SURVEY
Open-File Report 01-385


Troy, New York
2002

U.S. DEPARTMENT OF THE INTERIOR
GAIL A. NORTON, Secretary

U.S. GEOLOGICAL SURVEY
Gordon P. Eaton, Director



---

For additional information write to:

District Chief
U.S. Geological Survey
425 Jordan Road
Troy, NY 12180

Copies of this report can be purchased from:

U.S. Geological Survey
Branch of Information Services
Box 25286
Denver, CO 80225-0046

# CONTENTS



## FIGURES

## TABLES



## CONVERSION FACTORS, ABBREVIATIONS, AND VERTICAL DATUM

| Multiply | By | To obtain |
|---|---|---|
| | *Length* | |
| inch (in) | 25.4 | millimeter |
| foot (ft) | 0.3048 | meter |
| | *Flow Rate* | |
| gallons per minute (gal/min) | 0.06309 | liters per second |
| | *Temperature* | |
| degrees Fahrenheit | 5/9 x ($^{o}$ F— 32) | degrees Celsius |
| | *Transmissivity** | |
| foot squared per day | 0.09290 | meter squared per day |

**Sea level:** In this report sea level refers to the National Geodetic Vertical Datum of 1929 (NGVD of 1929) a geodetic datum derived from a general adjustment of the first-order level nets of both the United States and Canada, formerly called Sea Level Datum of 1929.

***Transmissivity:** The standard unit for transmissivity (*T*) is cubic foot per day per square foot times foot of aquifer thickness $[(ft^3/d)/ft^2]ft$ . In this report, the mathematically reduced form, foot squared per day ($ft^2/d$) , is used for convenience.

# Characterization of Fractures and Flow Zones in a Contaminated Shale at the Watervliet Arsenal, Albany County, New York

*By* John H. Williams and Frederick L. Paillet

## ABSTRACT

Flow zones in a fractured shale in and near a plume of volatile organic compounds at the Watervliet Arsenal in Albany County, N. Y. were characterized through the integrated analysis of geophysical logs and single- and cross-hole flow tests. Information on the fracture-flow network at the site was needed to design an effective ground-water monitoring system, estimate offsite contaminant migration, and evaluate potential containment and remedial actions.

Four newly drilled coreholes and four older monitoring wells were logged and tested to define the distribution and orientation of fractures that intersected a combined total of 500 feet of open hole. Analysis of borehole-wall image logs obtained with acoustic and optical televiewers indicated 79 subhorizontal to steeply dipping fractures with a wide range of dip directions. Analysis of fluid resistivity, temperature, and heat-pulse and electromagnetic flowmeter logs obtained under ambient and short-term stressed conditions identified 14 flow zones, which consist of one to several fractures and whose estimated transmissivity values range from 0.1 to more than 250 feet squared per day.

Cross-hole flow tests, which were used to characterize the hydraulic connection between fracture-flow zones intersected by the boreholes, entailed (1) injection into or extraction from boreholes that penetrated a single fracture-flow zone or whose zones were isolated by an inflatable packer, and (2) measurement of the transient response of water levels and flow in surrounding boreholes. Results indicate a well-connected fracture network with an estimated transmissivity of 80 to 250 feet squared per day that extends for at least 200 feet across the site. This interconnected fracture-flow network greatly affects the hydrology of the site and has important implications for contaminant monitoring and remedial actions.

## INTRODUCTION

Historical use of solvents within the main manufacturing area at the Watervliet Arsenal in Albany County, N. Y. (fig. 1) has resulted in the movement of dense non-aqueous fluids into the underlying bedrock and contamination of ground water with volatile organic compounds. The U. S. Geological Survey, in cooperation with the U. S. Army Corps of Engineers, conducted a study from September 2000 to May 2001 to characterize bedrock fracture-flow zones at the site as a basis for the design of an effective ground-water monitoring system, estimation of contaminant migration offsite, and evaluation of potential containment and remedial actions.

The site is underlain by the Normanskill Formation, a dark-gray shale of Ordovician age. The shale is overlain by 10 to 15 feet of artificial fill, alluvium, and glacial drift. The general direction of ground-water flow is southeastward toward the Hudson River, a regional discharge area.

Advanced borehole geophysical methods were used in the fracture and flow-zone characterization; these included borehole-wall imaging and single- and cross-hole flowmeter analysis. Four newly drilled coreholes and four older monitoring wells in and near


**Figure 1.** Location of study area at the Watervliet Arsenal, Albany County, N.Y.

the contamination plume were logged, and four cross-hole flow tests were conducted. This report summarizes the results of the geophysical logging and cross-hole testing and describes the fractures and flow zones at the site.

## FRACTURE CHARACTERIZATION

The distribution and orientation of fractures intersected by the four monitoring wells (34, 51, 58, and 59) and four coreholes (65, 68, 71, and 72) (fig. 2 and table 1) were interpreted through the analysis of borehole-wall image logs. Acoustic-televiewer logs were obtained in the open intervals of the wells and coreholes. Optical-televiewer logs were collected in monitoring well 34, the upper part of corehole 65, and corehole 68. Methods of analysis of borehole-wall image logs for fracture characterization is described by Williams and Johnson (2000). Examples of acoustic- and optical- televiewer logs and fracture analysis for a selected interval in monitoring well 34 are presented in figure 3.

The distribution and orientation of the fractures and bedding features intersected by the monitoring wells and coreholes are depicted in figure 4. The analysis identified 79 fractures within the total 500 ft of open hole logged in the eight wells and coreholes. The fractures are subhorizontal to steeply dipping and have a wide range of dip directions. Many fractures dip to the east at 50 to 60 degrees parallel to bedding.

## FLOW-ZONE CHARACTERIZATION

The distribution of flow zones intersected by the monitoring wells and coreholes was delineated through an integrated analysis of the borehole-wall image, fluid, and flowmeter logs. Flowmeter logs and fluid resistivity and temperature logs were collected under ambient and short-term stressed conditions. The flowmeter method for identifying flow zones in fractured bedrock is described by Paillet and others (1987). Vertical flow in the monitoring wells was measured under ambient and stressed conditions at selected depth stations with a heat-pulse flowmeter, whose lower detection limit is about 0.005 gallons per minute (gal/min). Vertical flow in the coreholes under ambient and stressed conditions were collected with an electromagnetic flowmeter, whose lower detection limit is about an order of magnitude higher than that of the heat-pulse flowmeter. The electromagnetic flowmeter was used in stationary and trolling (logging) modes. Stationary heat-pulse flowmeter measurements also were made under ambient conditions in coreholes 65, 68, and 71. The short-term flowmeter stress tests entailed the injection of 3 to 5 gal/min into the wells and coreholes except at corehole 72, which was pumped at 2 gal/min. Specific capacities of the wells and coreholes, as calculated from these tests, are presented in table 1.

The flowmeter method detects only flow zones whose transmissivity is within 1.5 to 2 orders of magnitude of the most transmissive zone in the borehole (Paillet, 1998). An example of this type of analysis showing the ambient and stressed fluid

**Table 1**. Record of logged monitoring wells and coreholes at the Watervliet Arsenal, Albany County, N.Y., 2000-01

[Locations are shown in fig. 2. (Gal/min)/ft, gallons per minute per foot.]

| Site number | USGS county number | Land-surface elevation, in feet | Hole depth, in feet | Casing depth, in feet | Date logged | Depth to water, in feet | Specific capacity, in (gal/min)/ft |
|---|---|---|---|---|---|---|---|
| **Monitoring well** | | | | | | | |
| 34 | A 656 | 18.56 | 31.5 | 16.5 | 9/14/00 | 9.55 | 1.2 |
| 51 | A 657 | 18.71 | 71 | 52.5 | 9/14/00 | 10.00 | none detected |
| 58 | A 654 | 20.54 | 82 | 64 | 9/14/00 | 10.74 | 0.002 |
| 59 | A 659 | 20.17 | 96 | 75 | 9/14/00 | 10.92 | 1.0 |
| **Corehole** | | | | | | | |
| 65 | A 655 | 18.69 | 165 | 21 | 12/1/00 | 9.24 | 1.3 |
| 68 | A 652 | 21.41 | 75 | 17.5 | 12/22/00 | 7.85 | 0.72 |
| 71 | A 658 | 20.69 | 105 | 21 | 12/14/00 | 9.60 | 1.1 |
| 72 | A 660 | 17.23 | 125 | 22 | 4/24/01 | 11.01 | 0.32 |

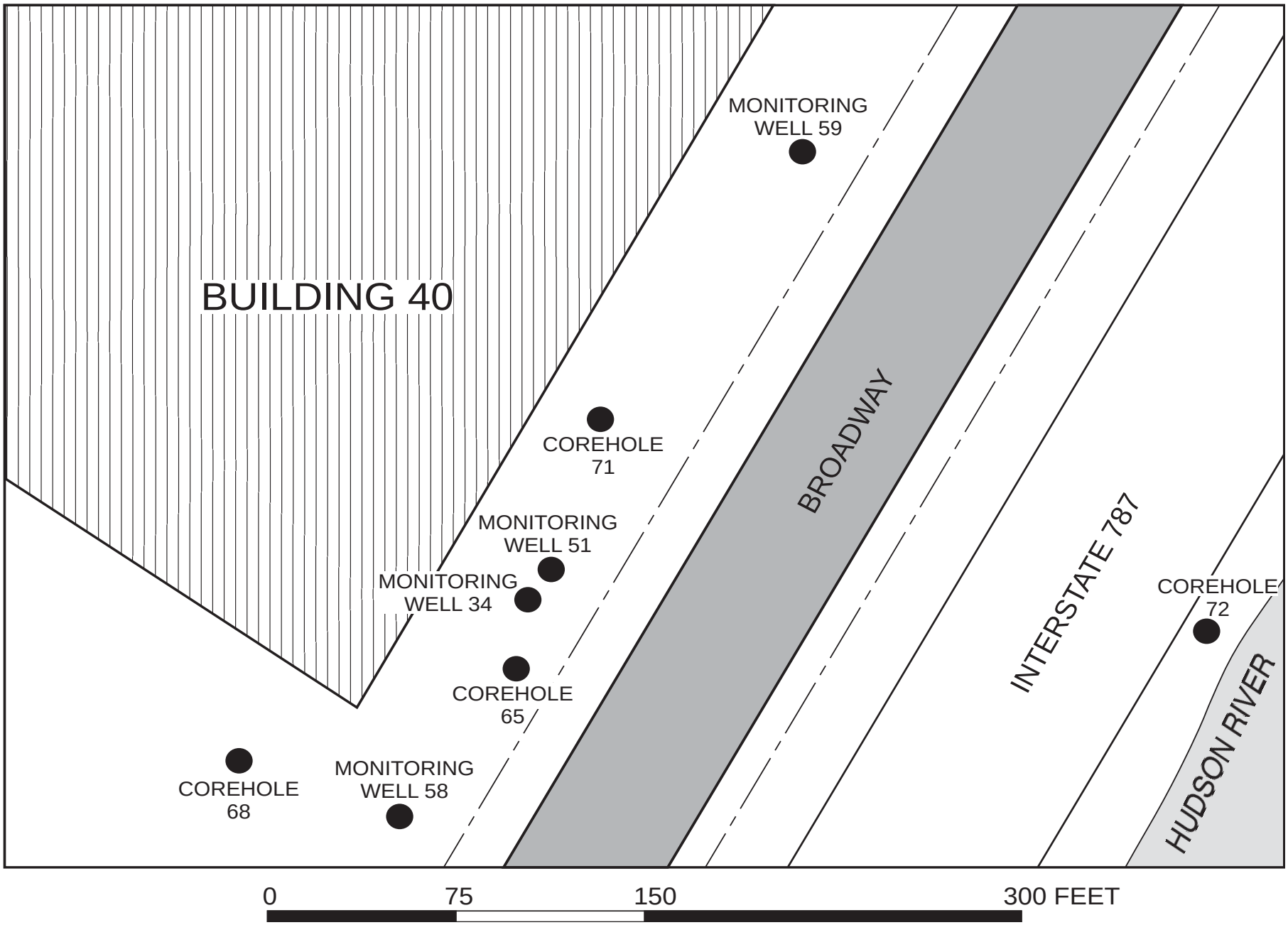


**Figure 2**.
Locations of logged and tested monitoring wells and coreholes. (Study area location is shown in fig. 1.)

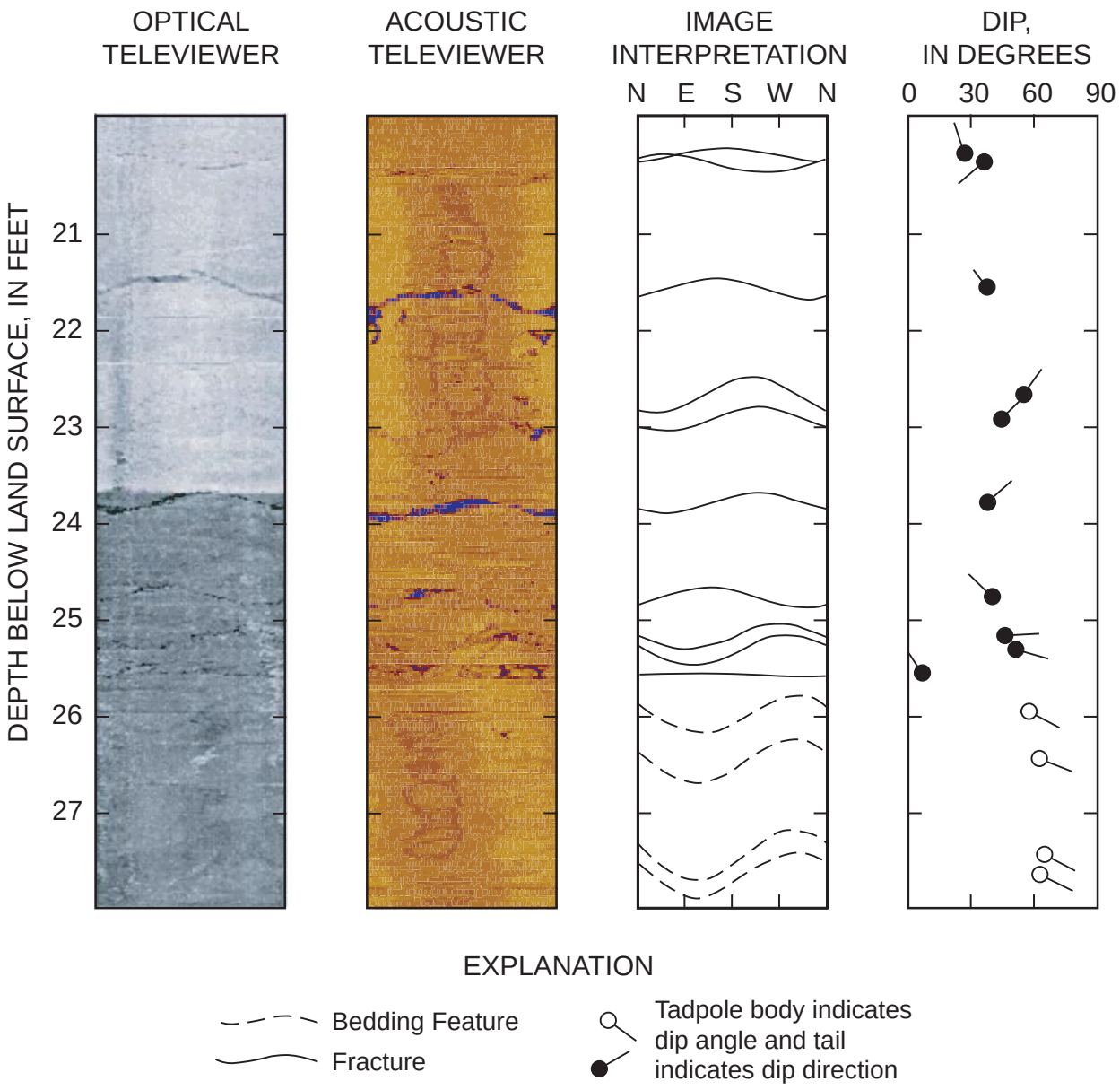


**Figure 3.** Acoustic- and optical-televiewer images from monitoring well 34 and analysis for the distribution and orientation of fractures and bedding. (Location is shown in fig. 2.)

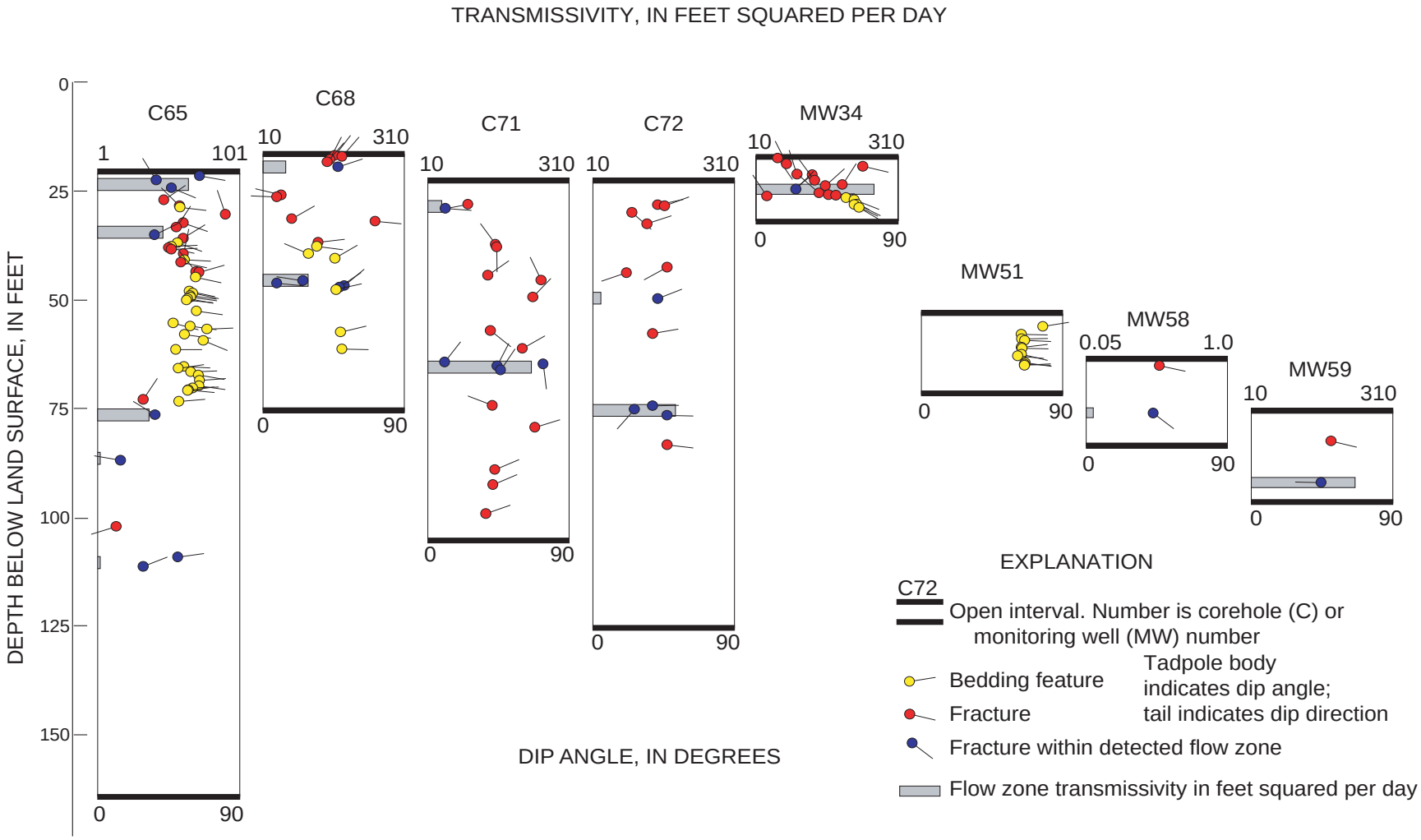


**Figure 4**. Distribution and orientation of fractures and bedding and detected flow zones intersected by the monitoring wells and coreholes. (Locations are shown in fig. 2.)

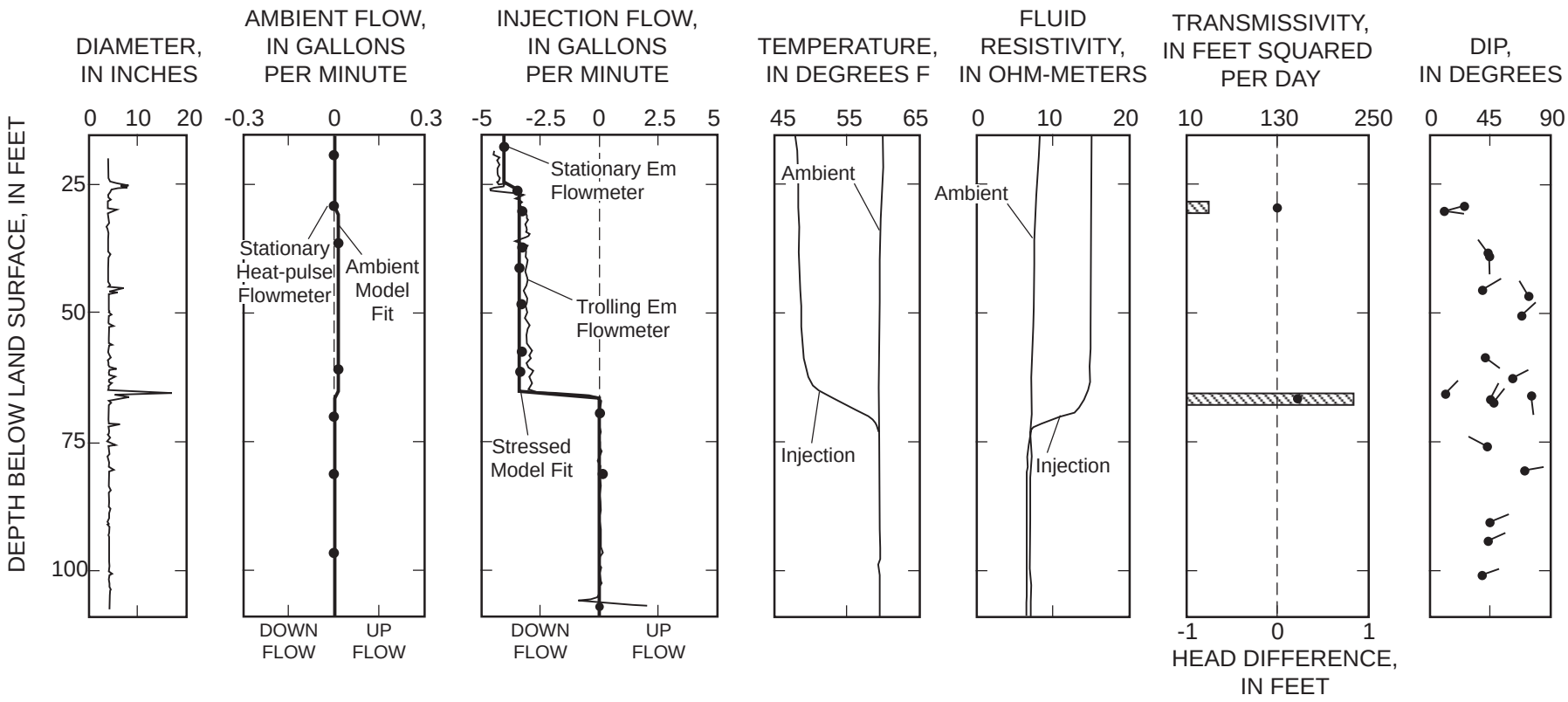


**Figure 5**. Wellbore diameter, fluid resistivity, temperature, and measured and simulated flow under ambient and injection conditions, transmissivity and hydraulic-head differences of flow zones, and fracture orientation for corehole 71. (Location is shown in fig. 2.)

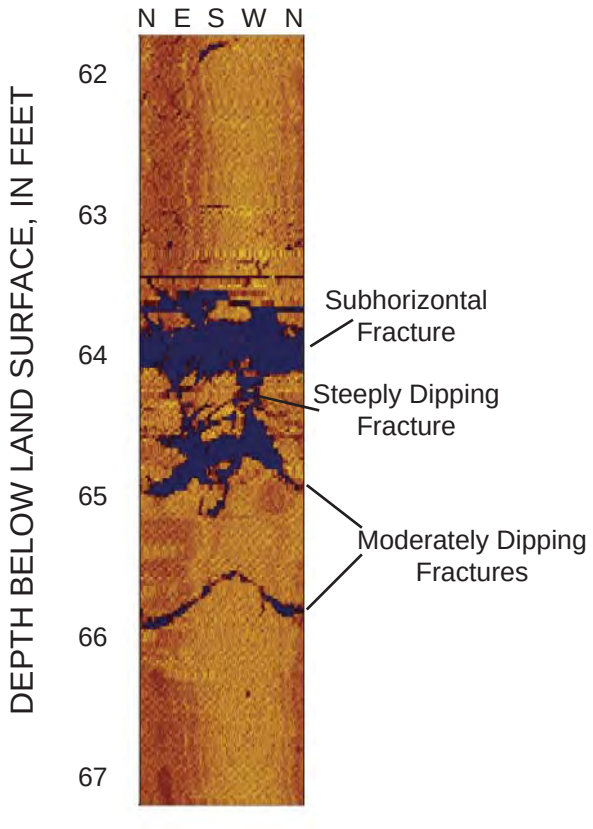


**Figure 6.** Acoustic-televiewer image of fractures in the flow zone at 65 feet at corehole 71. (Location is shown in fig. 2.)

resistivity, temperature, and flowmeter logs, and a delineation of flow zones in corehole 71 is presented in figure 5. The acoustic-televiewer image of the fractures within the flow zone at 65 ft in corehole 71 is presented in figure 6. The 65-ft flow zone consists of a large subhorizontal fracture, two moderately dipping fractures, and a steeply dipping fracture.

The distribution of detected flow zones intersected by the monitoring wells and coreholes is presented in figure 4 and table 2. Fourteen flow zones consisting of one to several fractures were detected in the total 500 ft of open hole logged in the eight wells and coreholes. Single-flow zones were detected in monitoring wells 34, 58, and 59; two flow zones were detected in each of coreholes 68, 71, and 72; five flow zones were detected in corehole 65; and no flow zones were detected in monitoring well 51.

A three-dimensional representation of the transmissive fractures intersected by the wells and coreholes is shown in figure 7. The representation is based on a simple radial projection of the fractures within the detected flow zones. The fractures are projected a radial distance of 50 ft according to their orientation measured at the borehole wall. Multiple fractures that have similar orientations within the same flow zone are displayed as a single combined feature.

## TRANSMISIVITY AND HYDRAULIC HEAD

The transmissivity and hydraulic head of the flow zones intersected by the monitoring wells and coreholes were estimated by flowmeter model analysis as described by Paillet (2000). In this method, measured ambient and stressed flows are matched to simulated flows by trial-and-error adjustment of flow-zone transmissivity and head. An example of the results from this type of analysis, depicting measured and simulated flow and estimated transmissivity and hydraulic-head differences of flow zones intersected by corehole 71, is shown in figure 5.

Estimated transmissivity ($T$) values for the fracture-flow zones range from 0.1 to 260 feet squared per day ($ft^2/d$) (fig. 4 and table 2); the highest of these estimates, 230 to 260 $ft^2/d$, are for zones penetrated by monitoring wells 34 and 59 and corehole 71. Lower values were estimated for coreholes 65, 68, and 72, these range from 3 to 110 $ft^2/d$. The $T$ value of the flow zone penetrated by monitoring well 58 is an order of magnitude lower than all other estimates.

Upward ambient flow from lower to upper fracture zones was measured in coreholes 65, 68, and 71. The smaller estimated hydraulic-head differences as estimated by the flowmeter analysis between zones in coreholes 65 and 71 than between zones in corehole 68 suggest a greater vertical connection between fractures near coreholes 65 and 71 than near corehole 68 (table 2).

Ambient hydraulic head in fractures intersected by monitoring wells 34 and 59 and coreholes 65 and 71 were similar (8.94 to 9.16 ft); the highest among these heads were in the fracture at monitoring well 59, the lower fractures at corehole 71, and the lower fractures at corehole 65. The head in the fracture at monitoring well 58 was about 0.5 ft higher than these heads. The heads in the fractures intersected by corehole 68 are about 3 ft higher than in most of the other fractures. The heads in fractures at corehole 72, nearest to the river, were about 2.5 ft lower than at most of the other boreholes.

**Table 2.** Estimated hydraulic properties of fracture-flow zones detected in the monitoring wells and coreholes at the Watervliet Arsenal, Albany County, N.Y., 2000-01.

[Locations are shown in fig. 2. Dashes indicate not determined. Multiple entries for zone depth indicate that the zones were grouped together for the cross-hole flow test.]

| Well or corehole no. | Zone depth, in feet | Zone head elevation, in feet | Transmissivity, in feet squared per day | | Storage | Hydraulic connection | |
|---|---|---|---|---|---|---|---|
| | | | Single-borehole | Cross-hole | | Well or corehole no. | Zone depth, in feet |
| 34 | 25 | 8.98 | 260 | 150 | $5 \times 10^{-5}$ | 71 | 65 |
| 34 | 25 | 8.98 | 260 | 100 | $5 \times 10^{-5}$ | 65 | 24 and 35 |
| 51 | - | 8.97 | - | - | - | - | - |
| 58 | 76 | 9.6 | 0.1 | - | - | - | - |
| 59 | 92 | 9.16 | 230 | 230 | $5 \times 10^{-5}$ | 71 | 65 |
| 59 | 92 | 9.16 | 230 | 250 | $1 \times 10^{-5}$ | 65 | 24 and 35 |
| 65 | 24<br>35 | 8.94 | 65<br>47 | 100 | $5 \times 10^{-5}$ | 34 | 25 |
| 65 | 24<br>35 | 8.94 | 65<br>47 | 100 | $1 \times 10^{-5}$ | 59 | 92 |
| 65 | 24<br>35 | 8.94 | 65<br>47 | 100 | 1 x 10-5 | 71 | 65 |
| 65 | 78<br>88<br>110 | 9.10 | 37<br>3<br>3 | 80 | $1 \times 10^{-4}$ | 71 | 65 |
| 68 | 19 | 12.04 | 58 | - | - | - | - |
| 68 | 45 | 12.79 | 110 | - | - | - | - |
| 71 | 28 | 8.92 | 40 | - | - | - | - |
| 71 | 65 | 9.02 | 230 | 230 | $5 \times 10^{-6}$ | 59 | 92 |
| 71 | 65 | 9.02 | 230 | 150 | $5 \times 10^{-6}$ | 34 | 25 |
| 71 | 65 | 9.02 | 230 | 100 | $1 \times 10^{-5}$ | 65 | 24 and 35 |
| 71 | 65 | 9.02 | 230 | 80 | $1 \times 10^{-4}$ | 65 | 78, 88, and 110 |
| 72 | 49 | 6.5 | 7 | - | - | - | - |
| 72 | 75 | 6.5 | 59 | - | - | - | - |

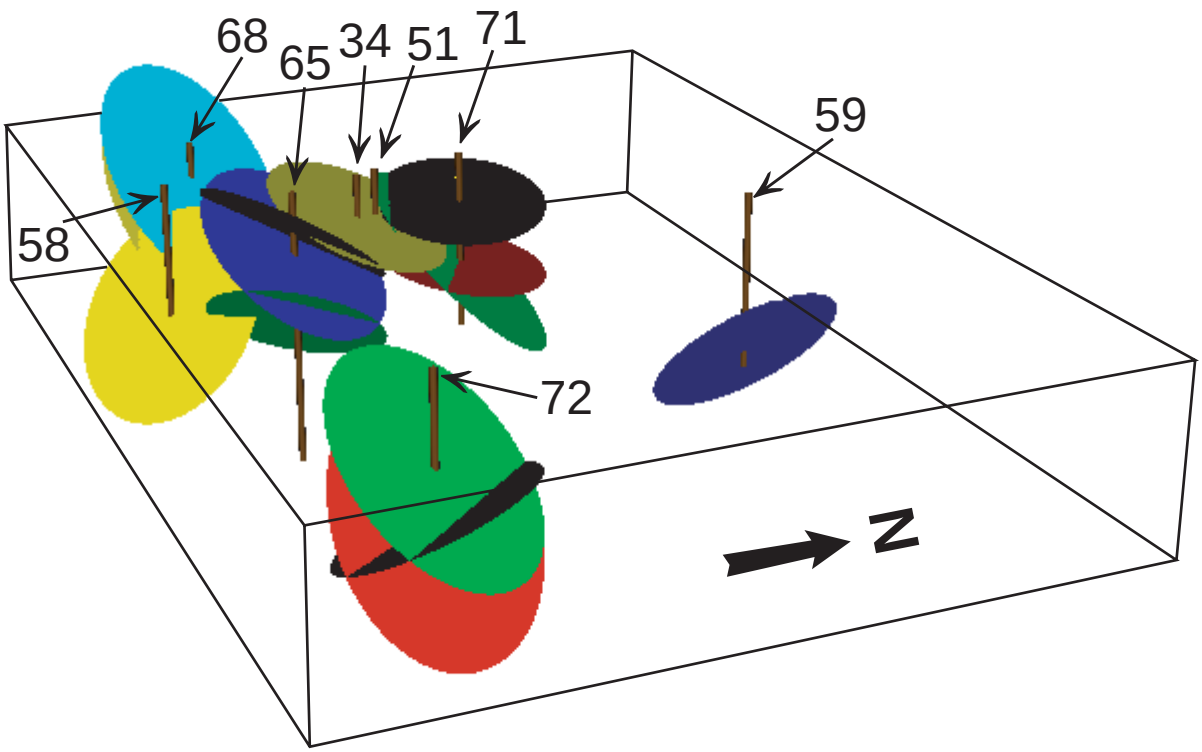


**Figure 7.** Three-dimensional representation of fracture-flow zones intersected by the monitoring wells and coreholes. (Locations are shown in fig. 2.)

## HYDRAULIC CONNECTION

The hydraulic connection between flow zones intersected by the monitoring wells and coreholes was characterized through an analysis of cross-hole flow tests as described by Paillet (1998). When a borehole that intersects one or more permeable fractures is stressed, the water-level effect extends outward along the fracture network. The generally differing water-level response among individual fractures induces a time-varying flow in an adjacent observation borehole between depths where fractures intersect that borehole. The water-level response also will cause water to flow from or into storage in the observation wellbore. Thus, if flow is measured at a depth station between or above the depth where such fractures intersect the observation borehole, the transient response to the stress can be recorded. This transient flow can be compared to model type curves representative of various fracture connection configurations that may be present between the boreholes. Once a specific type curve is recognized, the model's $T$ and storage coefficient ($S$) values can be adjusted until the simulation matches the measured response.

Although cross-hole flow tests provide a method to characterize the connections between fractures near pairs of boreholes, a given set of transient-flow data cannot be uniquely interpreted; that is, several different hydraulic connections might result in similar transient responses to a stress. The analysis can be simplified by stressing a borehole that intersects a single, permeable fracture zone to ensure that the water-level response produced by the stress is known to affect that zone only. If the stress induces flow in the observation borehole, that borehole's fracture zone that is most directly connected to the stressed borehole will be the outflow or inflow zone. The flow from or into this zone will vary over time, depending on the connections with other fractures and by movement of water from or into wellbore storage. The transient-flow type curve for the simplest configuration—where the stressed and observation boreholes are connected by a single fracture and flow in the observation borehole is from wellbore storage—is shown in figure 8.

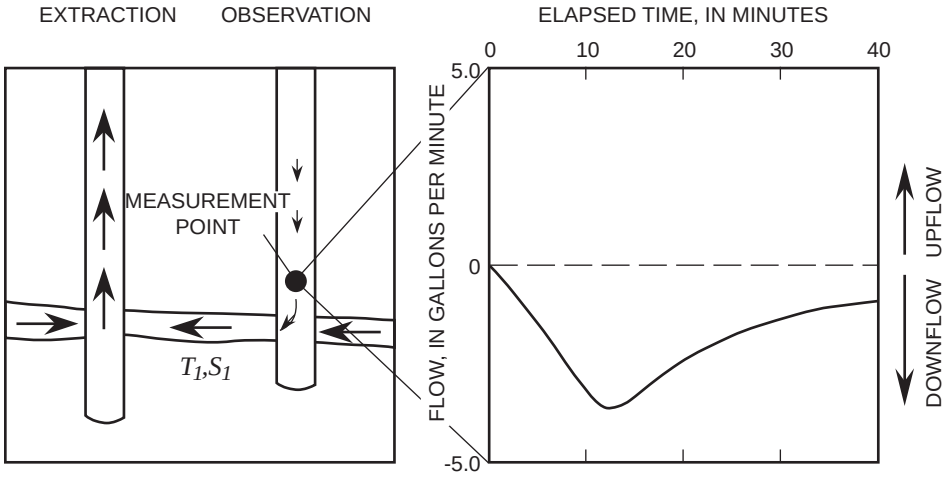


**Figure 8.** Cross-hole flow test of a single-fracture connection showing direction and relative amount of flow between extraction and observation boreholes and type curve for transient response where flow in the observation borehole is only from wellbore storage.

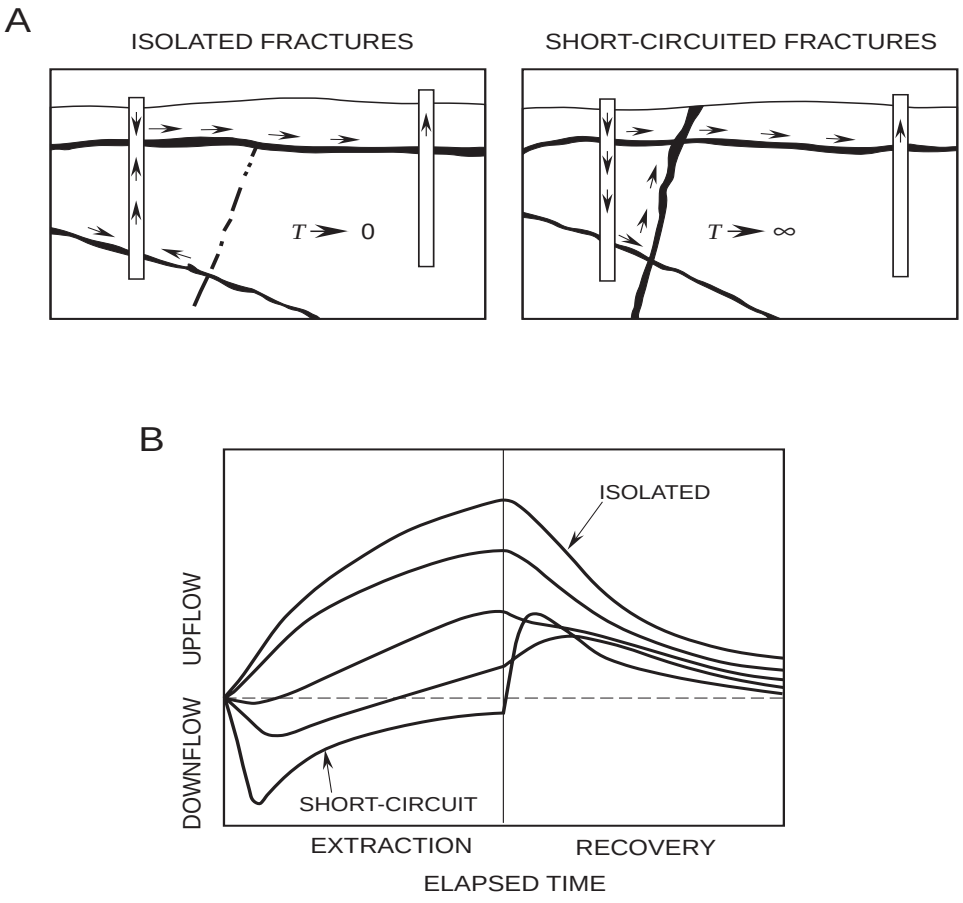


**Figure 9.** Cross-hole flow tests of fracture connections between extraction and observation boreholes: A. Isolated configuration where the transmissivity of the fracture connection approaches zero; and short-circuited configuration where the transmissivity of the fracture connection approaches infinity. B. Type-curve response corresponding to these two extremes, and to three intermediate connections.

The transient flow that develops in an observation borehole with two fracture zones in response to extraction is illustrated in figure 9. Flow between the fracture zones varies between two extreme configurations (fig. 9A). One extreme represents no hydraulic connection between the two fracture zones, other than the observation borehole. Here, the applied stress induces upflow from the lower zone into the upper zone, and this upflow increases continuously with time. When the stress ends, the upflow simply decays away (fig. 9B). At the other extreme, fractures in the area between boreholes provide a short circuit between the upper and lower zones. Here, the stress induces a transient downflow that fades away with time. The recovery induces a similar upflow response. In general, where the fracture connection has some finite *T* value, the flow response will lie somewhere between the two extremes.

The relative *T* value of the fracture zones in an observation borehole affects the transient flow response. The injection and recovery response for the short-circuited and isolated configurations where the fracture zones have equal *T* values, and where they differ by an order of magnitude is depicted in figure 10.

As presented earlier, single-hole flowmeter tests can provide estimated *T* values for fracture zones. Those *T* values can be used to determine the *S* values that give the best model fit to the cross-hole flow data. In general, the magnitude of the fracture-zone's *T* value determines how quickly the transient flow increases in response to the stress (fig. 11A). Commonly, the response time in the transient flow will simply confirm the *T* estimates given by the single-hole tests, although differences can occur because the cross-borehole test data apply to the area between boreholes, rather than to the immediate vicinity of one of the boreholes in the pair. The fracture-zone's *S* value determines the relative magnitude of the flow response (fig. 11B). The previously established *T* estimates and the type curve that most closely resembles the shape of the transient-flow response can be used be used to adjust the *S* values such that the simulated flow matches the measured flow.

Four cross-hole flow tests were completed at the Watervliet site. The stress for two of the cross-hole flow tests was applied by injection into boreholes believed to be on the periphery of the most contaminated area to minimize the amount of contaminated water to be disposed of and the spread of contaminants. Monitoring wells 34 and 59 were used for injection because they both intersected a single, zone; thus, the exact point at which the head change was applied to the fracture system was known. The injection rate in both tests was 4 gal/min. The other two tests were conducted by extraction from corehole 65. An inflatable packer set at 50 ft was used to isolate the upper and lower fracture groups in corehole 65 during these two tests. In the first of these tests, 1 gal/min was pumped from below the packer and in the second, 3 gal/min was pumped from above the packer. The extraction rate was increased from 3 to 6 gal/min during the latter part of the second test.

During the cross-hole tests, fluid logs, flow-meter profiles, and transient flowmeter measurements at selected depth(s) were made in the two coreholes that penetrate multiple flow zones and whose water levels were significantly affected by the stress. These were corehole 65 during injection into monitoring wells 34 and 59, and corehole 71 during injection into monitoring wells 34 and 59 and extraction from the lower and upper fracture zones in corehole 65. Flow was measured at a depth of 50 ft in corehole 71 in between the fractures at 28 and 65 ft. Corehole 65 was divided into an upper fracture group (fractures at 24 and 35 ft) and lower group (fractures at 78, 88, and 110 ft), and flow was measured at a depth of 60 ft in between. The transient-flow responses associated with single, isolated, and short-circuited fracture configurations, as shown in figures 8, 9, and 10, serve as the basic type curves to which the results of the Watervliet cross-hole tests were fit through adjustment of the *T* and *S* values.

### Injection into Monitoring Well 34

Injection at a rate of 4 gal/min into monitoring well 34 produced the following water-level increase in the monitoring wells and coreholes: 34 (5.14 ft), 59 (1.12 ft), 65 (2.51 ft), and 71 (1.24 ft) (fig. 12 and table 3). More than 80 percent of the measured water-level changes occurred within 15 minutes of the start of injection, and the changes paralleled each other and were less than 0.01 ft/min within 30 minutes. These water-level changes indicate a strong hydraulic connection between the boreholes. The close similarity of the water-level changes in corehole 71 to those in monitoring well 59, despite the much greater distance of the latter from the injection point, suggests an extremely direct connection between the two.

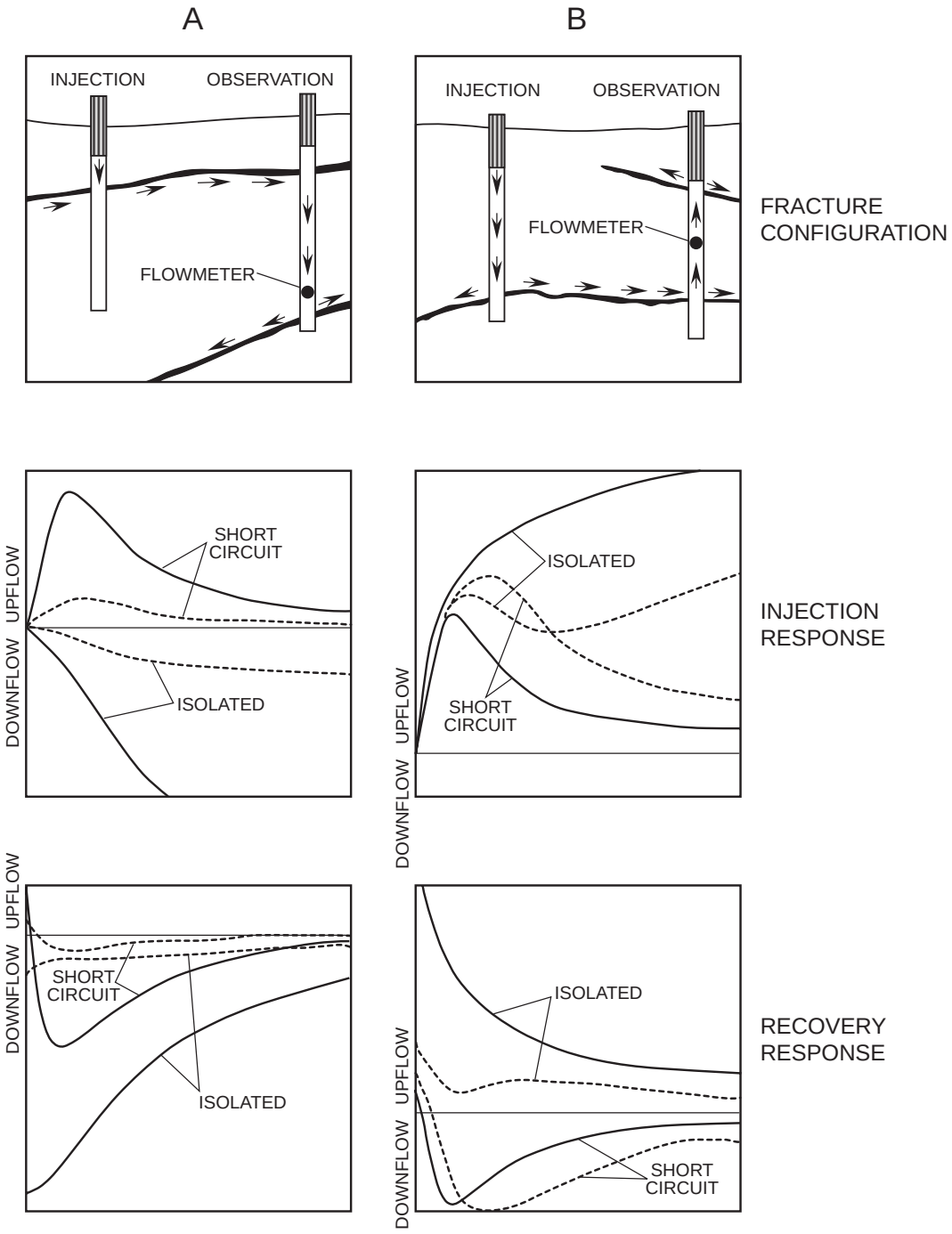


## EXPLANATION

Short-circuited and isolated examples with primary and secondary fracture $T$ values of 100 $ft^2/d$ are shown as a solid line. Short-circuited and isolated examples with primary and secondary fracture $T$ values of 100 $ft^2/d$ and 10 $ft^2/d$, respectively, are shown as a dashed line. Fracture $S$ values equal $1x10^{-5}$, borehole separation is 100 ft, and the injection rate is 10 gal/min for all examples.

**Figure 10.** Cross-hole flow tests of fracture connections between injection and observation boreholes and corresponding transient type-curve response for: A. A shallow fracture connection inducing flow to a deep fracture in the observation borehole. B. A deep fracture connection inducing flow to a shallow fracture in the observation borehole.

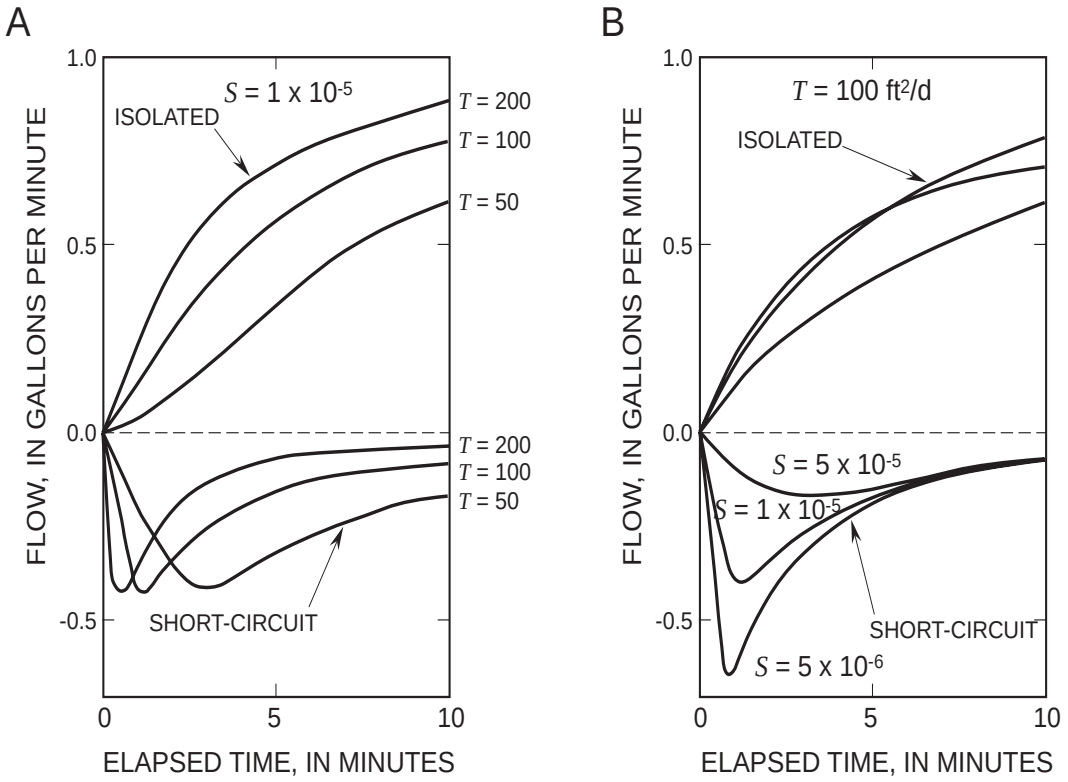


**Figure 11.** Example of the effects of variations in (A) fracture transmissivity, and (B) fracture storage coefficients on the shape and magnitude of cross-hole flow type curves for the fracture connections depicted in figure 9A.

Water-level changes in monitoring well 51 and corehole 68 were less than 0.05 ft.

Injection into monitoring well 34 more than tripled the rate of upflow from the 65-ft fracture zone to the 28-ft zone in corehole 71 in relation to ambient conditions. Model analysis of the cross-flow data indicates that the single fracture-flow zone at monitoring well 34 is directly connected to the 65-ft zone in corehole 71 (fig. 13A). A $T$ value of 150 $ft^2/d$ and $S$ value of 1 $x10^{-5}$ for the hydraulic connection between the boreholes provides a good fit between the measured and simulated flow. This $T$ estimate is somewhat smaller than those obtained in the single borehole tests and may indicate a constriction in the fracture connection between the boreholes. The single-fracture and short-circuited fracture configurations produce nearly identical type curves because the lower fractures at corehole 71 are much more transmissive than the upper fractures and therefore, dominate the response.

Injection into monitoring well 34 caused flow in corehole 65 to reverse from upward to downward between the upper fracture group (24 and 35 ft) and the lower fracture group (78 ft and deeper) (fig. 14). The 20-second maximum firing frequency of the heat-pulse flowmeter, together with equipment malfunctions, prevented effective capture of the early response of the direct connection between the fracture in borehole 34 and the upper fracture group at corehole 65 (fig. 13B). A fracture connection with a $T$ value of 100 $ft^2/d$ and $S$ value of 5 x $10^{-6}$ is consistent with the available data and single-hole test in corehole 65 (fig. 4 and table 2). The flow data agree with a model in which the upper and lower fracture groups in corehole 65 are isolated from each other during the first three minutes after the start of injection. The failure of the measured flow to continue to increase after 3 minutes indicates that the head change caused by the injection had propagated to the lower fracture group. This suggests a connection between the upper and lower fractures groups in the area near corehole 65.

The measured recovery was faster than the model predictions, which indicates that the head in the lower group increases more slowly during injection

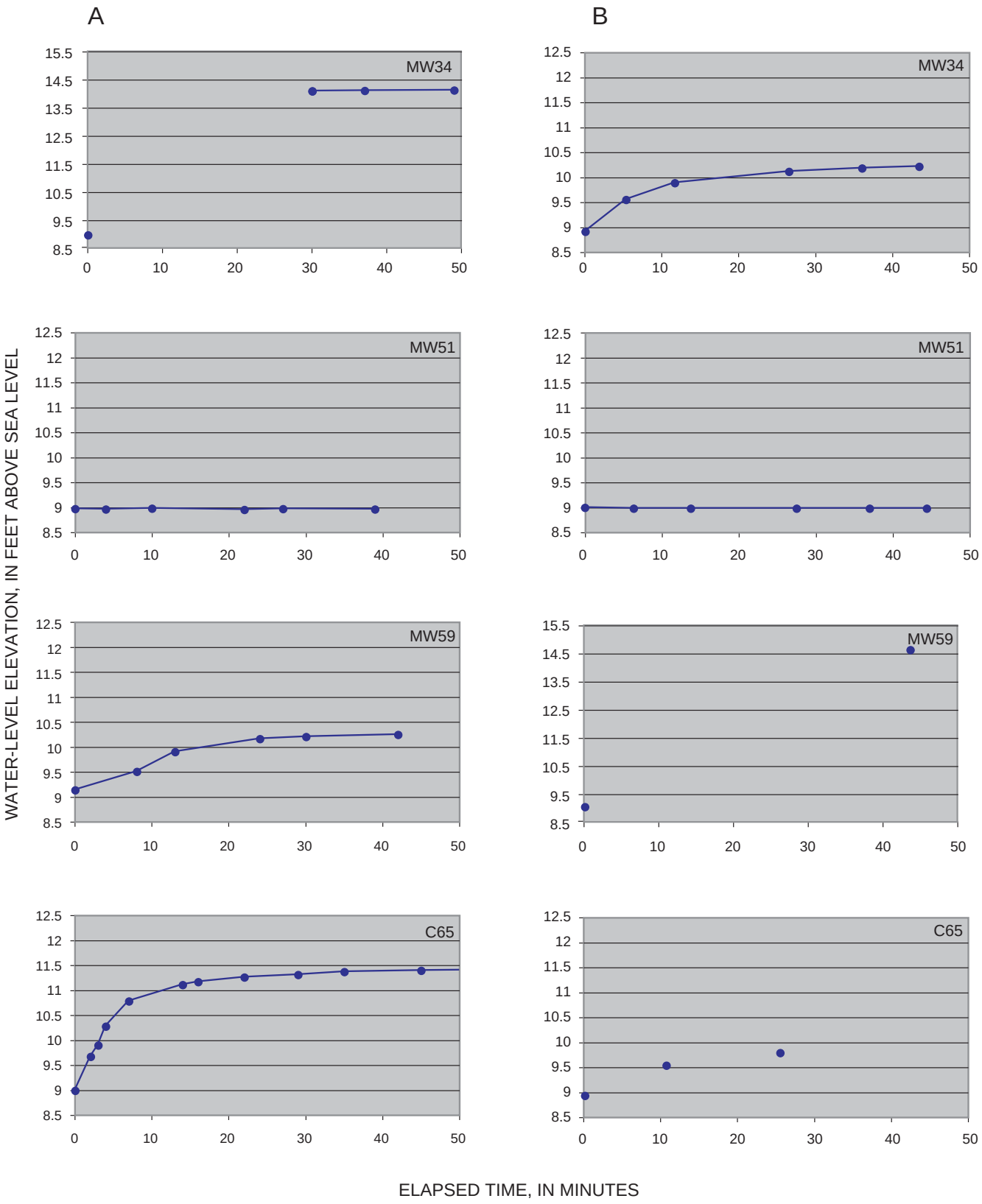


**Figure 12.** Water levels in the monitoring wells and coreholes for the cross-hole injection tests: A. Injection into monitoring well 34. B. Injection into monitoring well 59. (Locations are shown in fig. 2.)

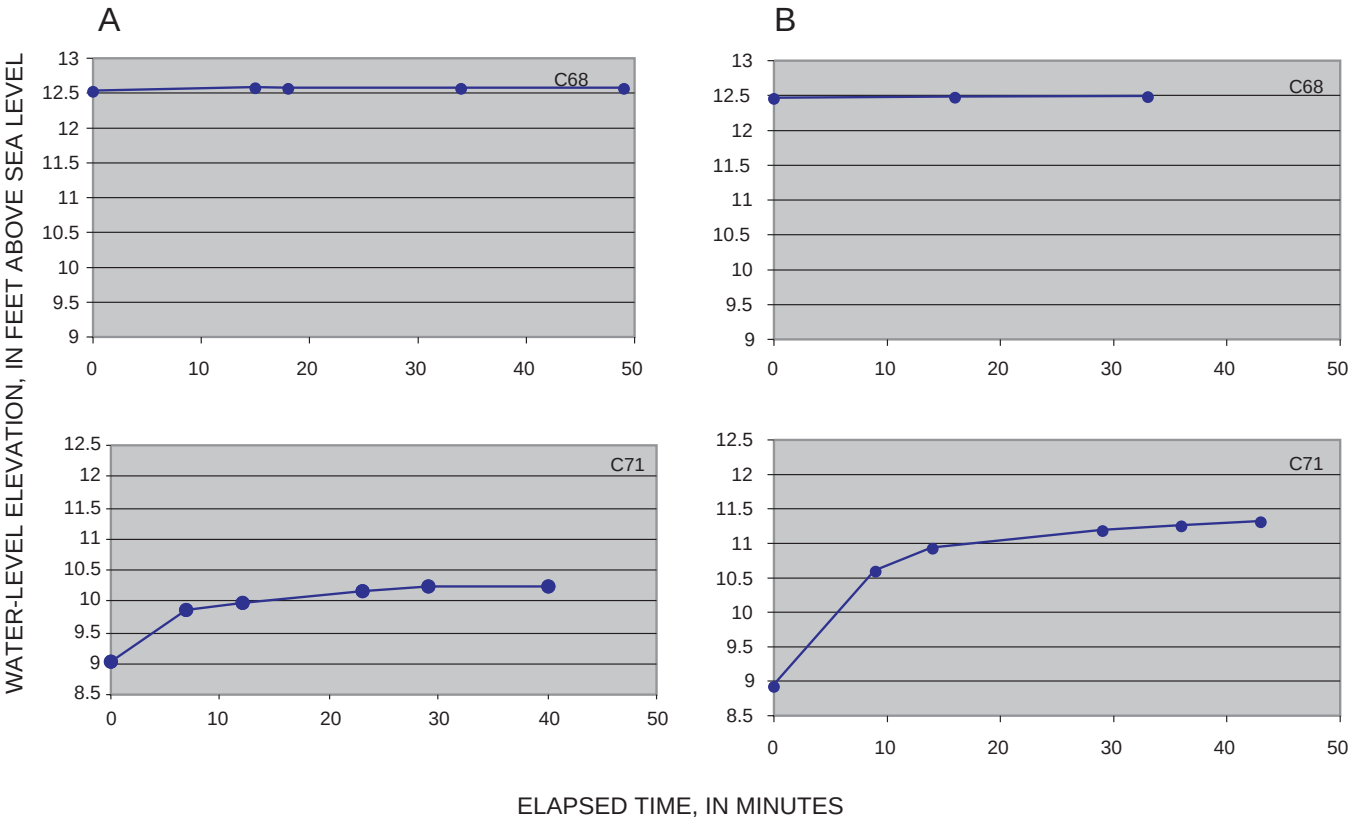


**Figure 12. (continued)** Water levels in the monitoring wells and coreholes for the cross-hole injection tests: A. Injection into monitoring well 34. B. Injection into monitoring well 59. (Locations are shown in fig. 2.)

than that in the upper group, then decreases more slowly during recovery. This results in a slower relaxation of the head in the lower group than in the upper zone during recovery. The result is a distinct "overshoot" during the early phase of recovery. Thus, the cross-hole test supports the *T* estimates for the fractures at corehole 65 and indicates a hydraulic connection between the upper and lower fracture groups. The connection is less direct than that between the shallow fractures at monitoring well 34 and corehole 65 because the measured flows lie closer to the isolated fracture prediction than to the strong upflow simulated for the short-circuited configuration depicted in figure 10A.

### Injection into Monitoring Well 59

Injection at a rate of 4 gal/min into monitoring well 59 produced the following water-level changes in the monitoring wells and coreholes: 34 (1.28 ft), 59 (~5 ft), 65 (0.85 ft), and 71 (2.39 ft) (fig. 12 and table 3). This response was similar to the response of the injection at monitoring well 34. The water-level changes in monitoring well 51 and corehole 68 were less than 0.05 ft.

Injection into monitoring well 59 increased the rate of upflow from the 65-ft fracture zone to the 28-ft zone in corehole 71 by almost an order of magnitude in relation to ambient conditions. The hydraulic connection between monitoring well 59 and corehole 71 is so direct that the transient flow was difficult to capture with the 20-second maximum firing frequency of the heat-pulse flowmeter (fig. 13C). Model-type curves representing isolated fractures and short-circuited fractures for the zones at 65 and 28 ft at corehole 71, based on the *T* value obtained from the single-hole tests and an assumed *S* value of $5 \times 10^{-5}$, are presented. The single-fracture type curve is omitted because it is virtually the same curve as the short-circuited configuration. The measured transient flow appears to lie about midway between the

**Table 3**. Water levels recorded in monitoring wells and coreholes during cross-hole flow tests at the Watervliet Arsenal, Albany County, N.Y., 2000-01.

[Time is in minutes. Water levels are in feet above sea level. Gal/min, gallons per minute. Dashes indicate no measurement. Locations are shown in fig. 2.]

| Corehole 65 | | Corehole 71 | | Monitoring well 59 | | Monitoring well 34 | | Corehole 68 | | Monitoring well 51 | | Monitoring well 58 | |
|---|---|---|---|---|---|---|---|---|---|---|---|---|---|
| Elapsed time | Water level | Elapsed time | Water level | Elapsed time | Water level | Elapsed time | Water level | Elapsed time | Water level | Elapsed time | Water level | Elapsed time | Water level |
| **Injection of 4 gal/min into monitoring well 34** | | | | | | | | | | | | | |
| 0 | 8.99 | 0 | 9.01 | 0 | 9.16 | 0 | 8.98 | 0 | 12.52 | 0 | 8.97 | - | - |
| 2 | 9.67 | 7 | 9.84 | 8 | 9.53 | 30 | 14.09 | 15 | 12.57 | 4 | 8.96 | - | - |
| 3 | 9.90 | 12 | 9.96 | 13 | 9.93 | 37 | 14.11 | 18 | 12.56 | 10 | 8.98 | - | - |
| 4 | 10.28 | 23 | 10.17 | 24 | 10.19 | 49 | 14.12 | 34 | 12.56 | 22 | 8.95 | - | - |
| 7 | 10.78 | 29 | 10.22 | 30 | 10.23 | - | - | 49 | 12.56 | 27 | 8.97 | - | - |
| 14 | 11.11 | 40 | 10.25 | 42 | 10.28 | - | - | - | - | 39 | 8.96 | - | - |
| 16 | 11.17 | - | - | - | - | - | - | - | - | - | - | - | - |
| 22 | 11.26 | - | - | - | - | - | - | - | - | - | - | - | - |
| 29 | 11.31 | - | - | - | - | - | - | - | - | - | - | - | - |
| 35 | 11.37 | - | - | - | - | - | - | - | - | - | - | - | - |
| 45 | 11.40 | - | - | - | - | - | - | - | - | - | - | - | - |
| 114 | 11.50 | - | - | - | - | - | - | - | - | - | - | - | - |
| **Injection of 4 gal/min into monitoring well 59** | | | | | | | | | | | | | |
| 0 | 8.92 | 0 | 8.92 | 0 | 9.12 | 0 | 8.90 | 0 | 12.45 | 0 | 9.00 | - | - |
| 10 | 9.52 | 9 | 10.59 | 40 | 14.65 | 5 | 9.53 | 16 | 12.47 | 6 | 8.99 | - | - |
| 24 | 9.77 | 14 | 10.92 | - | - | 11 | 9.86 | 33 | 12.48 | 13 | 8.99 | - | - |
| - | - | 29 | 11.18 | - | - | 25 | 10.08 | - | - | 26 | 8.99 | - | - |
| - | - | 36 | 11.25 | - | - | 34 | 10.15 | - | - | 35 | 8.99 | - | - |
| - | - | 43 | 11.31 | - | - | 41 | 10.18 | - | - | 42 | 8.99 | - | - |
| **Extraction of 1 gal/min from lower zone of monitoring well 65** | | | | | | | | | | | | | |
| 0 | 8.96 | 0 | 8.96 | 0 | 9.13 | 0 | 8.90 | 0 | 12.33 | 0 | 9.29 | 0 | 9.56 |
| 14 | 7.96 | 12 | 8.69 | 1 | 8.95 | 5 | 8.48 | 4 | 12.32 | 4 | 9.29 | 3 | 9.54 |
| 18 | 7.95 | 18 | 8.68 | 11 | 8.89 | 17 | 8.43 | 15 | 12.32 | 18 | 9.29 | 13 | 9.54 |
| 48 | 7.96 | 28 | 8.67 | 19 | 8.86 | 31 | 8.43 | 23 | 12.31 | 32 | 9.29 | 22 | 9.50 |
| - | - | 43 | 8.65 | 34 | 8.85 | 64 | 8.41 | 60 | 12.31 | 64 | 9.29 | 61 | 9.39 |
| - | - | 54 | 8.67 | 66 | 8.85 | 86 | 8.41 | 79 | 12.31 | 87 | 9.29 | 80 | 9.33 |
| - | - | 154 | 8.62 | 89 | 8.83 | 100 | 8.41 | 97 | 12.30 | 101 | 9.29 | 98 | 9.28 |
| - | - | 172 | 8.59 | 103 | 8.82 | 149 | 8.39 | 146 | 12.30 | 150 | 9.29 | 147 | 9.16 |
| - | - | - | - | 149 | 8.79 | - | - | - | - | - | - | - | - |

**Table 3**. (continued) Water levels recorded in monitoring wells and coreholes during cross-hole flow tests at the Watervliet Arsenal, Albany County, N.Y., 2000-01.

| Corehole 65 | | Corehole 71 | | Monitoring well 59 | | Monitoring well 34 | | Corehole 68 | | Monitoring well 51 | | Monitoring well 58 | |
|---|---|---|---|---|---|---|---|---|---|---|---|---|---|
| Elapsed time | Water level | Elapsed time | Water level | Elapsed time | Water level | Elapsed time | Water level | Elapsed time | Water level | Elapsed time | Water level | Elapsed time | Water level |
| **Extraction of 3 gal/min from upper zone of monitoring well 65 (increase to 6 gal/min at 155 min)** | | | | | | | | | | | | | |
| 0 | 9.00 | 0 | 8.94 | 0 | 9.17 | 0 | 8.94 | 0 | 12.36 | 0 | 9.29 | 0 | 9.53 |
| 3 | 3.82 | 5 | 8.51 | 15 | 8.47 | 5 | 8.00 | 11 | 12.35 | 13 | 9.29 | 7 | 9.55 |
| 8 | 1.83 | 8 | 8.34 | 31 | 8.33 | 9 | 7.97 | 26 | 12.34 | 28 | 9.27 | 10 | 9.55 |
| 17 | 0.67 | 10 | 8.31 | 46 | 8.69 | 17 | 7.47 | 37 | 12.34 | 41 | 9.28 | 19 | 9.55 |
| 22 | 1.28 | 11 | 8.30 | 57 | 8.31 | 23 | 7.03 | 53 | 12.34 | 54 | 9.28 | 24 | 9.53 |
| 39 | 2.62 | 15 | 8.10 | 105 | 8.31 | 40 | 6.99 | 65 | 12.33 | 104 | 9.28 | 38 | 9.48 |
| 47 | 2.55 | 22 | 8.03 | 118 | 8.25 | 48 | 7.17 | 112 | 12.29 | 162 | 9.28 | 52 | 9.42 |
| 61 | 2.58 | 29 | 8.03 | 165 | 7.92 | 62 | 7.18 | 146 | 12.29 | 171 | 9.28 | 64 | 9.39 |
| 88 | 2.51 | 37 | 8.05 | 172 | 7.73 | 103 | 7.16 | 167 | 12.28 | - | - | 110 | 9.24 |
| 106 | 2.51 | 44 | 8.03 | 188 | 7.59 | 115 | 7.11 | 175 | 12.27 | - | - | 166 | 9.04 |
| 113 | 2.51 | 70 | 7.99 | 201 | 7.54 | 166 | 6.19 | 190 | 12.25 | - | - | 174 | 8.97 |
| 160 | -9.96 | 91 | 7.97 | - | - | 171 | 5.84 | 207 | 12.23 | - | - | 189 | 8.87 |
| 170 | -18.54 | 136 | 7.96 | - | - | 186 | 5.65 | - | - | - | - | 198 | 8.79 |
| 185 | -18.84 | 156.5 | 7.83 | - | - | 200 | 5.62 | - | - | - | - | 208 | 8.71 |
| - | - | 158.5 | 7.71 | - | - | - | - | - | - | - | - | - | - |
| - | - | 159.5 | 7.63 | - | - | - | - | - | - | - | - | - | - |
| - | - | 164.5 | 7.50 | - | - | - | - | - | - | - | - | - | - |
| - | - | 169.5 | 7.41 | - | - | - | - | - | - | - | - | - | - |
| - | - | 174.5 | 7.38 | - | - | - | - | - | - | - | - | - | - |
| - | - | 178.5 | 7.33 | - | - | - | - | - | - | - | - | - | - |
| - | - | 187.5 | 7.35 | - | - | - | - | - | - | - | - | - | - |
| - | - | 192.5 | 7.23 | - | - | - | - | - | - | - | - | - | - |
| - | - | 197.5 | 7.22 | - | - | - | - | - | - | - | - | - | - |
| - | - | 202.5 | 7.20 | - | - | - | - | - | - | - | - | - | - |

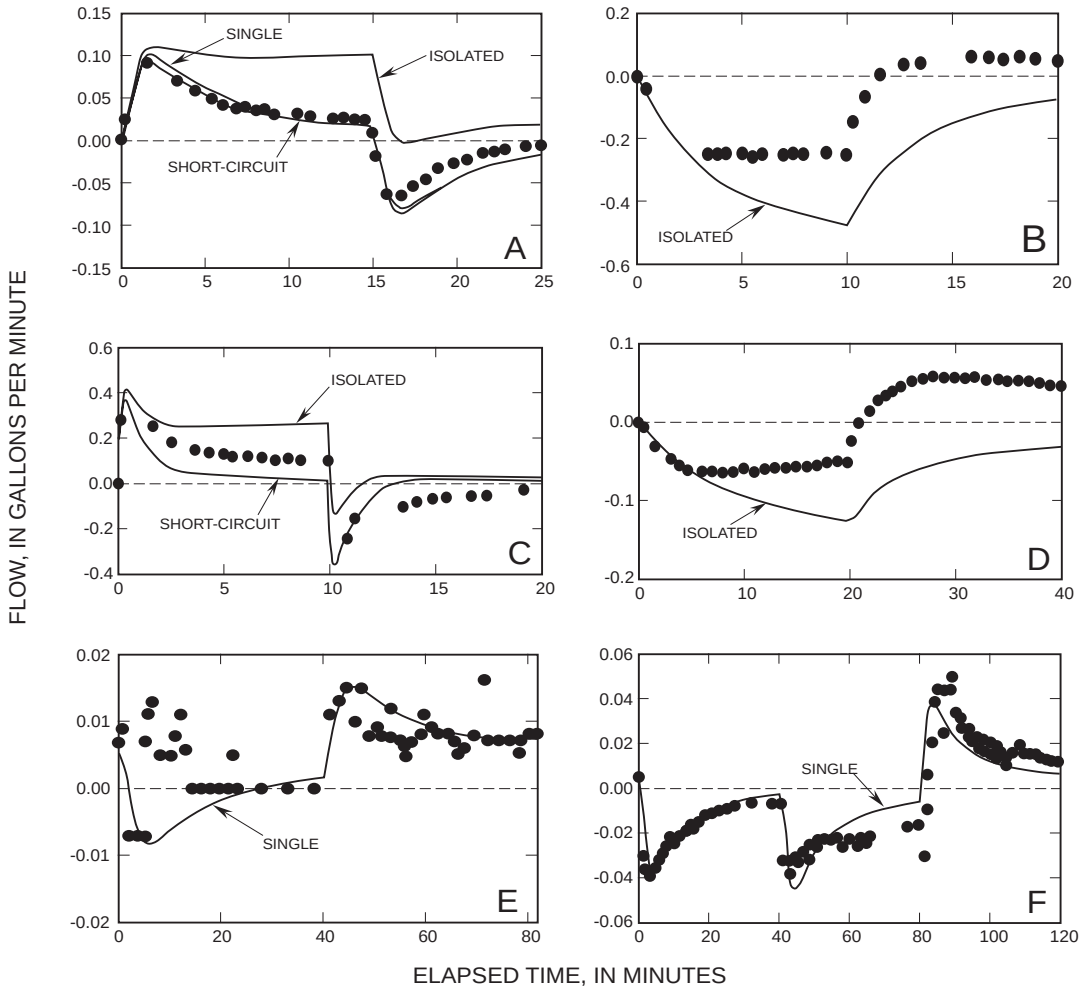


**Figure 13.** Measured flow (dots) and model type curves (solid lines) for the observation boreholes during the cross-hole tests: A. Corehole 71 with flowmeter at 50 ft during injection into monitoring well 34.
B. Corehole 65 with flowmeter at 60 ft during injection into monitoring well 34. C. Corehole 71 with flowmeter at 50 ft during the injection into monitoring well 59. D. Corehole 65 with flowmeter at 60 ft during injection into monitoring well 59. E. Corehole 71 with flowmeter at 50 ft during extraction from the lower part of corehole 65. F. Corehole 71 with flowmeter at 50 ft during extraction from the upper

completely isolated flow and short-circuited or single-fracture flow.

Injection into monitoring well 59 caused flow in corehole 65 to reverse from upward to downward (fig. 14). The downflow rate was less than one-half that obtained for the monitoring well 34 injection. A $T$ value of 250 $ft^2/d$ and $S$ value of $1 \times 10^{-5}$ for an isolated connection between the upper fracture group (24 and 35 ft) at corehole 65 and the 92-ft fracture zone at monitoring well 59 provide a good fit between measured and simulated flow at early times (fig. 13D). The measured flow's obvious lag behind the model simulation after about 5 minutes indicates a connection between the upper and lower groups of fractures near corehole 65. The expected overshoot during the recovery also is evident. Even so, the measured flow lies closer to the isolated configuration because the short-circuited configuration would predict strong upflow, as in figure 10A.

### Extraction from Lower Part of Corehole 65

Extraction at a rate of 1 gal/min from the lower part of corehole 65 produced the following drawdown in the monitoring wells and coreholes: 34 (0.51 ft), 58 (0.40), 59 (0.34 ft), upper part of 65 (1.00 ft), and 71 (0.37 ft) (fig. 15 and table 3). The water level in monitoring well 58 showed a delayed linear response, in contrast to the almost instantaneous logarithmic

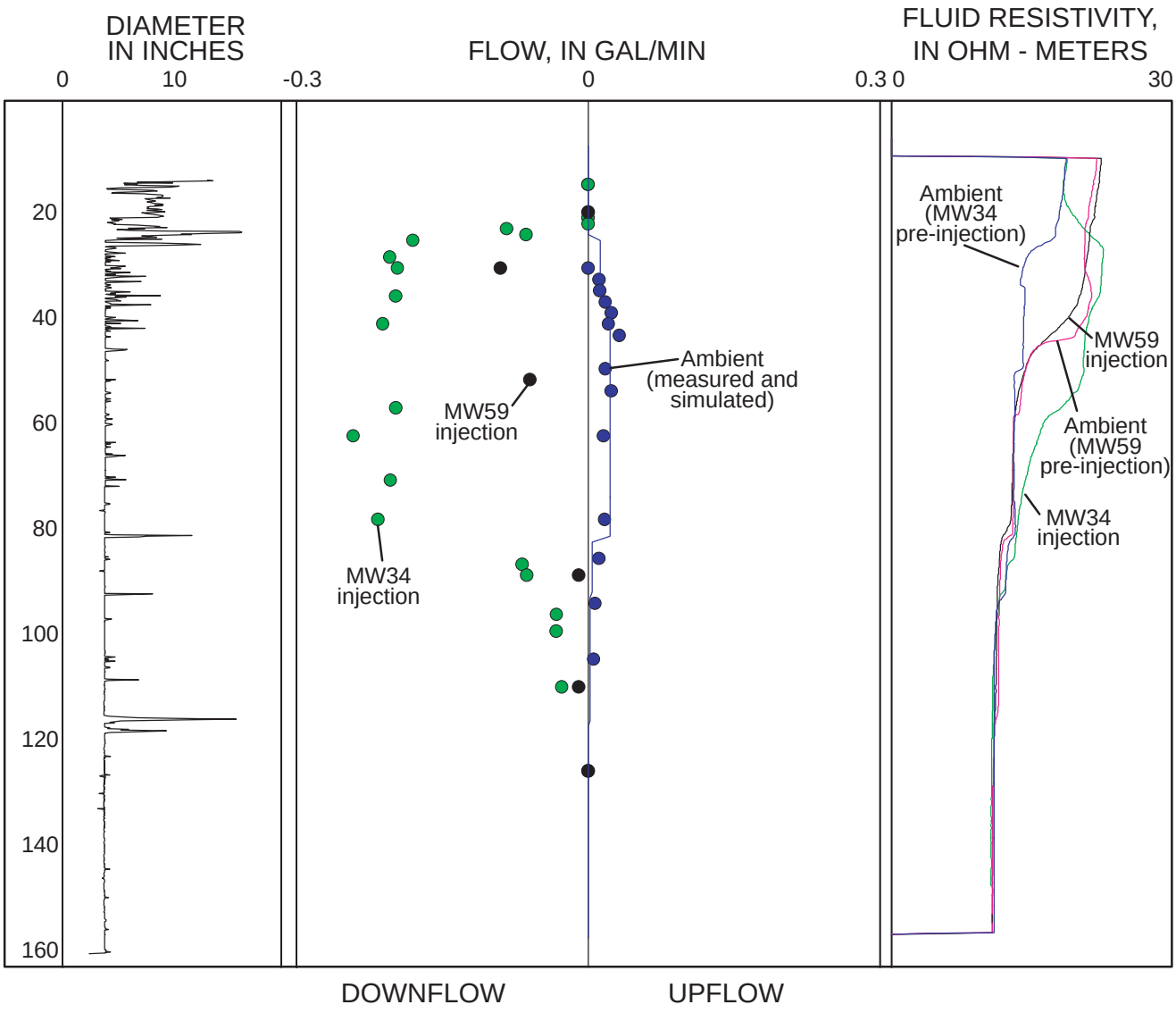


**Figure 14.** Wellbore diameter, flow, and fluid resistivity for corehole 65 during injection cross-hole tests at monitoring well 34 and 59. (Locations are shown in fig. 2.)

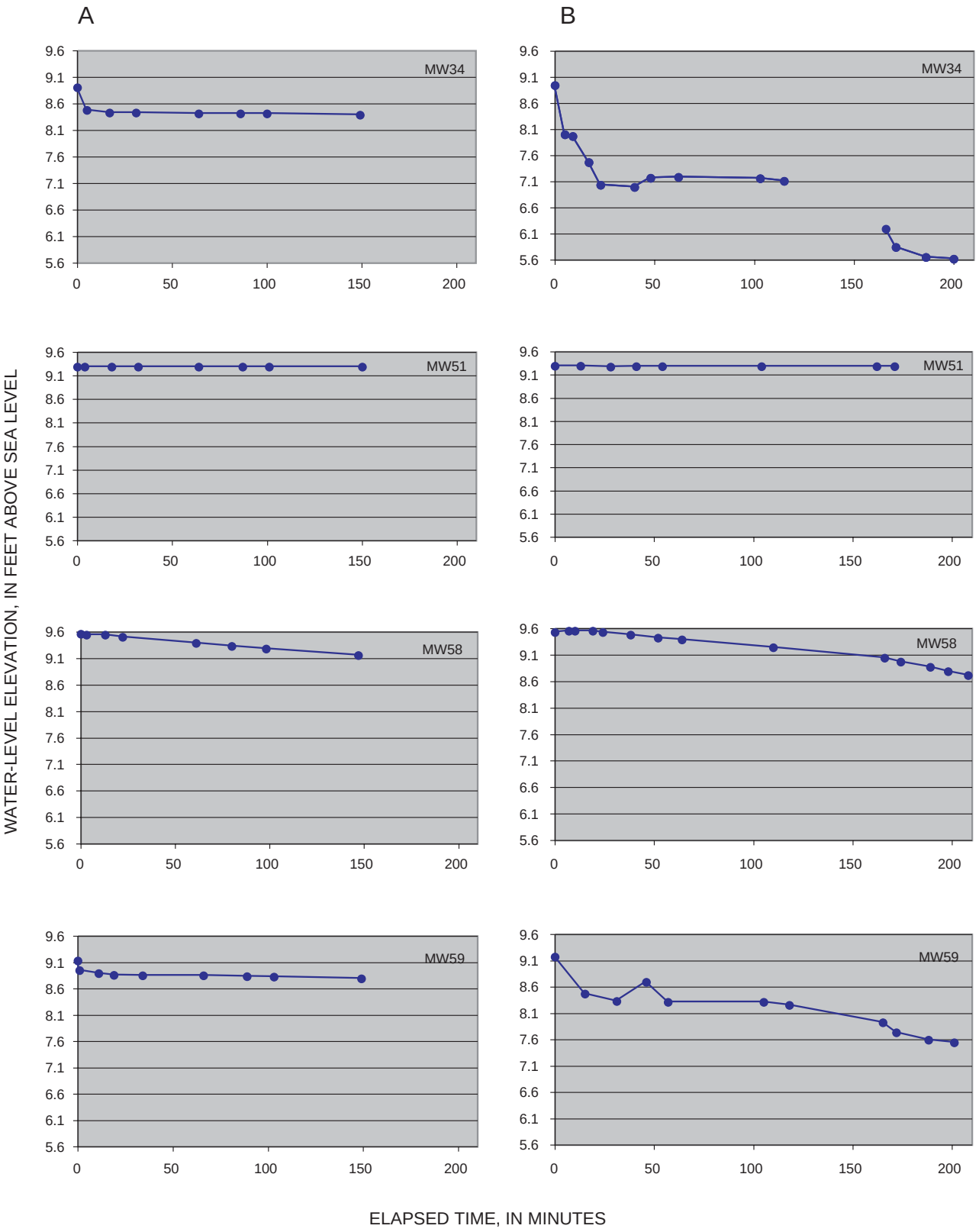


**Figure 15.** Water levels in the monitoring wells and coreholes for the cross-hole extraction tests: A. Extraction from lower part of corehole 65. B. Extraction from upper part of corehole 65. (Locations are shown in fig. 2.)

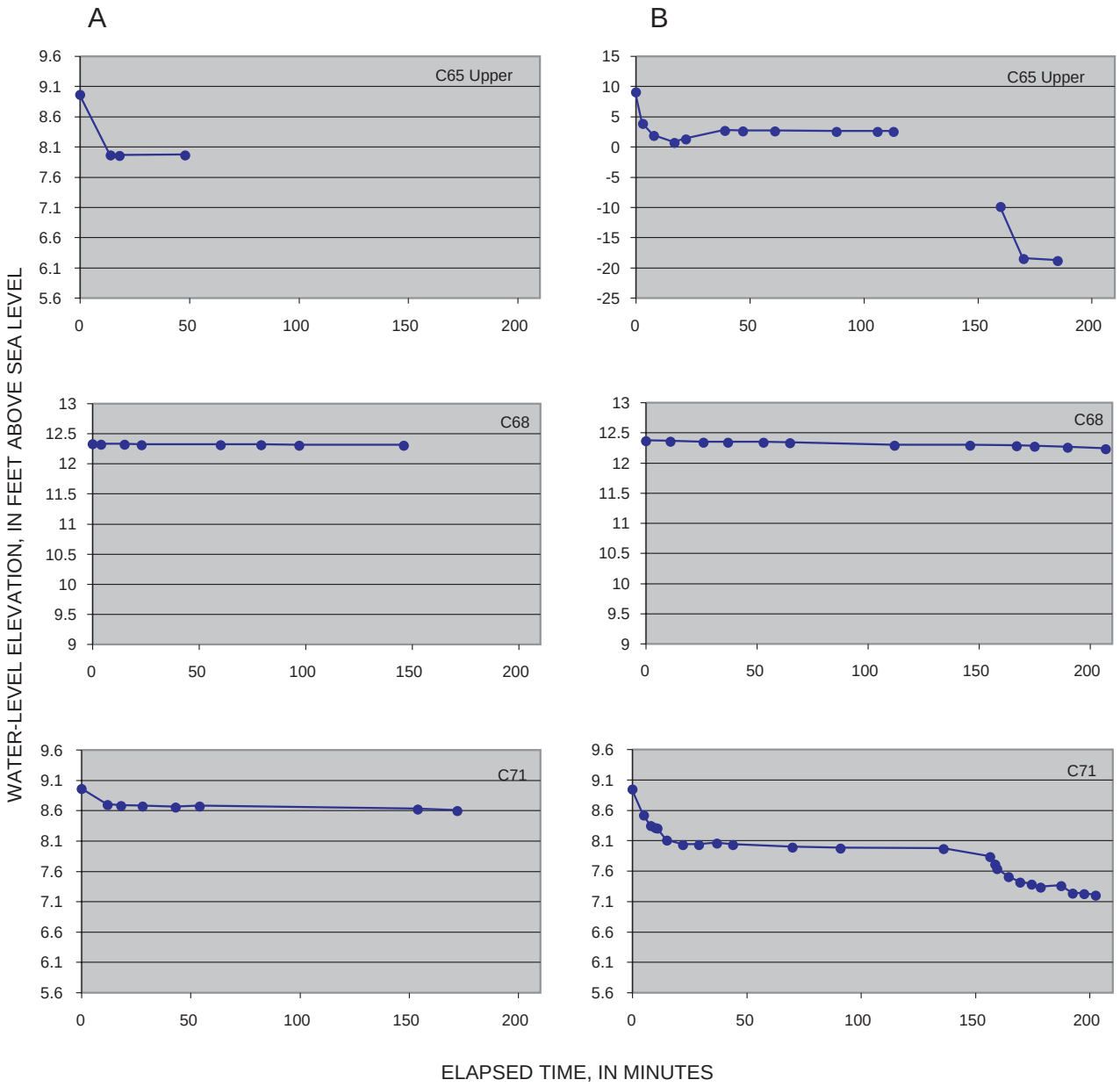


**Figure 15. (continued)** Water levels in the monitoring wells and coreholes for the cross-hole extraction tests: A. Extraction from lower part of corehole 65. B. Extraction from upper part of corehole 65. (Locations are shown in fig. 2.)

response in the other boreholes. This response is not surprising, given the low transmissivity of the flow zone in well 58 (fig. 4 and table 2). Water-level changes in monitoring well 51 and corehole 68 were less than 0.05 ft. The continuous water-level recorder in corehole 72 did not function properly during the extraction tests, and data were lost, but data recorded after the tests indicate that the water level in the corehole is affected by tides (fig. 16). Water-level changes based on the few manual measurements made during the tests are consistent with this tidal effect and did not appear to be affected by extraction from corehole 65.

The extraction induced a weak but measurable response in corehole 71 (fig. 13E). This response matches the type curve for a direct connection between the lower fracture group at corehole 65 and the fracture zone at 65 feet at corehole 71 if the irregular distribution of upflow after the initial downflow response to extraction is disregarded. The

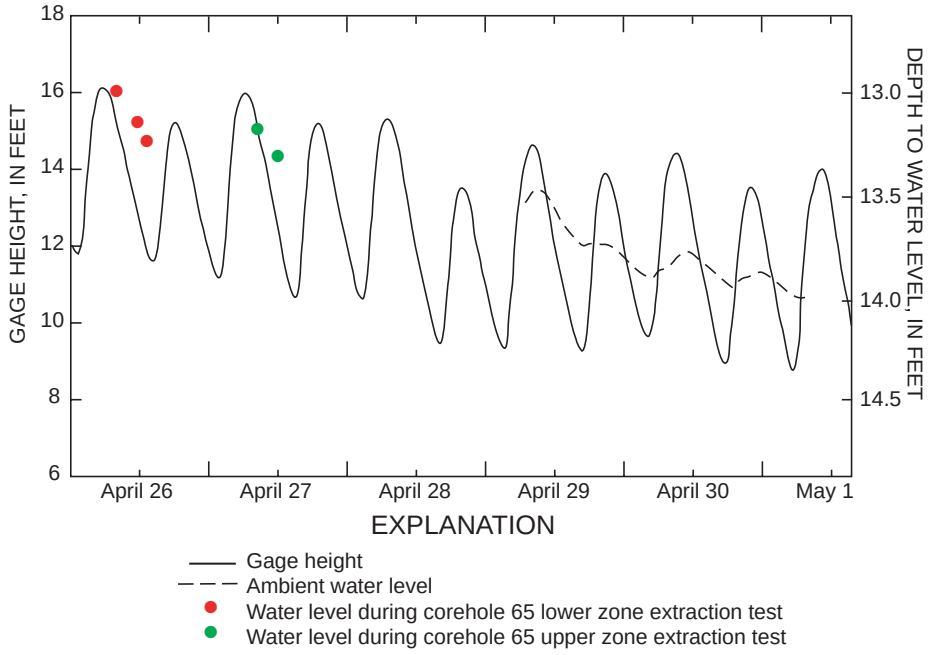


**Figure 16.** Depth to water level in corehole 72 and gage height in the adjacent Hudson River at Albany, April 26 to May 1, 2001. (Location is shown in fig. 2.)

response to extraction is poorly defined because the induced downflow is superimposed on a weak ambient upflow, which barely exceeds the 0.005 gal/min detection limit for the heat-pulse flowmeter. Thus, the induced downflow is forced to pass through flow values below the detection limit for the flowmeter until the downflow develops beyond the 0.005 gal/min detection limit. The irregular distribution of upflow data in the 5- to 15-minute period may be attributed to the buoyant rise of the heat pulse in a no-flow situation because the response to extraction exactly cancels the weak ambient flow. The response to recovery in the second half of this test is better defined, probably because the expected upflow response is added to the ambient upflow, and the measured flows are always above the detection limit.

A $T$ value of 80 $ft^2/d$ and $S$ value of $1 \times 10^{-4}$ for a single-fracture connection between the lower part of corehole 65 and the fracture zone at 65 feet at corehole 71 provide a reasonable fit of the measured and simulated flow (fig. 13E). This $T$ value falls between the values for the lower part of corehole 65 (43 $ft^2/d$) and the fracture zone at corehole 71 (230 $ft^2/d$) obtained from the single-hole tests (fig. 4 and table 2) and can plausibly represent an average $T$ value for the connection between the lower part of corehole 65 and deep fractures at corehole 71. The peak response occurs about 5 minutes after the start of extraction or recovery and coincides with the approximately 5 minute time interval after which the measured flow during the injection tests (figs. 13B and D) departs from the simulated response for the fracture groups at corehole 65. The facts that extraction from the lower part of corehole 65 induced a measurable response in corehole 71, and that the measured flow matches the expected response for a direct but weaker fracture connection, confirm the interpretation of the previous cross-hole tests that such a connection exists.

### Extraction from Upper Part of Corehole 65

Extraction at a rate of 3 gal/min from the upper part of corehole 65 produced the following drawdown in the monitoring wells and coreholes: 34 (1.83 ft), 58 (0.29), 59 (0.92 ft), upper part of 65 (6.49 ft), and 71 (0.98 ft) (fig. 15 and table 3). No measurable drawdown was detected in monitoring well 58 until after 30 minutes of extraction. Increasing the extraction rate to 6 gal/min resulted in the following additional drawdown: 34 (1.49 ft), 58 (0.53), 59 (0.71 ft), upper part of 65 (21.35 ft), and 71 (0.76 ft). The water level in corehole 68 dropped a total of 0.13 ft in a consistent manner during the test indicating it was possibly affected by the extraction. The water-level

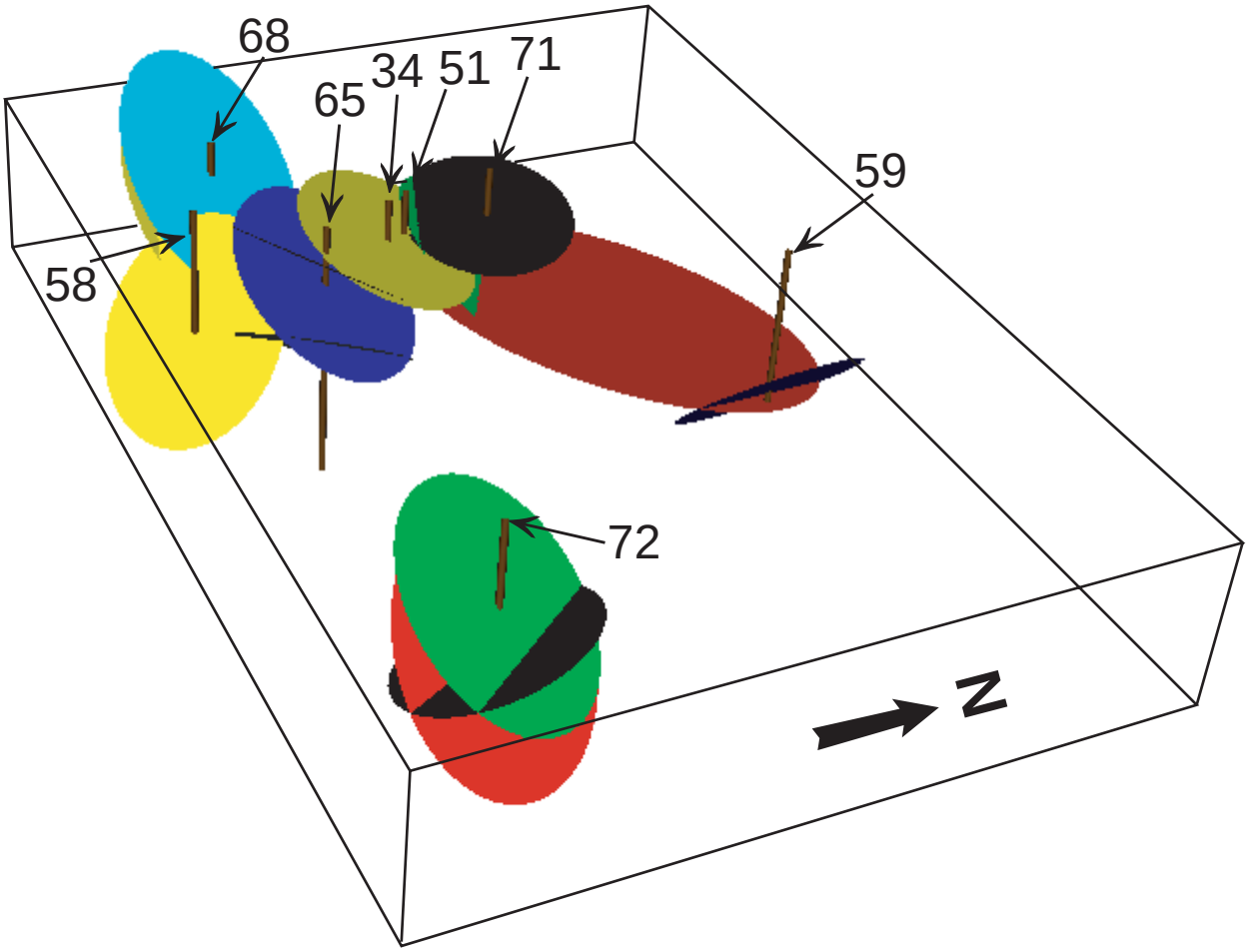


**Figure 17.** Three-dimensional representation of fracture-flow zones intersected by the monitoring wells and coreholes revised based on hydraulic connections. (Locations are shown in fig. 2.)

change in monitoring well 51 was less than 0.05 ft. The water-level change in corehole 72 seems to be consistent with tidal effects (fig. 16).

The measured flow in corehole 71 in response to extraction from the upper part of corehole 65 generally matches the simulated flow for a direct fracture connection with a *T* value of 100 $ft^2/d$ and *S* value of $1 \times 10^{-5}$, superimposed on the 0.005 gal/min ambient upflow (fig. 13F). No previous cross-hole tests were conducted between coreholes 65 and 71, but a direct fracture connection between the upper zone in corehole 65 and the lower zone in corehole 71 had been indicated by the other test analysis. These results support the presence of this connection and its relatively high transmissivity.

The simple radial projection of fracture-flow zones depicted in figure 7 provides a representation that is consistent with the hydraulic connections inferred from the cross-hole testing with one major exception the strong hydraulic connection between fractures in monitoring well 59 and corehole 71. A revised representation is presented in figure 17 that shows a projection of the subhorizontal fracture at 65 ft in corehole 71 to near corehole 59. The subhorizontal fracture in corehole 71 is a likely candidate for increased projection because of its high transmissivity and large apparent aperture, as seen in figure 6. The revised representation is by no means definitive or unique, but is consistent with all borehole-wall image and single- and cross-hole flow data collected at the Watervliet site.

## SUMMARY

The results of the geophysical logging and cross-hole testing indicate the presence of an

interconnected fracture network at the site, which greatly affects site hydrology and has important implications for contaminant monitoring and remedial actions. The fracture network includes a highly transmissive zone of well-connected fractures that is intersected at 25 ft (well 34), 92 ft (well 59), 24-35 ft (corehole 65), and 65 ft (corehole 71). The most direct hydraulic connection appears to be the one between the fractures at monitoring well 59 and corehole 71. The major fracture zone, which extends more than 200 ft across the site, is well connected, although less directly, to fractures at and below 78 ft at corehole 65. The poorly transmissive fracture at 76 ft at monitoring well 58 appears to be most strongly connected to the fractures at and below 78 ft at corehole 65. The transmissive fractures at 19 and 45 ft at corehole 68 appear to be only weakly connected with the fractures intersected by the other boreholes and are less connected to each other vertically than are the upper and lower fractures at coreholes 65 and 71. The transmissive fractures at corehole 72 are in hydraulic connection with the Hudson River but do not appear to be strongly connected with the fractures intersected by the other boreholes.

## REFERENCES CITED


Paillet, F. L., 1998, Flow modeling and permeability estimation using borehole logs in heterogeneous fractured formations: Water Resources Research, v. 34, no. 5, p. 997-1010.

_____, 2000, A field technique for estimating aquifer parameters using flow log data: Ground Water, v. 38, no. 4, p. 510-521.

Paillet, F.L., Hess, A. E., Cheng, C. H., and Hardin, E. L., 1987, Characterization of fracture permeability with high-resolution vertical flow measurements during borehole pumping: Ground Water, v. 25, no. 1, p. 28-40.

Williams, J. H. and Johnson, C. D., 2000, Borehole-wall imaging with acoustic and optical televiewers for fractured-bedrock aquifer investigations, in Proceedings of the Seventh International Symposium on Borehole Geophysics for Minerals, Geotechnical, and Groundwater Applications: October 24-26, 2000, Denver, Colo., Minerals and Geotechnical Logging Society, p. 43-53.

**Appendix F**

Goldstein et al., Remediation Journal, 2004

# Characterization and Pilot-Scale Studies for Chemical Oxidation Remediation of Fractured Shale

Kenneth J. Goldstein

Andrew R. Vitolins

Daria Navon

Beth L. Parker

Steven Chapman

Grant A. Anderson

*The distribution of volatile organic compounds (VOCs) in fractured shale overlain by thin (< 10 feet) overburden at the Watervliet Arsenal near Albany, New York, was initially determined by sampling water from the fracture network using packer systems in boreholes and also using conventional monitoring wells. Furthermore, short-term pumping and injection tests were conducted and the boreholes were logged using a variety of geophysical and hydrophysical tools. Tetrachloroethene is the dominant VOC in the groundwater, with lesser concentrations of trichloroethene and degradation products (cis-1,2-dichloroethene, trans-1,2-dichloroethene, and vinyl chloride). The vertical VOC distributions in the rock matrix were obtained from continuous-cored holes from which small rock samples, collected at many depths between 18 and 150 feet below ground surface, were analyzed. The rock core VOC concentrations were determined by methanol extraction of crushed rock followed by direct methanol injection onto a gas chromatograph and subsequent estimation of rock porewater VOC concentrations. The rock core data support the concept that diffusion-driven mass transfer has caused nearly all the VOC mass initially present in the fractures to now reside in the rock matrix, which has a porosity three or four orders of magnitude larger than the bulk fracture porosity. The results of the site characterization indicate that an effective site investigation strategy in fractured shale must include characterization of both the fracture and matrix contaminant distribution. These results also indicate that the most favorable remediation technologies for this fractured shale are those that will destroy VOCs in the rock matrix, particularly contaminants in the sorbed phase, and also destroy the VOC mass in the fractures including both dissolved and immiscible phases. The site characterization resulted in the selection of potassium permanganate for an* in situ *chemical oxidation pilot study. © 2004 Wiley Periodicals, Inc.*

## INTRODUCTION

It is generally recognized that geologic complexities pose some of the greatest challenges to site characterization and remediation. Fractured rock sites are among the most complex because of their considerable geologic heterogeneity and the nature of fluid flow and contaminant transport through fractured media (United States Environmental Protection Agency [US EPA], 2001). Until recently, the conventional view of fractured rock sites was that they are too complex to characterize and remediate. The most common remedial approach at fractured rock sites has been a containment strategy using groundwater extraction and treatment (US EPA, 2001).

Recent work has shown that in dual porosity systems such as fractured sedimentary rock, diffusive transport of contaminants initially present as DNAPL and aqueous phase


Published online in Wiley Interscience (www.interscience.wiley.com). DOI: 10.1002/rem.20019

mass in fractures into the matrix porewater will result in the transfer of the vast majority of contaminant mass into the rock matrix (Parker et al., 1994, 1997) with subsequent storage as aqueous and sorbed phase. This concept has important implications in the characterization and remediation of fractured bedrock sites in that treatment efficacy will depend almost entirely on the ability to treat the rock matrix, not the fractures. This article presents a case study describing the characterization and pilot-scale studies for chemical oxidation remediation of a fractured shale bedrock aquifer located at the Watervliet Arsenal (WVA) near Albany, New York.

## SITE BACKGROUND

The WVA, a national registered historic landmark, is the oldest continuously operating cannon manufacturing facility in the United States.

The WVA is a 140-acre government-owned installation located in the city of Watervliet, New York, which is west of the Hudson River and five miles north of the city of Albany. The WVA, a national registered historic landmark, is the oldest continuously operating cannon manufacturing facility in the United States. The WVA currently manufactures large-caliber cannons.

During a RCRA Facility Investigation (RFI), an area of groundwater contamination was discovered in the eastern portion of the WVA, adjacent to the site boundary and in front of Building 40—a former manufacturing building now used primarily for office space. Groundwater contaminants include chlorinated volatile organic compounds (VOCs), predominantly tetrachloroethene (PCE) and cis-1,2-dichloroethene (c-DCE), with a lesser percentage of trichloroethene (TCE) and vinyl chloride. PCE has been detected at aqueous concentrations as high as 170 mg/L, suggesting the presence of dense nonaqueous phase liquid (DNAPL). VOCs are present in the bedrock groundwater from 20 feet to more than 150 feet below ground surface (bgs).

The original source of the chlorinated VOCs is likely a former degreasing unit located in the northwestern portion of Building 40 (see Exhibit 1). It is estimated that the release(s) occurred more than 30 years ago. The Hudson River is located approximately 200 feet to the east of Building 40. Broadway Street (New York State Route 32) and a six-lane interstate highway (Interstate 787) are located between Building 40 and the Hudson River. The affected portion of the bedrock aquifer is not used as a source of potable water.

## PHYSICAL SETTING

### *Geology*

The major overburden unit consists of brown or dark gray silty sand with angular gravel. Overburden thickness in the vicinity of Building 40 ranges from approximately 10 feet bgs to the west of the building to approximately 19 feet bgs to the east of the building at the WVA property boundary. A thin layer of weathered shale bedrock, typically less than two or three feet thick, is present beneath the alluvium.

The bedrock underlying the site is black, medium-hard laminated shale, showing some characteristics of minor metamorphism. This shale has been identified as part of the Snake Hill Formation. The bedrock surface generally slopes to the east from an elevation of approximately 25 feet above mean sea level (amsl) west of Building 40 to an elevation of approximately 19 feet amsl at the WVA property boundary. The primary features identified in the bedrock in the Building 40 area during the various investigations


**Exhibit 1.** Building 40 at the WVA

include bedding planes, fractures, and mineral inclusions. Bedding planes dip to the east (median direction of 94 degrees) with a median dip of 54 degrees from horizontal. The strike of the bedding planes is north-south. Fractures are present along bedding planes and at angles to bedding. Fracture orientations range from subhorizontal to nearly vertical. Veins of calcite and pyrite are commonly present along fracture and bedding planes, particularly at depths greater than 100 feet.

### *Hydrogeology*

Groundwater flow in the vicinity of Building 40 is primarily controlled by the degree of fracturing within the bedrock aquifer. Based on sitewide groundwater elevations measured during multiple events, the predominant direction of groundwater in the Building 40 area is to the southeast toward the Hudson River. Hydraulic heads in the Building 40 area are upward, which is expected given the proximity to the regional discharge boundary at the Hudson River.

Extensive hydrogeologic characterization studies were performed in the bedrock aquifer in the Building 40 area. These are discussed in detail in the following sections.

## SITE CONCEPTUAL MODEL

The results of the successive stages of site characterization have been compiled into an integrated site conceptual model (see Exhibit 2). In this model, DNAPL, and dissolved-phase VOC concentrations indicating the likely presence of DNAPL, have been detected in the bedrock groundwater. Advective transport of the VOCs in the bedrock aquifer takes place through a well-connected fracture network. The original source of the VOCs

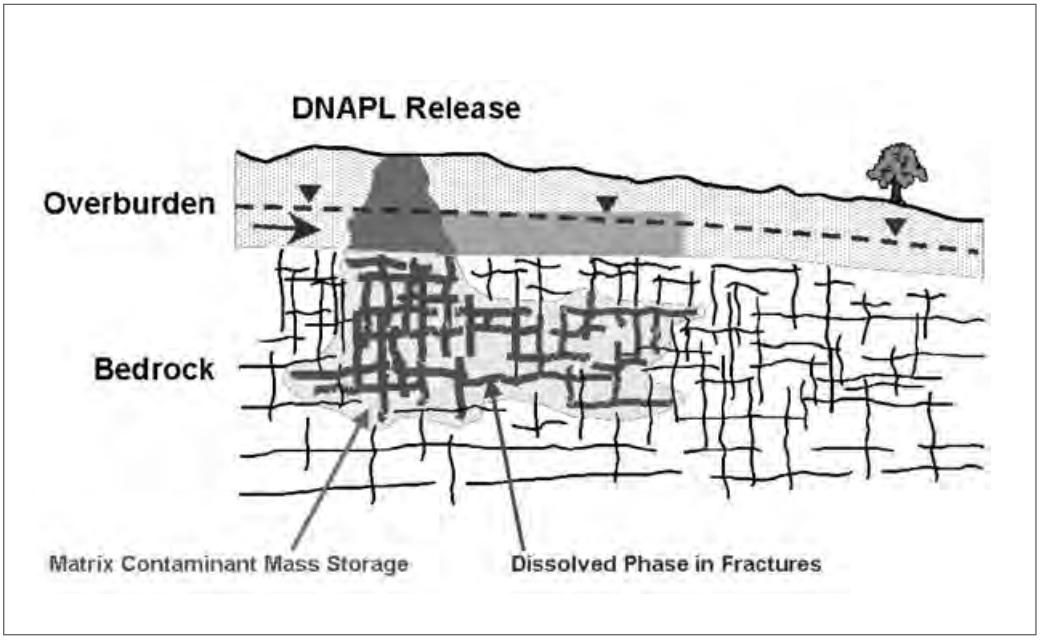


**Exhibit 2.** Site conceptual model

in the bedrock groundwater is presumed to be located in the northeastern portion of Building 40 (Exhibit 1). Since significant VOC concentrations were not detected in the overburden soil in this area, it is possible that the release occurred through a subsurface storm sewer that was once connected to floor drains in this area of Building 40.

Although fractures provide the primary pathway for advective transport of groundwater and VOCs through the bedrock aquifer, the ratio of the void space due to the presence of fractures to the bulk rock volume ("fracture porosity") is several orders of magnitude less than the porosity of the rock matrix ("matrix porosity")—meaning that the capacity of the rock matrix to store VOCs is orders of magnitude greater than the storage capacity in the fractures. Concentration gradients between VOCs present as DNAPL or at high concentrations in the fractures and the matrix porewater cause aqueous phase VOC mass to diffuse into the bedrock matrix. Contaminant sorption within the porous rock matrix further increases the matrix storage capacity, which may be especially important in shales with high organic carbon content. Although DNAPL may still exist in some fractures, the majority of the DNAPL that was initially present in the fractures has disappeared due to dissolution and diffusive mass transfer to the rock matrix. The result is that nearly all the VOC mass now resides in the rock matrix (as aqueous and sorbed phase) and not in the bedrock fractures. Given the lack of current surficial sources, it is presumed that releases of mass from the matrix back to the fractures is a significant source of the mobile VOCs in the groundwater.

This site conceptualization indicates that the only truly effective remediation technologies for the fractured bedrock aquifer are those that will treat the VOC mass in the rock matrix in addition to treating the VOC mass in the fractures. Failure to treat the VOC mass in the matrix where the majority of the mass now resides will result in rebound and ongoing diffusive transfer of VOCs out of the bedrock into the groundwater in the fractures following the remediation period.

| Characterization Technique | Purpose |
|---|---|
| Discrete Interval Packer Sampling | Delineate vertical and horizontal limits of VOC contamination in bedrock groundwater during drilling |
| Rock Core Testing | Evaluate the degree of VOC matrix contamination and identify matrix diffusion parameters. |
| Geophysical Testing | Identify location and nature of bedrock fractures. Identify flow zones and evaluate transmissivity and hydraulic head |
| Multilevel Monitoring Wells | Delineate vertical and horizontal limits of VOC contamination in the bedrock groundwater and monitor changes over time |

**Exhibit 3.** Site characterization techniques

## SITE CHARACTERIZATION

Site characterization activities in the Building 40 area were designed to provide the necessary information to confirm the conceptual model and provide sufficient data for the analysis of corrective measures alternatives. This information included:

1. The horizontal and vertical extent of VOC contamination in the fractured bedrock groundwater and in the bedrock matrix;
2. The physical properties of the bedrock;
3. The location, size, and interconnectivity of bedrock fractures in the study area; and
4. The transmissivity of the bedrock fractures and the associated VOC mass flux.

A summary of the site characterization techniques utilized for the project is provided in Exhibit 3. Testing locations are shown on the site map in Exhibit 4.

### *Discrete Interval Packer Sampling*

Discrete interval packer sampling was conducted during drilling of boreholes to provide preliminary information on the degree of VOC groundwater contamination and the hydraulic properties of the bedrock aquifer. Information gathered during the sampling was used to determine monitoring well depths and evaluate additional monitoring locations. Packer sampling was conducted at 20-foot intervals as each borehole was advanced into the bedrock. The isolated portion of each borehole was purged until three volumes had been removed. A groundwater sample was then collected for VOC analysis with a rapid laboratory turnaround time to aid in drilling decisions. Pumping rates and water levels in the isolated interval were monitored during purging to evaluate the relative hydraulic properties of each borehole interval. If an interval was pumped dry, the borehole was allowed to recharge, then was pumped dry again, before groundwater samples were collected.

### *Rock Core Testing*

Rock core testing was conducted to evaluate the physical properties of the rock matrix and the detailed distribution of VOC contamination. Continuous HQ-size bedrock cores (2.5-inch diameter) were collected in five-foot intervals from the competent bedrock

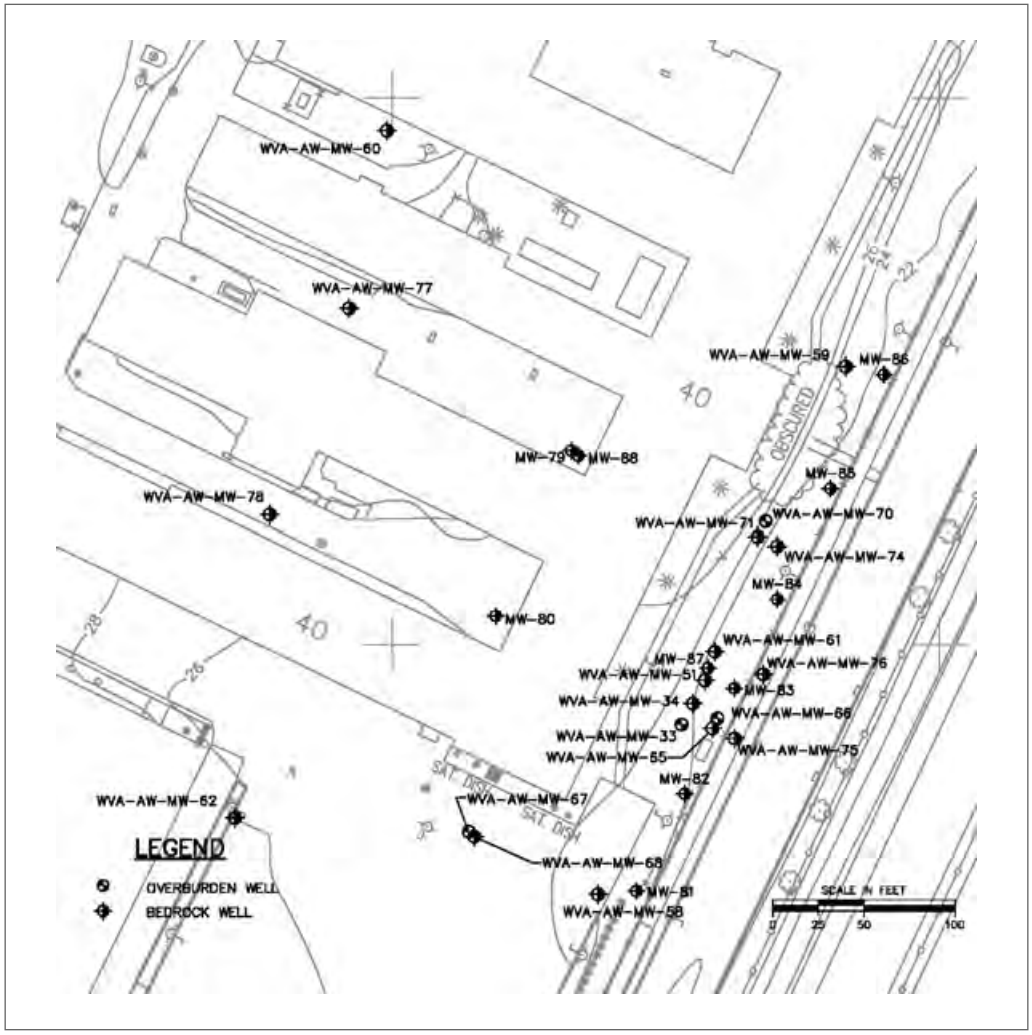


**Exhibit 4.** Site map

surface to the final depth of the well from five monitoring well boreholes (MW-74 and MW-75 in December 2001, and MW-80, MW-83, and MW-87 in October 2003). Samples from these cores were collected and analyzed using techniques developed at the University of Waterloo (UW).

Three types of samples were collected:

1. VOC samples, which were crushed and preserved in the field by placing in jars with methanol for extraction and later laboratory analysis;
2. Physical property samples consisting of intact sections of core that were analyzed for moisture content, matrix porosity, bulk density, specific gravity, hydraulic conductivity, and organic carbon content; and
3. Matrix diffusion samples consisting of intact sections of core designated for laboratory diffusion tests.

The protocol for collection of VOC samples included collection of samples at fractures (i.e., one of the fracture faces) and bedding planes, at lithologic changes, and from

matrix blocks between fractures. Sample lengths typically ranged from 0.1 to 0.4 feet of core, and averaged 0.2 feet. VOC samples were immediately wrapped in aluminum foil to minimize volatile losses and taken to an on-site field lab for crushing and processing. Prior to crushing, the outer rind of the core samples was chipped off to eliminate potential error from contact with the drilling fluids. Samples were then crushed with a hydraulic rock crusher using five stainless steel rock-crushing cells, which typically allowed samples from one core run to be processed. Between samples, the cells were decontaminated using a four-part wash and rinse sequence. The crushed rock samples were then placed into sample jars containing a known amount of HPLC grade methanol (MeOH) to extract and preserve the VOC mass. Excluding duplicates, and using the total cored interval, the average sample spacing was about 1.2 feet.

Five representative rock core samples were collected and sent to Golder Associates Ltd. (Golder) of Mississauga, Ontario, Canada, for analysis of selected physical and hydrogeologic parameters. Matrix diffusion tests were also performed on the rock cores to evaluate diffusion coefficients for the bedrock. Based on these tests, the average hydraulic conductivity of the shale matrix is approximately $1 \times 10^{-7}$ feet per day (ft/d) indicating that, as expected, advective groundwater transport in the bedrock is entirely controlled by fractures. The average porosity of the shale is approximately 2.3 percent, as compared to a typical range of 5 percent to 25 percent for sedimentary rocks (shale and sandstone). This low porosity is likely a result of the low-grade metamorphism to which the rock has been exposed. The average matrix diffusion coefficient (D) of the shale was $7.5 \times 10^{-7}$ cm$^2$/second.

Laboratory VOC analyses on the preserved crushed rock samples were conducted after allowing sufficient time for the VOCs to completely extract into the methanol (approximately six weeks). An aliquot of methanol was injected directly into a gas chromatograph (GC) for separation and quantification using a microelectron capture detector (μ-ECD). The list of analytes quantified included TCE, PCE, and the DCE isomers. The direct, on-column injection of methanol onto the gas chromatograph was tailored by UW for analysis of PCE, TCE, and relevant breakdown products so that the resulting detection limits were very low ($<$ 0.1 ug/L in MeOH for TCE and PCE, and $<$ 10 ug/L in MeOH for the DCE isomers). These were converted to equivalent porewater concentrations using bulk density, porosity, and sorption estimates, as well as rock sample and MeOH masses, as discussed below.

Laboratory VOC analyses on the preserved crushed rock were conducted after allowing sufficient time for the VOCs to completely extract into the methanol. . .

The laboratory analysis provided the total mass of each VOC per unit mass of wet crushed rock sample ($c_t$) (e.g., mg PCE per g wet rock) and included VOC mass present in the aqueous, sorbed, and DNAPL (if present) phases. Equivalent porewater concentrations ($c_w$) were estimated using:

$$c_W = c_t \frac{\rho_{bwet}}{R\phi} \qquad [1]$$

where $\rho_{bwet}$ is the rock wet bulk density (g/cm$^3$), $\phi$ is the porosity, and R is the retardation factor, accounting for VOC mass sorbed to organic carbon present in the rock. Retardation factors were estimated using the relation:

$$R = 1 + \left[\frac{\rho_b}{\phi}\right] K_d \qquad [2]$$

where $K_d$ is the distribution coefficient (mL/g) and $\rho_b$ is the dry rock bulk density (g/cm$^3$). It was assumed that sorption is rapid, linear, and reversible.

In converting total VOC concentrations to equivalent porewater concentrations, average values for porosity ($\phi = 0.023$) and bulk density ($\rho_b = 2.66$ g/cm$^3$) were used based on core samples analyzed by Golder. Distribution coefficients were estimated using the correlation $K_d = K_{oc} f_{oc}$, where literature values were used for the organic carbon partitioning coefficients ($K_{oc}$) of 380, 92, and 86 mL/g for PCE, TCE, and c-DCE, respectively (Table 12.1, Pankow & Cherry, 1996). Fraction organic carbon ($f_{oc}$) was measured by the Organic Geochemistry Lab at UW, according to the procedure outlined by Churcher and Dickhout (1987). Based on 15 samples collected from MW-74 and MW-75, $f_{oc}$ ranged from 0.31 percent to 0.68 percent, with an average of 0.40 percent, which was used in the retardation factor estimates. Using these parameters, average retardation factors of 177, 44, and 41 were estimated for PCE, TCE, and c-DCE, respectively. For samples where the estimated porewater concentration exceeded the aqueous solubility (~240 mg/L for PCE and 1,400 mg/L for TCE), it is likely that DNAPL was present. However, such inferences must be made with caution, considering uncertainty in parameters used to estimate the porewater concentrations, particularly the estimated retardation factors (for example, the effect of metamorphism on the sorption capacity of the organic carbon is not known). Porewater detection limits were approximately 0.16 µg/L, 0.04 µg/L, and 6 µg/L for TCE, PCE, and c-DCE, respectively, using Equation 1 and the above parameter values, assuming MeOH detection limits of 0.1 µg/L for PCE and TCE and 5.5 µg/L for c-DCE, and 60 mL of MeOH and 100 g of rock sample placed in each jar. However, reporting limits are higher due to potential for minor cross-contamination as evidenced by VOC contamination in field and laboratory blanks collected and analyzed with the rock core samples.

The results of the USGS survey indicated the presence of numerous fracture features, including identification of several other crosscutting fractures.

## Geophysical Analysis

The United States Geological Survey (USGS) performed several geophysical tests during the installation and completion of the monitoring wells installed during the site characterization activities. Characterization techniques utilized by the USGS are summarized in Exhibit 5. Detailed methods for the geophysical investigations performed by the USGS at the Building 40 area are discussed in a USGS Open File Report (Williams & Paillet, 2002).

The results of the USGS survey indicated the presence of numerous fracture features, including identification of several other crosscutting fractures. While the imaging data clearly showed the fractures present in each borehole, those data do not indicate the degree of interconnection of the fractures or if the fractures are transmissive. In order to address those data gaps, the USGS completed intra- and interborehole flowmeter and fluid temperature/resistivity testing. Each of these tests were completed under ambient and short-term injection or pumping conditions. During the injection/pumping conditions, the flow rates varied from 1 to 6 gallons per minute. The results of the interborehole testing indicated the presence of approximately 14 transmissive flow zones, which consisted of single or very closely spaced sets of fractures. A major north-south trending fracture flow system was also identified during the testing. The transmissivity values calculated ranged from 0.1 to more than 250 square feet per day (see Exhibit 6).

## Multilevel Monitoring Wells

Nine monitoring wells were completed with multilevel monitoring systems to allow for the evaluation of VOC concentrations in groundwater with depth. These multilevel sys-

| Characterization Technique | Purpose | Results Summary |
|---|---|---|
| Borehole-wall image logs (acoustic and optical televiewer) | Delineate distribution and orientation of fractures | 79 fractures identified in 500 feet of open hole in 8 wells and coreholes |
| Fluid and flowmeter logs (heat pulse flowmeter, electromagnetic flowmeter). Integrated analysis with borehole-wall image logs. | Distribution of fracture-flow zones intersected by the monitoring wells and coreholes | 14 flow zones consisting of one to several fractures were detected in 500 feet of open hole in 8 wells and coreholes |
| Flowmeter model analysis (see Paillet, 2000) | Determine transmissivity and hydraulic head of flow zones | Calculated transmissivities and ambient hydraulic heads for identified flow zones |
| Cross-hole flow tests (see Paillet, 1998) | Hydraulic connections between flow zones | Identified a major fracture feature oriented in north-south direction |

**Exhibit 5.** Geophysical characterization techniques

| No. | Zone Depth (ft) | Zone Head (ft) | Transmissivity $ft^2$/day | | Storage | Hydraulic Connection | |
|---|---|---|---|---|---|---|---|
| | | | Single Borehole | Cross-hole | | Well No. | Zone Depth (ft) |
| 34 | 25 | 8.98 | 260 | 150 | 5.0E-05 | 71 | 65 |
| 34 | 25 | 8.98 | 260 | 100 | 5.0E-05 | 65 | 24 and 35 |
| 51 | - | 8.97 | - | - | - | - | - |
| 58 | 76 | 9.6 | 0.1 | - | - | - | - |
| 59 | 92 | 9.16 | 230 | 230 | 5.0E-05 | 71 | 65 |
| 59 | 92 | 9.16 | 230 | 230 | 1.0E-05 | 65 | 24 and 35 |
| 65 | 24<br>35 | 8.94 | 65<br>47 | 100 | 5.0E-05 | 34 | 25 |
| 65 | 24<br>35 | 8.94 | 65<br>47 | 100 | 1.0E-05 | 59 | 92 |
| 65 | 24<br>35 | 8.94 | 65<br>47 | 100 | 1.0E-05 | 71 | 65 |
| 65 | 78<br>88<br>110 | 9.1 | 37<br>3<br>3 | 80 | 1.0E-04 | 71 | 65 |
| 68 | 19 | 12.04 | 58 | - | - | - | - |
| 68 | 45 | 12.79 | 110 | - | - | - | - |
| 71 | 28 | 8.92 | 40 | - | - | - | - |
| 71 | 65 | 9.02 | 230 | 230 | 5.0E-06 | 59 | 92 |
| 71 | 65 | 9.02 | 230 | 150 | 5.0E-06 | 34 | 25 |
| 71 | 65 | 9.02 | 230 | 100 | 1.0E-05 | 65 | 24 and 35 |
| 71 | 65 | 9.02 | 230 | 80 | 1.0E-04 | 65 | 78, 88, and 110 |
| 72 | 49 | 6.5 | 7 | - | - | - | - |
| 72 | 75 | 6.5 | 59 | - | - | - | - |

**Exhibit 6.** Summary of estimated hydraulic properties of fracture-flow zones (Williams & Paillet, 2002)

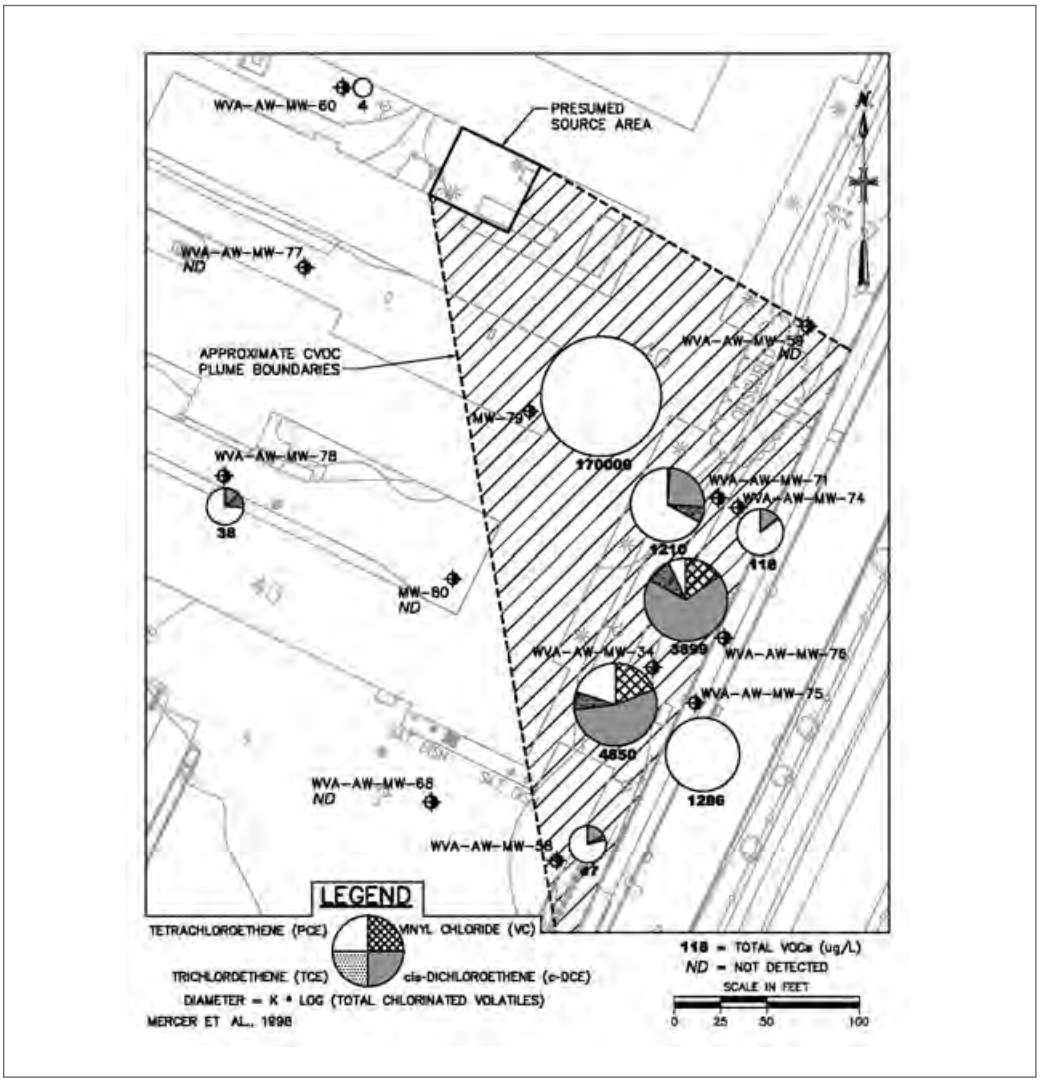


**Exhibit 7.** VOC distribution in groundwater (0–50 feet bgs)

tems were also used to evaluate fracture interconnectivity and hydraulic head distribution during subsequent testing. Multilevel monitoring well placement was based on the results of the discrete interval packer testing and the USGS geophysical analysis. Seven of the wells were completed with Westbay MP38 Multi-Level Sampling Systems. The remaining two wells were equipped with the Solinst Continuous Multi-Channel Tubing (CMT®) System.

## SITE CHARACTERIZATION RESULTS

### *Groundwater*

Exhibits 7, 8, and 9 present VOC concentrations in bedrock groundwater in the intervals from 0 to 50 feet bgs, 50 to 100 feet bgs, and 100 to 150 feet bgs, respectively. The data used to construct these figures were obtained from multilevel monitoring well sampling results, packer testing results, and long-term monitoring results. As shown on

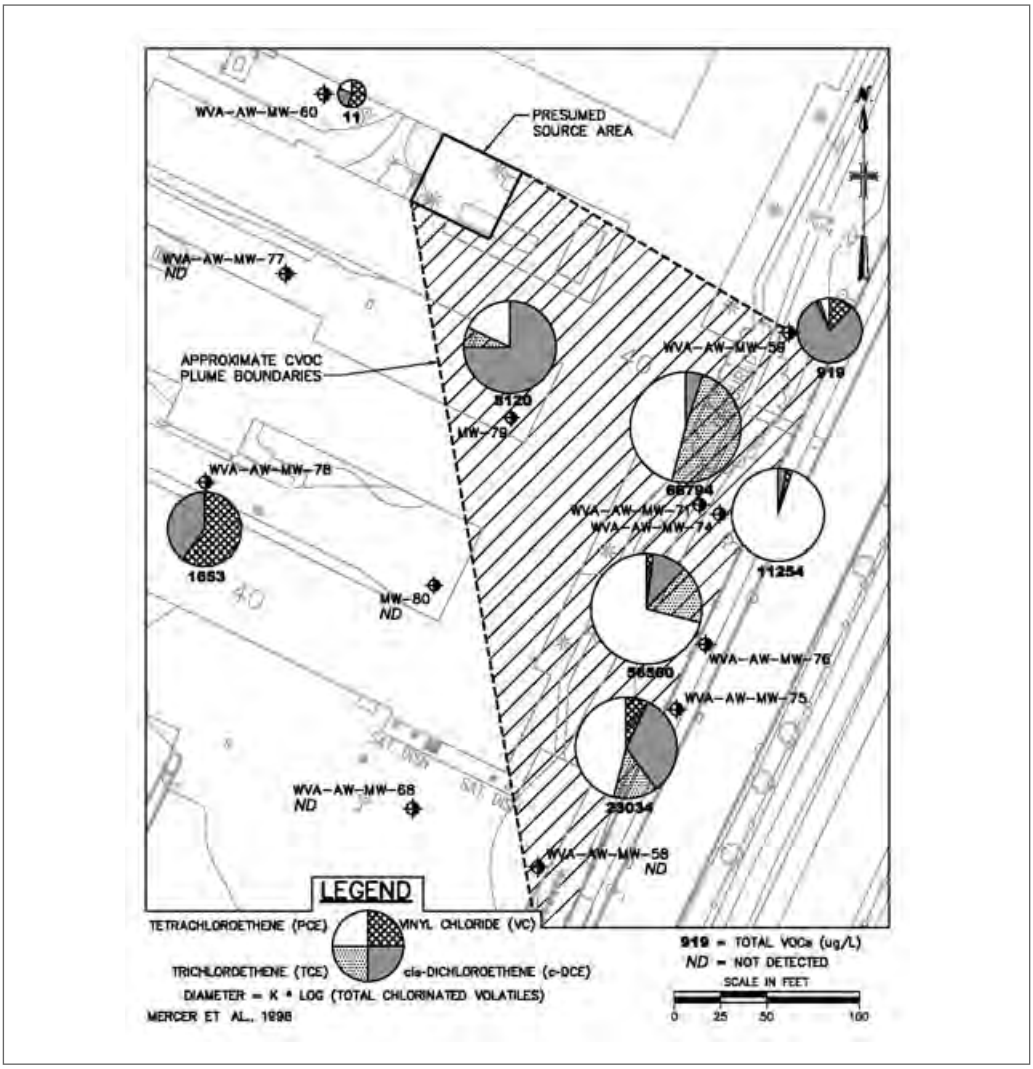


**Exhibit 8.** VOC distribution in groundwater (51–100 feet bgs)

these figures, the distribution of VOCs in the bedrock groundwater indicates a contaminant source in the northwestern portion of the building. This is supported by the fact that PCE was detected at a concentration of 170 mg/L in the 21 to 41 foot bgs interval in monitoring well MW-79, which is 85 percent of the aqueous solubility of PCE of 200 mg/L. The presence of PCE at such a high concentration near the bedrock surface suggests that monitoring well MW-79 is closer to a DNAPL source than the wells to the east of Building 40. The VOC distribution also indicates a predominant local bedrock groundwater flow direction toward the southeast.

## *Rock Matrix*

The results of the rock core VOC analyses conducted by the University of Waterloo show that several rock core samples contained PCE at estimated equivalent porewater concentrations approaching solubility. A representative rock core VOC profile from MW-87 (Exhibit 4) is shown in Exhibit 10.

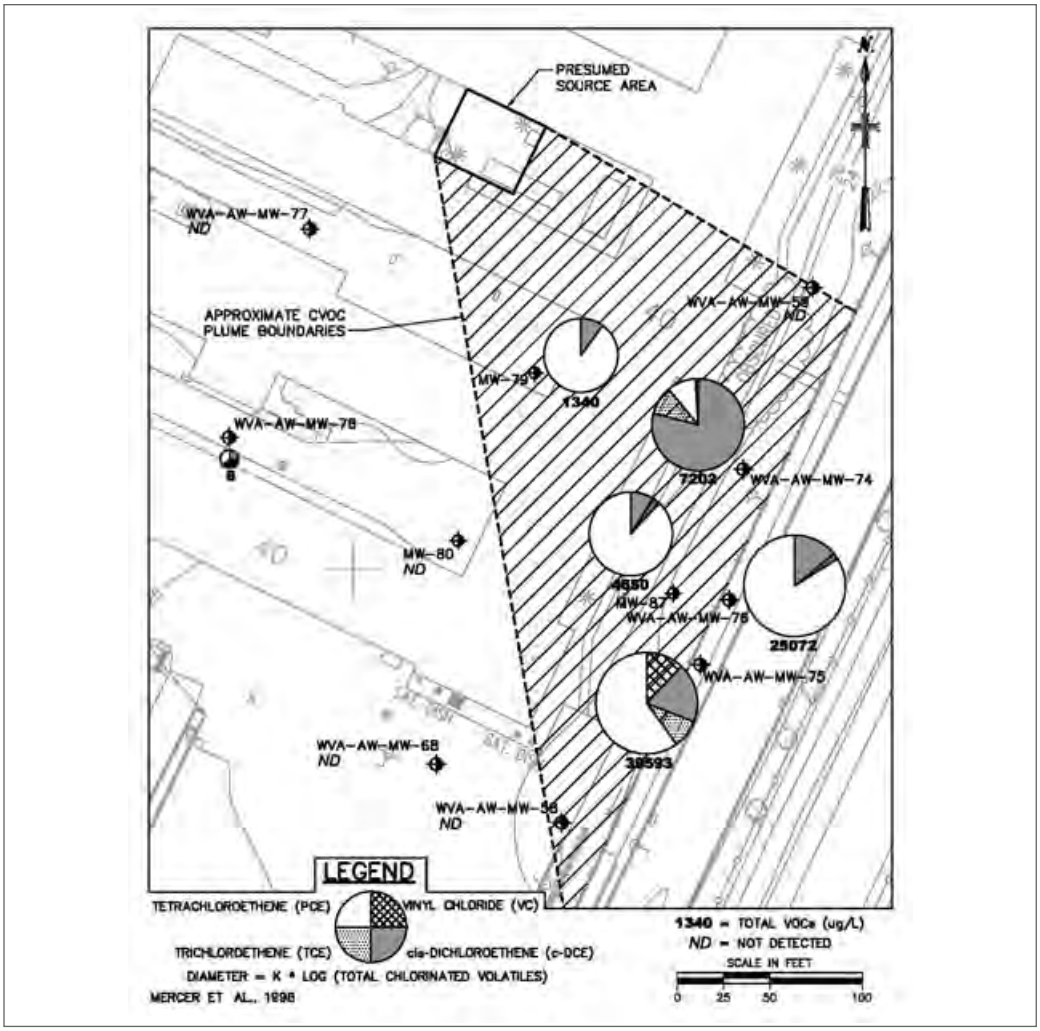


**Exhibit 9.** VOC distribution in groundwater (101–150 feet bgs)

The characterization data support the conceptual model in that although groundwater concentrations approaching solubility were detected in the bedrock fracture network, DNAPL was not observed in any of the fractures intersected by the borehole. At the same time, bedrock matrix porewater concentrations at and/or approaching solubility were detected in rock core samples collected in the same boreholes. The rock core data suggest contaminant transport in many fractures, indicating that the fracture network at the site is well connected. Since the storage capacity of the rock matrix is orders of magnitude greater than that of the bedrock fractures, these data confirm that the majority of the VOC mass is entrained in the rock matrix.

## *IN SITU* CHEMICAL OXIDATION PILOT STUDY

### *Pilot Study Overview*

In 2001 and 2002, an *in situ* chemical oxidation pilot study was conducted in the Building 40 area to evaluate the degree to which the VOCs in the bedrock groundwater and, more

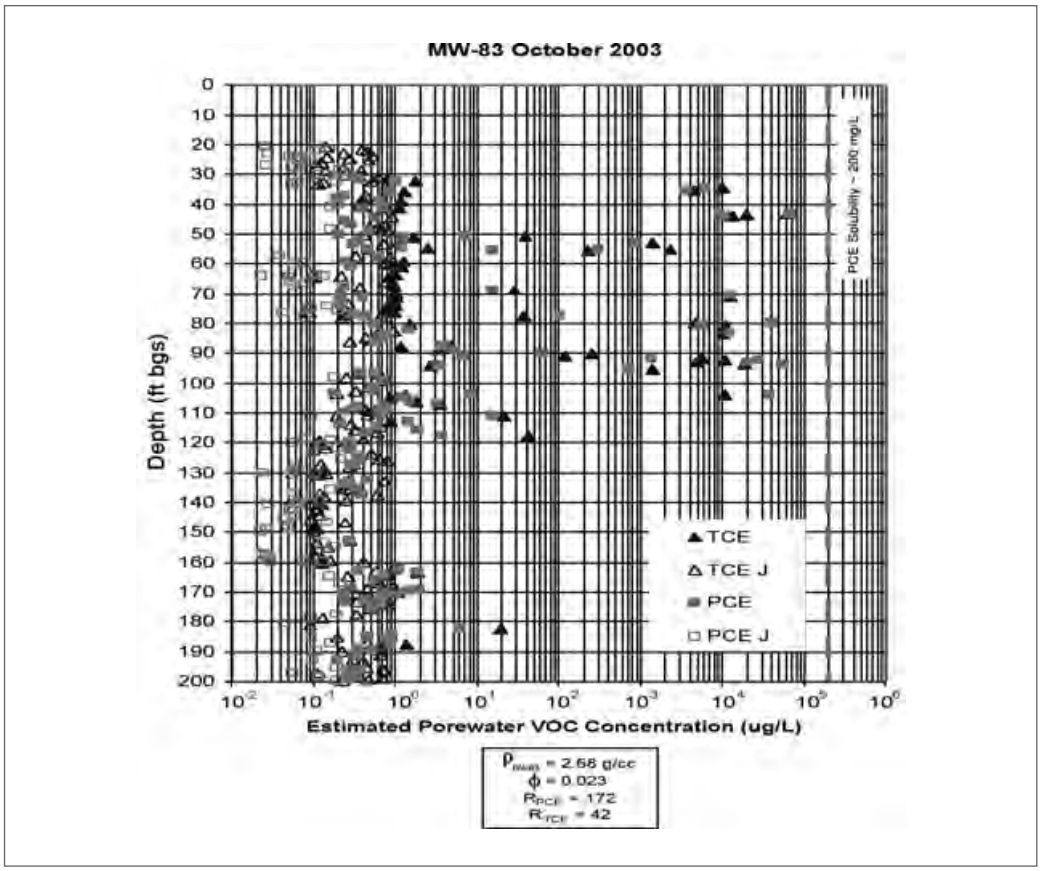


**Exhibit 10.** Example of VOC rock core sample profile

importantly, the bedrock matrix, could be treated using potassium permanganate ($KMnO_4$). $KMnO_4$ was selected as the oxidant because unreacted $MnO_4^-$ in solution is chemically stable and it can diffuse into media with low permeabilities (e.g., porous rock) over time. As contaminant concentrations decrease in the fractures following permanganate application, the concentration gradient leads matrix contamination to diffuse out of the rock matrix into the fractures. Application of excess $KMnO_4$ allows for diffusion of $MnO_4^-$ into the matrix at the same time as contamination is diffusing out of the matrix (i.e., the reactants move toward each other), speeding the treatment of aqueous and sorbed contamination within the rock matrix. The objectives of the pilot study were as follows:

- evaluate whether potassium permanganate could be effectively delivered and distributed through the bedrock treatment area;
- confirm that VOCs in the bedrock groundwater could be oxidized by the permanganate; and
- assess the persistence of permanganate in the subsurface.

The pilot study consisted of two phases of $KMnO_4$ solution application. The purpose of Phase 1 was to test delivery of $KMnO_4$ solution in a major transmissive zone (identified by geophysical testing) and monitor horizontal and vertical distribution in the contaminated area. Phase 2 was a longer-term permanganate delivery designed to flood certain areas with sufficient permanganate to evaluate residence time in the bedrock fractures.

In addition to the field portion of the pilot study, the University of Waterloo performed ongoing laboratory studies and numerical modeling to enhance understanding of field observations. These included rock oxidant demand (ROD) tests, permanganate invasion rate tests, and diffusion rate modeling. The methods and results of these studies will be presented in a separate publication.

## *Phase 1 $KMnO_4$ Injection*

At locations where permanganate was not detected, $Cl^-$ concentrations were generally stable.

During Phase 1 of the Pilot Study, approximately 8,000 gallons of a 2.5 percent solution of $KMnO_4$ were injected at MW-59 (Exhibit 4). MW-59 has its open interval between 76 and 96 feet bgs, and its static water level is typically 11 feet bgs. MW-59 was chosen for the Phase 1 injection because it intersects a highly transmissive zone that was expected (based on the geophysical tests) to be extensive and well connected over a large lateral and vertical area. During the injections, samples were collected from several wells and analyzed for field parameters (i.e., chloride, specific conductivity, and permanganate), as well as for VOC concentrations.

Specific conductivity was monitored as an indicator to impending arrival of $KMnO_4$ because a rise in specific conductivity can be measured prior to visually identifiable $KMnO_4$ due to dissolution of the potassium cation ($K^+$) and the permanganate anion ($MnO_4^-$). Since $MnO_4^-$ is consumed by reactions with VOCs and also organic carbon and minerals such as pyrite in the shale bedrock, it is expected that $K^+$ transport may be more rapid. As expected, increasing specific conductivities were measured prior to detection of permanganate at the locations where permanganate was later detected. Specific conductivities rose even at locations where $KMnO_4$ was not detected, reflecting the temporary increased ionic strength of groundwater in the vicinity of MW-59.

Chloride ($Cl^-$) was also monitored as an indicator to the impending arrival of $KMnO_4$. Since the oxidation of chlorinated solvents produces $Cl^-$. It was expected that $Cl^-$ would arrive at monitoring points before the $MnO_4^-$ front if it were pushed forward in advance of the reaction front. Contrary to expectations, $Cl^-$ concentrations decreased at most locations where permanganate was detected. At locations where permanganate was not detected, $Cl^-$ concentrations were generally stable. One possibility for why increased $Cl^-$ concentrations were not detected is that the increased ionic strength of the samples containing permanganate may have interfered with the chloride titration. Also, production of $Cl^-$ may not have been detectable because background concentrations of $Cl^-$ were relatively high, ranging from 200 to 350 mg/L.

## *Phase 2 $KMnO_4$ Injection*

Phase 2 consisted of $KMnO_4$ injections into MW-65 and MW-71 (see Exhibit 4) in April, May, and June 2002, with the purpose of flooding these areas and achieving $KMnO_4$ diffusion into the rock matrix. MW-65 and MW-71 were selected for the Phase 2 injections because they are both completed with Westbay® multilevel monitoring systems, which allow for the injection of $KMnO_4$ into multiple depth intervals in each well, either simultaneously or individually. During the Phase 2 injection period, MW-74 and MW-75, located adjacent to MW-71 and MW-65, respectively, were used as the primary monitoring locations. Both MW-74 and MW-75 are completed with Solinst® CMT multilevel monitoring systems. The Phase 2 injection fre-

quency was set at two weeks in order to maintain $KMnO_4$ concentrations of at least 1 percent for the duration of Phase 2.

All of the Westbay ports in both MW-65 and MW-71 were kept open during the injection period. Theoretically, when the $KMnO_4$ solution was fed into the casings and more than one port was open, the $KMnO_4$ entered each port at a relative rate in proportion to the transmissivity of each port interval. Thus, if one interval was much more transmissive than the others, it received nearly all of the injected volume. Both MW-65 and MW-71 have Westbay pumping ports situated at depth intervals with highly transmissive zones. Therefore, it is expected that the majority of the $KMnO_4$ solution left the Westbay systems through the ports associated with the high transmissivity zones. After completion of each Phase 2 injection, the high transmissivity Westbay ports were closed, and additional $KMnO_4$ solution was poured into the Westbay casings to bring the fluid level up to the ground surface with only the low transmissivity ports (i.e., port 3 in MW-71 and ports 4 and 6 in MW-65) open. This port configuration allowed for slow $KMnO_4$ distribution to the lower transmissivity zones in the bedrock. The $KMnO_4$ solution depth in the casing was monitored and adjusted as required to maintain at least five feet of head as compared to the highest open port. The permanganate solution levels in MW-65 dropped gradually; however, the MW-71 permanganate levels did not change, indicating that there was essentially no transmissivity in the open-port zones.

## *Pilot Study Monitoring*

The main objectives of the pilot study monitoring program were to confirm that the $KMnO_4$ being distributed in the fractured rock was, in fact, destroying chlorinated solvents and to assess the geochemical impacts on the system. During the pilot study, three synoptic sampling rounds were performed during which samples from all monitoring locations and depths in the pilot study area were collected and analyzed for VOCs, inorganic parameters, and $C_{12}/C_{13}$ isotopes.

A baseline sampling round was performed in February 2002, prior to Phase 1 injection. The two other full sampling rounds were performed in March 2002 and July 2002, immediately after the end of Phase 1 and Phase 2 injections, respectively. An additional full sampling event was performed in January 2003.

At the sampling locations where permanganate was detected, VOC concentrations diminished significantly, often to non detectable concentrations.

**Volatile Organic Compounds.** The results of VOC analyses from samples collected throughout the pilot study are shown in Exhibit 11. The March and July 2002 VOC results remained stable compared to the baseline pre-injection (February 2002) results, with the exception of the sampling locations where permanganate was detected during Phase 1 and Phase 2. At the sampling locations where permanganate was detected, VOC concentrations diminished significantly, often to nondetectable concentrations.

**Carbon Isotopes.** Carbon isotope ($\delta^{13}C$) analyses were performed to verify that decreases in VOC concentrations were the result of chemical oxidation, not displacement or other physical mechanisms. The method is based on the laboratory observation that $KMnO_4$ oxidation is preferential for the lighter isotope (i.e., destroys $^{12}C$ more rapidly than $^{13}C$), which causes the remaining VOC carbon to become enriched in the heavier isotope (i.e., $\delta^{13}C$ values become more positive). The University of Waterloo group has developed a method that enables the $\delta^{13}C$ analyses to be performed on samples contain-

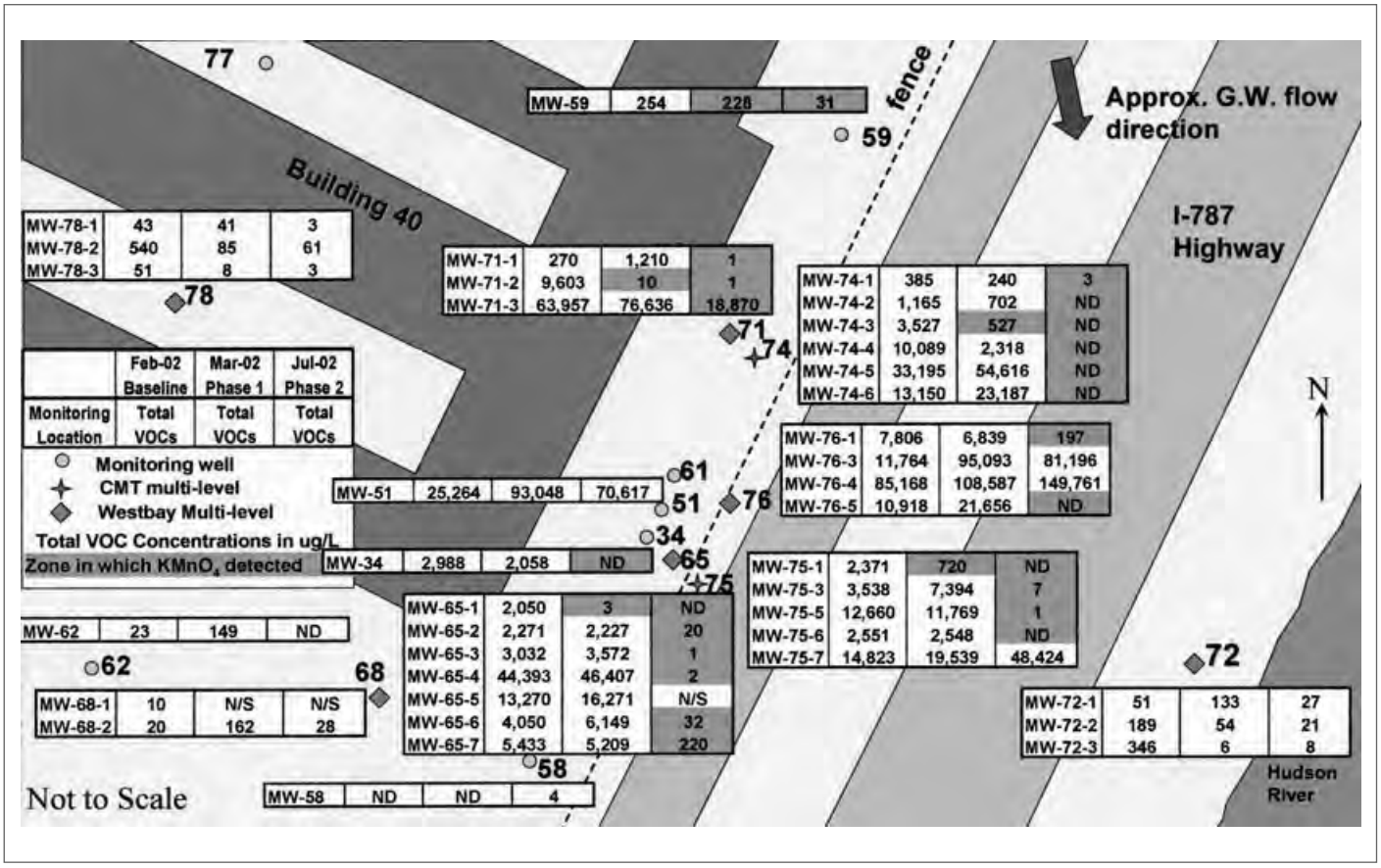


**Exhibit 11.** Pilot study VOC results

ing very low VOC concentrations. This is important because successful remediation causes the VOC concentrations to decline to very low levels and then to absence in many places. Representative sample results from monitoring zone 1 in MW-65 (i.e., MW-65-1) are shown in Exhibit 12. Significant isotopic shifts were observed on March 7, 2002, the day $KMnO_4$ was first detected at this location. In general, the extent of the isotopic shift effect increased as the number of substituted chlorines decreased. These data provided evidence of chlorinated VOC destruction.

Inorganic Parameters. As expected, at wells impacted by $KMnO_4$, concentrations of potassium rose significantly, from an average of 8 mg/L to 591 mg/L, while manganese

| Well ID | Date Sampled | PCE (ug/L) | TCE (ug/L) | c-DCE (ug/L) | Carbon Isotope ($\delta^{13}C$) PCE (‰) | TCE (‰) | c-DCE (‰) |
|---|---|---|---|---|---|---|---|
| MW-65-1 | 20-Feb-02 | 387 | 166 | 1356 | -30.57 | -30.03 | -31.65 |
| MW-65-1 | 06-Mar-02 | 1,961.5 | 387.6 | 1,948.8 | -30.86 | -34.22 | -31.76 |
| MW-65-1 | 07-Mar-02 | 1,282.6 | 4.9 | 210.4 | -19.48 | nd | 45.03 |
| MW-65-1 | 18-Mar-02 | 3.4 | nd | nd | nd | nd | nd |

**Exhibit 12.** Carbon isotope sample results for MW-65-1

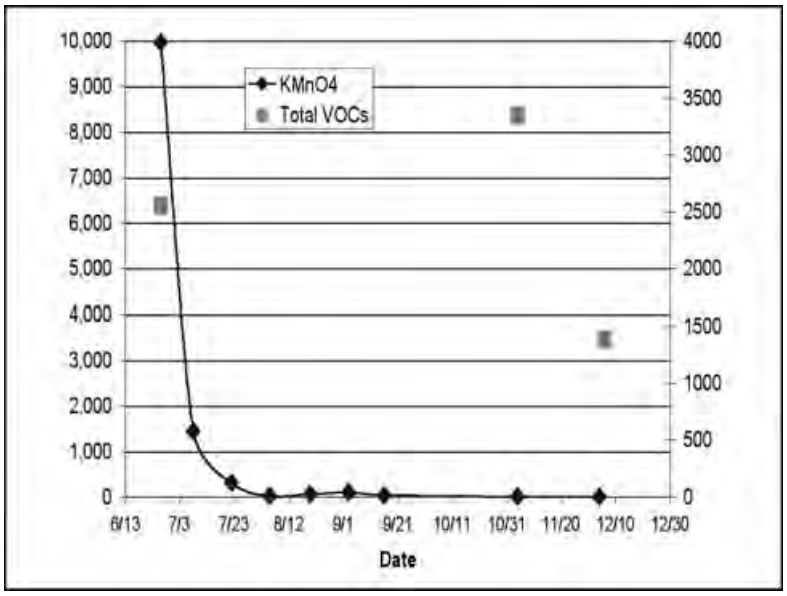


**Exhibit 13.** Rebound results at MW-75-6

($Mn^{2+}$) concentrations increased from an average of 0.5 mg/L to 179 mg/L. Sulfate concentrations also rose significantly, from an average of 38 mg/L to 868 mg/L. This is likely due to oxidation of reduced sulfur in pyritic minerals in the rock matrix and the presence of hydrogen sulfide in groundwater at greater depths. The geochemical changes that were observed are expected to have been temporary, and pre-injection conditions were likely reestablished after $KMnO_4$ concentrations diminished.

## *Rebound Monitoring*

It was anticipated that after the Phase 2 injections ceased, $KMnO_4$ concentrations would gradually diminish to below detection and VOC concentrations would gradually rise. This rebound in VOC concentrations is due to reverse diffusion from the rock matrix and cross-flow that can transport VOCs into the treated zone from any untreated zones (and flush injected $KMnO_4$ solution out of the monitored zones). Rebound monitoring was conducted to monitor the rate of $KMnO_4$ dissipation and subsequent VOC concentration rebound.

Monitoring wells 34, 74, 75, and 76 were selected for the rebound monitoring program because these wells all contained permanganate in at least one monitoring zone at the end of Phase 2 injections. During rebound monitoring, samples were analyzed for field parameters, including permanganate and chloride. Samples were analyzed for VOCs only if there was little or no permanganate in the sample.

Rebound monitoring results for MW-75-6 are shown in Exhibit 13. Rebound monitoring showed that permanganate persisted in the majority of the monitoring zones throughout the monitoring period (i.e., from June to December 2002). At many monitoring zones, there was a sharp decline in the permanganate concentration within the first one to three months of monitoring, followed by a slower decline as monitoring

continued. A January 2003 synoptic sampling event showed that VOC concentrations in groundwater rebounded from nearly nondetectable levels to their pre-injection concentrations within six months after $KMnO_4$ injections were halted.

## CONCLUSIONS

The site characterization showed the majority of the VOC mass in the bedrock aquifer in the vicinity of Building 40 is entrained within the shale bedrock matrix as aqueous and sorbed phase—not in the bedrock fractures. This confirmed the conceptual model and indicated that remediation of the site will require treatment of the rock matrix. The characterization also showed that the bedrock fracture network is interconnected and that the majority of the groundwater flow is present in a north-south trending fracture complex. The pilot study demonstrated that $KMnO_4$ could be distributed both vertically and horizontally throughout the treatment area using a small number of injection points. Carbon isotope analyses proved that VOC mass was destroyed during the pilot injections, as opposed to being displaced.

The results of the site characterization and pilot study have been used to design a full-scale corrective measure (CM) that focuses on source remediation through the treatment of the shale bedrock matrix as well as treatment of the VOCs in the bedrock groundwater. The CM, scheduled to start in summer 2004, involves the injection of high concentrations of sodium permanganate ($NaMnO_4$) into the bedrock aquifer using a phased injection process. Use of $NaMnO_4$ allows application of higher oxidant concentrations compared to $KMnO_4$ since the solubility limit is much higher. Injection of the permanganate will be performed for a period of five years, after which five years of groundwater monitoring will be conducted to evaluate long-term groundwater concentrations and the degree to which natural attenuation further decreases groundwater concentrations. Between injections, permanganate will be allowed to passively enter the system via the placement of solid permanganate pellets into the injection wells. VOC mass reduction will be evaluated through groundwater monitoring and mass flux analysis.

## ACKNOWLEDGMENTS

The U.S. Army Corps of Engineers, under Contract No. DACW31-94-D-0017, provided funding for this project. Stephen Wood and Grant Anderson of the U.S. Army Corps of Engineers, Baltimore District, provided project management and technical support. JoAnn Kellogg of the Watervliet Arsenal provided on-site support.

## REFERENCES

Churcher, P. L., & Dickhout, R. D. (1987). Analysis of ancient sediments for total organic carbon—Some new ideas. Journal of Geochemical Exploration, 29, 235–246.

Mercer, J. W., Noel, M. R., & Durant, N. D. (1998, December). Contaminant source identification based on chemical and degradation products distributions. The Professional Geologist, pp. 4–7.

Paillet, F. L. (1998). Flow modeling and permeability estimation using borehole logs in heterogeneous fractured formations. Water Resources Research, 34, 997–1010.

Paillet, F. L. (2000). A field technique for estimating aquifer parameters using flow log data. Ground Water, 38, 510–521.

Pankow, J. F., & Cherry, J. A. (Eds.). (1996). Dense chlorinated solvents and other DNAPLs in groundwater. Portland, OR: Waterloo Press.

Parker, B. L., Gillham, R. W., & Cherry, J. A. (1994). Diffusive disappearance of immiscible-phase organic liquids in fractured geologic media. Ground Water, 32, 805–820.

Parker, B. L., McWhorter, D. B., & Cherry, J. A. (1997). Diffusive loss of nonaqueous phase organic solvents from idealized fracture networks in geologic media. Ground Water, 35, 1077–1088.

United States Environmental Protection Agency (US EPA). (2001). The state-of-the practice of characterization and remediation of contaminated ground water at fractured rock sites. Office of Solid Waste and Emergency Response. EPA 542-R-01-010. Retrieved July 27, 2004, from http://www.clu-in.org/pub1.cfm

Williams, J. H., & Paillet, F. L. (2002). Characterization of fractures and flow zones in contaminated shale at the Watervliet Arsenal, Albany County, New York. USGS Open-File Report 01-385. Retrieved July 27, 2004, from http://water.usgs.gov/ogw/bgas/publications/OFR-01-385/

---

**Kenneth J. Goldstein** is a vice president at Malcolm Pirnie, Inc. in White Plains, New York. He is a certified groundwater professional and hydrogeologist with over 20 years of experience in contaminant hydrogeology. His focus is on the development and implementation of *in situ* remedial technologies for the restoration of sites contaminated by chlorinated hydrocarbons, petroleum hydrocarbons, and heavy metals.

**Andrew R. Vitolins** is a project hydrogeologist at Malcolm Pirnie, Inc. in Albany, New York. He is a professional geologist and has over nine years of experience in environmental restoration and water resources.

**Daria Navon** is a project engineer at Malcolm Pirnie, Inc. in Tampa, Florida. She is a professional engineer with eight years of experience in remedial investigation and design at hazardous waste sites.

**Beth L. Parker** is a research assistant professor in the Department of Earth Sciences at the University of Waterloo, Ontario, Canada. Her research focuses on field characterization and behavior of industrial organic contaminants in fractured and unfractured low-permeability geologic media and in sandy aquifers, with an emphasis on the interplay of molecular diffusion with other processes affecting contaminant behavior, and also on the development of new techniques for site investigation and remediation.

**Steven Chapman** is a research hydrogeologist in the Department of Earth Sciences at the University of Waterloo, Ontario, Canada. He is a professional engineer with a master of science degree (Hydrogeology) from the University of Waterloo, and has ten years of experience in site characterization, remediation trials, and modeling at contaminated sites.

**Grant A. Anderson** is a professional geophysicist/hydrogeologist with the U.S. Army Corps of Engineers, Baltimore District. He has 25 years of experience in environmental and exploration geophysics, ordnance detection, hydrogeology, groundwater modeling, and remedial system design.

---

**Appendix G**

Parker, EPA/NGWA Portland Conference Paper, 2007

**Chlorinated Solvent Source and Plume Behavior in Fractured Sedimentary Rock from Field Studies (former title)**

**Investigating Contaminated Sites on Fractured Rock Using the DFN Approach**

Beth L. Parker

Professor and NSERC Chair in Groundwater Contamination in Fractured Media,
School of Engineering, University of Guelph
Guelph, Ontario, Canada N1G 2W1
bparker@uoguelph.ca
Tel: 519-824-4120 Ext. 53642

**Abstract**

This presentation provides an overview of a major field - focused program of studies aimed at improved investigation methods and understanding organic contaminant source zones and plumes in fractured porous sedimentary rock. This research began in 1997, when intensive field studies were initiated at a TCE contaminated site on steeply dipping and faulted sandstone in California. Now, with collaborations involving several disciplines (analytical chemistry, mathematical modelling, geophysics, microbiology), the program includes three other sites contaminated with chlorinated solvents in addition to the California site: a Wisconsin site on flat-lying sandstone and two sites in Ontario on flat-lying dolostone. These four sites have important differences so that they are broadly representative of sedimentary rock but they have several aspects in common, including: much site data from earlier conventional investigations, contamination initially caused decades ago by DNAPL flow into the rock, sufficient matrix porosity (2-20 %) to allow diffusion-driven chemical mass transfer between fractures and the rock matrix causing strong influence on contaminant behaviour, deep contaminant occurrence (greater than 350 m below ground surface at one site), and each site receives much regulatory attention. Also, the plume fronts advance at rates much slower than the average linear groundwater velocity in the fracture networks. Based on the field results obtained to date, a general conceptual model for the formation and long-term evolution of source zones and plumes in fractured porous sedimentary rock is proposed. This conceptual framework is being tested and the various processes quantified through field investigations using a suite of high-resolution techniques that I refer to as the **d**iscrete-**f**racture **n**etwork (DFN) investigation approach. This then allows application of DFN numerical models, such as FRACTRAN and HydroGeoSphere, to simulate flow and contaminant transport at these sites. Conventional field methods used in fractured rock studies are poorly suited for plume delineation or characterization and therefore, new methods are being developed and used at all of the sites. In the DFN approach, emphasis for data acquisition is on data specific to individual fractures and the fracture network as well as the rock matrix blocks between fractures so that the characteristics and interactions between these two domains can be discerned. Hence, the spatial scale of measurements on continuous rock core and also in the core holes must be exceptionally detailed. Rock core contaminant analyses at each site confirm that nearly all of the contaminant mass now resides in the low-permeability rock matrix although the down-gradient transport occurs in numerous, well-connected fractures. Therefore, quantifying the interactions between these domains is

essential for improving the understanding of individual site conditions regarding the prediction of plume behavior and/or response to site remediation. The investigations at the field sites will continue for several years.

## Introduction and Background

The behaviour of contaminants in fractured rock is now one of the few remaining scientific frontiers in physical hydrogeology. The status of knowledge concerning groundwater flow and contaminant migration in fractured rock has been reviewed by the U.S. National Research Council (NRC, 1996), Lapcevic et al. (1999), Berkowitz (2002) and Neuman (2005). These reviews detail considerable published literature concerning the conceptual nature of fractures and hydraulic conditions in fracture networks based on borehole investigations in uncontaminated fractured rock (primarily based on work by the petroleum industry, USGS studies of the Mirror Lake granitic system in New Hampshire and investigations of prospective radioactive waste repositories). Furthermore, many publications concern mathematical models representing hypothetical or idealized fracture networks for contaminant behaviour in fractured rock systems (e.g., Smith and Schwartz, 1984; 1993; Sudicky and McLaren, 1992; Therrien and Sudicky, 1996; and many others). However, these modelling endeavours generally do not represent actual field sites or any particular type of rock, and field data of actual contaminant distributions and contaminant behaviour in fractured rock, particularly sedimentary rock, are almost non-existent.

Current concepts for the nature of contaminant plumes in fractured rock are quite speculative and parameterization of model inputs is inadequately supported by field data. Although many techniques for borehole logging and hydraulic testing exist (e.g. review by Sara, 2003), general agreement in the literature indicates these techniques are severely limited in their prospects for providing quantitative information about the length and interconnectivity of the fractures in fracture networks (NRC, 1996; Berkowitz, 2002). Unlike behaviour in igneous rock, contaminants in sedimentary rock can reside predominately in the porous rock matrix while downgradient transport occurs in the fractures. Therefore, determination of the contaminant distribution in sedimentary rock requires measurement of contaminant concentrations in both the fracture network and the rock matrix. Most literature pertaining to groundwater flow and solute behaviour in fractured rock concerns igneous rock such as granite. Several countries have proposed creation of deep repositories for radioactive waste in granitic rock and the search for and assessment of prospective sites has involved intensive field studies. However, these studies have not involved existing contaminant plumes as such plumes do not (yet) exist in these environments (i.e., no radioactive waste has been disposed of in this type of rock). The research has included tracer experiments but their spatial scale is small in relation to the relevant plume scale. The literature contains no well-documented cases of industrial contaminant plumes in any type of fractured rock.

In essence, the state of knowledge at this time concerning actual contaminant plumes in fractured rock is where the understanding of contaminant plumes in granular porous media (sand & gravel aquifers) was in the 1950's. Back then, vague concepts existed for plumes but no plumes had been delineated / characterized in any detail to show what reality was really like. However, the difficulty of the challenge posed by fractured rock is much greater

than that posed then by granular media because the scale of variability and complexity imposed by fracture networks is so much greater, as well as increased costs per borehole given greater depths and need for comprehensive monitoring is so much greater. Also, an important contribution to the understanding of contaminant behaviour in granular aquifers has been large-scale, natural-flow tracer experiments with detailed 3-D monitoring to examine effects of heterogeneity on dispersion (e.g. Sudicky 1986, Garabedian et al. 1991). Such natural-gradient experiments at relevant spatial scales have not been conducted in fractured rock and are generally cost-prohibitive. Therefore, for fractured rock there is no alternative but to rely on intensive studies of actual contaminated sites to gain insights concerning plume formation and evolution and quantify the influences of the various processes such as advection, dispersion and degradation. In essence, the plumes represent long-term, large-scale tracer experiments, and is the thrust of my research program in fractured sedimentary rock at the University of Guelph based in Ontario, Canada.

**Origin and Nature of the DFN Approach**

Ten years ago I initiated use of chemical analyses (rock core VOC analyses) done at very closely spaced vertical intervals on contaminated sandstone core in the style presented in Figure 1 to determine the nature of the contaminant distribution at a location in California where TCE had entered sandstone decades earlier and this has led to a systematic way for investigating contaminated bedrock following what I now refer to as the discrete - fracture network (DFN) approach represented in the Figure 2 flow chart. This core-focused field study grew out of conceptual modelling supported by analytical modelling concerning dissolution and diffusion effects on chlorinated solvent DNAPL in fractured porous geologic media represented by fractured clay and fractured sandstone with literature derived parameters (Parker et al., 1994; 1997). From the rock core analyses done at the California sandstone site mentioned above, it was evident that the DNAPL had initially flowed primarily downward through a network of many interconnected fractures, spaced 1-5 m apart, and that over the subsequent years or decades, all or nearly all of the immiscible phase liquid has been transferred by dissolution and diffusion into the rock matrix blocks between the fractures where the mass now resides in the dissolved and sorbed phases. Comparison of the rock core contaminant profiles with groundwater analyses done on samples from conventional monitoring wells and multilevel systems (MLSs) showed that these water analyses gave misleading results because of effects of vertical flow in the holes when the holes were open, allowing cross contamination between fractures with different initial concentrations (Sterling et al., 2005). Conventional methods of borehole geophysics and hydrophysics also gave misleading results about flow in the sense that the aim is to understand the flow in the fracture network during ambient conditions not the disturbed flow imposed by the open borehole. From this initial experience a decade ago and subsequent experience at other sites where the rock core VOC analyses method has been applied, the DFN approach was designed to determine the distribution, transport and fate of contaminants in sedimentary rock and it has now been applied to some degree at more than 18 sites with chlorinated solvent contamination, from which four were selected as focus of a long-term intensive field studies. Two of these are in the USA (California and Wisconsin) and two in Canada (Cambridge and Guelph in the Province of Ontario). Table 1 provides a summary of the hydrogeologic conditions.

Chlorinated solvents have been in the subsurface beneath many industrial properties for several decades allowing plumes to migrate down-gradient several hundreds to thousands of metres or more. These contaminants can now serve as tracers to study contaminant migration over the relevant large space and time scales most relevant in contaminant hydrogeology. Chlorinated solvent compounds are not naturally occurring in the environment, hence, even extremely low level detects (possible due to exceptional measurement sensitivity) serve as reliable evidence of contamination over several orders of magnitude. The physical and chemical properties of the common chlorinated solvents make them good indicators of the physical hydrogeologic system characteristics, including the fracture network connectivity and distribution of groundwater flow.

**Table 1:** Summary of contaminant types, site hydrogeology and causes of the contamination at the four field research sites.

| Field Site/ Owner | Rock Type | Major Parent Chemicals | Degradation Products (in order of abundance) | Entered ground water (main period) | Water table depth and Max. cont. depth (meters bgs) | Overburden Thickness and Type (meters) | Cause of Contamination/ Comments |
|---|---|---|---|---|---|---|---|
| Cambridge Ontario | Dolostone aquifer on shale aquitard; flat lying | Metolachlor, TCE | None | 1978-1990 | 20m<br>150 m into shale | 25-35 Glacial; sand and silt, and thin basal till | Agricultural chemical packaging; no DNAPL found; metolachlor plume goes to a municipal well; below MCLs; |
| Guelph, Ontario | Dolostone aquifer on shale aquitard; flat lying | TCE, minor PCE | cis-DCE, VC | 1990s | 3-4 m<br>50 m but may be deeper | 3-5 Till | Auto-parts manufacturing; small lateral plume extent expected; no DNAPL found |
| Simi, California | Sandstone with siltstone, shale interbeds; 30° dip | TCE, minor TCA | cis-DCE, 1,1-DCE, t-DCE, VC | 1950s-1960s | 15- 100 m<br>>300 m | 0-5 Alluvium | Rocket engine testing, research; many plumes from many different source areas; no DNAPL found<br>NE area focus |
| Wisconsin | Sandstone and minor dolostone with minor siltstone; flat lying | PCE, TCE, TCA, Ketones | cis-DCE, 1,1-DCA, 1,1-DCE, VC | 1950s-1960s | above grade-25 m<br>Nearly all mass shallower than 60 m | 7-40 Glacial sand, silt and clay layers | Solvent recycling; plume extends ~3km from source zone; 35,000L DNAPL pumped out and residual DNAPL remains |

The research based on the DFN approach applied at the four study sites has two general goals:

(1) to develop and demonstrate the effectiveness of an approach that relies on several new field methods for determining the nature, extent and controls on the transport and fate of organic contaminants in fractured sedimentary rock; and

(2) to develop a field-verified general conceptual model for contaminant migration and fate in fractured sedimentary rock with emphasis on chlorinated solvents.

The overall approach is to perform 3-D high resolution characterization and associated process studies based on the DFN framework where both the fracture network and matrix properties are studied in appropriate detail at the four study sites. Organic

contaminants of industrial origin have existed in the rock at these sites for decades while migrating primarily under natural groundwater flow conditions. The sites offer appropriate diversity in characteristics (Table 1) to provide a strong framework for assessing the general conceptual model.

The research goal is to understand the formation and evolution of existing relatively extensive contaminant plumes and investigations of the groundwater flow governing the plumes must be directed at the flow conditions causing contaminant transport. This flow is referred to here as the natural or ambient flow regime, even though there may be influences caused by pumping of water supply wells. This emphasis on natural flow conditions is an important distinction in the DFN approach because it means that flow conditions created by open boreholes or imposed during hydraulic testing are only minimally relevant. The challenge, therefore, is to develop methods for borehole data acquisition that pertain most directly to the ambient flow in the fracture network. Essentially all conventional fractured-rock borehole test methods relevant to the hydraulic conditions and properties, except for depth-discrete multilevel monitoring, (see comprehensive review by Sara, 2003), are done in open holes into which data acquisition equipment is inserted downhole. Flow metering, fluid resistivity and conventional downhole temperature logging and full-hole borehole dilution tests pertain to imposed (forced advection) hydraulic conditions, by applied fluid pressure as in the case of packer tests or vertical flow in the open hole caused by the hole itself (borehole cross connection between fractures). Therefore, in this research program, emphasis is on identifying and /or developing new methods aimed at understanding the borehole properties and flow regime under the ambient flow conditions. Price and Williams (1993), Sterling et al. (2005) and others have demonstrated that open holes in fractured rock commonly have borehole cross connection that disturbs the hydrochemical conditions. Hence, minimizing borehole cross connection is necessary while data are being acquired from the holes, a particularly important caution when investigating contaminated zones. Immediately after drilling each hole, the hole is sealed, usually using a FLUTe liner but sometimes using packer strings or the Solinst continuous modular packer system. In addition to the prevention of cross connection, FLUTe lined holes provide two other advantages: measurements of hydraulic conductivity continuous down the hole when the liner is first installed and temperature profiling in the water column inside the installed liner.

**Figure 1**: Schematic diagram illustrating use of rock core contaminant analyses to identify migration pathways by identification of diffusion haloes associated with active fractures.

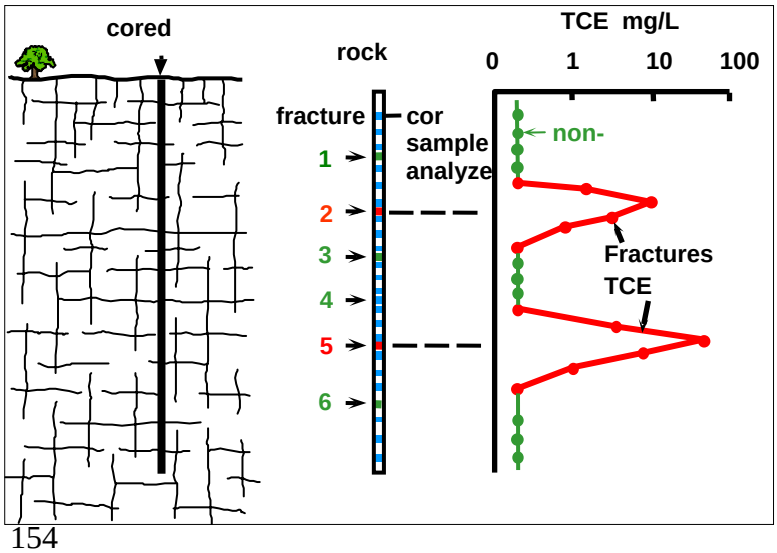


The studies are directed at understanding the behaviour and fate of contaminants, primarily common volatile organic contaminants (i.e. chlorinated solvents), in fractured sedimentary rock with emphasis on the formation and evolution of plumes (spatial scales of 100s to 1000s of meters in longitudinal extent), and therefore, the research

seeks to conduct those field and laboratory measurements needed for this particular scale of understanding. Although several numerical discrete-fracture-network (DFN) models exist for simulating contaminant transport and fate at the plume scale, no actual plumes at fractured rock field sites have been monitored at the range of scales necessary for both the fracture network and the matrix conditions needed to calibrate or verify any of these models.

**Figure 2**: DFN approach for site study

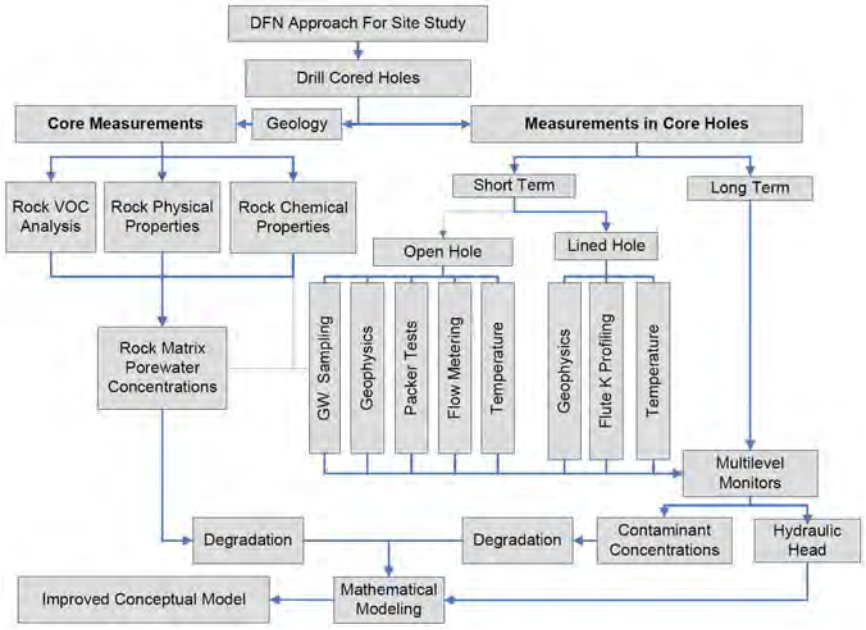


## Role of Rock Core Contaminant Analyses

The distribution of contaminants within chlorinated solvent plumes in fractured sedimentary rock has strong spatial variability due to heterogeneity in source zone contaminant mass distributions, fracture network and matrix characteristics accompanied by temporal variability in groundwater flow. To measure the scale of these variabilities requires application of a specific combination of unconventional and conventional field and laboratory methods. The research activities involve development and testing of several methods recently developed to complement the existing array of tools and techniques to advance the depth-discrete data sets to support the DFN field approach (Figure 2).

One major reason why so little is known about contaminant migration and fate in fractured sedimentary rock is that traditional research approaches involve only sampling water from the fractures. However, field studies using the rock core VOC analysis method show contaminant mass storage is dominated by the rock matrix rather than the fractures, and the contaminant concentrations in the fractures and the matrix are not in equilibrium (Hurley and Parker, 2002; Sterling et al., 2005; Parker et al., in review). This disequilibrium between fracture and matrix zones is evident in the rock core concentration profile from the California site shown in Figure 3. Therefore, sampling only the groundwater from the fractures cannot provide the overall mass distribution. Furthermore, when conventional boreholes are drilled, the water from a fracture in one section of the borehole migrates to another section of the borehole due to differences in head between the two sections. This creates an un-natural flow and contaminant transport condition within the system known as borehole cross-connection.

This condition will also persist across the screened interval of a conventional monitoring well, and as a result, results from sampling the well do not reflect the natural system (Price and Williams, 1993; Sterling et al., 2005).

Rock core analyses provide contaminant mass and phase distributions more relevant to contaminant behaviour than those obtained from monitoring wells or other types of borehole water sampling alone. The determination of the nature and extent of the contamination, with emphasis on elucidating the internal anatomy of contaminant plumes (including contaminant distribution in the rock matrix where groundwater is nearly immobile due to low permeability), is the foundation for understanding the processes governing the contaminant distribution.

**Figure 3**: Example of rock core analysis results for TCE in sandstone at a location near TCE DNAPL source zone at the California site. All analyses are much below TCE solubility indicating lack of DNAPL presence. (modified from Sterling et al. 2005)

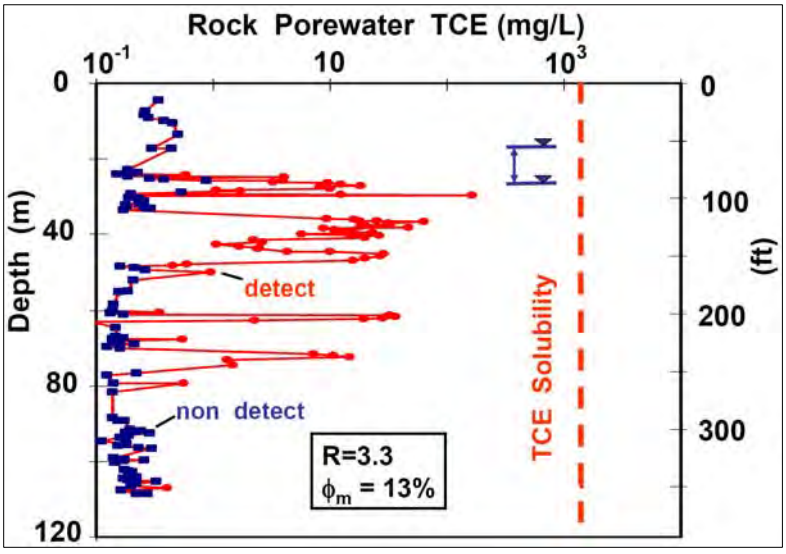


The rock-core based approach has several advantages over conventional methods for contaminant investigations in fractured sedimentary rock. For example, it provides a time-integrated finger print of plume behaviour. In the rock matrix block, the extent of the halo evolving outward from each fracture can increase over several decades, depending on the duration of the dense, non-aqueous phase liquid (DNAPL) source. This allows the halo extent to be used as an indicator of the age of contamination (time since contaminant arrival) on a fracture by fracture basis. In contrast to analyses pertaining to the rock matrix, which generally has low permeability, groundwater sampling in the borehole using depth-discrete multi-level groundwater monitoring systems allows the current chemical concentrations in the hydraulically active factures to be determined and permits evaluation of plume variability over time. However, drilling and related borehole cross connection effects can influence the results of groundwater sampling. The rock core analysis method avoids this problem because the low permeability matrix is not easily cross connected during drilling and core retrieval prior to sample collection (Sterling et al., 2005). In addition, the rock core contaminant analyses provide a direct measure of contaminant mass storage because the pore space in the rock matrix constitutes nearly the entire contaminant mass storage volume; the exception is the potentially large contaminant mass percentage stored in the fractures if DNAPL persists. However for the rock core analyses to show the actual mass distribution with useful accuracy, the samples must be collected from the core at closely spaced interval (Lawrence et al., 2006).

## General Conceptual Model

Parker et al. (1994; 1997) proposed a new conceptual model for chlorinated solvent DNAPL source zones, supported using analytical models for DNAPL behaviour in water-saturated fractured porous media such as clay and sedimentary rock. In this model, the immobile DNAPL film in the fracture dissolves into the contiguous water film in the fracture, establishing an aqueous concentration gradient driving mass into the porous matrix by diffusion. This mass transfer can cause complete dissolution of the DNAPL phase after some period of time that depends on the thickness of the DNAPL film (i.e., fracture aperture and initial fracture DNAPL saturation) and the diffusion driven mass transfer rate into the matrix; however, this time is short relative to the time elapsed since contamination of these sites (decades ago). Building on the work of Parker et al. (1994; 1997), VanderKwaak and Sudicky (1996) developed a numerical model to show the dissolution time is dramatically shortened when active groundwater flow is present in the fracture containing the DNAPL. In this model, the 'source zone' evolves relatively rapidly (i.e., DNAPL dissolution followed by continued changes in concentration distribution and contaminant flux from the source to the plume) and has a strong influence on plume development and internal concentration behaviour. The lack of DNAPL persistence in all or major parts of the source zone represents a major difference between typical source zones in fractured porous sedimentary rock and those of granular aquifers where DNAPL as free product and / or residual can persist for extremely long times (Pankow and Cherry, 1996). The conceptual model for complete loss of the DNAPL phase from chlorinated solvent source zones has been assessed at the field sites using closely spaced sampling of continuous rock core at each of the four field sites. These results support the conclusion that the DNAPL phase has completely dissolved away (Hurley and Parker, 2002; Sterling et al., 2005; Parker et al., in review) and all or nearly all of the mass is stored in the matrix (Goldstein et al., 2004). Complete dissolution of the DNAPL phase may not occur when the DNAPL is of low effective solubility as complex mixture of compounds, such as at the Wisconsin site and sites with creosote, coal tars and PCBs.

Another major conclusion from applications of the rock core VOC method in zones where DNAPL contamination had occurred is that the concentration profiles (concentration vs. depth) indicate the occurrence of numerous pathways for contaminant migration in each hole, consistent with observations of fracture occurrence in the cores. However, the existence of numerous active fractures is not consistent with results of conventional borehole fluid resistivity and temperature logging and borehole flow metering that typically indicate only two or three active fractures in each hole (Sterling et al., 2005; Pehme et al, 2007). Therefore, the rock core VOC results support the conceptual model for fractured sedimentary rock in which the DNAPL initially occupied many, mostly small to intermediate aperture fractures, and then dissolved away allowing the mass to be transferred by diffusion into the nearby matrix. Groundwater flow through the DNAPL zone in the fractured rock causes a down-gradient dissolved-phase plume to form. In this conceptual model, the plume forms in a network of many interconnected fractures of variable aperture and length without dominance over long distances of any large-aperture fractures. The evolution of a chlorinated solvent source zone and plume in fractured sedimentary rock is illustrated in cross-section at three stages in Figure 4, illustrating the strong influence of diffusive mass transfer into the low permeability matrix blocks both in the source zone and plume.

In the past few years, the conceptual model for chlorinated solvent DNAPL behaviour in fractured porous media outlined above has been combined with a conceptual model for the formation and evolution of contaminant plumes from the source zone, referred to here as *the*

*general conceptual model for source zones and plumes*. This model, which includes DNAPL disappearance after several years or a couple of decades and plume formation in networks of many interconnected fractures within a porous medium, has been represented stylistically with simulations using 2-D discrete fracture models (e.g., FRACTRAN by Sudicky and McLaren, 1992) with assignment of fracture and matrix parameters consistent with borehole measurements in the field and laboratory measurements on core samples (see Figure 5).

In studies of contaminant migration in granular media (i.e. non-indurated geologic deposits), the plug flow advance of plume fronts is estimated using the average linear groundwater velocity ($\bar{v}$) which is the Darcy flux divided by the effective porosity relevant to transport. This porosity is commonly between 0.2 – 0.4 (Freeze and Cherry, 1979).

The $\bar{v}$ concept is also applicable to fractured rock in which many interconnected fractures exist, in which case the $\bar{v}$ is the Darcy flux divided by the bulk fracture porosity ($q/\phi_{fb}$). For intact fractured rock, typical values of $\phi_{fb}$ are $10^{-3}$ to $10^{-5}$. The overall magnitude of Darcy flux variations in fractured rock terrain are generally in the same general range as in granular media terrain and therefore the calculated $\bar{v}$ range typical of fractured rock is orders of magnitude larger than that of granular media. For example, $\bar{v}$ in fractured sedimentary rock is generally on the order of a kilometre to tens of kilometres per year. The potential consequences of such high $\bar{v}$ values to plume expansion and arrival at receptors are large and therefore there is emphasis in the research program on acquiring field data that more reliably determine $\bar{v}$.

Although existing evidence indicates that $\bar{v}$ in the fractured rock aquifers at the four field sites is very large (in the range indicated above typical of fractured rock), the results of the plume investigations conducted to date indicate that the actual plume fronts over decades have advanced at rates which are orders of magnitude smaller than the respective $\bar{v}$'s. Therefore, studies are aimed at quantifying the processes responsible this apparent strong plume front retardation relative to groundwater advection. These studies then have two thrusts: i) improved estimates of $\bar{v}$ based on better measurements of Darcy flux and bulk fracture porosity and ii) more detailed examinations of plume front travel. Plume front retardation is a concept initially established by Foster (1975), further illucidated by Freeze and Cherry (1979) and represented in several DFN modelling papers (e.g Grisak and Pickens, 1980; Lipson et al., 2005) but it has not previously been demonstrated. Greatest confidence in $\bar{v}$ values must come from comparisons of $\bar{v}$ results obtained from independent methods. Therefore, effort is being directed at determining $\bar{v}$ using methods based on temperature, chemical, dilution (borehole dilution) or environmental isotopes (atmospheric tritium and/ or carbon-14). Although the groundwater flow is governed by Darcian flow, the methods in this latter group do not involve measurements of the parameters used in Darcy Law (i.e. K, head gradient) and therefore the results are independent of Darcy-based calculations for $\bar{v}$.

**Temperature Measurement in Sealed Boreholes for Identification of Active Fractures**

The detection of all fractures in which significant flow occurs is a critical data requirement for the DFN approach. Furthermore, the capability of quantifying the amount of fracture flow in individual fractures over a range of several orders of magnitude is necessary.

Various possibilities to acquire such data down-hole have been assessed and the most insightful method proved to be high-resolution temperature logging inside lined holes. The power of this approach is gained from two independent advances: 1) improved sensitivity to monitor temperature variability to 0.0001 $^{o}$C (probe capability) under ambient temperature conditions and when heat is added (active line source) and its dissipation is monitored, as realized (Pehme et al., accepted 2006; Pehme et al., 2007a; 2007b); and 2) utilization of FLUTe liners to temporarily seal the borehole but provide access to static water column inside the liner, allowing measurement of ambient temperature distributions. When temperature logging is done in open bore holes (i.e., holes without liners), as is conventional practice, the vertical flow in the open hole typically swamps the minor but important, temperature signals and therefore larger number of hydraulically active fractures that likely occur in many holes are not identified. The temperature profiling research provides substantial supporting data concerning hydraulically active fractures at each of the four field sites (Pehme et al., submitted). Most recently, an important advance in this temperature logging technology has been initiated involving a prototype for identifying hydraulically active fractures in lined boreholes to resolve flow direction and flow rate under natural flow conditions.

**Contaminant Degradation**

The behaviour and fate of organic contaminants in fractured sedimentary rock are influenced by physical processes (advection, dispersion and diffusion), sorption and in some cases biotic and abiotic degradation. Little peer-reviewed literature exists about chlorinated solvent degradation in fractured sedimentary rock and none examines abiotic versus biotic degradation pathways or evaluates where this degradation is occurring (fractures versus rock matrix). Long term groundwater sampling at all of the field sites shows occurrences of compounds typical of biotic TCE degradation (cis- and trans- 1,2-dichloroethene and in some cases vinyl chloride). Pierce et al. (in prep) examined TCE degradation at the California site and concluded both biotic and abiotic degradation occurs in these sandstones. However, whether this degradation occurs solely in the fractures or in the rock matrix was not determined. Based on a study at the Wisconsin site source zone, Austin (2005) showed abundant chlorinated solvent degradation products in monitoring wells; if this degradation occurred prior to entry of the mixed organic wastes into the subsurface (either in the overburden soils or bedrock) or during storage prior to their release to the subsurface was not determined. The two Canadian sites have less abundant transformation products compared to the US sites, which may be due to the different rock types (differences in mineralogy and pore structure/connectivity) and/or the length of time since contaminants entered the subsurface (15-20 years ago for the Canadian sites versus 40-50 years at the US sites).

**Simulating Plumes Using DFN Numerical Models**

Although the research is focused on the field studies, mathematical models play an important role in the interpretation of field information and testing and validating components of the general conceptual model. Existing models will be used with emphasis on discrete-fracture network (DFN) numerical models (e.g., FRACTRAN, FEFLOW, FRACMAN, HEATFLOW and HydroGeoSphere) for contaminant behaviour and fate. Both

DFN and equivalent porous media (EPM) models will be used to represent groundwater flow. In the DFN models, the fracture networks are generated with many discrete fracture elements and each fracture is usually assigned statistically-derived parameters including length, spacing, orientation, and aperture. The DFN models most relevant to this research are those in which the fractures are superimposed onto a porous rock matrix allowing advection, diffusion, sorption and degradation of contaminants in both the matrix and fractures. The numerical models selected for this part of the IRC research are those that also include rigorous representation of the diffusion-driven contaminant mass transfer between fractures and the rock matrix.

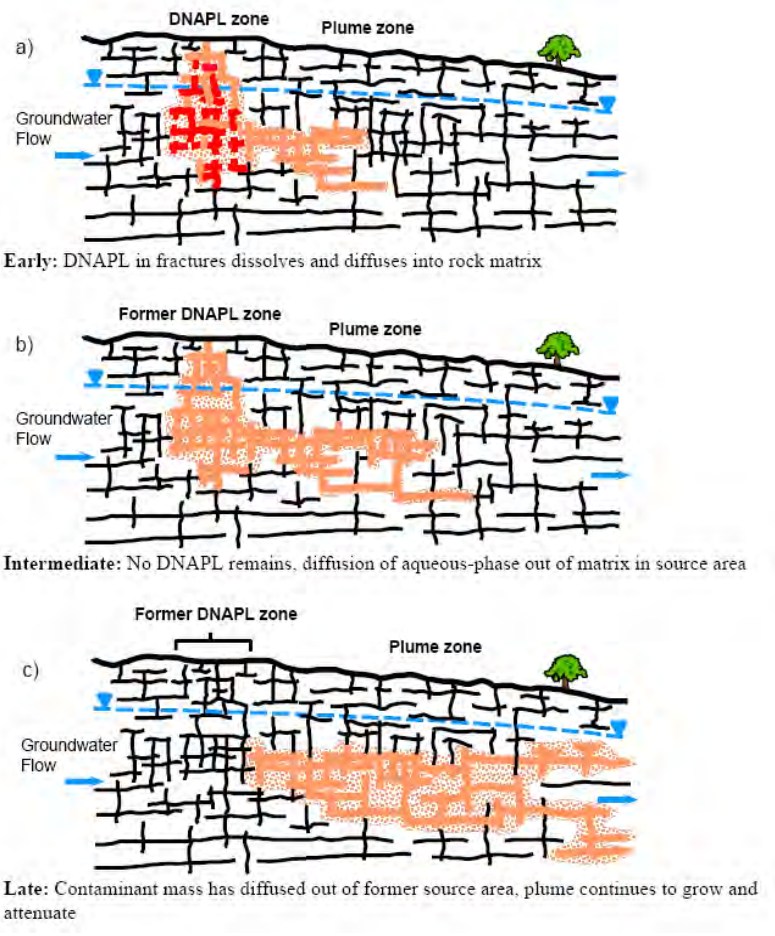


Figure 4: The discrete fracture network (DFN) approach for investigating contaminated sites on fractured sedimentary rock, includes intensive data acquisition from contaminated cores and from the corehole. Open hole conditions are minimized. Illustration of conceptual stages in the time evolution of source zone and plume at chlorinated solvent DNAPL sites on fractured porous sedimentary rock: a) DNAPL flows in fracture network and begins to dissolve and diffuse into rock matrix. DNAPL flow ceases soon after DNAPL input to the rock ceases. b) All DNAPL mass has dissolved completely and the contaminant mass now exists almost entirely in the rock matrix as dissolved and sorbed mass due to diffusion driven mass transfer. Therefore, the source zone no longer has DNAPL and there is not distinct difference in contaminant state between the zone initially referred to as the source zone and the plume. c) Groundwater flow through the initial DNAPL source zone has caused complete mass translocation from much of the initial source zone into the downgradient plume ; the plume front is migrating only slowly or is stable or shrinking due to the combined effects of matrix diffusion and degradation.

The main objective of the DFN modelling of contaminant transport is to achieve good similarities between contaminant distributions at the field sites and the simulated distributions while maintaining consistency/reasonableness between the field information and the model boundary conditions and model parameter assignments. The contaminant plume characteristics and plume geometry over time (temporal evolution) for both the fractures and the rock matrix represented by DFN numerical simulations of the plumes must show reasonable similarities to the field information constrained by the appropriate boundary conditions and parameter values in order to field verify the general DFN conceptual model. For the DFN plume simulations using numerical models to serve their purpose, the 3-D

plume shapes must be mapped and show similarities to the model results for both the fractures and the matrix. Also, the fracture network responsible for the contaminant transport must have large numbers of interconnected, hydraulically active fractures. This task is particularly challenging for fractured rock because some of the model input parameters, such as fracture interconnectiveness, cannot be measured directly (Berkowitz, 2002). Fracture connectivity is, in effect, a result of statistical assignments in the model but it cannot be determined explicitly in the field. Also, uncertainty is associated with the timing and mass of DNAPL inputs into the rock decades ago that eventually resulted in today's contaminant distributions. Nevertheless, application of detailed spatial resolution, field techniques for both the fractures and the rock matrix, and comparisons with distributions from model simulations can narrow the knowledge gap.

When the DFN models are used to simulate groundwater flow and contaminant transport, the hydraulic head, water velocity, and water flux distributions in each of the many thousands of fractures in the network are displayed. In the field, such measurements cannot be made in thousands of fractures but 1-D profiles at selected locations (i.e., boreholes) can be made to the degree necessary for model versus field comparisons at useful spatial scales. This is shown in Figure 5, with 2-D FRACTRAN simulations of the California site and comparison of a field TCE concentration profile derived from rock core compared to a vertical profile through the model output. The extremely detailed profiles of head (Meyer et al., submitted) and groundwater contaminant concentrations from particular boreholes (i.e., exceptionally small spacing between monitoring points particularly in the multilevel monitoring systems) and the extremely detailed contaminant concentrations (concentration versus depth profiles) obtained from the rock matrix (e.g., Sterling et al., 2005; Goldstein et al., 2004) will provide information with unprecedented detail supporting the DFN approach. The high-resolution ambient temperature profiling described by Pehme et al. (in press) provides another independent avenue for comparison between DFN model simulations and the field. Molson et al. (2007) indicate the nature of this modelling approach.

A key input parameter for DFN modelling of contaminant migration is fracture aperture and fracture network geometry, which is difficult to quantify appropriately. There is no alternative but to rely on use of the Cubic Law in conjunction with borehole hydraulic tests to obtain depth discrete hydraulic conductivity values from which values for hydraulic aperture are derived. For this, two types of tests are primarily used: straddle packer injection tests and FLUTe hydraulic conductivity profiling. The straddle packer tests are conventional in their general design however the equipment and procedures have been find-tuned to maximize potential for acquiring more accurate hydraulic apertures. The FLUTe profiling is done in the same holes as the packer testing and the types of data sets taken together provide much stronger bases for deriving information about fracture aperture and the nature of the fracture network local to the borehole. Information about the larger-scale nature of the fracture network is derived from pumping tests, cross-hole hydraulic tomography and plume behaviour over decades.

The patterns of fractures in sedimentary rock are much different than those in igneous rock, which have been the emphasis of most of the hydrologic research pertaining to DFN issues in the context of groundwater flow. However, interest concerning insights from geological observations of fractures in sedimentary rock is increasing (NRC, 1996). For example, Graham Wall (2006) used sedimentological and structural geology principles in field studies of outcrops of peritidal and basinal carbonate sequences in fold-thrust settings to

examine the development of fractures in these rocks. Cooke et al. (2006) summarize recent structural geology and fracture mechanics studies on relatively undeformed carbonate rock sequences to provide important insight into the major controls on groundwater flow paths in these rocks. Efforts are being made at the four field sites to incorporate such geological approaches into the development of concepts for the geometry of the fracture networks. For the Cambridge and Guelph sites, quarries excavated into the dolostone formations situated nearby are being examined for fracture network geometry (style). One of the difficulties inherent in quarry observations is the separation of the effects of blasting from natural characteristics. Nevertheless, quarries can provide useful information. At the California site, many natural outcrops on site and in areas adjacent to the site are being used for fracture network observations.

Figure 5: Example of DFN simulations using FRACTRAN (2-D numerical model; cross section display) of TCE plume in fractured sandstone with fracture and matrix properties consistent with those of the California site: a) source location on fracture network domain; aperture distribution shown, b) TCE plume (no degradation) after 50 years, and c) stylistic comparison of rock core TCE profiles 75m from source at 50 years.

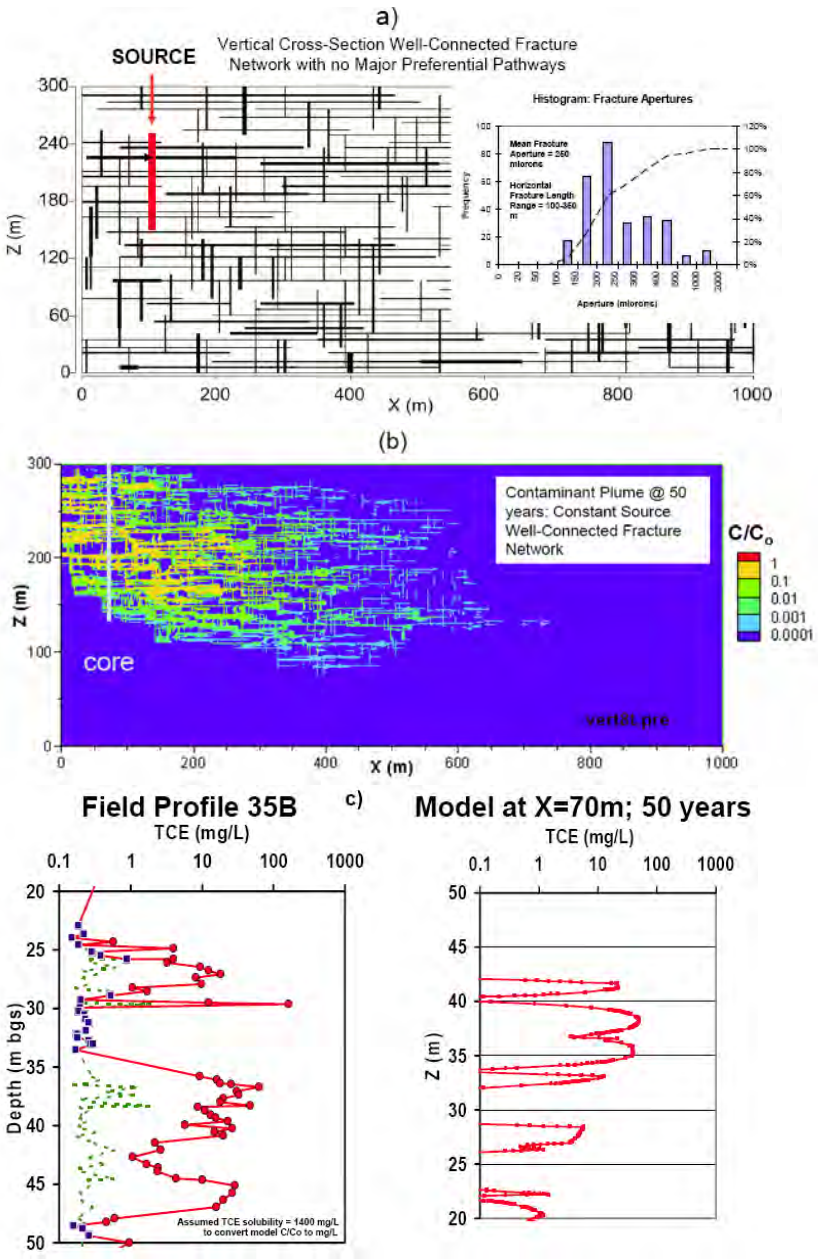


## Concluding Remarks

This research program based on intensive field studies at the four sites has show that, even though there are substantial hydrogeologic complexities attributed to fracture networks in rock, the source zones and plumes are readily amenable to insightful investigations relying on intensive data acquisition (i.e. multiple, independent and high-resolution data sets) from continuous core and from the coreholes. In the early years of this research, there was concern that contaminant migration would occur almost exclusively along a few, major pathways (i.e. "superhighways") resulting in sparse random and/or chaotic contaminant pathways that would prove to be difficult to locate, hence not easy to delineate or monitor (i.e. non-plumes) using a reasonable number of boreholes or wells for the search. This 'old' conceptual model

leaves one with considerable uncertainty and may lead to overly conservative decision-making, such as excessive or inappropriate characterization and/or remediation. Although the plumes found at the four field sites are not yet fully delineated, enough information has been acquired to conclude that very large numbers of fractures are involved in the contaminant migration, and hence plume formation, causing strong transverse horizontal and vertical dispersion of the plume. Therefore, the plumes in sedimentary rock are relatively large targets and easy to detect. This likely derives from the fracture networks being quite systematic, which is a reasonable expectation given the propensity for bedding plane partings and joints in sedimentary rocks to be systematic and orderly. However, plume characterization sufficient for understanding and predicting plume behavior is more challenging given internal variability of contaminant concentrations and flow distributions. The hydrogeologically favorable attributes of many sedimentary rock types may not be common in other rock types such as crystalline rock.

Contaminant plumes in granular media (i.e. sand and gravel aquifers) generally show only minimal attenuation when degradation is slow or non existent because dispersion alone is incapable of strong overall attenuation influence. In fractured sedimentary rock, however, strong transverse dispersion in the fracture network combined with matrix diffusion can result in very strong plume attenuation. Although the average linear groundwater velocity in fractured networks is much larger than in granular aquifers, the plume fronts in fractured sedimentary rock can advance much slower due to the matrix diffusion effects and sorption in the rock matrix. Thus, there are large dissimilarities between plume behavior in fractured sedimentary rocks and granular aquifers.

It would be unreasonable to claim that a general conceptual model for source zones and plumes in sedimentary rock can be founded on model testing / verification at as few as four field sites. Therefore, data from many other sites are also being examined. For example, the same rock core VOC analysis method used at the four intensive study sites has been applied to more than two dozen other sites where chlorinated solvents occur in fractured sedimentary rock. Also, other components of the DFN field approach are being applied at other sites, such as the high-resolution temperature profiling inside lined holes. Although the number of holes analyzed at each of these other sites using the DFN methods is smaller than at each of the four intensive study sites, the data are valuable for comparing the style of the information to that predicted by the general conceptual model.

## Acknowledgements

This research program has benefited continually from: the collaboration and encouragement of John Cherry, Distinguished Professor Emeritus, University of Waterloo (UW), the skillful field and modeling efforts of Steven Chapman, MSc Research Associate (UW) and the dedicated analytical laboratory efforts of Maria Gorecka, MSc Research Associate (UW). The rock core VOC analysis method has steadily advanced due to the collaboration with Tadeusz Górecki (Professor, Chemistry, UW). Innovations in borehole temperature logging were brought to the research program by Peeter Pehme and John Greenhouse (Professor Emeritus, UW) and insights on karst hydrology provided by Jérôme Perrin, post-doctoral fellow (UW). Physical property measurements including measurements of effective diffusion coefficients of rock core samples were performed in a laboratory

supervised by Frank Barone (Golder Associates) and Edison Amirtharaj (UW) has done additional matrix property measurements. Robert Ingleton and Paul Johnson provided skilled technical assistance in the field at the Ontario field sites, field work at the California site benefits greatly from the assistance of MWH and Haley and Aldrich, and at the Wisconsin site by GeoTrans. Important advances were made by the following students who completed MSc theses within the research program: D.C. Austin, L.S. Burns, J.C. Hurley, J.R. Meyer, J.H. Plett, S.N. Sterling and C.M. Turner.

The research program is funded by the Natural Sciences and Engineering Research Council of Canada (NSERC), the University Consortium for Field-Focused Groundwater Contamination Research and the site owners: The Boeing Company, Hydrite Chemical Company, Syngenta Crop Protection Canada and Guelph Tool Inc. Also important are the collaborations with and technical assistance from the following groundwater technology companies: Westbay Instruments (Schlumberger), Flexible Liner Underground Technologies (FLUTe) and Solinst Canada; and most recently, additional support from R.J. Burnside & Associates, AquaResource Inc., GeoSyntec, City of Guelph, Regional Municipality of Waterloo and Schlumberger Canada.

**References**

Austin, D.C., 2005. Hydrogeologic controls on contaminant distribution within a multi-component DNAPL zone in a sedimentary rock aquifer in south central Wisconsin. M.Sc. thesis, Department of Earth Sciences, University of Waterloo.

Berkowitz, B. 2002. Characterizing flow and transport in fractured geologic media: a review. *Advances in Water Resources*, 25(8): 861-884.

Britt, S.L., B.L. Parker and J.A. Cherry. Field testing the Snap Sampler™ – A comparison with low flow, volume purging and the polyethylene diffusion bag sampler. For submission to *Ground Water Monitoring and Remediation*.

Cherry, J.A., B.L. Parker and C. Keller, 2007. A new depth-discrete multilevel monitoring approach for fractured rock. *Ground Water Monitoring and Remediation*, 27(2): 57-70.

Cooke, M.L., J.A. Simo, C.A. Underwood, P. Rijken. 2006. Mechanical stratigraphic controls on fracture patterns with carbonates and implications for groundwater flow. *Sedimentary Geology*, 184: 225-239.

Foster, S.S.D. 1975. The chalk groundwater tritium anomaly – a possible explanation. *Journal of Hydrology*, 25: 159–165.

Freeze, R.A. and J.A. Cherry, 1979. *Ground Water*, Englewood Cliffs, NJ: Prentice-Hall Inc.

Garabedian, S.P., D.R. LeBlanc, L.W. Gelhar and M.A.Celia, 1991. Large-scale natural gradient tracer test in sand and gravel, Cape Cod, Massachusetts. II. Analysis of spatial moments for a nonreactive tracer. Water Resources Research WRERAQ, 27(5): 911-924.

Goldstein, K.J., A.R. Vitolins, D. Navon, B.L. Parker, S.W. Chapman, and G.A. Anderson. 2004. Characterization and pilot-scale studies for chemical oxidation remediation of fractured shale. *Remediation*, 14(4): 19-37.

Graham Wall, B.R. 2006. Influence of depositional setting and sedimentary fabric on mechanical layer evolution in carbonate aquifers. *Sedimentary Geology*, 184(3-4): 203-224.

Grisak, G.E. and J.F Pickens, 1980. Solute transport through fractured media: 1. The effect of matrix diffusion. *Water Resources Research*, 16(4): 719-730.

Hurley, J.C. and Parker, B.L. 2002. Rock core investigation of DNAPL penetration and TCE mobility in fractured sandstone. In: *Ground and Water: Theory to Practice***,** Proceedings of the 55th Canadian Geotechnical and 3rd Joint IAH-CNC and CGS Groundwater Specialty Conferences. Eds. Stolle D., A.R. Piggott and J.J. Crowder, Southern Ontario Section of the Canadian Geotechnical Society.

Keller, C., 2007. Liners and packers: Similarities and differences. . *Proc. Of EPA/NGWA Fractured Rock Conference: State of the Science and Measuring Success in Remediation*, Sept. 24-26, 2007, Portland, ME.

Keller, C.E., J.A. Cherry and B.L. Parker. A new method for fracture identification and continuous hydraulic conductivity profiling in fractured rock boreholes. For submission to Groundwater Monitoring and Remediation.

Lapcevic, P. A., K. S. Novakowski and E. A. Sudicky, 1999. Groundwater flow and solute transport in fractured media. In: *The Handbook of Groundwater Engineering*, J. W. Delleur ed., chap.17, 17-39.

Lawrence, A., M. Stuart, C. Cheney, N. Jones and R. Moss, 2006. Investigating the scale of structural controls on chlorinated hydrocarbon distributions in the fractured-porous unsaturated zone of a sandstone aquifer in the UK. *Hydrogeology Journal*, 14: 1470-1482.

Lipson, D.S., B.H. Kueper and M.J. Gefell, 2005. Matrix diffusion-derived plume attenuation in fractured bedrock. *Ground Water*, 43(1): 30-39.

Meyer, J.R., B.L. Parker, and J.A. Cherry. Use of detailed hydraulic head versus depth profiles for defining hydrogeologic units in flat laying fractured sedimentary rock. Submitted to *Journal of Environmental Geology*.

Molson, J.W., E.O. Frind, 2005. HEATFLOW, A 3D groundwater flow and thermal energy/mass transport model for porous and fractured porous media, version 2.0, University of Waterloo.

Molson, J.W., P. Pehme, J.A. Cherry and B.L. Parker, 2007. Numerical analysis of heat transport within fractured sedimentary rock: Implications for temperature probes. *Proc. Of EPA/NGWA Fractured Rock Conference: State of the Science and Measuring Success in Remediation*, Sept. 24-26, 2007, Portland, ME.

Neuman, S.P. 2005. Trends, prospects and challenges in quantifying flow and transport through fractured rocks. *Hydrogeology Journal*, 13:124-147.

Pankow, J.F. and Cherry, J.A. (eds.) 1996. *Dense Chlorinated Solvents and other DNAPLs in Groundwater: History, behaviour, and remediation*. Waterloo Press, Guelph, Ont., 522 p.

Parker, B.L., L.S. Burns, C.M. Turner and J.A. Cherry. DNAPL origin for deep herbicide and TCE contamination in a dolostone aquifer. *Journal of Contaminant Hydrology*, Submitted 2006.

Parker, B.L., D.B. McWhorter and J.A. Cherry, 1997. Diffusive loss of non-aqueous phase organic solvents from idealized fracture networks in geologic media. *Ground Water*, 35(6): 1077-1088.

Parker, B.L., R.W. Gillham and J.A. Cherry, 1994. Diffusive disappearance of immiscible phase organic liquids in fractured geologic media. *Ground Water*, 32(5): 805-820.

Pehme, P.E., J.P. Greenhouse and B.L. Parker. The active line source temperature logging technique and its application in fractured rock hydrology. *Journal of Environmental & Engineering Geophysics*, Accepted 2006.

Pehme, P., J. Greenhouse and B.L. Parker, 2007. The Active Line Source (ALS) technique, a method to improve detection of hydraulically active fractures and estimate rock thermal

conductivity. *Proceedings, 60th Canadian Geotechnical Conf. & 8th Joint CGS/IAH-CNC Groundwater Conf,* Oct. 21-24, 2007. Ottawa, ON.

Pehme, P., B.L. Parker and J.A. Cherry, 2007. The potential for compromised interpretations when based on open borehole geophysical data in fractured rock. *Proc. Of EPA/NGWA Fractured Rock Conference: State of the Science and Measuring Success in Remediation*, Sept. 24-26, 2007, Portland, ME.

Pierce, A.A., 2005. Isotopic and hydrogeochemical investigation of major ion origin and trichloroethene degradation in fractured sandstone. M.Sc. thesis, Department of Earth Science, University of Waterloo.

Pierce, A.A., B.L. Parker, R. Aravena, J.A. Cherry. Field evidence for TCE degradation mechanisms in fractured sandstone. For submission to Journal of Contaminant Hydrology.

Price, M. and A. Williams, 1993. The influence of unlined boreholes on groundwater chemistry: A comparative study using pore-water extraction and packer sampling. *Journal of the Institute of Water and Environmental Management*, 7(6): 651-659.

Sara, M.N, 2003. *Site Assessment and Remediation Handbook*. 2nd Edition. New York: Lewis Publishers

Smith, L., and F.W. Schwartz. 1984. An analysis of the influence of fracture geometry on mass transport in fractured media. *Water Resources Research*, 20(9):1241-1252.

Smith, L., and F.W. Schwartz. 1993. Solute transport through fracture networks. In *Flow and Contaminant Transport in Fractured Rocks*, J. Bear, C. F. Tsang, and G. de Marsily, eds. New York: Academic Press.

Sterling, S.N., B.L. Parker, J.A. Cherry, J.H. Williams, J.W. Lane Jr., and F.P. Haeni, 2005. Vertical cross contamination of trichloroethylene in a borehole in fractured sandstone. *Ground Water*, 43(4): 557-573.

Sudicky, E.A., 1986. A natural gradient experiment on solute transport in a sand aquifer: Spatial variability of hydraulic conductivity and its role in the dispersion process. *Water Resources Research*, 22(13): 2069-2082.

Sudicky, E.A., and R.G. McLaren. 1992. The Laplace transform Galerkin technique for large scale simulation of mass transport in discretely fractured porous formations. *Water Resources Research*, 28(2):499-514.

Therrien, R. and E. Sudicky. 1996. A three dimensional analysis of variably-saturated flow and soluble transport in discretely fractured porous media. *Journal of Contaminant Hydrology*, 23, (1-2): 1-44.

U.S. National Research Council. 1996. *Rock Fractures and Fluid Flow: Contemporary Understanding and Applications.* National Academy of Sciences, 551 pp. (see chap. 6, Field scale flow and transport models: p. 301-403)

Vanderkwaak, J.E. and E.A. Sudicky. 1996. Dissolution of non-aqueous phase and aqueous phase contaminant transport in discretely fractured porous media. *Journal Contaminant Hydrology*, 23(1-2), 45-68.

**Biographical Sketch**

Beth L. Parker has a Bachelors degree in environmental science/ economics from Allegheny College, a Masters degree in environmental engineering from Duke University and a Ph.D. in hydrogeology from the University of Waterloo. She was a research faculty member in the Earth Sciences Department at the University of Waterloo from 1996 to 2007. She is currently

a professor in the School of Engineering at the University of Guelph and holder of the NSERC Industrial Research Chair in Groundwater Contamination in Fractured Media. Her research involves field studies of transport, fate and remediation of chlorinated solvents in diverse hydrogeologic environments including fractured rock, clayey aquitards and sandy aquifers.

# Appendix H

A Conceptual Model for the Fracture Network in Contaminated Shale Based on Multiple Lines of Evidence (Draft Manuscript, March 2008)

# A Conceptual Model for the Fracture Network in Contaminated Shale Based on Multiple Lines of Evidence

Beth L. Parker[1], Steven W. Chapman[2], John A. Cherry[3]

[1] School of Engineering, University of Guelph
50 Stone Road East, Guelph, Ontario, Canada N1G 2W1
Phone: 519-824-4120 Ext. 53642, Fax: 519-836-0227
bparker@uoguelph.ca

[2] School of Engineering, University of Guelph
50 Stone Road East, Guelph, Ontario, Canada N1G 2W1
Phone / Fax: 506-454-2173
schapman@uoguelph.ca

[3] Department of Earth and Environmental Sciences, University of Waterloo
200 University Avenue West, Waterloo, Ontario, Canada N2L 3G1
Phone: 519-888-4567 Ext. 34516, Fax: 519-883-0220
cherryja@uwaterloo.ca

A Manuscript in Preparation for Submission to:

Ground Water

**Draft** March 31, 2008

NOTE: This document is a draft in preparation intended for submission to a peer-review journal, tentatively intended to be Ground Water. This draft, although not entirely complete at this time, contains essentially all of the main points that will be included in the final version of the manuscript. This draft is intended for inclusion in the ESTCP report as an appendix or attachment. In the next few weeks, while the report draft is being reviewed by ESTCP, this manuscript draft will be edited and brought to final form for submission to the Journal.

**Abstract**

Investigations were conducted in fractured shale contaminated with volatile organic chemicals (VOCs), primarily PCE and its degradation products TCE and cis-1,2-DCE, between top of rock at 3 to 6 m depth to the bottom of the zone of contamination at 45 to 60 m depth. In the initial stage, transmissive fractures or fracture zones were identified in eight boreholes using water injection or withdrawal tests, including intensive borehole flow metering in the open hole water columns and cross-hole monitoring. The number of flow zones totaled fourteen in 140 m of open hole and ranged from none to five per hole. However, acoustic televiewing identified seventy-nine fractures in this total hole length, but televiewing cannot distinguish non-transmissive from transmissive fractures. Subsequent studies at this site, including collection of detailed hydraulic head profiles and determination of vertical profiles of VOC concentrations in groundwater using borehole sampling while drilling and multilevel monitoring systems, and VOC concentrations measured at an average spacing of 0.3 m along continuous rock core, indicate that the fracture network includes many fractures that have advective groundwater flow under ambient conditions, uninfluenced by open-hole cross-connections.

Consideration of fracture identifications from rock core visual inspections, borehole televiewing and rock core VOC profiles indicate spacing of active fractures in vertical holes on the order of one to four meters. The contaminants in the bedrock at this site have performed the role of a long term (decades) tracer test providing insight concerning the fracture network unattainable by other means, indicating a well-interconnected fracture network, both vertically and horizontally. This network allowed chlorinated solvents as DNAPL to penetrate deep and following the period of DNAPL flow, fostered diffusion-driven dissolved phase contaminant mass transfer from the fractures into the low permeability fracture network, where nearly all of the contaminant mass now resides. This conceptual model for the fracture network is supported by permanganate distributions determined during pilot scale and full scale remediation. Although the literature concerning occurrence of transmissive fractures in sedimentary rock based on conventional hydraulic tests and borehole flow metering typically shows only a few fractures / fracture zones per hole, many more hydraulically active fractures are likely common but have gone undetected because of the insensitivity of flow metering in open holes to the presence of most of the active fractures occurring at the location under ambient flow conditions.

**List of Figures**

**List of Tables**

## Introduction

Investigations of contaminated sites on bedrock commonly have data obtained providing information about the nature of the fracture network. Fracture network characteristics strongly influence both groundwater flow and contaminant transport. Also, selection of effective insitu remediation technologies requires knowledge of the fracture network. Fracture network characteristics are typically examined through various measurements made in boreholes and through borehole-to-borehole hydraulic tests and/or forced advection tracer tests. Based on a thorough literature review of fractured rock characteristics in the context of contaminant transport, Berkowitz (2002) indicates that there is a paucity of field information regarding the quantitative nature of fracture networks and the parameters least understood and most difficult to measure are fracture length and fracture network connectivity. Information concerning fracture connectivity is minimal because each borehole provides only a one-dimensional view and the number of boreholes per site that can be drilled is limited. In situations where bedrock is exposed at ground surface or on quarry walls or outcrops (e.g. Cooke et al., 2006) fracture mapping along 2-D planes has provided additional insights but nevertheless lack the third dimension and information about fracture hydraulic transmissivity (i.e. the fracture traces do not distinguish between hydraulically open or closed fractures). There is also uncertainty whether the excavation or weathering due to exposure has caused changes to the visible portion of the fracture network compared to a buried version of the same feature. Therefore, the lengths of many or perhaps all of the fractures identified in each hole are indeterminant with any direct measurement means, and a complete deterministic approach to characterizing specific details of fracture networks in 3-D is not possible. However, the style of fracture network, referred to here as a fracture network conceptual model (FNCM), is discernible and important as discussed in this paper.

Although direct determinations of fracture lengths/connectivity is infeasible, indirect approaches for gaining insight concerning these network features have been attempted based primarily on combinations of borehole hydraulic and/or flow tests and forced-gradient tracer tests involving measurements in individual holes combined with cross-borehole tests. These hydraulic-based techniques have provided site-specific fracture network conceptual models for several sites (e.g. Sweden tunnel site, Mirror Lake site, Nevada test site – Add References). Use of hydraulic methods combined with borehole and/or outcrop fracture mapping is standard practice,

performed to varying degrees depending on perceived importance of detail. More sensitive research approaches have been developed and proposed recently (e.g. Lapsevic, Paillet, Yeh and Illman - refer to cross-hole hydraulic tomography work of Illman and others and forced gradient tracer tests e.g. USGS Mirror Lake work).

Another approach for determining hydraulic connectivity between boreholes in fractured rock involves the flow meter pulse method described by Lapcevic et al. (1993) and Williams and Paillet (2002a, 2002b). This approach was applied comprehensively along with borehole geophysics at the contaminated shale bedrock site near Albany, NY which is the focus of this paper, resulting in a conceptual model for the fracture network. In this conceptual model, a few hydraulically transmissive fractures (generally between 1 to 5) were found in each hole and the borehole-to-borehole tests show hydraulic connectivity between some of the identified transmissive fractures (Table 1).

Based on the few transmissive fractures identified in each hole and the observed hydraulic cross-hole responses between some of these fractures, Williams and Paillet (2002) provided a three-dimensional interpretation of the geometric configuration of the fracture network, thereby representing the fracture network conceptual model for the site. This conceptual fracture network includes only a small total number of major fractures or fracture zones. The presence of many more fractures with / without hydraulic activity were identified on borehole geophysical logs but the hydraulic tests and flow metering were unable to assign hydraulic activity or transmissivity to any of them. Fracture network conceptual models for several other bedrock sites are reported in the literature based on borehole and cross-hole testing, showing general similarities to that presented by Williams and Paillet (2002) in that the fracture networks are comprised of a small number of hydraulically connected major transmissive fracture or fracture zones (examples - Paillet, 1993; Paillet, 1998; check for paper on carbonate site in Illinois, Mirror Lake work).

None of the field studies providing fracture network conceptual models indicated above involved determinations of contaminant distributions and therefore, it is not known whether the fracture network models are consistent with contaminant transport in such fracture networks. In general hydraulic methods have limitations due to tool measurement sensitivity and dominance of high K zones in boreholes and effects from cross-connections. Also, while research has been extensive

at crystalline rock sites (igneous and metamorphic rock) driven by the radioactive waste industry, insights from such fracture networks may not be relevant to sedimentary rock sites.

There is widespread recognition of the need for fracture network conceptual models (FNCMs) suitable for understanding and prediction of contaminant distributions and migration. Studies of contaminant transport in fracture networks for which FNCMs have been published are limited almost entirely to numerical modeling to simulate development of plumes in hypothetical systems (e.g. Smith and Schwartz, 1984; Smith and Schwartz, 1993; Sudicky and McLaren, 1992; Therrien and Sudicky, 1996). However, these FNCMs are stylized on fracture network maps for outcrops, and have not been verified using field data such as contaminant distributions to ascertain whether transport in conceptualized networks actually produce realistic contaminant distributions. Various numerical models for simulating contaminant transport and plume evolution have been developed with capabilities for inclusion of large numbers of fractures in two or three-dimensions incorporating substantial complexity (variability) involving fracture spacing, aperture, orientation, length and therefore, connectivity (e.g. Fractran, Feflow, Fracman, HydroGeoSphere). However, these numerical models will have limited usefulness in contaminated site investigations until such time as field verifications are accomplished.

This paper reports on a field study in fractured shale bedrock where PCE DNAPL entered the subsurface at least 40 years ago. Site data including several conventional and new high-resolution depth discrete data sets were used to develop a conceptual model for the fracture network consistent with the contaminant distributions. The unconventional data sets using the contaminant distribution data (collected in high resolution 3-D format) that essentially represents a long term natural gradient tracer experiment were essential for distinguishing the two fracture network conceptual models for the site (the one favored in this paper presented later, and the contrasting conceptual model mentioned previously by Williams and Paillet (2002). Using the same study site investigated by Williams and Paillet (2002) provided the opportunity to evolve the site conceptual model for the fracture network from that based only on hydraulic testing and flow metering to a different one consistent with contaminant distribution data and borehole geophysical fracture mapping (e.g. via optical and acoustic televiewer).

The contamination comprises chlorinated solvents, primarily PCE and its degradation products, occurring in fractured shale and this contamination has evolved to its current distribution since

chlorinated solvent DNAPLs entered the subsurface several decades ago. This study involved application of many different investigative methods including rock core and borehole logging, borehole flow metering, pumping tests, rock core contaminant analyses, groundwater contamination analyses and large-scale solute tracer injection experiments involving permanganate to assess remediation potential of ISCO. Goldstein et al. (2004) reported on the overall performance of this pilot-scale trial in the remediation context, we have used these results and more recent injections to assist in the development of the fracture network conceptual model.

**Site Description**

The study area occupies part of the Watervleit Arsenal near Albany, NY in an area of a former manufacturing building (Building 40) where chlorinated solvents were used for degreasing, with releases suspected to have occurred more than three decades ago (Goldstein et al., 2004). The Ordovician-age shale in the study area site is overlain by 3 to 5 m of artificial fill, alluvium and glacial deposits. Chlorinated solvent contamination in the shale was discovered when the first monitoring wells in the area were drilled in 1995 [check]. The study area is located near the Hudson River (Figure 1a) which is incised into the shale bedrock. The shale is a hard somewhat metamorphosed sedimentary rock in which groundwater flow is entirely through fractures. Figure 1b shows the nature of the shale observed in rock core. The land surface in the study area has elevations of about 5.0 to 6.5 m above sea level (ASL) and the bottom of the Hudson River near the study area is approximately 6 m below sea level [check]. Figure 2 shows the locations of monitoring wells, multilevel monitoring systems and coreholes in the study area, including the ones reported on by Williams and Paillet (200) and also the general area of chlorinated solvent contamination in the shale indicated by sampling the wells and coreholes. Except for one monitoring well located near the Hudson River (not shown on Figure 2) all of the monitoring locations are west of the local road and highway (U.S. Interstate 787) that forms the eastern boundary of the primary study area.

The water table in the study area is generally about 2.5 to 3.5 m below ground surface (bgs) [check] and is almost always higher than the river level which averages about 0.6 m ASL with a tidal variation of about 1.2 m (http://waterdata.usgs.gov/ny/nwis/dv/?site_no=01359139). Therefore, the general direction of groundwater flow in the study area is towards the Hudson

River, and the solvent contamination emanating from the study area is transported to the Hudson River where it goes undetected due to the large flow causing dilution. The specific locations and timing of chlorinated solvent releases and entry into the shale are unknown, however information on historical solvent usage at the site and results of site investigations suggest that the solvent releases occurred more than three decades ago, with some releases suspected from a former degreasing unit located in the northwest portion of the Building 40 area.

**Initial Site Conceptual Model**

The initial FNCM was developed by Williams and Paillet (2002) based on borehole wall imaging and fluid and flow meter logs to identify 'flow zones' in the fracture network. Cross-hole hydraulic tests combined with borehole flow metering in the unstressed holes were used to identify the connections between boreholes. This initial study involved four monitoring wells and four coreholes ranging in depth from 10 to 50 m. Seventy nine fractures were identified by borehole imaging of the 140 m of open hole in these eight holes. Many fractures dip to the east at 50 to 60 degrees parallel to bedding, although fractures occur also at angles to bedding with orientations from subhorizontal to nearly vertical. Borehole imaging provides no information as to whether or not a fracture is open and/or has active groundwater flow. Therefore, these identified fractures are referred to as 'imaging fractures' to distinguish them from hydraulically active fractures. Borehole imaging does not detect fractures with apertures smaller than about 0.5 mm and hydraulically active fractures (HA fractures) can have apertures much smaller than this and therefore can go unidentified by borehole imaging.

The flow zones identified by Williams and Paillet (2002) are those fractures indicated by flow metering done using heat pulse and/or electromagnetic devices. Fluid resistivity and temperature logs conducted in the water column in the open holes also contributed to identification of flow zones. These various types of borehole measurements were conducted under ambient conditions and under forced gradient conditions imposed by pumping or injection. These measurements pertain to flow in the water column, either upward or downward. Under ambient conditions flow in the water column occurs due to inflow to the hole from one or more fractures and outflow from one or more other fractures. This inflow and outflow is caused by head differentials set up by the larger-scale ambient groundwater flow system, perturbed locally by each borehole that

creates cross connecting flow between fractures. Williams and Paillet (2002) detected fourteen transmissive flow zones in the 140 m of open hole exposed in the eight holes (Table 1). Single flow zones were detected in wells 34, 58 and 59, two flow zones were identified in each of coreholes 68, 71 and 72, no flow zones were found in well 51 and five were found in corehole 65. Therefore, the total number of fractures showing hydraulic activity, including ambient and forced gradient conditions, were much fewer than the total number of imaging fractures, and the imaging fractures exclude small fractures (apertures <0.5 mm) where they intersect the holes.

Williams and Paillet (2002) first identified the flow zones and then developed their conceptual model for connections between these zones. Figure 3a shows the flow zones and their transmissivities determined for four of the eight holes. The transmissivity values were obtained using borehole flow metering during cross-hole hydraulic tests using the modeling procedure described by Paillet (1998). Some flow zones have only one fracture and other have two or in some cases more. For example, the flow zone at about 20 m depth in hole 71 shows four fractures (Figure 3a), including a subhorizontal fracture, a steeply dipping fracture and two moderately dipping fractures. Figure 3b shows the conceptual model for the fracture system proposed by Williams and Paillet (2002) in which the fractures in the flow zones are connected between holes by transmissive zones represented as extensive domains where fractures are well connected. This figure shows the individual fractures intersecting the boreholes at each flow zone but does not project these individual fractures much distance from each hole, and the conceptual model for the fracture network implies other connected fractures occur in the transmissive zones connecting from hole to hole. Williams and Paillet (2002) indicate that this representation is “by no means definitive or unique but is consistent with all borehole wall image and single and cross-hole flow data collected at the Watervleit site”. Following on from the development of the FNCM based on borehole geophysical / hydrophysical testing, investigations focused on contaminant distributions provide additional data sets for FNCM development.

**Methods**

The field investigations at the study site, beyond the borehole geophysical and cross-hole hydraulic testing reported on by Williams and Paillet (2002) involved four main activities:

(i) Groundwater sampling while drilling to determine the VOC distributions;

(ii) Installation of depth-discrete multilevel monitoring systems to determine hydraulic head profiles and for groundwater sampling;

(iii) Rock coring to determine the VOC distribution in the rock matrix; and

(iv) Pilot-scale injections of dissolved permanganate to assess the feasibility of effectively distributing permanganate in the fracture network contaminated domain, followed by full-scale permanganate injections for a two year period.

The data acquired from each of these activities provided different insights concerning the nature of the fracture network. The first data acquisition activity involved collecting water samples from the bottom interval of boreholes during drilling. In this method, the hole was advanced to a specified depth, say 15 m below surface, and an inflated packer then set at 9 m depth and a groundwater sample collected by pumping from below the packer after a period of purging to remove the drilling water (add details on purge volumes and sample collection). This type of sampling was done in several cored holes (including MW-51, 58, 59, 61, 64, 65, 71; Figure 2) drilled to depths between 20 and 50 m below ground surface. The water samples were packed in coolers and sent to an EPA certified laboratory for analysis by method 8260 (check).

The second activity involved installation of depth-discrete multilevel monitoring systems (MLS) for monitoring hydraulic head and groundwater sampling in three episodes. The first involved installation of Westbay MP Systems (described by Black et al., 1986) in six holes, each having between two and seven monitoring ports. In the next episode, CMT systems (described by Einarson and Cherry, 2002), each with five or six ports were installed in two holes. In the final episode, FLUTe multilevel systems (described by Cherry et al., 2007) with nine ports each were installed in five holes. The Westbay systems were used in the early stage primarily for groundwater sampling and later on for injecting permanganate solutions as part of the pilot scale remediation trial. The CMT systems were used primarily for monitoring during the pilot-scale remediation trial and longer term monitoring in the full scale permanganate remediation. The FLUTe systems were used primarily for early arrival and distribution monitoring of permanganate in the full-scale remediation program. All of the MLSs were used initially for hydraulic head measurements.

The third data acquisition activity involved collection of continuous rock core for contaminant analysis from six holes drilled to depths between 12 to 60 m below land surface (five of the six

extended to at least 45 m depth) (Table 2, locations shown in Figure 1). The cores were collected in 1.52 m lengths using conventional water circulation diamond bit rotary coring during field episodes in 2001 and 2003. Immediately on arrival of each core run at surface, the core was examined quickly and small pieces, generally 5 to 10 cm long, were broken off from the core, crushed using a hydraulic rock crushing unit in stainless steel crushing cells, and immediately placed in bottles or vials with a known volume of high purity methanol. Generally 4 to 7 samples were collected from each 1.52 m core run, with average sample spacing from 0.21 to 0.37 m for the six holes (Table 2) with an overall average of 0.28 m. The vials containing the crushed rock were then shipped to a fixed lab for completion of extraction of the VOC mass into the methanol (via periodic shaking and storage in a cold room over an approximately six week period). The methanol extract was then analyzed for a short-list of target analytes (PCE, TCE and DCE isomers) using a sensitive method providing low method detection limits (<10 μg/L for PCE and TCE, <10 μg/L for the DCE isomers) involving direct on-column injection of an aliquot of the methanol extract on a gas chromatograph (GC) equipped with a micro electron capture detector (μ-ECD) (Reference). More details on methods are provided by Hurley and Parker (2002) and Sterling et al. (2005).

## RESULTS AND DISCUSSION

### Hydraulic Head

The MLS hydraulic head profiles typically show gradual change with depth with only one or two major inflections of slope rather than numerous distinct changes in slope. Figure 4 shows head profiles from three FLUTe systems, which are the most detailed profiles because they had the most monitoring ports. In these profiles, the highest head values occur in the deepest part of each hole, below 25 m depth where there is minimal vertical variation and the head values above 25 m in the holes are lower and with a strong but gradual decline upward indicating a distinct upward hydraulic gradient in this upper zone. The higher head in the lower zone indicates leakage upward from this zone into the shallower zone. Examination of vertical components of hydraulic gradient indicated by the head profiles, including those from the conventional monitoring well clusters, indicates widespread upward components of the hydraulic gradient, indicating the study area is located in a groundwater discharge area. This is consistent with the position of the study

area in the broader scale topography, positioned at the base of a broad hill and close to the Hudson River. The head profiles are relevant to the nature of the fracture network and the contaminant distribution, as discussed below.

The orderly nature typical of the head profiles is indicative of a fracture network with many well interconnected fractures. The general lack of narrow zones showing distinctly low or high head relative to monitoring intervals above and below indicates lack of major through-going dominantly transmissive flow zones because such zones should either draw flow lines to them or have flow lines diverging from them depending on their position in the overall flow system. The three head profiles shown in Figure 4 and the other MLS profiles (e.g. CMT head profiles in Figure 6) show similarity across the site concerning the deep higher head zone with minimal head differentials between ports and the shallower zone with lower head and strong upward head decline. This suggests broad consistency of fracture network characteristics governing the bulk hydraulic conductivity and possibly anisotropy in these two zones. The minimal head differentials between monitoring intervals in the lower zone suggest stronger vertical fracture network hydraulic connectivity in this zone relative to the shallow zone where the substantial head differentials suggest lesser vertical connectivity. The presence of strong upward hydraulic gradient components in the shallower zone does not infer that the vertical component of groundwater flow is strong relative to the horizontal components. The horizontal component of flow towards the Hudson River likely dominates due to the boundary conditions on the groundwater flow system.

**Distribution of VOCs in Groundwater**

Of the holes sampled for VOCs using the single packer method during drilling, at least five were within the contaminant plume and showed presence of VOCs. Major features of the VOCs versus depth profiles are the presence of VOCs in nearly all sample intervals and large concentrations particularly deep in some of the holes. Figure 5 shows results from two of the holes (MW-65 and MW-71; Figure 2) indicating very large total VOC concentrations (PCE, TCE, cis-DCE, VC) (e.g. 94 mg/L in the 26-32 m depth interval in MW-71, 15 mg/L in the 30.5 to 36.5 m depth interval in MW-65). Figure 6 shows the head profiles measured with CMT systems at two locations alongside the total VOC concentrations from groundwater sampling of the CMT

systems in February 2002 [include?] and January 2003. Both locations show upward component of hydraulic gradient except possibly at the bottom of the holes and highest VOC concentrations at depth below 20 m bgs. The results shown in Figures 5 and 6, consistent with results throughout the site, indicate deep VOC contamination even though there is widespread occurrence of upward directed groundwater flow indicated by the head profiles. The most plausible explanation for the occurrence of deep VOCs is DNAPL flow in a vertically well-interconnected fracture network. Without downward DNAPL flow counter-direction to upward groundwater flow, such deep occurrence of VOCs would not be expected since dissolved VOCs transported by groundwater could not go deep against the vertical components of the hydraulic gradient. VOCs were found in the bottom most sampling intervals, indicating the bottom of the VOC contaminated zone is below the bottom of these holes at depth greater than 40 to 45 m.

The physical principles governing the entry and flow of DNAPL in fractures are presented by Kueper and McWhorter (1991) and McWhorter and Kueper (1996) and O'Hara et al. (2000) conducted a laboratory experiment where DNAPL entered and flowed in fractures. These studies and others indicate that DNAPL with physical properties typical of chlorinated solvents can enter and flow in fractures with very small apertures (e.g. less than 10 or 20 microns). For DNAPL entry and flow to occur in initially water saturated fractures, there needs to be sufficient accumulation of free-product DNAPL on top of the open fractures to overcome the DNAPL entry pressure, and then sufficient free-product DNAPL to sustain flow in the fractures. However, if the fractures generally have small aperture so that the DNAPL storage capacity is small, minimal free-product DNAPL can cause flow over substantial distances along fractures. Kueper and McWhorter (1991) also suggest DNAPL cannot flow in the direction counter to the hydraulic gradient if the gradient is very large (i.e. range of 0.3 to 0.5 or greater in a vertical fracture). None of the hydraulic head profiles measured at the Watervleit site indicate upward gradient components approaching this range, and therefore downward DNAPL flow counter to upward groundwater flow is consistent with the site data.

**Contaminant Distributions in Rock Core**

The rock core VOC analyses were done based on the premise that initially the DNAPL flowed in the fractured network during a relatively short period of time after the DNAPL releases occurred,

and at the end of the DNAPL flow episode, the DNAPL was motionless in the fracture network, where it occurs as filaments, ganglia and globules surrounded by water (i.e. the DNAPL is the water wetting liquid in the duel liquid phase system). There were presumably a few DNAPL release episodes over the decades during which chlorinated solvents were used for manufacturing at the Watervleit Arsenal, although the exact locations and timing of the releases are unknown. In the second part of the premise on which the rock core VOC method was based, the DNAPL dissolves into the contiguous water in the fractures and, as dissolved phase, the VOCs diffuse into the rock matrix blocks between fractures where the contaminant mass then resides as dissolved and sorbed mass removed from the active groundwater flow system in the fracture network. The conceptual model on which this premise is based was presented by Parker et al. (1994, 1997), who showed that, after a period of years or decades, all or nearly all of the DNAPL mass can be converted to the dissolved and sorbed mass stored in the rock matrix, if the fractures have small apertures and if the rock matrix allows for substantial diffusion. Vanderkwaak and Sudicky (1996) used a numerical model to show that active groundwater flow in the fractures containing DNAPL can greatly shorten the time and interval needed for DNAPL disappearance, with part of the mass transferred by diffusion to the rock matrix in the zone of initial DNAPL occurrence, and the rest of the mass being transported by groundwater downgradient where it forms a plume in the fracture network with most mass residing in the rock matrix.

Figure 7 illustrates the concepts described above and shows conceptually the approach for using the rock core VOC analysis method in investigations of fracture networks at fractured sedimentary rock sites. In Figure 7a the DNAPL has entered the fractured network and dissolution has produced a downgradient contaminant plume where diffusion halos occur in the rock matrix adjacent to all of the fractures where contaminant transport has occurred. Figure 7b shows conceptually what is expected from rock core VOC analyses done on samples collected at appropriate spacing along a continuously cored hold in porous sedimentary rock. Each fracture along which contaminant transport has occurred over substantial time has a diffusion halo identified by the rock core VOC profile. In this view, the rock core VOC profiles show distinct halo shapes because the system is idealized as a regular two-dimension network, but in the field more complex profiles are expected due to the third dimension and other network complexities causing overlapping or interfering halos.

Figure 8 shows four of the six rock core VOC profiles done at the Watervleit site (Table 2) prior to full-scale permanganate remediation extending to depths between 45 to 61 m bgs, indicating the concentrations of PCE and TCE, which are the dominant VOCs found in the rock core. The other two locations were either shallow (MW-88 to 12 m bgs) to had minimal contamination (MW-80). The VOC concentrations are expressed as micrograms of dissolved VOC mass per litre of groundwater, representing values calculated (partitioned) from the actual measured values that represent the total VOC mass in the sample. Goldstein et al. (2004) and Sterling et al. (2005) describe the calculation procedure. PCE generally has the highest concentrations and was the main chlorinated solvent used and released at the site, and TCE is likely a product of degradation from the PCE. These four rock core VOC profiles show numerous high concentration 'peaks' separated by intervals of much lower concentration and/or non-detects. These rock core results are consistent with the occurrence of VOC contamination at nearly all depths found in monitoring wells and MLSs. Therefore, the rock core VOC results support the interpretation that DNAPL flowed deep into the rock through a network with numerous well connected fractures.

The rock core VOC analysis results show the presence of substantial VOC occurrence in the rock matrix, which is consistent with the long time since chlorinated solvent DNAPL apparently first entered the subsurface decades ago with the diffusion related properties of the shale. Table 3 provides the results of laboratory measurements of effective diffusion coefficients for chloride and related diffusion rock matrix properties and parameters (including porosity, organic carbon content and matrix permeability) for five rock core samples from five coreholes taken from depths ranging from 12 to 41 m bgs. The measurements were performed by Golder Associates. Rock matrix porosity was calculated from the measured dry density (ASTM Method D4531-86) and specific gravity (ASTM Method 845-92), providing a range from 1.9 to 3.1% with a mean of 2.3%. Porosity determined on seven samples from one location over depths ranging from 12 to 53 m bgs from water content and volume of water-saturated rock sample at the University of Waterloo indicated lower values, ranging from 0.7 to 1.3% with a mean of 1.1%. The lower porosity values compared to the Golder results suggest the samples may not have been fully water saturated and/or that some of the porosity is not interconnected [more details].

The porosity values for the shale at the study site are at the low end of the range for sedimentary rock matrix porosities reported by Freeze and Cherry (1979) and Parker et al. (1994) and also at the low end for shale [check Grathwohl, 1998; Potter et al., 2005, other references]. The matrix

porosity values are at the low end likely because this shale has been subjected to low grade metamorphism (reference). However, although the porosity values are at the low end of the range for sedimentary rock, the effective diffusion coefficients for chloride (tortuosity range of 0.032 to 0.071 with a mean of 0.048) in the shale do not appear to be skewed towards the low end of laboratory measured values for sedimentary rock based on values of Parker et al. (1994) and [Grathwohl, 1998 – check]. This inconsistency between the relatively small matrix porosity values and the chloride effective diffusion values is likely due to enhanced diffusion paths provided by microfractures [more support - cite Tom Al unpublished results and personal communication concerning presence of microfractures?].

The PCE concentration distribution profile in the rock matrix emanating from PCE saturated water in a fracture was simulated using a 1-D analytical solution (e.g. equation 3-62 in Grathwohl, 1998) with results displayed in Figure 9. The PCE concentration was held constant at the fracture at solubility of 200 mg/L (Table A1, Pankow and Cherry, 1996) and the rock matrix was assumed homogeneous with mean porosity ($\phi$) and effective diffusion coefficient ($D_e$) values shown in Table 3. Figure 9 shows profiles for 40 year diffusion scenarios with and without sorption attributed to the solid-phase organic carbon in the shale. For the scenario with sorption, the PCE retardation factor (R) was estimated using the well-known relation $R = 1 + (\rho_b / \phi) K_d$ applying the mean porosity ($\phi$) and dry bulk density ($\rho_b$) values (Table 3). The distribution coefficient ($K_d$) was estimated from $K_d = K_{oc} f_{oc}$ using a literature organic carbon partition coefficient ($K_{oc}$) of 364 mL/g (Table A1, Pankow and Cherry, 1996). The average fraction of organic carbon content ($f_{oc}$) from the Golder measurements, which used the Walkley-Black wet oxidation method (Walkley, 1947), all fell within a narrow range with a mean of 0.28% (Table 3). Measurements of $f_{oc}$ at the University of Waterloo using a combustion method (Churcher and Dickhout, 1987) on 15 samples from MW-74 and MW-75 provided somewhat higher $f_{oc}$ values ranging from 0.31 to 0.68% with a mean of 0.40%. The latter was used in the R estimate, providing a PCE R of 170. However, the sorptive nature of the organic carbon in this slightly metamorphosed shale and use of the correlation is somewhat uncertain. The difference in the diffusion profiles indicates strong influence of sorption. Without sorption, the diffusion front (assumed at 5 μg/L) migrates 140 cm into the rock from the fracture and with sorption the front goes only 11 cm into the matrix.

The four rock core VOC profiles displayed in Figure 8 show numerous distinct peaks, typically indicated by one or two relatively high concentration values and separated by samples with concentrations a few orders of magnitude lower or non-detections. Given that the number of peaks in each hole ranges from 9 to 17 (Table 2) and each peak is generally identified based on only one high concentration sample, and that the average sample spacing per corehole is approximately 30 cm for the profiles shown in Figure 8, the number of peaks encountered is consistent with the simulated 1-D diffusion profile with sorption (Figure 9) which suggest limited matrix penetration. The average spacing of fractures identified as contamination migration pathways in the subsampled coreholes ranges from about 2.7 to 4.4 m for the four coreholes shown in Figure 8. It is also interesting to note the positions of the flow zones identified via borehole flow testing at MW-83 versus the contaminant distribution via rock core subsampling (Figure 8c) indicating nearly all of the peaks and contaminant mass occurs in zones not identified as 'flow zones'. Based on the information presented above, it is apparent that the presence of numerous rock core VOC peaks in each of the four profiles in Figure 8 supports a fracture network conceptual model in which there are numerous fractures along which contaminant migration has occurred, either as DNAPL flow and/or dissolved phase transport. The rock core VOC profiles also indicate that fractures allowing contaminant migration occur throughout the vertical thickness examined, from near top of rock to depths of 45 m or more.

**Permanganate Injections**

Additional insight on the interconnectivity of the fracture network can be obtained based on results of monitoring of the distribution of permanganate and associated parameters / reaction products (e.g. specific conductivity, sodium from the $NaMnO_4$ injection solution, sulfate produced from pyrite oxidation) during pilot-scale and full-scale injections conducted at the Watervliet site. Results of pilot-scale injections, conducted in 2001 and 2002, are provided by Goldstein et al. (2004) which showed the ability to effectively distribution permanganate in the fracture network. Here the focus is on monitoring conducted during early stages of the full-scale implementation of permanganate remediation. For monitoring of breakthrough and distribution of permanganate and other parameters, five temporary 9-port FLUTe multilevel systems (described by Cherry et al., 2007) were installed in MW-79 and IW-1 to IW-4 located

immediately east of Building 40 (Figure 2). These systems were intended for short-term monitoring and then removal to allow these holes to be utilized for later injections. The FLUTe system has particular advantages for breakthrough monitoring, given the very small storage volumes in the sampling port interval thus requiring minimal purging. However the system was limited to short-term monitoring, since the liner material (polyurethane-coated Nylon) degrades in the presence of permanganate; however, following this work a new version more resistant to degradation by permanganate was developed using a polyester liner material.

The following focuses on two early injection episodes in MW-90 (Inj#1: 8500 L of 10% $NaMnO_4$ solution injected over a two day period in Sept. 2004, Inj#2: 17000 L of 10% $NaMnO_4$ solution injected over an eleven day period in Feb. 2005) and one in MW-79 (Inj#3: 17 000 L of 5% $NaMnO_4$ solution injected over a two day period in May 2005, focusing on a zone isolated in the borehole from 21 to 45 m bgs using an inflatable packer). For the first two injection episodes in MW-90, no $MnO_4$ was observed in any of the FLUTe multilevels during or after the injections, however elevated conductivity, sodium and/or sulfate concentrations was observed in several zones at the two closest FLUTe multilevels at MW-79 (ports 3-6) and IW-4 (ports 5-9), which were the main systems monitored during these injections. This suggests consumption of the $MnO_4$ prior to reaching these monitored zones. For the third injection episode at MW-79 following removal of the FLUTe system from this hole, permanganate arrival was observed in several ports at IW-1, IW-2 and IW-3 during the injection (Figure 10) based on twice daily sampling, with breakthrough after one day of injection at IW-2 and IW-3 and after two days at IW-1 located further away from MW-79. The figure also shows locations of the flow zones identified via borehole flow metering during ambient and pumping conditions prior to the FLUTe installations, indicating arrival of permanganate at several ports where ‘flow zones’ were not identified. Besides the zones with $MnO_4$ arrival, Figure 9 also shows monitoring zones with elevated conductivity, sodium and/or sulfate from the injections, indicating these zones were also affected by the injections but that the $MnO_4$ was consumed before reaching them, which is not surprising given the large oxidant demand of the rock determined from lab batch tests and assessed via mineralogical analysis. Overall, the distribution of permanganate and reaction products determined from detailed monitoring using multilevel systems shows the fracture network is well-interconnected between the injection and monitoring locations.

**Revised Conceptual Model**

A revised conceptual model for the fracture network (FNCM) at the Watervliet site was created using the results of the diverse type of field information presented above. This FNCM is quite different from the initial FNCM described by Williams and Paillet (2002), which was fully consistent with the single borehole and cross-borehole flow metering data pertaining to forced-gradient hydraulic conditions on which the model was based. The revised conceptual model presented here maintains consistency with the hydraulic flow metering data, but also accounts for the contaminant distributions obtained from analyses of water samples from boreholes, wells, and MLSs and rock core VOC analyses. The main difference between the two FNCMs is that the revised one contains many more transmissive fractures and that groundwater flow and contaminant transport occurs in large numbers of these fractures.

The initial evidence for the revised FNCM was the VOC distribution indicated by the analyses of groundwater samples collected while drilling, which showed deep contamination strongly inconsistent with the initial FNCM. Groundwater samples from MLSs and the rock core VOC analyses also show deep VOC occurrence, seemingly inconsistent with the upward directed component of groundwater flow indicated by hydraulic head profiles. However, deep VOC occurrence is reasonably attributable to downward DNAPL flow, counter direction to groundwater flow, in a fracture network with many connected vertical and sub-vertical fractures. If the seventeen fractures or fracture zones included in the initial FNCM shown on Figure 3b were to have dominant influence on DNAPL flow, deep VOCs would be unexpected. Also, none of the seventeen fractures shown on Figure 3b are vertical or even steeply dipping and of the many more imaging fractures shown on Figure 3a few are steeply dipping. Therefore, the steeply dipping fractures likely most important for allowing deep DNAPL flow went undetected in the borehole imaging. Borehole imaging cannot identify fractures with apertures at the borehole wall smaller than 0.5 to 1 mm. The steeply dipping fractures may generally have apertures below this detection limit and, because all of the boreholes are vertical, the probability of boreholes encountering near vertical and vertical fractures is low and therefore, there is a propensity for these fractures to be underrepresented in fracture identifications using borehole imaging. The permanganate injections during the pilot test showed that the fracture network has strong connectivity in the horizontal direction not dependent on the flow zone connectivity identified in the initial site study. In combination, the pilot and full scale permanganate injections are

supportive of the revised FNCM in which there are ubiquitous fractures with strong interconnectivity in all directions to at least the bottom of the study domain at 45 to 60 m bgs.

In the quest to characterize fracture networks for purposes of contaminant transport, an important network 'property' is fracture spacing. Three types of data were obtained that provide insight concerning fracture spacing: the rock core visual descriptions, the borehole imaging logs, and the rock core VOC profiles. Each of these provides an independent estimate of the fractures 'detected' in holes at the Watervliet site. The average fracture spacing for the four coreholes shown in Figure 8 (and summarized in Table 2) ranges from about 0.25 to 0.32 m when all core breaks are included, which covers about 176 m total length of rock core. However, many of these were identified as drilling induced breaks (mostly along bedding) so that the spacing of real fractures is likely much lower [provide spacing of fractures that appear to be real based on logs]. The borehole imaging reported by Williams and Paillet (2002) identified 79 fractures in 140 m of total open hole, which provides a mean fracture spacing of 1.8 m. Most of these fractures appear in the four deepest holes out of the eight holes logged, as shown in Figure 3a. The logged and imaging fractures are not necessarily transmissive, and the use of only vertical holes causes bias towards under identification as previously noted.

The fracture frequency based on the rock core VOC analyses varies from hole to hole, as indicated by Table 2. Overall, the four rock core VOC profiles shown in Figure 8 showed 54 peaks over the 176 m of rock core for an average fracture spacing of 3.3 m. Therefore, overall the three different indicators of fracture spacing provide a range from about 0.3 m based on the rock core logs to about 3.3 m based on the rock core VOC profiles. Each of these fracture identifier methods has inherent biases. The borehole imaging and rock core VOC method is expected to underestimate the number of fractures in which active groundwater flow under ambient conditions occur, and the rock core descriptive logs should overestimate the number of fractures when the potential corebreaks due to drilling are included in the estimates. Overall the data suggests that spacing of hydraulically active fractures is on the order of perhaps 1 to 3 m.

**Summary and Implications**

Sedimentary bedrock underlies many industrialized areas and therefore contaminated sites in fractured sedimentary rock are common. Prospects for understanding and predicting contaminant transport and fate at these sites are limited by the lack of information concerning the fracture network characteristics. Outcrops only rarely provide much information about site specific network characteristics because overburden is generally extensive and weathering alterations are typically severe. Therefore, boreholes are the critical source of information. To understand fracture networks in the context of contaminant fate and transport at sites where contaminants already exist in the system (i.e. plumes exist) the focus must be directed at the network as it relates to groundwater flow under the site ambient conditions governing the evolution of the plumes in the past and the likely conditions in the future. Therefore, the fractures of interest are those that are hydraulically transmissive and also have sufficient flow to be influential in contaminant transport. Hence, the borehole information of most relevance is that which provides insight concerning fractures with significant groundwater flow for contaminant transport.

In the conventional approach used for investigations of contaminated bedrock sites, borehole imaging logs (i.e. optical or acoustic televiewing) are commonly obtained, typically indicating presence of many fractures but these logs cannot distinguish closed or cemented fractures from those that are hydraulically transmissive. The other component of the conventional approach to borehole information acquisition involves hydraulic testing (i.e. packer tests) for transmissivity and borehole flow metering. Packer tests commonly indicate presence of transmissive fractures at many depths in holes, but borehole flow metering typically shows very few hydraulically active fractures or flow zones, such as was obtained at the Watervliet site. This relatively small number of flow zones detected in open holes by flow metering and fluid resistivity and temperature logging can be attributed to the dominance of short-circuiting flow in the holes that masks effects of other fractures (Pehme et al., 2007; Pehme et al., in progress). Cross-connection effects prevent investigation of the ambient flow system.

The VOC distributions at the Watervliet site obtained from groundwater and rock core analyses and the hydraulic head profiles indicate that the fracture network governing ambient groundwater flow and contaminant transport has a large number of hydraulically active fractures in each hole with strong connectivity in all directions throughout the network, so that DNAPL flowed deep

through many fractures and dissolved phase contamination has become dispersed throughout the subsurface domain in the area investigated. The end result after decades of contamination residing in the system is the contaminant mass now resides almost exclusively in the rock matrix because of diffusion-driven mass transfer from fractures into the rock matrix blocks between fractures. This diffusive mass transfer has occurred in a large number of fractures, providing a very large fracture surface area across which the mass transfer occurs. This has major implications for in situ remediation, in that treatment fluids injected into the system must circulate through the large numbers of fractures in the network to have potential for treatment effectiveness. The pilot scale and full scale permanganate injections at the Watervliet site confirmed the revised conceptual model that has a large number of connected fractures throughout the investigated domain. The results of this study indicate that the focus of contaminated site investigations directed at understanding contaminant transport and fate and / or in situ remediation should be directed at identifying the fractures exhibiting active groundwater flow under ambient flow conditions and, for this purpose, the existing contaminant distributions and detailed hydraulic head profiles can provide critical insights.

**Acknowledgements**

The data on which this paper is based resulted from investigations conducted at the Watervliet Arsenal over a nine year period from 1998 to 2006. Several organizations and many individuals were involved, with the lead organization being the U.S. Army Corps of Engineers represented by Grant Anderson and Stephen Wood. Malcolm Pirnie Inc. (MP) managed the program of site investigations and provided much of the field support. Ken Goldstein of MP was the overall investigation program leader, Andrew Vitolins was the lead field project manager and Daria Navon provided essential program support. JoAnn Kellogg of the Watervliet Arsenal provided on-site support. Funding was provided by the U.S. Army Corps of Engineers and the Department of Defense funding program ESTCP.

## References


Berkowitz, B. 2002. Characterizing flow and transport in fractured geologic media: a review. Advances in Water Resources, 25(8): 861-884.

Black, W.H., H.R. Smith, and F.D. Patton, 1986. Multiple-level ground water monitoring with the MP system. Proceedings of the Conference on Surface and Borehole Geophysical Methods and Ground Water Instrumentation, National Water Well Association, Dublin, OH, pp. 41–60.

Cherry, J.A., Parker, B.L., Keller, C. 2007. A new depth-discrete multilevel monitoring approach for fractured rock. Ground Water Monitoring & Remediation, 27(2), 57-70.

Churcher, P.L., and Dickhout, R.D. 1987. Analysis of ancient sediments for total organic carbon - some new ideas, Journal of Geochemical Exploration, 29, 235-246.

Cooke, M.L., J.A. Simo, C.A. Underwood, P. Rijken. 2006. Mechanical stratigraphic controls on fracture patterns with carbonates and implications for groundwater flow. Sedimentary Geology, 184: 225-239.

Freeze, R.A., and Cherry, J.A. 1979. Groundwater. Prentice Hall, Englewood Cliffs, NJ.

Grathwohl, P., 1998. Diffusion in Natural Porous Media: Contaminant Transport, Sorption / Desorption and Dissolution Kinetics. Kluwer Academic Publishers, Boston, MA.

Hao, Y., T.-C. J. Yeh, W. A. Illman, K. Ando, K.-C. Hsu. 2007. Hydraulic tomography for detecting fracture connectivity. Ground Water, in press.

Hurley, J.C. and Parker, B.L. 2002. Rock core investigation of DNAPL penetration and TCE mobility in fractured sandstone. In: Ground and Water: Theory to Practice, Proceedings of the 55th Canadian Geotechnical and 3rd Joint IAH-CNC and CGS Groundwater Specialty Conferences. Eds. Stolle D., A.R. Piggott and J.J. Crowder, Southern Ontario Section of the Canadian Geotechnical Society, October 20-23, Niagara Falls, Ontario, pp. 473-480.

Illman, W. A., A. J. Craig, and X. Liu. 2007. Practical issues in imaging hydraulic conductivity through hydraulic tomography, Ground Water, 46(1): 120-132.

Kueper, B.H., and D.B. McWhorter. 1991. The Behavior of Dense, Nonaqueous Phase Liquids in Fractured Clay and Rock. Ground Water, 29:716-728.

Lapcevic, P.A., Novakowski, K.C., Paillet, F.L. 1993. Analysis of flow in an observation well intersecting a single fracture. Journal of Hydrology 151, 227–239.

McWhorter, D.B., and B.H. Kueper. 1996. Mechanics and mathematics of the movement of dense non-aqueous phase liquids (DNAPLs) in porous media. In Dense Chlorinated Solvents and other DNAPLs in Groundwater; History, Behavior, and Remediation. Edited by J.F. Pankow and J.A. Cherry. Rockwood, ON: Waterloo Press: 89-128.

O'Hara, S.K., B.L. Parker, P.R. Jorgensen, and J.A. Cherry. 2000. Trichloroethene DNAPL flow and mass distribution in naturally fractured clay: Evidence of aperture variability. Water Resources Research, 36:135-147.

Paillet, F.L., Hess, A.E., Cheng, C.H., Hardin, E.L. 1987. Characterization of fracture permeability with high-resolution vertical flow measurements during borehole pumping. Ground Water 25, 28–40.

Paillet, F.L. 1993. Using borehole geophysics and cross-borehole flow testing to define hydraulic connections between fracture zones in bedrock aquifers. Journal of Applied Geophysics 30, 261-279.

Paillet, F.L. 1998. Flow modeling and permeability estimation using borehole flow logs in heterogeneous fractured formations. Water Resources Research 34, 997–1010.

Paillet, F.L. 2000. A field technique for estimating aquifer parameters using flow log data. Ground Water, 38(4): 510-521.

Paillet, F.L. 2001. Hydraulic head applications of flow logs in the study of heterogeneous aquifers. Ground Water 39, 667–675.

Parker, B.L., D.B. McWhorter and J.A. Cherry, 1997. Diffusive loss of non-aqueous phase organic solvents from idealized fracture networks in geologic media. Ground Water, 35(6): 1077-1088.

Parker, B.L., R.W. Gillham and J.A. Cherry, 1994. Diffusive disappearance of immiscible phase organic liquids in fractured geologic media. Ground Water, 32(5): 805-820.

Parker, B.L. 2007. Investigating contaminated sites on fractured rock using the DFN approach. Proceedings of the 2007 U.S. EPA/NGWA Fractured Rock Conference: State of the Science and Measuring Success in Remediation, Sept. 24-26, 2007, Portland, Maine, pp. 150-168.

Pehme, P., Greenhouse, J., Parker, B. 2007. The active line source (ALS) technique, a method to improve detection of hydraulically active fractures and estimate rock thermal conductivity. Proceedings of the 60th Canadian Geotechnical Conference & 8th Joint CGS/IAH-CNC Groundwater Conference, October 21-24, 2007, Ottawa, Ontario, pp. 302-309.

Pehme et al., in progress

Potter, P.E., Maynard, J.B., Depetris, P.J., 2005. Mud & Mudstones. Springer, 205pp.

Smith, L., and F.W. Schwartz. 1984. An analysis of the influence of fracture geometry on mass transport in fractured media. Water Resources Research, 20(9):1241-1252.

Smith, L., and F.W. Schwartz. 1993. Solute transport through fracture networks. In Flow and Contaminant Transport in Fractured Rocks, J. Bear, C. F. Tsang, and G. de Marsily, eds. New York: Academic Press.

Sterling, S.N., B.L. Parker, J.A. Cherry, J.H. Williams, J.W. Lane Jr., and F.P. Haeni, 2005. Vertical cross contamination of trichloroethylene in a borehole in fractured sandstone. Ground Water, 43(4): 557-573.

Sudicky, E.A., and R.G. McLaren. 1992. The Laplace transform Galerkin technique for large scale simulation of mass transport in discretely fractured porous formations. Water Resources Research, 28(2):499-514.

Therrien, R. and E. Sudicky. 1996. A three dimensional analysis of variably-saturated flow and soluble transport in discretely fractured porous media. Journal of Contaminant Hydrology, 23, (1-2): 1-44.

Vanderkwaak, J.E. and E.A. Sudicky. 1996. Dissolution of non-aqueous phase and aqueous phase contaminant transport in discretely fractured porous media. Journal Contaminant Hydrology, 23(1-2), 45-68.

Williams, J.H. and F. Paillet. 2002a. Characterization of Fractures and Flow Zones in a Contaminated Shale at the Watervliet Arsenal, Albany County, New York. U.S. Geological Survey Open-File Report 01-385.

Williams, J.H., and Paillet, F.L. 2002b. Using flowmeter pulse tests to define hydraulic connections in the subsurface: a fractured shale example. Journal of Hydrology, 265: 100-117.

Yeh, T.J., Illman, W.A., Kruger, A., Sudicky, E., Daniels, J. 2006. New technology to improve the understanding of contaminant migration in fractured geological settings. Geological Society of America, 2006 Annual Meeting, Philadelphia, PA, Oct. 22-25, 2006, Abstracts with Programs - Geological Society of America, 38(7): 462.

| Well or Corehole No. | Zone Depth (m) | Zone Head (m ASL) | Transmissivity ($cm^2/s$) | | Hydraulic Connection | |
|---|---|---|---|---|---|---|
| | | | Single-borehole | Cross-borehole | Well or Corehole No. | Zone Depth (m) |
| 34 | 7.6 | 2.74 | 2.80 | 1.61 | 71 | 19.8 |
| 34 | 7.6 | 2.74 | 2.80 | 1.08 | 65 | 7.3 and 10.7 |
| 51 | - | 2.73 | - | - | - | - |
| 58 | 23.2 | 2.93 | 0.001 | - | - | - |
| 59 | 28.0 | 2.79 | 2.47 | 2.47 | 71 | 19.8 |
| 59 | 28.0 | 2.79 | 2.47 | 2.69 | 65 | 7.3 and 10.7 |
| 65 | 7.3 | 2.72 | 0.70 | 1.08 | 34 | 7.6 |
| | 10.7 | | 0.51 | | | |
| 65 | 7.3 | 2.72 | 0.70 | 1.08 | 59 | 28.0 |
| | 10.7 | | 0.51 | | | |
| 65 | 7.3 | 2.72 | 0.70 | 1.08 | 71 | 19.8 |
| | 10.7 | | 0.51 | | | |
| 65 | 23.8 | 2.77 | 0.40 | 0.86 | 71 | 19.8 |
| | 26.8 | | 0.03 | | | |
| | 33.5 | | 0.03 | | | |
| 68 | 5.8 | 3.67 | 0.62 | - | - | - |
| 68 | 13.7 | 3.90 | 1.18 | - | - | - |
| 71 | 8.5 | 2.72 | 0.43 | - | - | - |
| 71 | 19.8 | 2.75 | 2.47 | 2.47 | 59 | 28.0 |
| 71 | 19.8 | 2.75 | 2.47 | 1.61 | 34 | 7.6 |
| 71 | 19.8 | 2.75 | 2.47 | 1.08 | 65 | 7.3 and 10.7 |
| 71 | 19.8 | 2.75 | 2.47 | 0.86 | 65 | 23.8, 26.8 and 33.6 |
| 72 | 14.9 | 1.98 | 0.08 | - | - | - |
| 72 | 22.9 | 1.98 | 0.63 | - | - | - |

Table 1: Positions and estimated hydraulic head and transmissivities for the flow zones identified in the first site investigation (2000-2001) (adapted from Williams and Paillet, 2002).

| Corehole ID | Date Drilled | Top of Bedrock (m bgs) | Cored Interval (m bgs) | Total Rock Core Length (m) | Number of Rock Core VOC Samples | Average VOC Sample Spacing (m) | Numer of VOC Peaks Observed |
|---|---|---|---|---|---|---|---|
| MW-74 | Dec 2001 | 5.6 | 6.1 - 45.7 | 39.6 | 112 | 0.35 | 9 |
| MW-75 | Dec 2001 | 5.0 | 5.3 - 45.9 | 40.5 | 109 | 0.37 | 13 |
| MW-80 | Oct 2003 | 3.0 | 4.6 - 45.7 | 41.1 | 184 | 0.22 | none (minimal VOCs in this area) |
| MW-83 | Oct 2003 | 4.4 | 5.9 - 61.1 | 55.2 | 216 | 0.26 | 17 |
| MW-87 | Oct 2003 | 3.8 | 5.3 - 46.0 | 40.7 | 150 | 0.27 | 15 |
| MW-88 | Oct 2003 | 4.1 | 5.5 - 12.2 | 6.7 | 32 | 0.21 | 6 |
| | | | **Totals** | **223.9** | **803.0** | **0.28** | **60** |

Table 2: Summary of coreholes sampled for rock core VOC analyses.

| Borehole ID | Depth (m bgs) | Dry Bulk Density (g/cm3) | Total Porosity (%) | Organic Carbon Content (%) | Matrix Hydraulic Conductivity (cm/s) | Chloride Matrix Diffusion Coefficient ($cm^2/s$) | Matrix Tortuosity Factor |
|---|---|---|---|---|---|---|---|
| MW 64 | 40.7 - 41.1 | 2.68 | 2.4 | 0.26 | 3.3E-09 | 6.4E-07 | 0.042 |
| MW 65 | 12.2 - 13.7 | 2.66 | 1.9 | 0.29 | 6.3E-10 | 7.1E-07 | 0.047 |
| MW 68 | 19.8 - 21.3 | 2.65 | 1.9 | 0.28 | 1.0E-10 | 1.1E-06 | 0.071 |
| MW 71 | 21.5 - 23.0 | 2.66 | 3.1 | 0.27 | 1.8E-09 | 4.8E-07 | 0.032 |
| MW 72 | 12.0 - 12.3 | 2.65 | 2.4 | 0.29 | 3.6E-11 | 8.4E-07 | 0.056 |
| | **Average** | 2.66 | 2.3 | 0.28 | 1.2E-09 | 7.5E-07 | 0.050 |

Table 3: Summary of measured matrix parameters by Golder Associates.

(a)

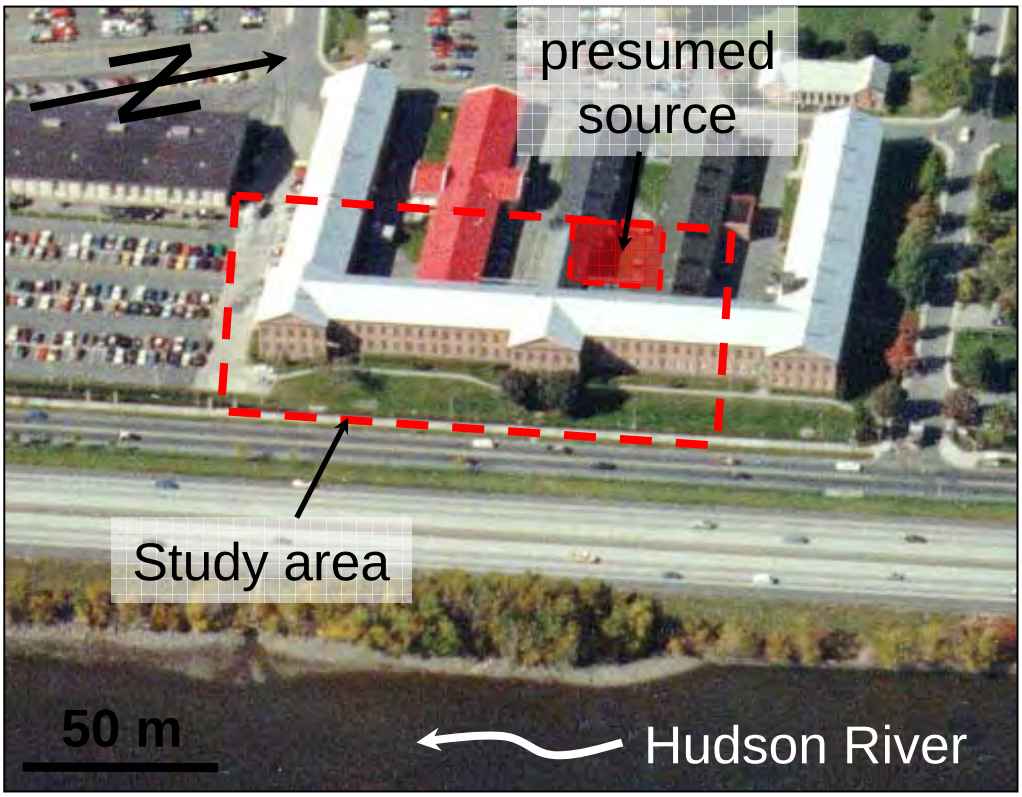


(b)

Figure 1: Photos showing (a) aerial view of the study site, and (b) typical rock core run and fracture features.

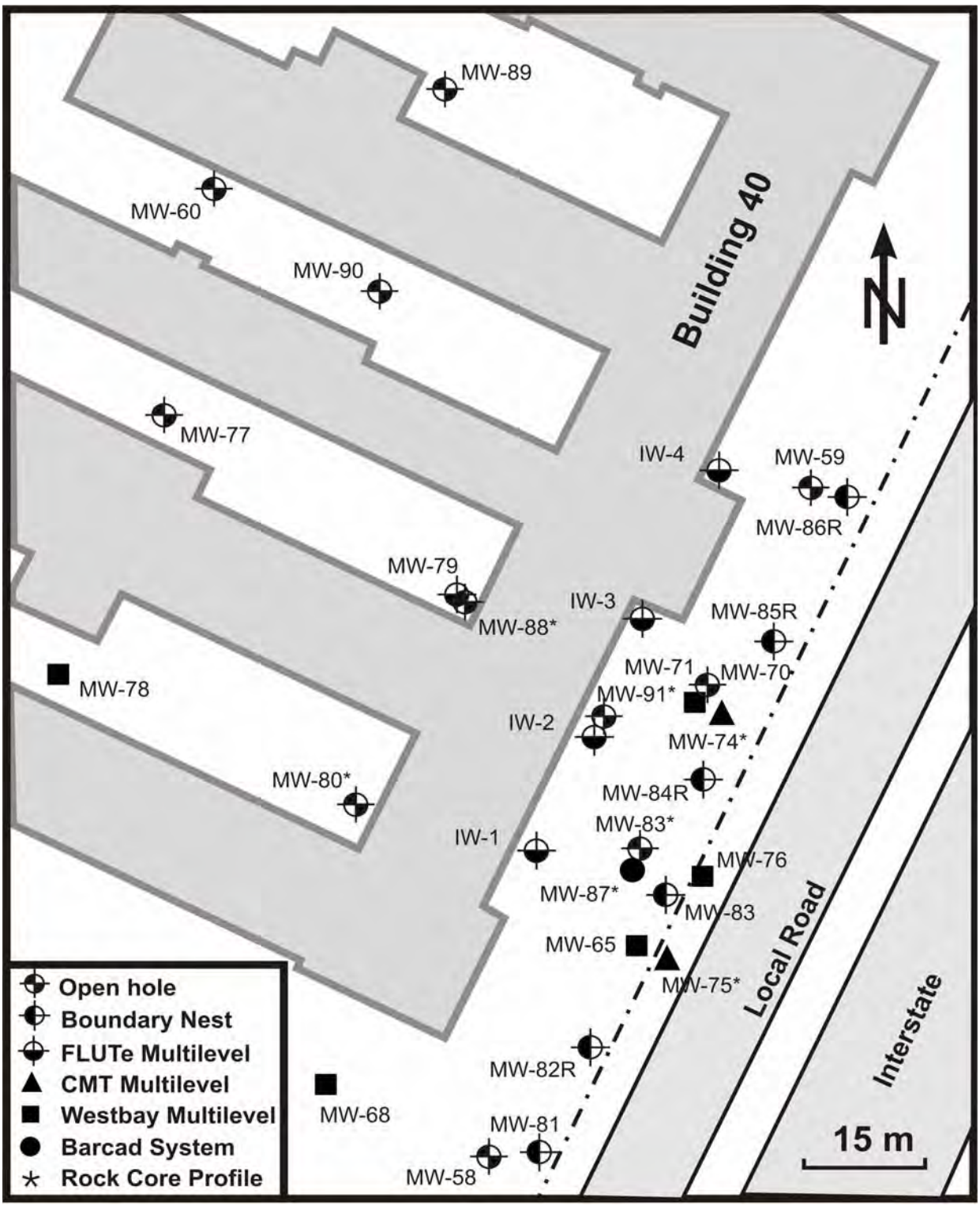


Figure 2: Site map showing locations of coreholes, wells and multilevel systems.

(a)

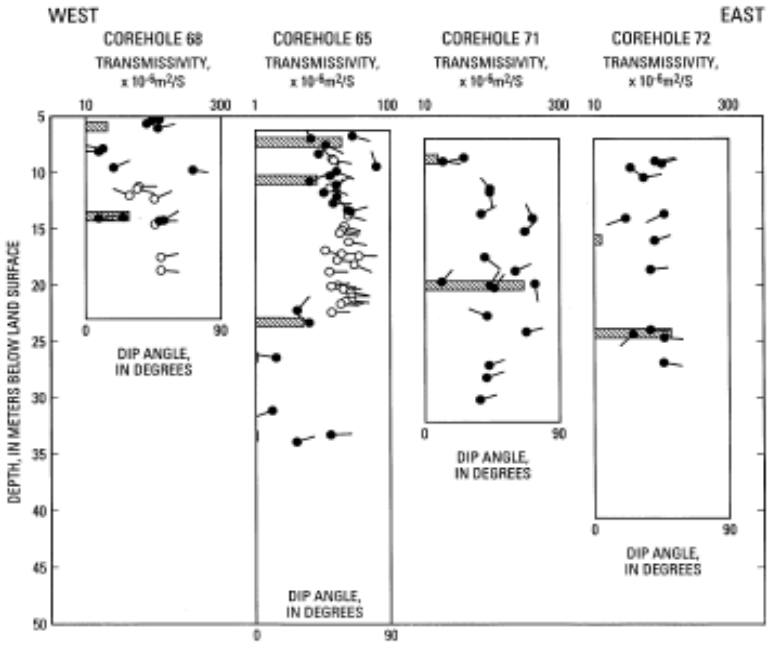


(b)

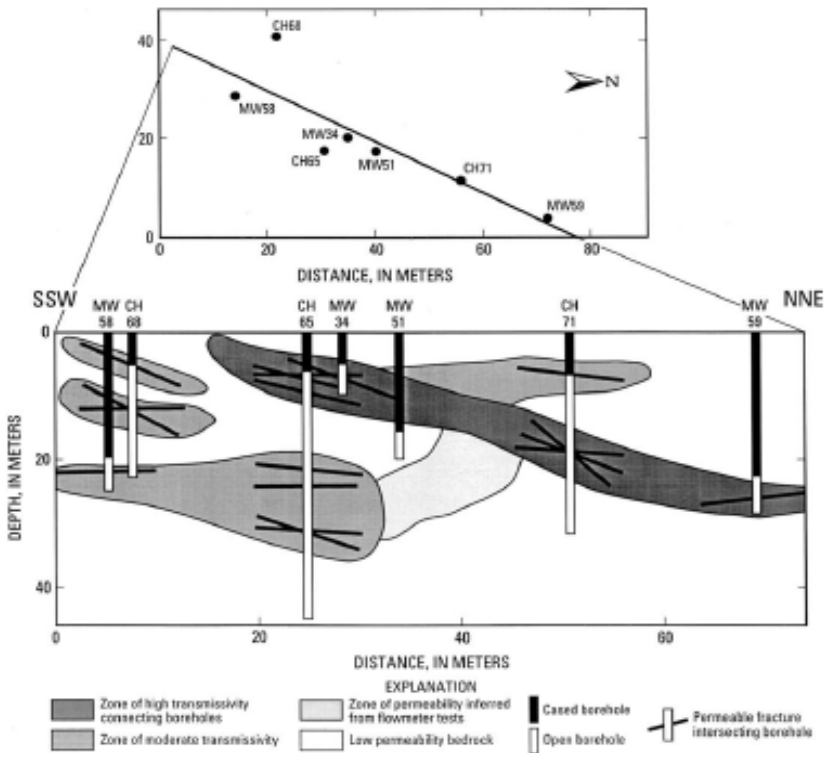


Figure 3: (a) USGS flow meter and televiewer log interpretations for four coreholes showing two or three flow zones in each hole (Figure 7, Williams and Paillet, 2002), and (b) conceptual model of few large/long continuous fractures or fracture zones without emphasis of smaller fractures (Figure 12, Williams and Paillet, 2002).

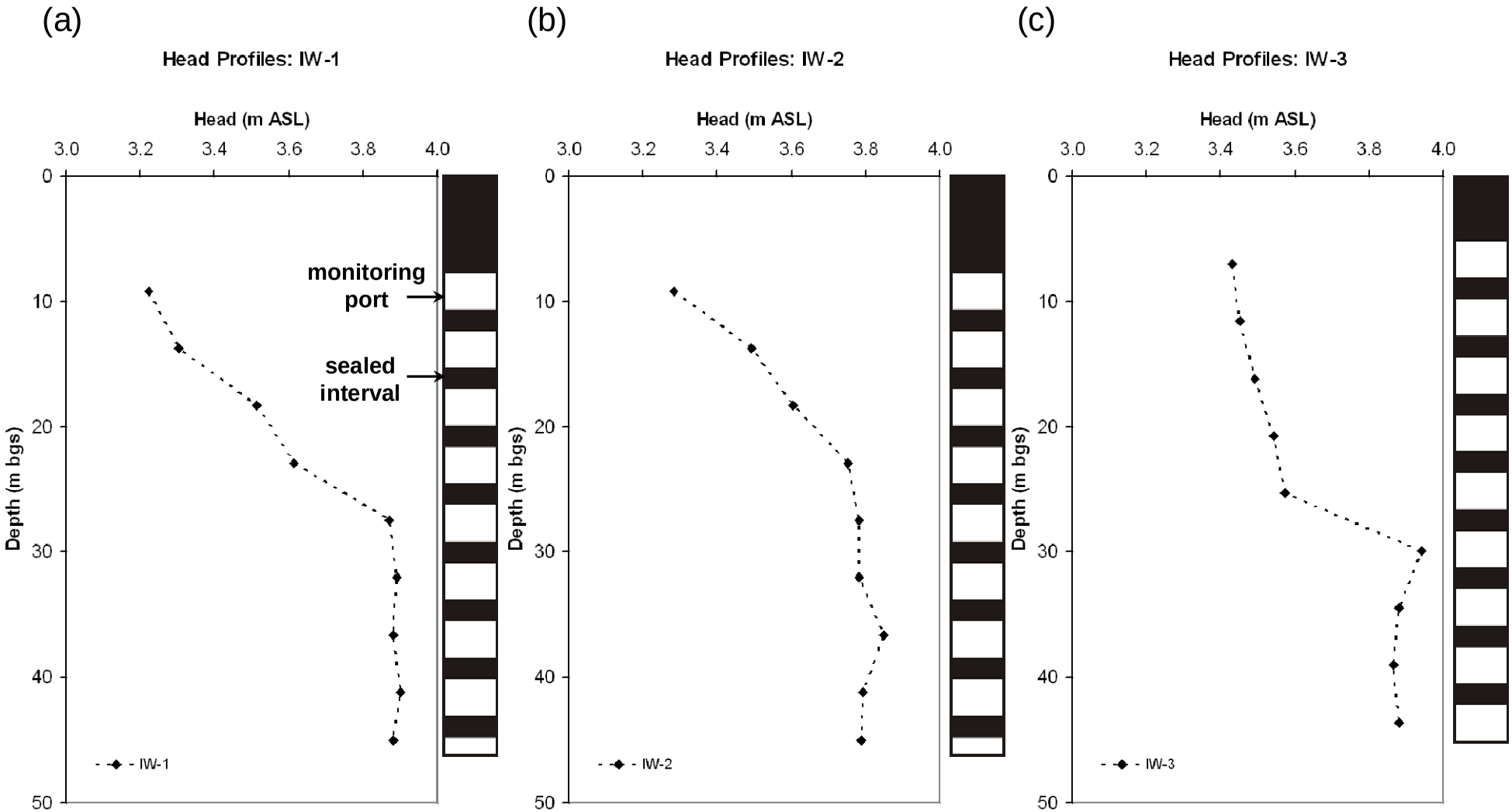


Figure 4: Hydraulic head profiles measured in three nine-port FLUTe multilevel systems: (a) IW-1, (b) IW-2 and (c) IW-3.

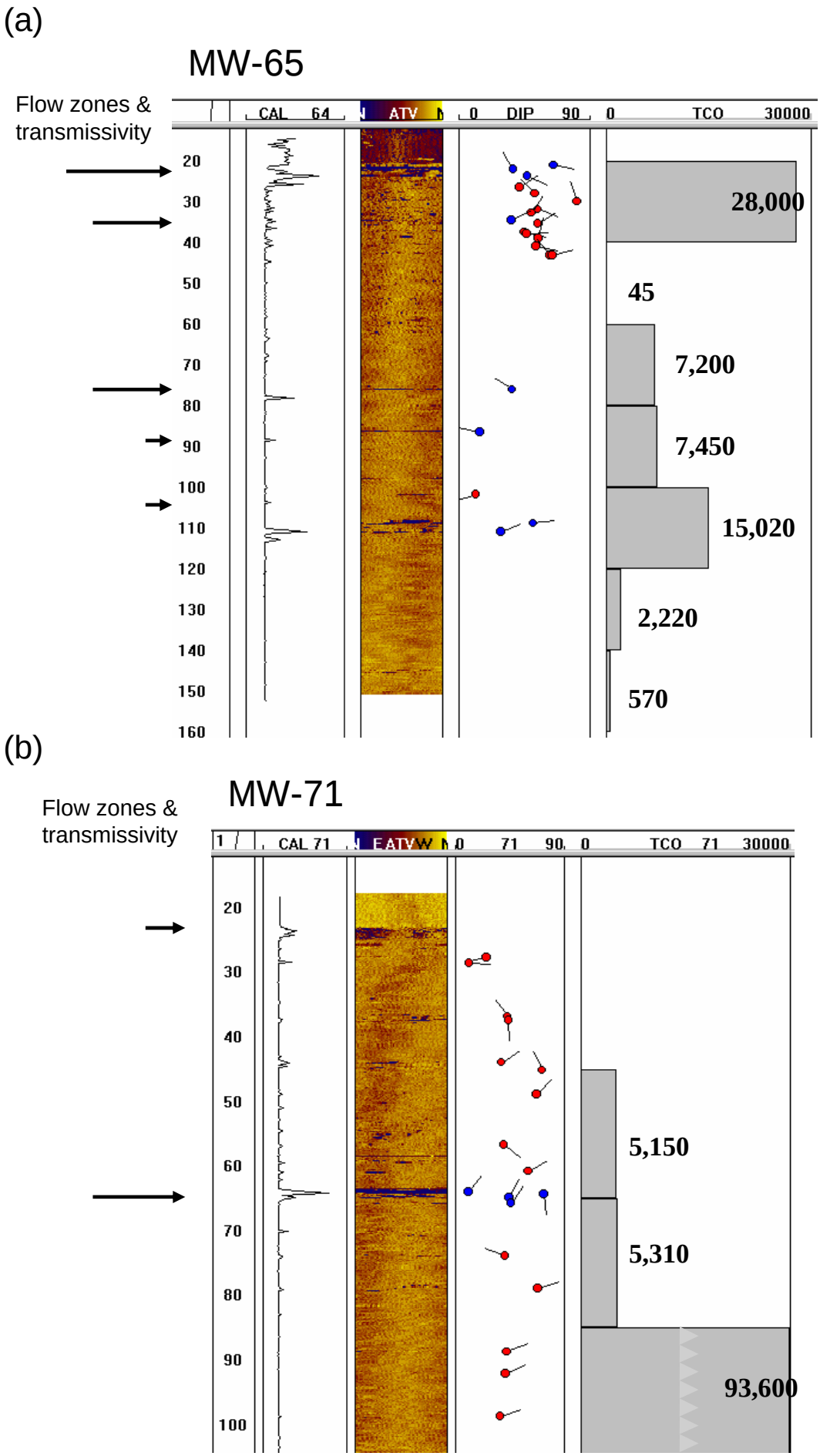


Figure 5: Comparison of geophysics, flow zones and VOCs from groundwater samples collected during drilling at coreholes: (a) MW-65, and (b) MW-71 (data from USGS, VOC data from Malcolm Pirnie Inc.).

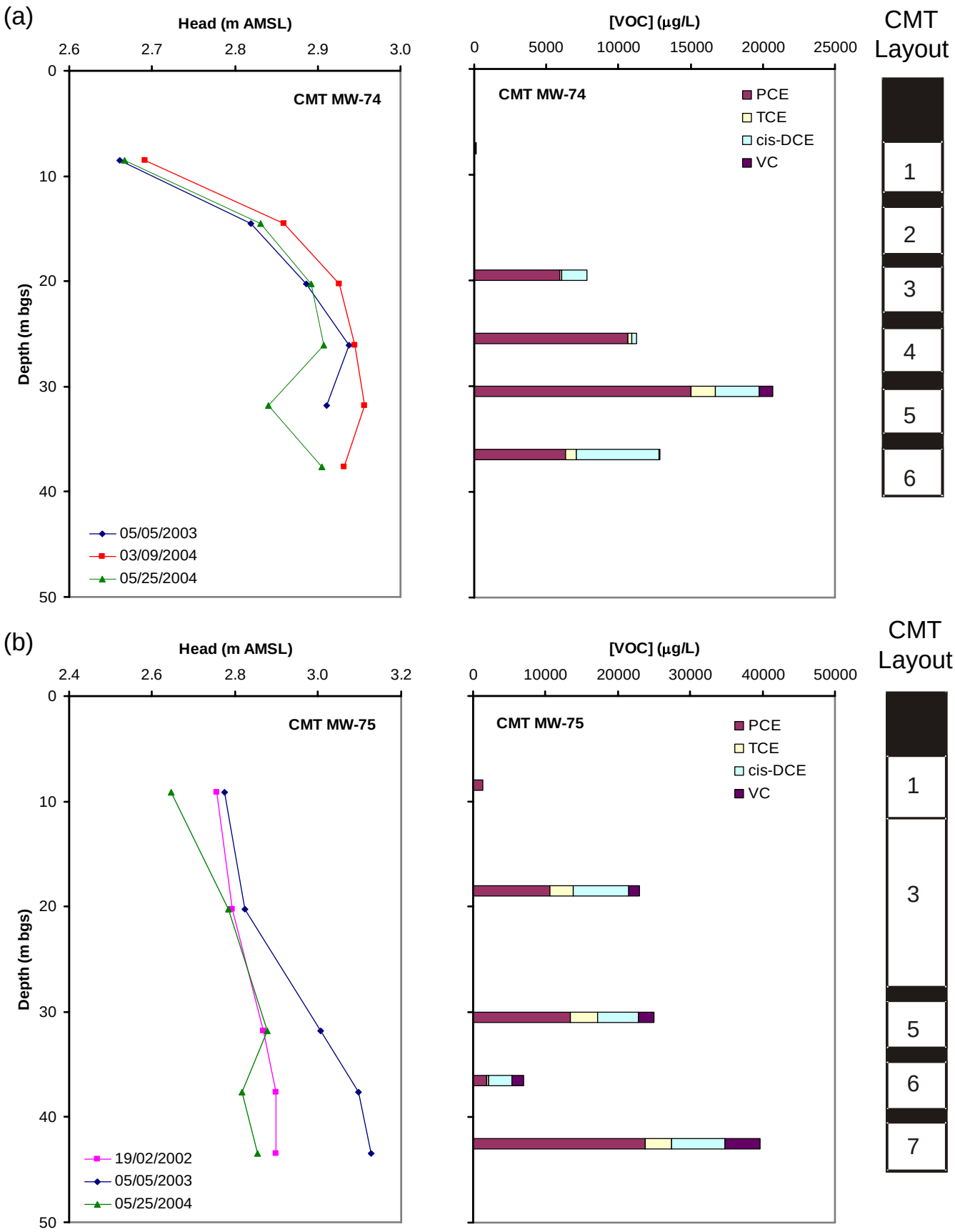


Figure 6: Plots of head profiles and VOCs in CMT multilevels: (a) MW-74 and (b) MW-75.

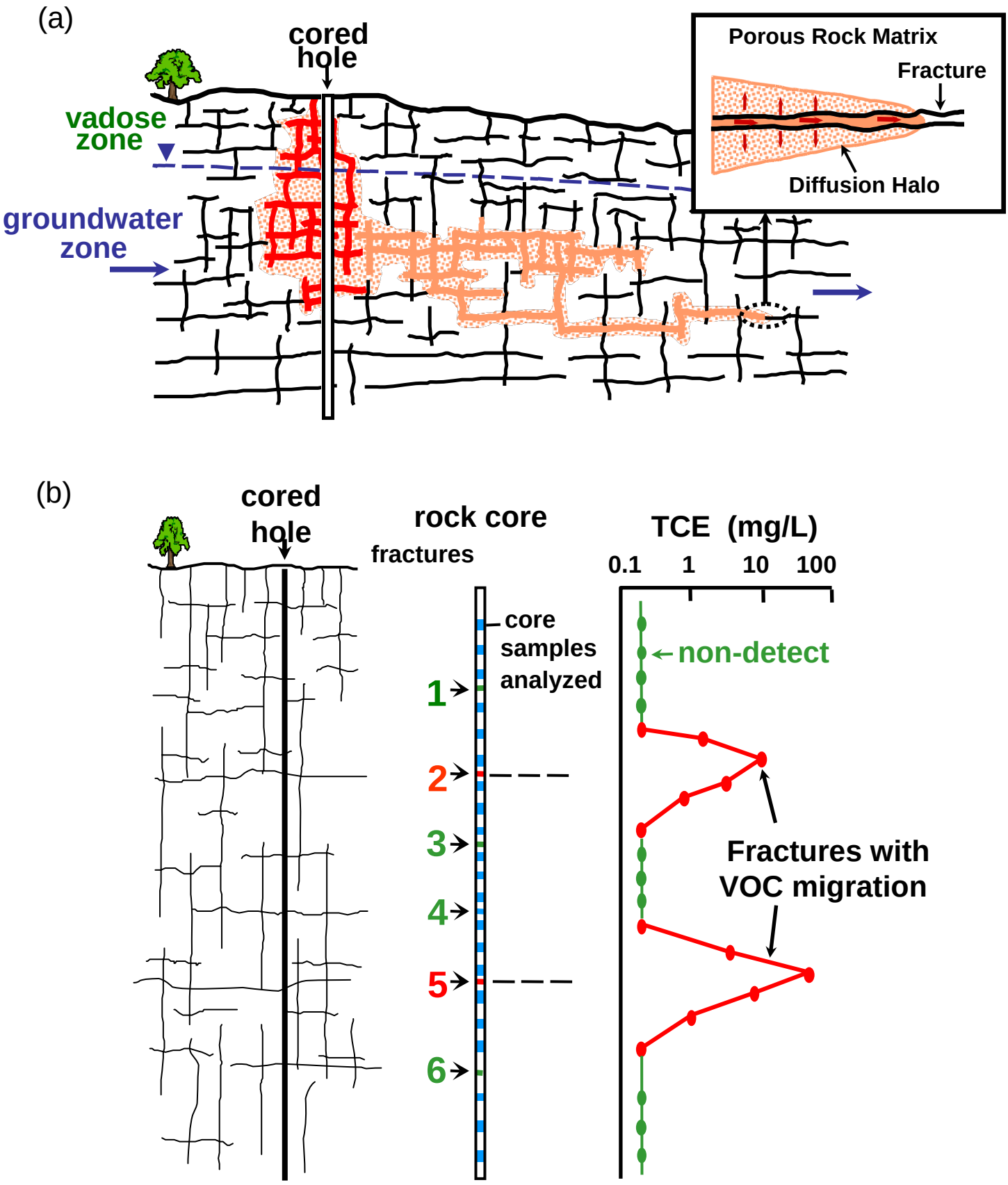


Figure 7: Schematic of (a) collection of vertical continuous cores through a source zone where DNAPL entered the ground decades ago and since has largely or completely disappeared due to dissolution in fracture flow and diffusion into the rock matrix (inset shows schematic of diffusion halo developed in the rock matrix away from a fracture, and (b) rock core subsampling for VOCs to identify migration pathways.

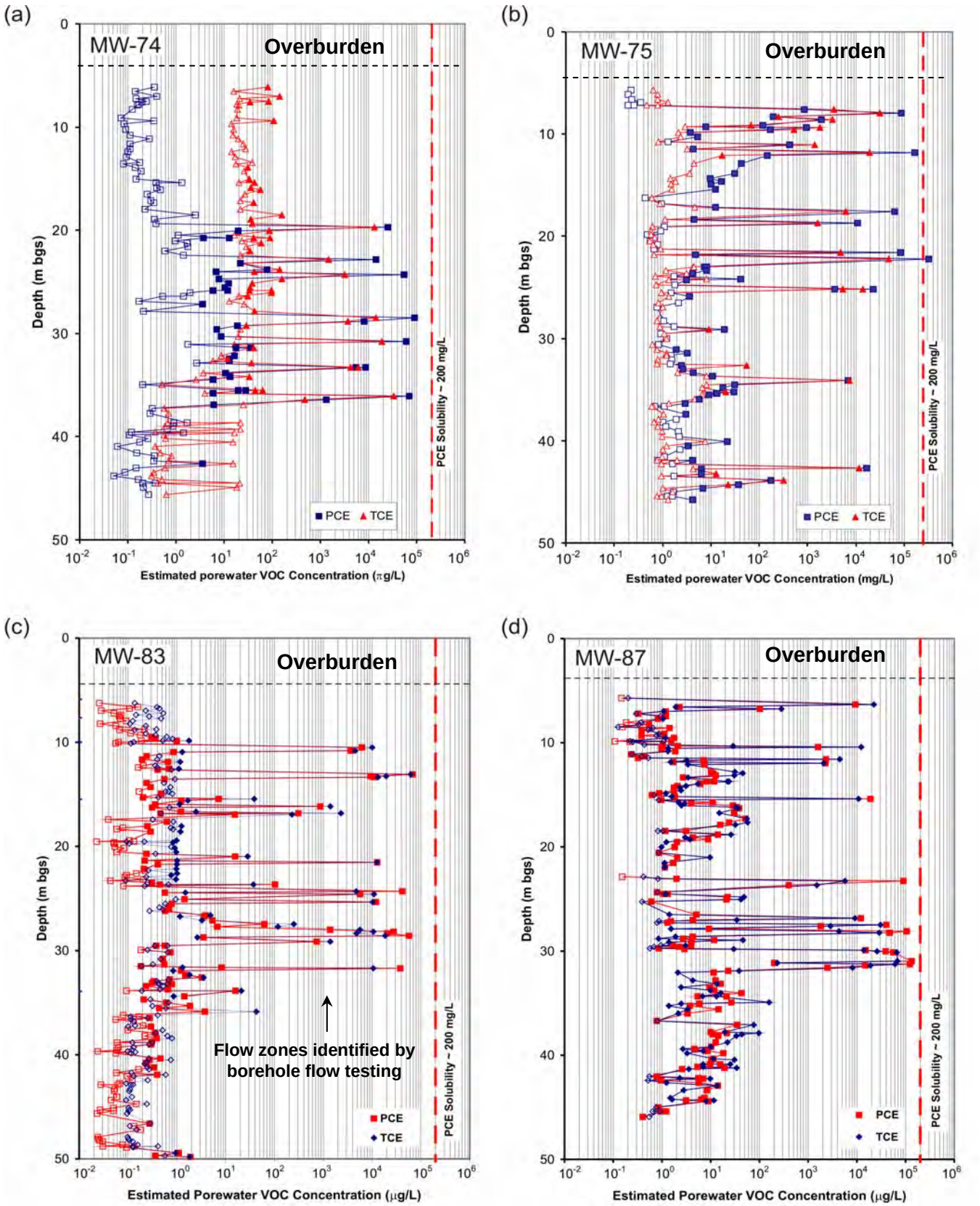


Figure 8: Rock core VOC profiles: (a) MW-74 and (b) MW-75 collected in 2001, and (c) MW-83 and (d) MW-87 collected in 2003.

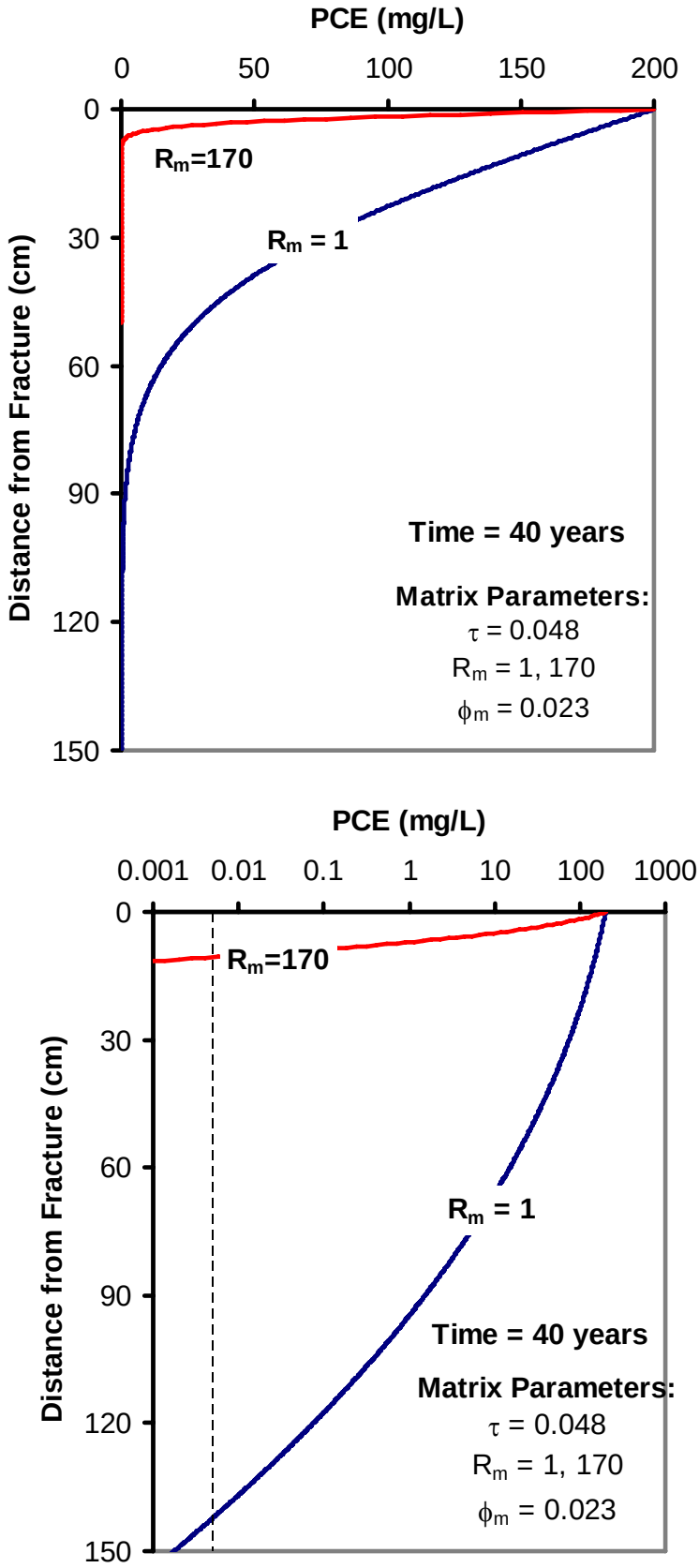


Figure 9: Simulated 1-D PCE diffusion profiles into rock matrix after 40 years from a fracture with PCE at solubility for cases with no sorption and including sorption (R=170).

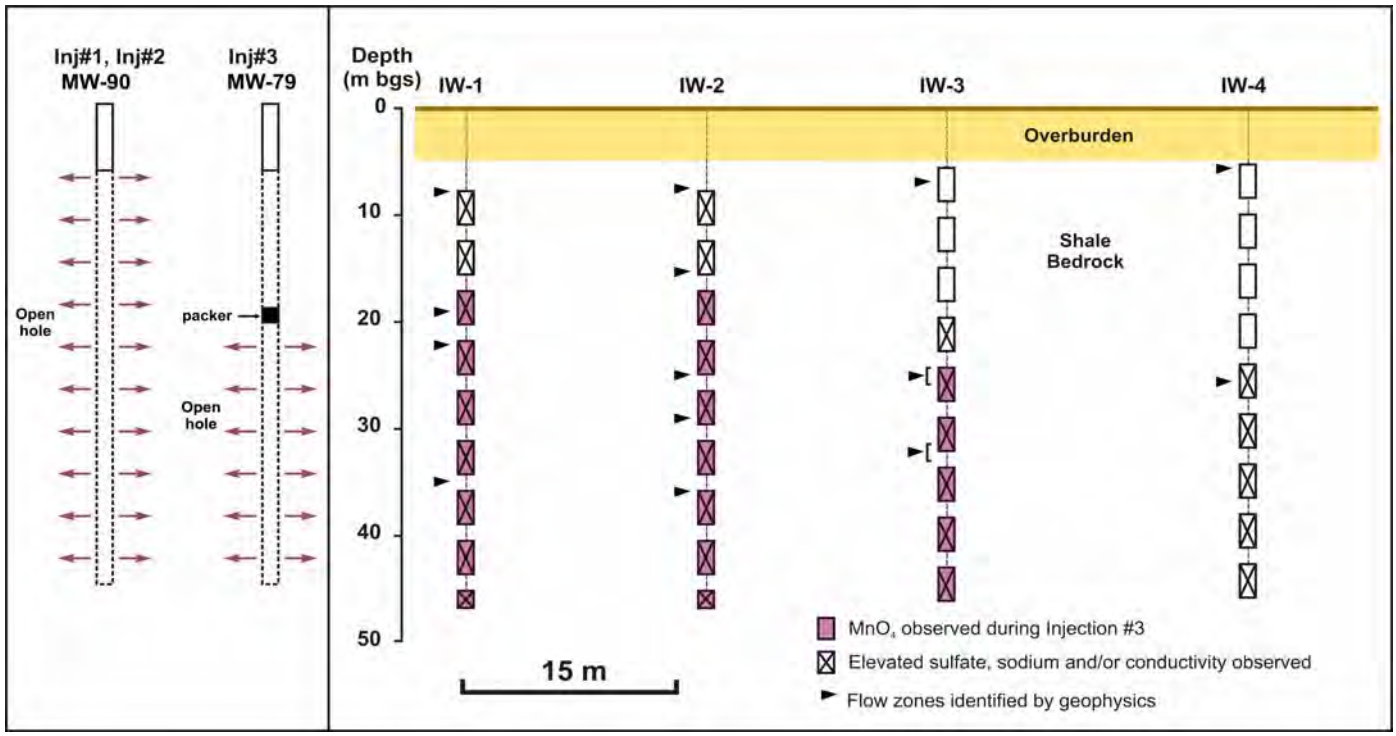


Figure 10: Distribution of permanganate and elevated sulfate and/or other injection-related parameters (sodium, conductivity) along transect of FLUTe multilevel wells observed during permanganate injections at MW-90 (two injections) and MW-79 (one injection).

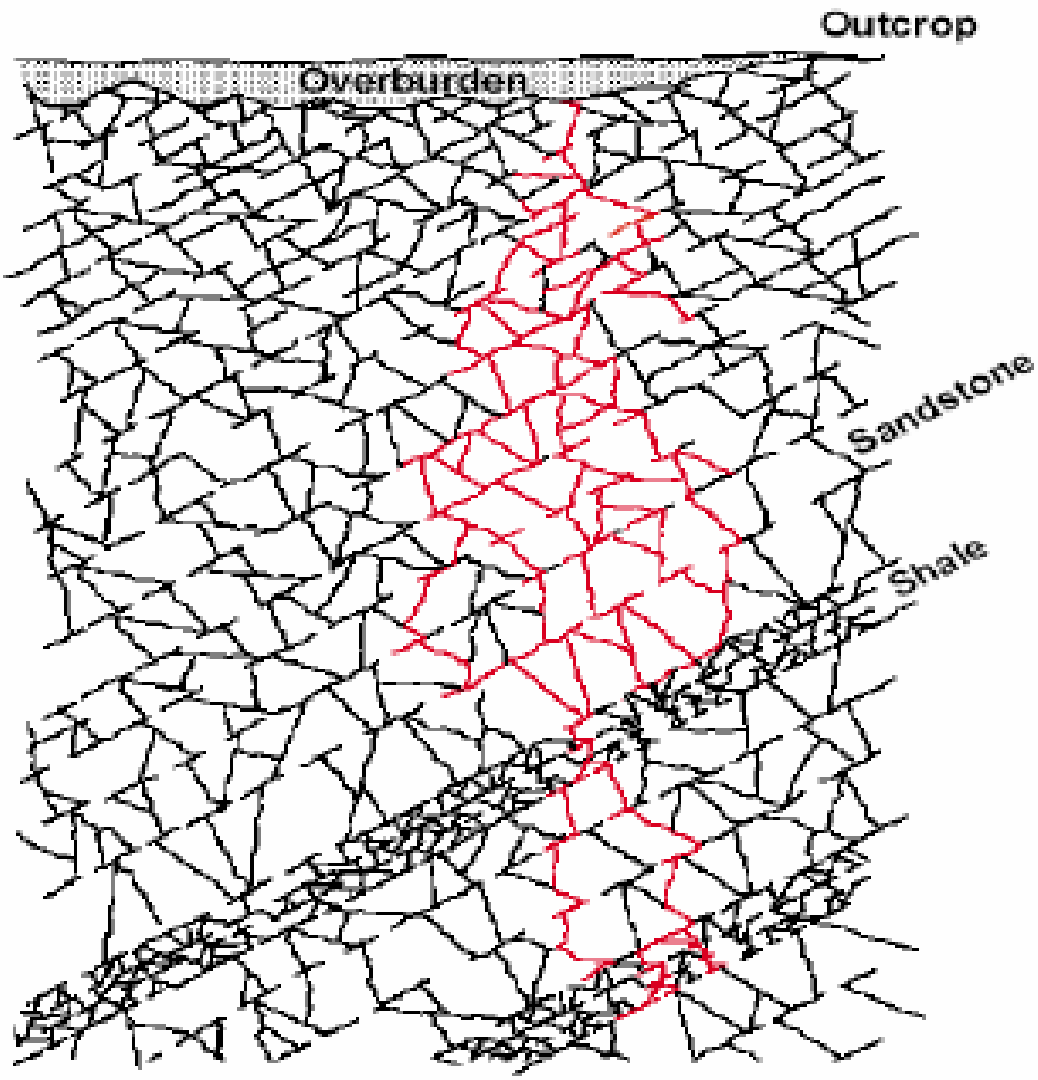


Note: this is a version of a fracture network model created for a different site, a version representative of Watervliet conditions will be included in the next manuscript revision.

Figure 11: Conceptual model of fracture network.